THE IDENTIFICATION OF A NOVEL RAS NANOCLUSTER REGULATOR

Thesis submitted in accordance with the requirements of the University of Liverpool for the degree of Doctor in Philosophy

Stephanie Puy Lam Mo

August 2020

Abstract

Ras proteins are crucial for the regulation of cellular proliferation, differentiation, and survival. These small GTPases act as a binary on/off switch, which reversibly binds to GTP or GDP, respectively. In humans, there are four Ras isoforms: KRAS4A, KRAS4B, HRAS and NRAS. They share almost complete sequence homology (~85%), however differ in the last 25 amino acids, termed the hypervariable region. This region is responsible for the specific localisation of the different Ras isoforms at the plasma membrane, where they occupy distinct non-overlapping nucleotide-dependent nanoclusters. These transient Ras nanoclusters are essential signalling platforms that recruit various effectors for Ras activation. Although, Ras activity is crucial for the normal functions of a living cell, it can also be detrimental, for example, in cancer. Mutations of the *Ras* gene renders them constitutively active and are highly prevalent in cancers (~17%). This has led to many efforts into the development of a Ras inhibitor as a cancer treatment. However, it has shown to be challenging, therefore, complementary research into understanding the regulation of Ras function and localisation has also been of importance as a possible indirect therapeutic.

Since the discovery of Ras, only a handful of Ras nanocluster regulators have been found. Therefore, the main aim of this project is to be able to identify a novel interactor of Ras with a particular interest in the organisation of Ras nanoclusters. Here, APEX2 was used to perform an unbiased screen of the proximal protein microenvironment in different Ras isoforms (KRAS4B, HRAS and NRAS). Nearby proteins were labelled with biotin generated by the APEX2-Ras and later enriched for mass spectrometry analysis. Nearly 3000 proteins were identified, with a group of phospholipid-binding proteins called annexins being amongst the top hits. Investigations into the relationship between Ras and annexins revealed that both HRAS WT and G12V interact with annexin 6. The spatial patterning of Ras proteins on the plasma membrane in the presence of annexin 6 demonstrated that this membrane-related protein could be a novel negative regulator of Ras nanoclustering.

Acknowledgements

‘You are capable of achieving anything you set your mind to’.

I have received support from all walks of life during my time here. With each individual bringing different qualities that have helped me through the journey. My close friends have provided immense support and inspiration, which has been so fundamentally important in helping me push through. My family have shown me encouragement in their unique ways. Starting with my parents being the yin and yang to my work ethics, from my father telling me to be better and work harder, to my mother saying that I have achieved more than they had ever imagined for me. My brother for reminding me to have a work-life balance by opening my eyes to a world other than studying. You have all individually contributed to helping me grow as a person and have been the support and love that I needed to get through this unique time of my life. I thank you all so much for being the amazing people that you are and for sticking by me at not only my best but also during my worst.

I would also like to express my gratitude to my supervisor: Professor Ian Prior, whom without I would not be on this PhD programme. He has given me guidance and opportunities to better myself as a scientist, as well as shared his knowledge on Ras and fastidiousness when it comes to figure making. I have also valued the advice and support sought from Professor Judy Coulson and Professor Chris Sanderson, as well as the technical support provided by colleagues and staff at other establishments during this project.

Table of Contents

List of Figures

List of Tables

List of Appendixes

List of Abbreviations

A	Alanine
ACN	Acetonitrile
AF6	Afadin 6
Ambic	Ammonium bicarbonate
ANXA	Annexin
APEX	Ascorbate peroxidase
APT1	Acyl protein thioesterase 1
Arf	ADP-ribosylation factor
ARF2	Arf-like protein 2
ASPP2	Apoptosis-stimulating proteins of p53 2
BiFC	Biomolecular fluorescence complementation
BioAMP	Biotinoyl-5'-AMP
BioID	Promiscuous biotin ligase identification
BirA	Biotin ligase
BP	Biotin phenol
BSA	Bovine serum albumin
C	Cysteine
CaM	Calmodulin
CAV1	Caveolin-1
CFC	Cardiofaciocutaneous syndrome
CO_2	Carbon dioxide
CON	Control
CRD	Cysteine-rich domain
CS	Costello syndrome
D	Aspartate

DAB	Diaminobenzidine
DHHC9-GCP16	Aspartate–histidine–histidine–cysteine domain-containing 9-Golgi complex-associated protein of 16kDa
DMEM	Dulbecco's Modified Eagle's Medium
DNA	Deoxyribonucleic acid
dNTP	Deoxynucleoside triphosphate
DTT	Dithiothreitol
EGF	Epidermal growth factor
EGFR	Epidermal growth factor receptor
EM	Electron microscopy
EMARS	Enzyme-mediated activation of radical source
ER	Endoplasmic reticulum
ERK	Extracellular Signal-Regulated Kinase
EZR	Ezrin
FGF	Fibroblast growth factor
FLIM	Fluorescence lifetime imaging
FLOT1	Flotillin-1
FRET	Fluorescence resonance energy transfer
FTase	Farnesyltransferase
FTIs	Farnesyltransferase inhibitors
G	G-binding motif
Gal-1	Galectin 1
Gal-3	Galectin 3
GAP	GTPase-activating protein
GDP	Guanosine diphosphate
GEF	Guanine-nucleotide exchange factor
GFP	Green fluorescent protein

GO	Gene ontology
GPCR	G-protein coupled receptor
GTP	Guanosine triphosphate
GTPases	Small guanosine triphosphates
G3BP2	GTPase-activating protein-binding protein 2
H_2O	Water
H_2O_2	Hydrogen peroxide
HCl	Hydrochloric acid
HRAS	Harvey rat sarcoma
HRP	Horseradish peroxidase
HVR	Hypervariable region
IAA	Iodoactamide
ICMT	Isoprenylcysteine carboxylmethyltransferase
IF	Immunofluorescence
IGF	Insulin-like growth factor
IMM	Inner mitochondrial membrane
IP	Immunoprecipitation
IκB	Inhibitor of nuclear factor kappa B
KRAS	Kirsten rat sarcoma
KSR	Kinase Suppressor of Ras
LaA	Lamin
L_d	Liquid disordered
LFA-1	Lymphocyte function-associated antigen 1
LFQ	Label-free quantification
L_o	Liquid ordered
MEFs	Mouse embryonic fibroblasts
MEK	Mitogen-activated protein kinase kinase

MPI	Mammalian protease inhibitor
NaCL	Sodium Chloride
NaF	Sodium Fluoride
NFκB	Nuclear factor kappa B
NHDF	Normal human dermal fibroblasts
NPM	Nucleophosmin
NRAS	Neuroblastoma rat sarcoma
NSAID	Nonsteroidal anti-inflammatory drug
NSCLC	Non-small cell lung carcinoma
NT	Non-targeting
OMM	Outer mitochondrial membrane
PAT	Palmitoyl acyltransferase
PBS	Phosphate buffered saline
PC	Phosphatidylcholine
PCR	Polymerase chain reaction
PDEδ	Phosphodiesterase-δ
PE	Phosphatidylethanolamine
PI3K	Phosphoinositide 3-kinase
PI3P	Phosphatidylinositol 3-phosphate
PI4P	Phosphatidylinositol 4-phosphate
PIP2	Phosphatidylinositol 4,5-biphosphate
PKC	Protein kinase C
PLCε	Phospholipase C ε
PM	Plasma membrane
PMSF	Phenylmethylsulfonyl fluoride
PS	Phosphatidylserine
PTB	Phosphotyrosine-binding

PTM	Post-translational modification
R	Arginine
RA	Ras association domain
Ral-GDS	Ral guanine nucleotide dissociation stimulator
Ras	Rat sarcoma
RASSF	Ras association domain family
RBD	Ras binding domain
RCE1	Ras-converting enzyme 1
RE	Restriction endonuclease
RFP	Red fluorescent protein
RIN1	Ras and Rab interactor 1
RIPA	Radioimmunoprecipitation assay
RTK	Receptor tyrosine kinase
S	Serine
SDS-PAGE	Sodium dodecyl sulphate polyacrylamide gel electrophoresis
SE	Sensitised emission
SEPT2	Septin-2
SH2	Src homology 2
SILAC	Stable isotope labeling by amino acids in cell culture
siRNA	Short interfering RNA
SPH	Sphingomyelin
SPPLAT	Selective proteomic proximity labelling assay using tyramide
SS	Serum-starved
STIM	Stimulated
TAE	Tris-acetate-EDTA
TBE	Tris-borate-EDTA

TBST	Tris-buffered saline with Tween
TCR	T cell receptor
TF	Transcription factor
tH	Truncated HRAS membrane anchor
Tiam1	T cell lymphoma invasion and metastasis-inducing protein 1
tK	Truncated KRAS membrane anchor
TOPO	Topoisomerase
U	Untransfected
V	Valine
WT	Wild type

CHAPTER ONE

Introduction

1.1. THE RAS SUPERFAMILY OF SMALL GTPASES

1.1.1. Small GTPases

In humans, the Ras superfamily consists of over 160 small guanosine triphosphatases (GTPases), which all share a fundamental role of GTP binding and hydrolysis (Qu *et al.*, 2019). These proteins are further subdivided based on their sequence homology and function into the following groups: Ras, Rho, Ran, Rab and ADP-ribosylation factor (Arf) (Qu *et al.*, 2019). For example, the Ras subfamily regulates cellular proliferation, Rho and Ran members are involved in actin dynamics and nuclear transport, respectively (Bishop and Hall, 2000; Macara, 2001). Whereas Rab and Arf subfamilies are fundamental for vesicular movement (Segev, 2001; D'Souza-Schorey and Chavrier, 2006).

All of these monomeric proteins together with their associated regulators and effectors play a central role for a plethora of signal transduction pathways, ranging from the regulation of gene expression to vesicular transport. They have a high affinity for guanosine triphosphate (GTP) and guanosine diphosphate (GDP) at their conserved ~20kDa G-domain located at the N-terminus. This domain contains two important regions: switch I and switch II, which undergo conformational changes when GTP-bound (Milburn *et al.*, 1990). Rendering the GTPase active and allowing for tight binding of effectors, which propagates its subsequent signalling pathway (Scolnick, Papageorge and Shih, 1979).

Regulatory proteins such as guanine-nucleotide exchange factors (GEFs) and GTPase-activating proteins (GAPs) promote the exchange of GDP/GTP in most GTPases (Cherfils and Zeghouf, 2013). During this cycle, GEFs regulate the conversion of GDP to GTP, whereas GAPs stimulate GTP hydrolysis. Although, small GTPases have intrinsic hydrolysis activity, the rate is relatively low in some members such as the Ras subfamily and therefore require additional aid from GAPs (Bourne, Sanders and McCormick, 1990). However, there are certain atypical GTPases that do not undergo the GDP/GTP cycle, instead they are regulated on a transcriptional level (Haga and Ridley, 2016).

1.1.2. Discovery of Ras

The founding members of the Ras superfamily emerged through the isolation of transforming retroviruses in rodent models, whereby oncogenic viruses induced sarcomas in infected rodents. Ras research first dates back to 1964, where murine leukaemia virus extracted from leukaemic rats were found to trigger the production of sarcomas in new-born rodents (Harvey, 1964). Another murine sarcoma retrovirus was discovered in the later years following a serial passage of a mouse leukaemic virus in Wister-Furth rats (Kirsten and Mayer, 1967). The highly expressed gene product responsible for the cellular transformation in these virally infected cells was a 21kDa protein (p21), which differed in gene sequence between the Harvey and Kirsten sarcoma viruses. An alternative form of this p21 protein was later shown to be constitutively expressed at a low level in normal healthy cells (Ellis *et al.*, 1981).

Human homologs of these genes responsible for inducing rat sarcomas (Ras) were later discovered and were named *KRAS* and *HRAS*, respectively after its initial discovery in Kirsten- and Harvey- rat sarcoma viruses. The link between the human and viral form of *RAS* was made by the hybridisation of specific probes for viral *RAS* genes to DNA isolated from NIH-3T3 cells transformed with DNA from bladder and lung carcinoma cells. This revealed restriction fragments that were homologous to the transforming genes present in the sarcoma viruses (Der, Krontiris and Cooper, 1982). This was later supported by the detection of *HRAS* and *KRAS* in human tumour cell lines of bladder and lung carcinomas, respectively (Hall *et al.*, 1983; Shimizu, Goldfarb, Suard, *et al.*, 1983).

By 1983, the third Ras member was identified. Transforming sequences were found in DNA isolated from fibrosarcoma and rhabdomyosarcoma cell lines, which resulted in the morphological transformation of NIH-3T3 cells (Marshall, Hall and Weiss, 1982). Similarly, DNA from a human neuroblastoma cell line, SK-N-SH also showed to transform NIH-3T3 cells (Shimizu, Goldfarb, Perucho, *et al.*, 1983). The DNA isolated from these different studies were shown to be identical and related to the other *RAS* genes. This third

Ras gene was later named neuroblastoma rat sarcoma (*NRAS*) (Marshall, Hall and Weiss, 1982; Hall *et al.*, 1983; Shimizu, Goldfarb, Perucho, *et al.*, 1983).

The transforming property of Ras was found to be due to a single point mutation. In T24 human bladder carcinoma cells, Ras was activated by the substitution of guanosine instead of thymidine, which altered the twelfth amino acid from a glycine to a valine (G12V) (Reddy *et al.*, 1982). The first clinical case reporting of mutated KRAS in a lung cancer biopsy was the beginning to the discovery of the wide prevalence of mutated Ras in numerous human cancers (Santos *et al.*, 1984).

1.2. THE RAS SUBFAMILY

1.2.1. Ras members

The Ras subfamily consists of 36 members that all affect similar cellular processes such as proliferation, growth, and gene expression. Aside from the initial founding members: KRAS, HRAS and NRAS, other members include MRAS, RRAS, RAP, RAL and RIT (Qu *et al.*, 2019).

The genes: *KRAS*, *HRAS* and *NRAS* encode for four different Ras proteins: KRAS4A, KRAS4B, HRAS and NRAS, of which are all ubiquitously expressed; however, expression levels vary dependent on the tissue type. The two isoforms of KRAS are the product of alternate splicing, which results in different fourth exons of the *KRAS* gene (hereafter KRAS4B will be referred to KRAS, unless otherwise stated) (Newlaczyl, Coulson and Prior, 2017).

1.2.2. Structure

Each of the three Ras genes differ in DNA length: 35kb (KRAS), 3kb (HRAS) and 7kb (NRAS) and are also located on different chromosomes: 12p12.1, 11p15.5 and 1p13.2, respectively (Popescu *et al.*, 1985; Zabel *et al.*, 1985). Despite the differences in DNA length, these genes all encode for four coding exons each, which result in very similar sized proteins of 188-9 amino acids (21kDa) that share high sequence homology (~90%) in the

first 166 amino acids but vastly differ in the remaining sequence. These represent the G-domain and membrane targeting regions, respectively (Lowy and Willumsen, 1993).

1.2.2.1. G-domain

Binding of GDP/GTP, Ras effectors and regulators occurs within the first half of the catalytic G-domain. This is called the effector lobe (aa 1-86) and shares the identical DNA sequence amongst all the Ras isoforms. Whereas the allosteric lobe (aa 87-166) differs between the Ras isoforms and only share an approximate 82% sequence match. The allosteric lobe has shown to play a role in communicating with the effector lobe in order to modulate Ras-membrane interactions (Parker and Mattos, 2015).

Crystal structures of Ras have revealed that the catalytic domain consists of six-stranded β-sheets, which forms the hydrophobic core (*Fig. 1.1*). Surrounding the core are five α-helices, which are interconnected by ten hydrophilic loops. Amongst this polypeptide chain are five conserved GDP/GTP (G) binding motifs: G1, G2, G3, G4 and G5. These regions are fundamental for GDP/GTP exchange, GTP hydrolysis and GTP-induced conformational changes (Gorfe, Grant and McCammon, 2008).

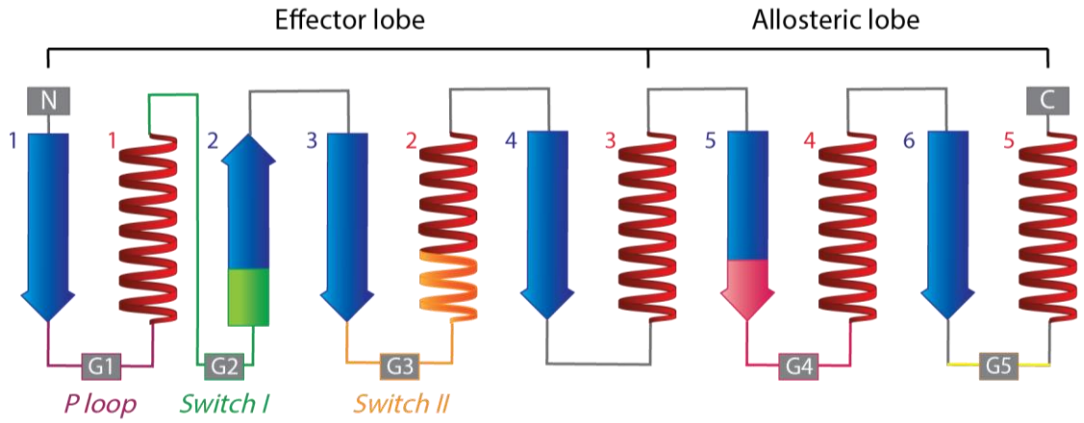

Figure 1.1| Schematic of the G catalytic domain - The composition of the catalytic domain is made up of β-strands (blue arrows), α-helices (red helices) and interconnecting loops (lines). Each G-binding motif is highlighted.

The first motif, G1 (aa 10-17) represents the P-loop (GXXXXGKS/T), which connects the β1 strand to the α1 helix. The P-loop also binds GDP or GTP by forming bonds with the α- and β-phosphates on the nucleotides via its NH_2 groups on the main chain and lysine side

chain (Milburn *et al.*, 1990; Schlichting *et al.*, 1990). The second motif, G2 also more commonly known as switch I (aa 30-38), contains the N-terminus of the β2 strand and its preluding neighbour loop, L2 (Milburn *et al.*, 1990; Bourne, Sanders and McCormick, 1991). Conformational changes to L2 occur when bound to GTP (Tong *et al.*, 1989; Milburn *et al.*, 1990). Here, the invariant threonine residue (Thr-35) on the loop interacts with the γ-phosphate of GTP (Pai *et al.*, 1989). As a result, the orientation of Thr-35 is altered, allowing it to bind tightly to a crucial magnesium (Mg^{2+}) co-factor via its hydroxyl side chain (John *et al.*, 1993). The third motif, G3 represents switch II (aa 59-76) and consists of the L4 loop and α2 helix. The NH_2 backbone of residues 60 and 61 form hydrogen bonds with the γ-phosphate, which induces conformational changes to the L4 loop and alters the orientation of α2 (Milburn *et al.*, 1990; Stouten *et al.*, 1993)

The P-loop, switch I and switch II regions are all components of the effector lobe (Pai *et al.*, 1989). Whereas the allosteric lobe is composed of the remaining G motifs: G4 (aa 112-119) and G5 (143-147). Together these motifs along with G1 aid the tight binding of the nucleotide via their interactions with the guanine base and β-phosphate, respectively (Parker and Mattos, 2015). The fourth motif, G4 is composed of the β5 strand and L8 loop. Its N/TKXD motif mediates guanine specificity via its Asp side chain and stabilises the guanine-binding site through bonds between its Asn and Lys side chains with residues 13 and 14 in G1. Lastly, the fifth motif, G5 is found in the loop, between the β6 strand and α5 helix. It predominantly stabilises nucleotide binding via its SAK motif but can also bind directly to guanine via its Ala group (Bourne, Sanders and McCormick, 1991). Altogether, the allosteric lobe plays a crucial role in the intercommunication between the effector lobe, membrane targeting domain and the plasma membrane.

In more recent times, a switch III region was discovered using HRAS. It consists of the β2-β3 loop and the α5 helix, which together with α4 and the hypervariable region (HVR) reorients the G-domain accordingly to the plasma membrane during Ras activation (Abankwa *et al.*, 2008).

1.2.2.2. Membrane targeting domain

Unlike the G-domain, the membrane targeting domain (aa 166-188/189)/HVR is specific for each Ras isoform (Hancock, Paterson and Marshall, 1990). This region is divided into a linker domain and a targeting domain (*Fig.1.2*). The linker domain has shown to stabilise Ras localisation at the plasma membrane and other subcellular regions (Prior and Hancock, 2001). Whereas the targeting domain is a site for post-translational modifications (PTMs) that are required for membrane trafficking and localisation (Laude and Prior, 2008). At the C-terminal of the targeting domain is a CAAX motif, whereby C is cysteine, A is usually an aliphatic amino acid like isoleucine, leucine or valine and X is serine or methionine. This motif plays an important role for membrane localisation of which will be discussed in section 1.4 (Reiss *et al.*, 1990). Collectively, both the linker and targeting domains contribute to the precise localisation of Ras to the inner plasma membrane as well as other intracellular compartments (S. J. Plowman and Hancock, 2005; Wright and Philips, 2006; Laude and Prior, 2008; Henis, Hancock and Prior, 2009; Prior and Hancock, 2012).

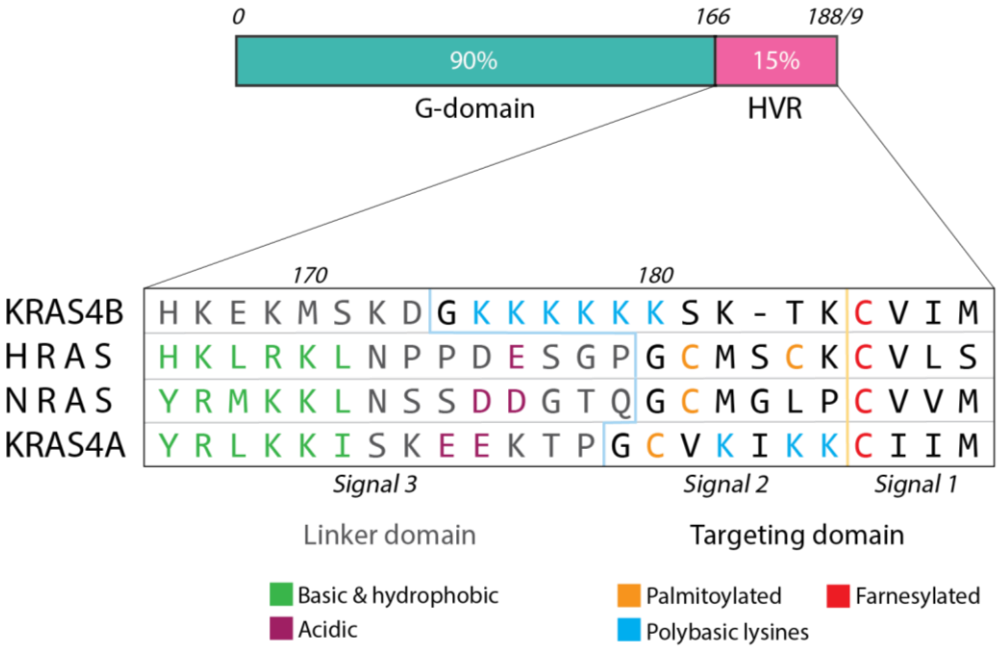

Figure 1.2| Ras sequence – Sequence homology between the different Ras isoforms for the two main components: G-domain and HVR are displayed. Important residues from the HVR that form the three signals required for membrane targeting are highlighted for each Ras isoform.

1.3. RAS SIGNALLING

1.3.1. Receptor tyrosine kinase pathway

Cell surface receptors transmit external signals to a multitude of signalling pathways to elicit a relevant biological response (Lemmon and Schlessinger, 2010). Receptor tyrosine kinases (RTKs) are fundamental receptors for Ras activation. These receptors can be triggered by growth factors such as epidermal growth factor (EGF), insulin-like growth factor (IGF) and fibroblast growth factor (FGF) (Fantl, Johnson and Williams, 1993). Ligand binding at the extracellular region of RTKs induces receptor oligomerisation, which releases the cis-autoinhibition and triggers trans-autophosphorylation of the cytoplasmic tyrosine kinase domains (Lemmon and Schlessinger, 2010). These phosphotyrosine residues become the docking sites for proteins that contain a Src homology-2 (SH2) or a phosphotyrosine-binding (PTB) domain (Wagner *et al.*, 2013). In the context of Ras activation, the SH2/SH3 domain-containing adaptor protein: Grb2 binds to the autosphosphorylated RTK and recruits a Ras-GEF called Son-of Sevenless (Sos) via its SH3 domain (Rozakis-Adcock *et al.*, 1993). This activates Sos, which in turn promotes the exchange of GDP for GTP on Ras (Buday and Downward, 1993).

1.3.2. Ras activation

1.3.2.1. GEFs

The off-rate for GDP ($t_{1/2}$ = 6 min, k_{off} = $2x10^{-3}s^{-1}$) in Ras is relatively slow, therefore GEFs are required to accelerate this GDP/GTP exchange rate (Hunter *et al.*, 2015). Aside from Sos, other types of Ras GEFs include RAPGEF, RASGRP and RASGRF (Bos, Rehmann and Wittinghofer, 2007). These GEFs catalyses the dissociation of GDP from Ras by reducing its nucleotide affinity via modifications to the nucleotide-binding site. However, GEFs do not favour whether GDP or GTP binds, instead the cellular concentration of GDP versus GTP determines whether Ras is GDP or GTP-bound, respectively (Boriack-Sjodin *et al.*, 1998).

1.3.2.2. Conformational switch

As mentioned previously, the switch I (aa 30-38) and II (aa 59-76) regions are located within the G-domain and play an important role in the binding of GDP/GTP (Pai *et al.*, 1989; Milburn *et al.*, 1990). When GEF is bound, it interacts with these switch regions to perturb the binding of GDP and the Mg^{2+} ion. Typically, GEF binds the switch I region and pulls this switch region away, resulting in the opening of the nucleotide binding site. In the context of Sos, it displaces this region with a helical hairpin. Then, uses the hydrophobic Ala-59 residue on the switch II domain to repel the Mg^{2+} ion from the Mg^{2+} binding site (Wittinghofer *et al.*, 1991; John *et al.*, 1993).

Conformational changes amongst the P-loop, switch I and switch II regions result in GDP being displaced (Boriack-Sjodin *et al.*, 1998). Ras becomes GTP-bound, i.e., active, when the cellular concentration of GTP exceeds GDP by approximately tenfold in the cytoplasm. Once GTP-bound, GEF is displaced. Here, switch I and II regions are held in an active conformation due to the hydrogen bonds between the γ-phosphate oxygens and the main chain NH groups of the two residues: Thr35 and Gly60 (Pai *et al.*, 1989; Wittinghofer *et al.*, 1991).

There are two different conformations of Ras in its GTP-bound state: state 1 ('open') and state 2 ('closed'). The open conformation favours nucleotide exchange and is less capable of effector interactions, whereas the closed conformation encourages effector binding and GTP hydrolysis (Shima *et al.*, 2010). Different Ras isoforms are thought to favour a particular state, for example, KRAS is predominantly found in an open state, whereas HRAS and NRAS is preferential to the closed state (Gorfe, Grant and McCammon, 2008; Parker *et al.*, 2018).

1.3.2.3. GTP hydrolysis

Additional GTPase activity is required from Ras GAPs, such as p120GAP and RASA1, to accelerate GTP hydrolysis of Ras due to its relatively low intrinsic GTPase rate ($t_{1/2}$ = 16 mins, k_{off} =$6x10^{-4}s^{-1}$) (Hunter *et al.*, 2015). In HRAS, GAP stabilises the interaction between

the Gly61 residue (from the switch II region) and H_2O molecule (Frech *et al.*, 1994). In addition, it inserts a catalytic arginine finger near the β- and γ-phosphates, which contains a main chain carbonyl group that aids the extraction of a hydrogen atom from the water molecule (Kötting *et al.*, 2008). The resulting hydroxyl ion is involved in the nucleophilic attack on the γ-phosphate of GTP, which cleaves the phosphomonoester bond, thus releasing the phosphate and returning the switch regions back to its flexible GDP-bound conformation (Scheffzek *et al.*, 1997).

1.3.3. Ras effector pathway

1.3.3.1. Effector binding

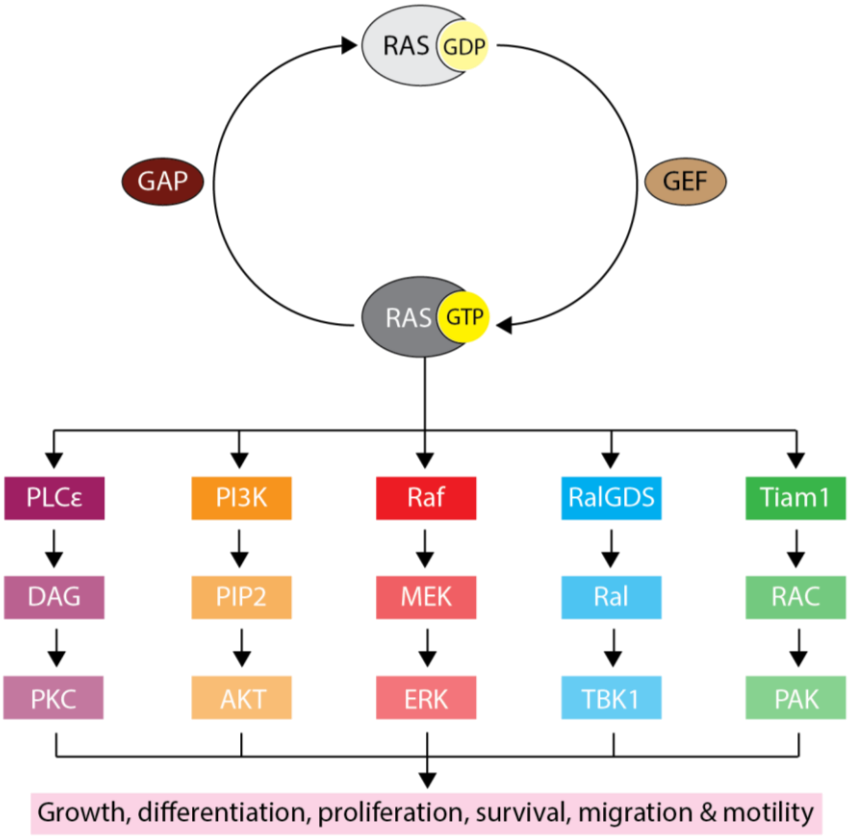

Figure 1.3| Schematic of Ras effector pathways – Exchange of GDP to GTP via GEF leads to activation of Ras. As a result, conformational change occurs, allowing GTP-bound Ras to bind to an effector and activate its downstream pathway.

In its active conformation i.e., bound to GTP, the core effector domain within the switch I region forms a loop on the surface, providing a platform for high affinity Ras effector

binding. This effector binding region is identical amongst all four Ras isoforms (Spoerner *et al.*, 2001). To date, over 10 different classes of Ras effectors have been discovered, where several classes consist of different isoforms. Examples include Raf, phosphoinositide 3-kinase (PI3K), Ral guanine nucleotide dissociation stimulator (RalGDS), T cell lymphoma invasion and metastasis-inducing protein 1 (Tiam1), Afadin 6 (AF6), RIN (Ras and Rab interactor), Ras association domain family (RASSF), phospholipase C ε (PLCε) and GAP (Sjölander *et al.*, 1991; Dickson *et al.*, 1992; Kuriyama *et al.*, 1996; Rajalingam *et al.*, 2007).

These Ras effectors are defined as proteins that preferentially bind to GTP-bound Ras, whereby mutations within the core effector domain would lead to impairment of this interaction. They are further characterised by the presence of a Ras binding domain (RBD) or Ras association domains (RA), which differs in sequence between the Ras effectors. However, common to all is their topology of a ubiquitin fold consisting of a ββαββαβ tertiary structure (Nassar *et al.*, 1995).

1.3.3.2. Raf/MAPK pathway

The Raf/MAPK pathway and PI3K/Akt pathway are key downstream signalling pathways of Ras. The Raf family of serine/threonine kinases consist of three members: a-Raf, b-Raf and c-Raf. These proteins are involved in the Raf-MEK (mitogen-activated protein kinase kinase)-ERK (extracellular signal-regulated kinases) cascade, which ultimately regulates processes such as proliferation, differentiation, cell survival and cell motility (Leevers, Paterson and Marshall, 1994).

Ras activation leads to the recruitment of cytosolic Raf to the plasma membrane (Vojtek, Hollenberg and Cooper, 1993). Dimerization of Raf is a fundamental step for Raf activation. However, the prerequisites of this process are unclear and of debate whether monomeric or dimeric active Ras mediates the formation of Raf dimers or alternatively, Raf dimers induce Ras dimerization (Inouye *et al.*, 2000; Rushworth *et al.*, 2006; Rajakulendran *et al.*, 2009; Ritt *et al.*, 2010; Nan *et al.*, 2015; Ambrogio *et al.*, 2018; Travers *et al.*, 2018). All three Raf members can dimerise with each other, but for Ras signalling, there is a preference for b-

Raf-c-Raf heterodimers (Weber *et al.*, 2001; Garnett *et al.*, 2005; Rushworth *et al.*, 2006; Ritt *et al.*, 2010). In addition to dimerization, the Raf cysteine-rich domain (CRD) also needs to engage with Ras via its farnesyl group as well as membrane phospholipids in order to release the autoinhibition, thus allowing for full Raf activation to occur (Ghosh *et al.*, 1996; Luo *et al.*, 1997; Cutler *et al.*, 1998; Hekman *et al.*, 2002; Terrell and Morrison, 2019).

When Raf dimerizes, the Raf kinase domains come in contact, which leads to transactivation. This induces its catalytic activity, allowing it to phosphorylate MEK proteins: MEK1 (MAP2K1) and MEK2 (MAP2K2). These in turn phosphorylates ERK1 and 2 (also known as MAPK3 and MAPK1) (Howe *et al.*, 1992; Leevers and Marshall, 1992). The activated ERK proteins dimerizes and activates a variety of nuclear transcription factors (TFs) such as ETS1/2, Myc, JUN, FOS, NF-κB and AP-1, as well as other kinases like JNK (Chang *et al.*, 2003). As a result, cells enter S-phase and the expression of negative regulators such as Sprouty and MAPK phosphatases (dual specificity phosphatases 1-6) are induced (Ozaki *et al.*, 2001; Kidger *et al.*, 2017).

1.3.3.3. PI3K/Akt pathway

Another well-characterised Ras effector pathway involves PI3K proteins, which are important for cell survival and proliferation (Sjölander *et al.*, 1991; Rodriguez-Viciana *et al.*, 1994). These heterodimeric proteins are lipid kinases that consist of a p85 regulatory subunit and a p110α catalytic subunit (Gupta *et al.*, 2007). They bind to GTP-Ras via their RBD and consequently become activated. The activated PI3K catalyses the conversion of a phospholipid component of the plasma membrane, phosphatidylinositol (4,5)-biphosphate (PIP_2) into phosphatidylinositol (3,4,5)-triphosphate (PIP_3). The latter recruits inactive cytosolic Akt to the plasma membrane via the engagement of the PH domain of Akt (Ebner *et al.*, 2017). In addition to Akt, PIP_3 also recruits PDK1 to the plasma membrane. PDK1 along with TORC2 phosphorylate the threonine and serine residues of Akt (Hemmings and Restuccia, 2012). This results in the activation of Akt, which dissociates from the plasma membrane to activate a series of cytosolic and nuclear proteins that promote cell survival

via the inhibition of proapoptotic pathways (Rameh and Cantley, 1999). Examples include preventing apoptosis via phosphorylation of Mdm2, negatively regulating proapoptotic Bcl-2 members: BAD and BAX as well as inhibiting NF-κB (nuclear factor kappa B) via the phosphorylation of IκB (inhibitor of NFκB) (Brunet, Datta and Greenberg, 2001; Ogawara *et al.*, 2002).

1.4. LOCALISATION

1.4.1. Post-translational modifications

Ras proteins are first synthesised on cytosolic free polysomes (Prior and Hancock, 2012). Then trafficked to the plasma membrane following a series of PTMs, which generate isoform-specific membrane anchors that allow for precise localisation amongst the inner leaflet of the plasma membrane (Hancock, Paterson and Marshall, 1990; Casey and Seabra, 1996; Boyartchuk, Ashby and Rine, 1997; Dai *et al.*, 1998).

1.4.1.1. First signal: farnesylation, proteolysis and methylation

All Ras isoforms undergo CAAX processing, which consists of three obligate steps: farnesylation, proteolysis and carboxyl methylation (*Fig. 1.2*) (Casey and Seabra, 1996; Boyartchuk, Ashby and Rine, 1997; Dai *et al.*, 1998). The first PTM occurs when the globular hydrophilic Ras protein encounters farnesyltransferase (FTase) in the cytosol (Casey and Seabra, 1996). Here, FTase catalyses the addition of a 15-carbon farnesyl isoprenoid lipid to the cysteine residue of the CAAX motif via a stable thioester linkage. As a result, the farnesylated Ras is able to traffic and bind to the cytosolic face of the endoplasmic reticulum (ER) membrane (Choy *et al.*, 1999), where an integral membrane endoprotease: Ras-converting enzyme 1 (RCE1) is located (Boyartchuk, Ashby and Rine, 1997). This enzyme cleaves the C-terminal AAX tripeptide. The resulting terminal farnesylated cysteine residue is next methylated by an ER resident enzyme, isoprenylcysteine carboxylmethyltransferase (ICMT) to produce a hydrophobic tail that can interact with the phospholipid bilayer (Dai *et al.*, 1998). These three PTMs generates the first signal required for membrane targeting.

1.4.1.2. Second signal: polylysine residues or palmitoyl groups

A second signal is necessary for membrane targeting as it stabilises the weak interaction generated by the initial PTMs. Subsequent steps following CAAX processing are dependent on the Ras isoform (Choy *et al.*, 1999). For KRAS4B, the farnesyl group is sufficient for direct trafficking from the ER to the inner plasma membrane due to the presence of polybasic hexa-lysine residues (aa 175-180). These positively charged residues facilitate membrane localisation as they interact electrostatically with the negatively charged phospholipids present within the membrane (Hancock, Paterson and Marshall, 1990).

Contrastingly, additional PTMs are required for HRAS, NRAS and KRAS4A. These Ras isoforms undergo an exocytic pathway to the plasma membrane via the Golgi, where they are either mono- or di-palmitoylated (Hancock, Paterson and Marshall, 1990; Choy *et al.*, 1999; Apolloni *et al.*, 2000). This process occurs on the cytosolic face of the Golgi membrane via a palmitoyl acyltransferase (PAT) called DHHC domain-containing 9-Golgi complex-associated protein of 16kDa (DHHC9-GCP16) (Swarthout *et al.*, 2005). This heterodimeric protein complex adds a 16C palmitic acid on to one (NRAS - C181, KRAS4A – C180) or two (HRAS – C181 and C184) cysteine residues via a thioester bond. As a result of this protein modification, the C-terminal becomes more hydrophobic (Hancock *et al.*, 1989).

1.4.1.3. Third signal: basic and acidic residues

For HRAS, the combination of the farnesyl group and two palmitoyl groups are sufficient for stable membrane interactions. Whilst the monopalmitoylated NRAS and KRAS4A require a third signal to increase its membrane stability. A study revealed that palmitoylated Ras isoforms have a stretch of six basic residues at the linker domain of the HVR, which contributes to membrane localisation via electrostatic interactions. In addition, a pair of acidic residues that are also present in the linker domain of NRAS and KRAS4A have been shown to stabilise palmitoylation. Moreover, KRAS4A has an additional basic patch that provides further membrane affinity (Laude and Prior, 2008).

1.4.2. Endomembrane trafficking

The addition of these lipid groups renders Ras more lipophilic and thus aiding its association with membranes (*Fig.1.4*). Studies have shown evidence of Ras localisation and signalling on subcellular membranes of various organelles such as ER, Golgi, endosomes and mitochondria (Choy *et al.*, 1999; Rebollo, Pérez-Sala and Martínez-A, 1999; Chiu *et al.*, 2002; Lu *et al.*, 2009). The ability of the different Ras isoforms to associate with endomembranes vary between isoforms (NRAS>HRAS>KRAS) (Choy *et al.*, 1999). But overall, majority of Ras localisation and signalling occurs in the plasma membrane, despite a larger abundance of endomembranes within the cell. This non-equilibrium localisation is maintained by the combination of changes in membrane affinities, unidirectional vesicular trafficking, and chaperone proteins. Together, these regulate trafficking of Ras proteins leaked from the plasma membrane and prevent rapid diffusion of Ras proteins to intracellular membranes (Schmick, Kraemer and Bastiaens, 2015).

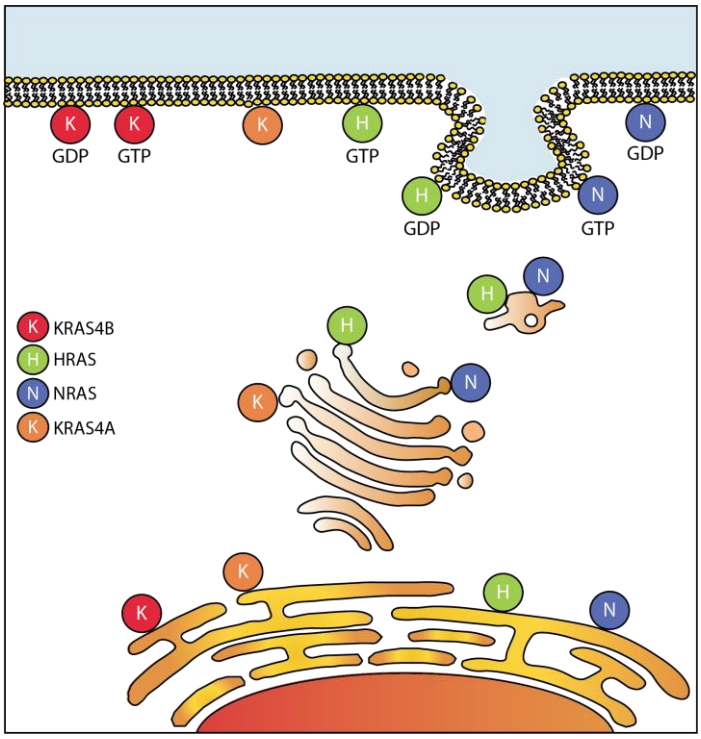

Figure 1.4| Ras localisation – Trafficking of Ras isoforms from the ER to the plasma membrane through different mechanisms. At the plasma membrane, Ras isoforms occupy distinct nucleotide-dependent non-overlapping nanoclusters.

1.4.2.1. Modulation of Ras trafficking

Ras proteins can become detached from the plasma membrane via different processes. For KRAS, dissociation from the plasma membrane can occur either spontaneously, indirectly via the constitutive internalisation of the plasma membrane or by processes regulated by calmodulin (CaM) or protein kinase C (PKC) (Bivona *et al.*, 2006; Schmick, Kraemer and Bastiaens, 2015; Agamasu *et al.*, 2019). In a calcium-dependent manner, CaM binds to the farnesyl side chain of KRAS via its hydrophobic binding pocket, independent of whether KRAS is GDP- or GTP-bound (Agamasu *et al.*, 2019; Grant *et al.*, 2020). As a result, CaM extracts KRAS from the plasma membrane due to its higher affinity for KRAS. However, the underlying molecular mechanism is still unclear due to inconsistencies in the literature (Sperlich *et al.*, 2016; Agamasu *et al.*, 2019; Grant *et al.*, 2020). Alternatively, KRAS is able to interact with other intracellular membranes, as a result of phosphorylation by PKC. This enzyme phosphorylates the S181 residue of the polybasic region, allowing KRAS to rapidly dissociate from the plasma membrane (Bivona *et al.*, 2006).

Whereas, for the palmitoylated Ras isoforms, HRAS and NRAS, removal of their palmitoyl groups i.e., depalmitoylation is sufficient to reduce their affinity to the plasma membrane. Dissimilar to farnesylation, palmitoylation is reversible. This process can only occur at the Golgi, whereas the reverse process, depalmitoylation, is ubiquitous (Rocks *et al.*, 2010). However, typically, depalmitoylation occurs at the plasma membrane via an enzyme called acyl protein thioesterase 1 (APT1) (Duncan and Gilman, 1998; Rocks *et al.*, 2005). This cytosolic enzyme is first localised to the plasma membrane via self-palmitoylation before it cleaves the thioester bond between Ras and the palmitoyl group/s (Kong *et al.*, 2013). As a result, the Ras protein loses its avidity for the plasma membrane and undergoes retrograde trafficking to other membranes (Rocks *et al.*, 2005). Although, non-vesicular trafficking of depalmitoylated proteins can also occur (Goodwin *et al.*, 2005). These depalmitoylated Ras proteins can re-enter the Golgi, where repalmitoylation occurs and cycles these proteins back to the plasma membrane via vesicular trafficking (Choy *et al.*, 1999; Apolloni *et al.*, 2000; Goodwin *et al.*, 2005; Rocks *et al.*, 2005).

The constant cycling between palmitoylation and depalmitoylation allows for dynamic trafficking between the Golgi, plasma membrane and other subcellular membranes. The spill over of palmitoylated Ras can be redistributed to other subcellular membranes, however depalmitoylation occurs ubiquitously at a rapid rate (Rocks *et al.*, 2010). The kinetics of the palmitoylation/depalmitoylation cycle varies between the different isoforms due to the differences in the number of palmitoyl groups present. HRAS (<20 min) has a longer half-life than NRAS (< 5 min), since the additional palmitate group increases the duration of the membrane interaction (Rocks *et al.*, 2005). These differences could account in part for the isoform-specific activity (Rocks *et al.*, 2005)

In the cytosol, Ras isoforms can diffuse freely until they encounter a membrane by binding to chaperone proteins called phosphodiesterase-δ (PDEδ). This cytosolic GDI-like solubilising factor binds to farnesylated Ras and shields their hydrophobic farneyl tail from the aqueous environment, thus enhancing its diffusion around the cytoplasm (Chandra *et al.*, 2012; Schmick *et al.*, 2014). Only depalmitoylated HRAS and NRAS can bind PDEδ, since palmitoyl groups interfere with this interaction. Once bound, these Ras proteins can explore the cell interior at a faster rate, thereby increasing the encounter frequency with the Golgi, where it can become repalmitoylated and shuttled back to the plasma membrane (Chandra *et al.*, 2012). Trapping of KRAS at the perinuclear membranes can occur when the KRAS-PDEδ complex encounters GTP-bound Arf-like protein 2 (Arl2) (Ismail *et al.*, 2011). This G-protein binds to PDEδ via its allosteric site, inducing a conformational change that releases Ras from PDEδ at the perinuclear membranes, where it is shuttled off into recycling endosomes that re-localise Ras to the plasma membrane (Chandra *et al.*, 2012; Schmick *et al.*, 2014). This process aids the enrichment of KRAS at the plasma membrane, thus opposing leakage to other endomembranes (Schmick, Kraemer and Bastiaens, 2015).

1.4.2.2. Endoplasmic reticulum and Golgi

Both HRAS and NRAS have shown to signal from the ER and Golgi, as illustrated by the engagement of c-Raf to their oncogenic variants at these subcellular locations (Chiu *et al.*,

2002). In addition, endogenous palmitoylation-deficient HRAS responded to mitogens independently of endocytosis in both the ER and Golgi. Therefore, this type of activation does not depend on activated epidermal growth factor receptors (EGFRs) (Chiu *et al.*, 2002). The observed Ras activation in the Golgi was later suggested to be the result of depalmitoylated Ras-GTP, which had trafficked back to the Golgi from the plasma membrane either via a non-vesicular or vesicular route (Goodwin *et al.*, 2005; Rocks *et al.*, 2005). However, others have also suggested an alternative model, whereby *in situ* activation of HRAS and NRAS occur in the Golgi (Bivona *et al.*, 2003; Mor *et al.*, 2007). For example, T cell receptor (TCR) engagement alone resulted in the accumulation of palmitoylated Ras-GTP at the Golgi but not on the plasma membrane. However, redistribution of palmitoylated Ras-GTP to both the Golgi and plasma membrane occurs during co-stimulation of TCR and co-receptor, lymphocyte function-associated antigen 1 (LFA-1) (Mor *et al.*, 2007).

1.4.2.3. Mitochondria

All three Ras isoforms have shown to localise to the mitochondria. It appears that interaction with Bcl-2 directs their trafficking to the mitochondria. (Rebollo, Pérez-Sala and Martínez-A, 1999). A later study suggested that both KRAS and NRAS contributes to the normal morphology of mitochondria. Whereby, KRAS localised to the outer mitochondria membrane (OMM), whereas NRAS was able to localise to both the OMM and inner mitochondria membrane (IMM) independent of PTMs (Wolfman *et al.*, 2006). At the OMM, KRAS can interact with Bcl-XL, which eventually leads to apoptosis (Bivona *et al.*, 2006).

1.4.2.4. Endosomes

Studies have demonstrated that all Ras isoforms can localise on endosomes. In the clathrin-dependent route, KRAS is internalised from the plasma membrane via clathrin-coated pits and transported along an endosomal pathway, in which KRAS can become activated in late endosomes before being eventually targeted to lysosomes (Lu *et al.*, 2009). Similarly, receptor-mediated Ras activation at the plasma membrane can activate RIN1, which in turn

stimulates Rab5A-mediated internalisation of Ras and thus attenuates cell surface receptor signalling (Tall *et al.*, 2001).

Palmitoylated isoforms have shown to traffic via recycling endosomes along the exocytic pathway from the Golgi to the plasma membrane. (Misaki *et al.*, 2010). Whereby, the interaction with the endosomal membrane is stabilised by ubiquitination (Jura *et al.*, 2006). The detection of c-Raf interaction with HRAS at the endosomal membrane also indicates that in addition to Ras localisation, signalling can also occur on endosomes (Roy, Wyse and Hancock, 2002).

1.4.2.5. Nucleus

At current, there is a lack of substantial evidence for Ras localisation at the nucleus. One study detected HRAS in the nuclear extracts from mouse fibroblast cells. Its appearance in the nuclei fluctuated with the cell cycle, whereby peak HRAS detection occurred during S phase (Contente, Yeh and Friedman, 2011). In another study, confocal microscopy and subcellular fractionation of normal human dermal fibroblasts (NHDF) and HEK293 cells were used to demonstrate localisation of KRAS4B to the nucleolus, of which appeared to be dependent on its interaction with the nucleolar protein, nucleolin (Birchenall-Roberts *et al.*, 2006).

1.4.2.6. Subcellular signalling

Ras signalling has shown to differ between the subcellular locations, which also often results in different outcomes. An example being the involvement of Ras in thymic selection. Here, Ras signalling occurs at the plasma membrane during negative selection, but in the Golgi for positive selection where the kinetics are much slower (Daniels *et al.*, 2006). This also correlates with another study which reported that more transient and dynamic (mins) signalling occurs at the plasma membrane compared to endomembranes, where activity was longer (>1hr) and more sustained (Chiu *et al.*, 2002).

Interestingly, a proteomic study using green fluorescent protein (GFP)-tagged KRAS and NRAS chimeras that consisted of different organelle-specific targeting motifs at the C-

terminus revealed that Golgi-Ras and mitochondrial-Ras displayed similar signalling outputs in terms of phosphoproteome responses as plasma membrane-Ras, particularly in KRAS. Whereas, responses in ER/Golgi-Ras and endo-Ras were relatively low (Hernandez-Valladares and Prior, 2015).

More recently, HRAS signalling in different subcellular regions was investigated using multiple biochemical networks: the interactome, phosphoproteome and transcriptome. Results revealed a vast difference in these networks amongst the various locations: plasma membrane, ER and Golgi. Their main findings showed that the majority of phosphorylation events as a result of HRAS activation were detected at the plasma membrane, whereas on a transcriptional basis, most genes were regulated when Ras signalled from the ER (Santra *et al.*, 2019).

Studies exploring Ras subcellular localisation have often exhibit discrepancies, which could be due to the uses of different cell models and methodology. Many of these were conducted using subcellular fractionation, which could result in false positives (Choy *et al.*, 1999; Rebollo, Pérez-Sala and Martínez-A, 1999). In addition, many of the earlier studies lacked *in vivo* models. However, overall, it is evident that Ras localises to different subcellular locations, but the extent of their signalling is most likely context dependent.

1.5. RAS NANOCLUSTERS

1.5.1. Plasma membrane

The plasma membrane is a complex and dynamic platform. Whereby, the fluid mosaic model depicts a non-equilibrium mixture of lipids and proteins organised to form the phospholipid bilayer (Singer and Nicolson, 1972).

1.5.1.1. Composition

The four major phospholipids that constitute more than half of the lipid composition of the plasma membrane include: sphingomyelin (SPH), phosphatidylcholine (PC), phosphatidylethanolamine (PE) and phosphatidylserine (PS) (Spector and Yorek, 1985). SPH and PC make up the majority of the outer membrane, whereas the inner membrane is

predominantly composed of PE, PS and phosphatidylinositol (PI) (Connor *et al.*, 1992). Additionally, glycolipids and cholesterol are also present in the plasma membrane, where they contribute to 5-10% and 30-40% of the membrane lipid composition, respectively (Spector and Yorek, 1985; Warnock *et al.*, 1993).

1.5.1.2. Microdomains

Among the plasma membrane, these lipid species are non-uniformly distributed and can laterally segregate into functional microdomains. This is due to the interaction between the saturated lipids and sterols, which can either be in a liquid ordered (L_o) or disordered (L_d) phase (Kusumi and Sako, 1996; Silvius, Del Giudice and Lafleur, 1996; Filippov, Orädd and Lindblom, 2004). Both phases are fluid and therefore allow for motion, however L_o phase is dependent on cholesterol and enriched in saturated lipids whereas L_d phase is low in cholesterol (Filippov, Orädd and Lindblom, 2004). This results in the generation of an array of lipid microenvironments, which act like signalling platforms that differ in dynamics. These are crucial for biological processes as they facilitate signal transduction (Prior *et al.*, 2001).

The presence of the two phases allow for lipid rafts to be assembled. These have often been defined as non-ionic detergent resistant glycosphingolipid- and cholesterol-rich membrane compartments (Simons and Sampaio, 2011). However, this model has often been controversial due to the lack of technology with the spatial and temporal capacity to directly investigate these dynamic nanoscale structures (Munro, 2003). In addition to lipid rafts, other membrane microdomains exists such as caveolae, clathrin-coated pits and focal adhesions (Hooper, 1999).

1.5.2. Properties of Ras nanoclusters

Ras proteins predominantly localise on the inner plasma membrane. Here, they undergo constant diffusion with similar rates as free lipids and can assemble into transient distinct nanoscale domains (Murakoshi *et al.*, 2004; Tian *et al.*, 2007). The specific localisation of Ras nanoclusters on the plasma membrane is determined by the isoform as well as to their

nucleotide state, i.e. GDP- or GTP-bound (*Fig.1.5*) (Prior *et al.*, 2003). The combination of their unique membrane anchors and G-domain allow for the formation of these spatially distinct nanoclusters. Although, the minimal membrane anchor is also sufficient for nanoclustering albeit slightly different to full-length Ras (Zhou *et al.*, 2017). These Ras nanoclusters are fundamental platforms for effector binding and downstream activation. They function as switches that convert ligand input into high-fidelity Ras signal transduction via an analogue-digital-analogue circuit (Tian *et al.*, 2007).

At the plasma membrane, around 44% of the Ras proteins assemble into nanoclusters. These immobile nanodomains are highly dynamic with a turnover of 0.1-1 second, dependent on its nucleotide state. The diameter of a nanocluster can span from 12 to 20nm and can contain around 6-7 Ras proteins, which could exist as dimers, trimers and other high ordered oligomer (Murakoshi *et al.*, 2004; S.J. Plowman and Hancock, 2005). There have been suggestions that dimers exist as the intermediate structure on the plasma membrane, where it forms the foundation for further oligomerisation and thus nanocluster formation (Tian *et al.*, 2010; Sarkar-Banerjee *et al.*, 2017). The remaining 56% of Ras proteins diffuse freely as mobile monomers (S.J. Plowman and Hancock, 2005).

Earlier studies on Ras nanoclusters used relatively crude techniques. One methodology facilitated the use of non-ionic detergents at low temperatures to isolate the detergent-resistant membrane fraction, which supposedly contains lipid rafts that are rich in SPH, cholesterol and glycolipids. This essentially solubilised the majority of the plasma membrane with the exception of these tightly packed membrane components. However, this process could introduce artefacts by ultimately generating artificial domains, therefore this membrane model was not ideal for reflecting the *in vivo* state (Heerklotz, 2002). Similarly, the use of sucrose density-gradient ultracentrifugation also carried the risk of perturbing membrane structures (Song *et al.*, 1996). The evolution of high-resolution microscopy has been instrumental in providing more of an insight to the properties of Ras nanoclusters. For example, immunogold electron microscopy (EM) has been commonly used to visualise 2D

sheets of plasma membrane labelled with gold against Ras in order to analyse their spatial distribution (Parton and Hancock, 2004).

1.5.3. Regulators of Ras nanoclustering

The assembly of Ras nanoclusters depend on other factors. The three main components that are of importance include the actin cytoskeleton, lipid microenvironment as well as various regulatory proteins (Elad-Sfadia *et al.*, 2004; Plowman *et al.*, 2005; Belanis *et al.*, 2008; Zhou *et al.*, 2014). The proteome and lipidome microenvironments of Ras nanoclusters are generally not well-understood with only a few numbers of Ras nanocluster regulators having been identified to date. These include nucleolin, nucleophosmin (NPM), caveolin (CAV-1), galectin 1 (Gal-1), galectin 3 (Gal-3) and apoptosis-stimulating of p53 protein 2 (ASPP2).

1.5.3.1. Nucleolin and NPM

Both nucleolin and NPM are nucleolar proteins that can traffic to the cytoplasm. They are both involved in ribosome biogenesis and chromatin remodelling, however one study revealed that these nucleolar proteins were able to localise to the plasma membrane where they might be involved in the regulation of Ras nanoclustering (Inder *et al.*, 2009a; Abdelmohsen and Gorospe, 2012; Box *et al.*, 2016).

Using affinity chromatography, NPM and nucleolin were found to bind to the HVR of KRAS (Inder *et al.*, 2009a). Specifically, the N-terminal of NPM was responsible for binding the C-terminal polybasic domain of KRAS. This interaction was further enhanced when the farnesyl group was blocked, which coincided with later results whereby interaction between NPM/nucleolin and KRAS was seen at the plasma membrane, where the farnesyl group is hidden in the lipid bilayer. Lastly, EM immunogold labelling revealed that both NPM and nucleolin increased KRAS WT and KG12V expression at the plasma membrane, which corresponded to an increase in ERK activation. However, only NPM was able to increase KRAS nanoclustering (Inder *et al.*, 2009a). Although, the exact mechanism is unclear, the authors suggested that nucleolin might act like a chaperone protein and aid the

localisation of KRAS to the plasma membrane, whereas NPM interacts with KRAS at the plasma membrane in order to regulate their clustering (Inder, Hill and Hancock, 2010).

1.5.3.2. CAV-1

As mentioned previously, caveolae are a type of plasma membrane microdomain. These small invaginations enriched with cholesterol and glycosphingolipids span between 50-80nm (Örtegren *et al.*, 2004). One of the major components of caveolae is CAV1 (Rothberg *et al.*, 1992). Depletion of CAV1 affects the membrane lipid profile and organisation, in particular the glycosphingolipid and sphingolipid biosynthesis pathway become desregulated. Clustering of PS was also observed in CAV1-KD cells, suggesting that CAV1 modulates the organisation of PS at the plasma membrane. Similarly, CAV1 appears to play a role in the organisation of Ras nanoclusters. Whereby the effect of CAV1 depletion differed between the different isoforms, KRAS nanoclustering was enhanced whereas HRAS nanoclustering was reduced. Overall, it appears that CAV1 can alter Ras nanoclustering via its role in modulating the lipid composition of the plasma membrane (Ariotti *et al.*, 2014).

1.5.3.3. Gal-1 and Gal-3

Galectins are defined by their conserved β-galactoside binding sites located in their carbohydrate recognition domains. Similar to Ras, they are synthesised in the cytosol, where they can reside or alternatively traffic to the nucleus. Some galectins can also undergo a non-classical secretory pathway (Johannes, Jacob and Leffler, 2018). Two members of the galectin family, Gal-1 and Gal-3 have found to play important roles in the regulation of specific Ras nanoclusters (Belanis *et al.*, 2008; Shalom-Feuerstein *et al.*, 2008).

An initial study showed that Gal-1 was recruited to the plasma membrane as a result of HRAS activation (Paz *et al.*, 2001). Results revealed that Gal-1 was important for active HRAS nanoclustering, since decreased HG12V clustering was seen with reduced Gal-1 expression (Prior *et al.*, 2003). Using a combination of high-resolution microscopy techniques such as EM, fluorescence lifetime imaging-fluorescence resonance energy

transfer (FLIM-FRET) and biomolecular fluorescence complementation (BiFC) microscopy, it was demonstrated that Gal-1 is an important component of active HRAS nanoclusters. Interestingly, it appeared that Gal-1 aided the stabilisation of these structures and as a result, prolonged Raf activation. In addition, Gal-1 can also function as a chaperone protein that aids the transport of depalmitoylated HRAS to the Golgi (Belanis *et al.*, 2008). Previously, computational modelling showed that Gal-1 bound directly to the C-terminal farnesyl group of active HRAS via its hydrophobic prenyl-binding pocket (Rotblat *et al.*, 2004). However, this model has since been revised by another group, which showed that the interaction occurs indirectly via its association with the RBD of Ras effectors. This newer theory proposes that Gal-1 is recruited to Ras effectors like Raf as a result of Ras activation. It is suggested that the ability of Gal-1 to dimerise and therefore generate Gal-1 dimers could in turn stabilise the Raf dimers (Blaževitš *et al.*, 2016). Altogether, Gal-1 appears to be a HRAS-GTP specific nanocluster regulator.

Another important regulator of Ras nanoclustering is Gal-3 (Shalom-Feuerstein *et al.*, 2008). Active KRAS appears to recruit Gal-3 to the plasma membrane, whereby the hydrophobic pocket of the carbohydrate recognition domain of Gal-3 is responsible for binding the farnesyl group of KRAS. Here, Gal-3 acts as a scaffold for the formation of KRAS-GTP nanoclusters. Its fundamental role in KRAS biology was demonstrated by the reduction in downstream Ras signalling and transformative potential in the presence of impaired Gal-3 that harbour mutated prenyl binding pockets (Shalom-Feuerstein *et al.*, 2008).

1.5.3.4. ASPP2

Unlike other Ras nanocluster regulators mentioned, ASPP2 is the only regulator to date that has shown to enhance clustering of all Ras isoforms (Posada *et al.*, 2016). In oncogenic G12V mutants of KRAS, HRAS and NRAS, ASPP2 increased Ras effector signalling but with an outcome of promoting senescence and reducing mammosphere formation. Interestingly, ASPP2 was found to block Gal-1 regulated nanoclustering, thus diverting the cellular fate from pro-tumourigenic to anti-tumourigenic. Although it is unclear how ASPP2

interacts with Ras, it has been previously shown that ASPP2 can induce Raf dimerization and therefore the authors suggested that ASPP2 might act in a similar manner to Gal-1 in inducing the observed nanoclustering effects (Z. Wang *et al.*, 2013; Posada *et al.*, 2016).

1.5.4. Ras isoform-dependent nanoclusters

The microenvironment of isoform-specific nanoclusters differ and exhibit dissimilarities in their dependence for actin, lipid species and types of proteins for their assembly and localisation (Elad-Sfadia *et al.*, 2004; Plowman *et al.*, 2005; Belanis *et al.*, 2008; Zhou *et al.*, 2014).

1.5.4.1. KRAS

The KRAS membrane anchor comprises of basics residues that allow for electrostatic interactions with the anionic lipids amongst the plasma membrane. This is further complicated by the G-domain, which adopts different orientations with respect to the plasma membrane depending on whether its GDP or GTP-bound (Abankwa *et al.*, 2010). However, one study has shown that the membrane anchor does not simply engage the plasma membrane as a result of electrostatics. Instead, the membrane anchor encodes a complex lipid sorting code. The combination of the prenyl group along with the code determines the dynamic conformation of the membrane anchor and thus the residues involved in membrane binding, which ultimately defines the lipid preferences (Zhou *et al.*, 2017).

As a result of this lipid-sorting code, KRAS nanoclusters localise in PS enriched non-raft, i.e. cholesterol-independent, regions of the membrane (Prior *et al.*, 2003; Zhou *et al.*, 2014). These clusters are also dependent on another lipid species, phosphatidic acid (PA) and actin (Plowman *et al.*, 2005; Zhou *et al.*, 2014). In its GTP-bound form, KRAS also interacts with a regulatory protein, Gal-3, which promotes the activation of both Raf and PI3K (Elad-Sfadia *et al.*, 2004).

1.5.4.2. HRAS and NRAS

GDP-bound HRAS nanoclusters are cholesterol- and actin-dependent; in contrast to GTP-bound nanoclusters (Prior *et al.*, 2003; Zhou *et al.*, 2014). Regulatory protein, Gal-1 binds

to and stabilises GTP-bound HRAS nanoclusters. Additionally, Gal-1 diverts the activation towards the Raf pathway as opposed to the PI3K pathway (Belanis *et al.*, 2008).

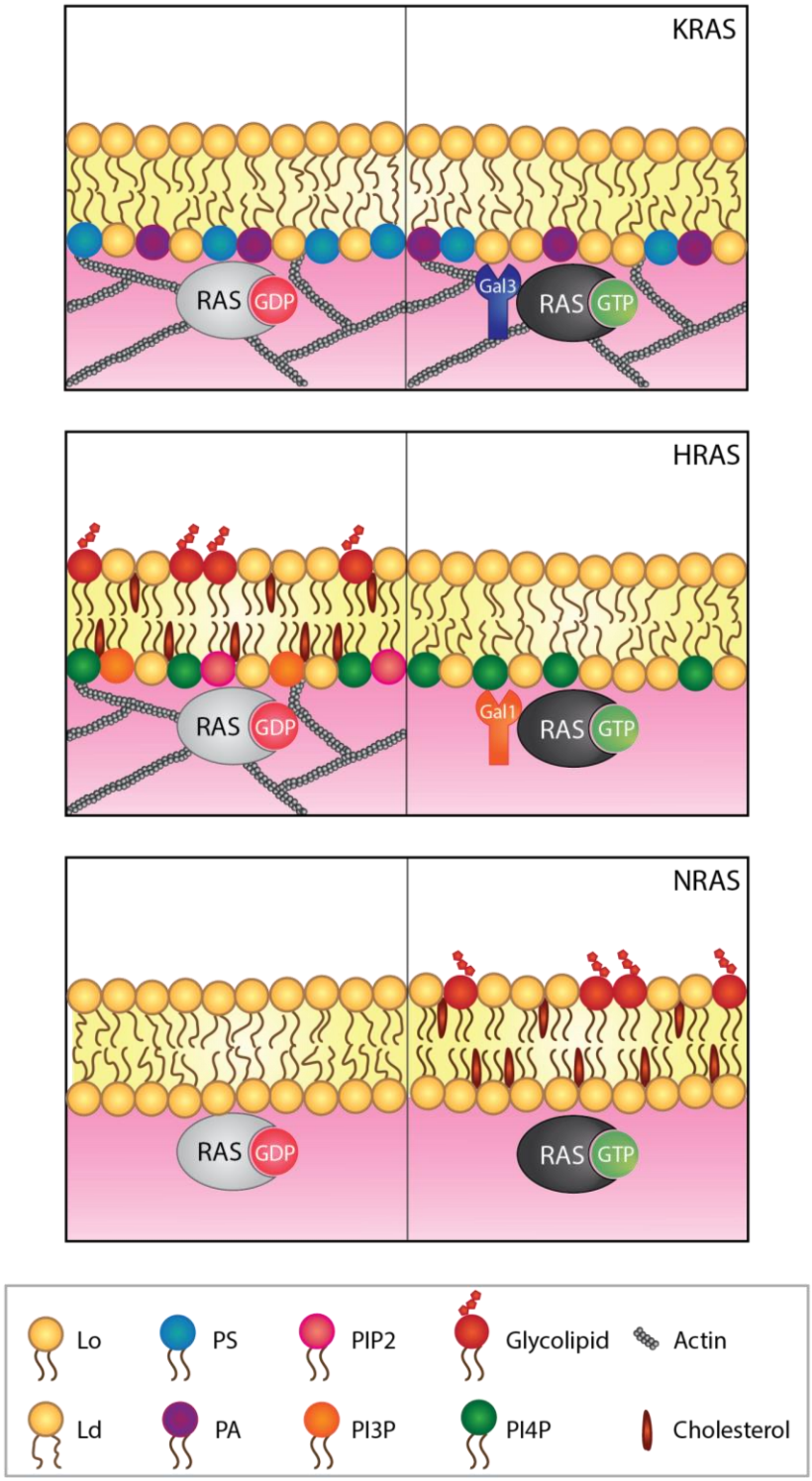

Figure 1.5| Schematic of isoform- and nucleotide-dependent Ras nanoclusters – Nanoclusters (represented by the Ras molecule) occupy either L_d non-lipid rafts or L_o lipid rafts, which vary in lipid composition, dependence on actin and regulatory proteins.

Phosphatidylinositol 4-phosphate (PI_4P) is present in both active and non-active HRAS nanoclusters, however PIP_2 and phosphatidylinositol 3-phosphate (PI_3P) are preferentially associated with the latter (Zhou *et al.*, 2014). For both KRAS and HRAS, the cluster lifetimes for inactive Ras (<0.1s) is significantly shorter than active Ras (0.5-1s) (Murakoshi *et al.*, 2004). However, this is unknown for NRAS, which has only been shown to be dependent on cholesterol when active (Roy *et al.*, 2005).

Altogether, it appears that KRAS nanoclusters localise within non-raft membranes irrespective of nucleotide state, whereas HRAS and NRAS nanoclusters laterally segregate between raft and non-raft regions depending on whether GDP- or GTP-bound (Prior *et al.*, 2003; Roy *et al.*, 2005). However, it is likely that this is an oversimplification of the nanocluster microenvironments. Nonetheless, further studies and higher resolution techniques will help unravel and provide a better insight into these complex nano-organisations.

1.6. ROLE IN CANCER

1.6.1. Oncogenic Ras

Normal cells require stimulatory signals to transition from a quiescent state to an activated proliferative state. However, in the presence of an oncogene, i.e. a gene with transformative potential, a cell can become self-sufficient and propagate its own cellular growth and proliferation (Hanahan and Weinberg, 2011). The Ras proto-oncogene can become oncogenic when an activating mutation occurs within its gene, leading to aberrant constitutive cellular signalling (Marshall, Hall and Weiss, 1982). These mutations are common and are responsible for the high number of Ras-related cancer cases (Mo, Coulson and Prior, 2018).

In cancer, majority of these Ras mutations occur at codons 12, 13 and 61, which are located within the P-loop and switch II region, respectively (Mo, Coulson and Prior, 2018). Normally, the amino acid at codons 12 and 13 is glycine, however mutations at these positions often result in a single base substitution. As a result, glycine can convert into

different amino acids (with the exception of proline) such as alanine (A), arginine (R) aspartate (D), cysteine (C), serine (S) or valine (V) (Muñoz-Maldonado, Zimmer and Medová, 2019). As a result of the mutation, GTP hydrolysis is hindered as it prevents the entry of the arginine finger of GAP into the GTPase site (Scheffzek *et al.*, 1997).

Similarly, mutations at glutamine-61 impairs both the GAP-mediated and intrinsic GTPase activity (Frech *et al.*, 1994). Other less common mutations such as A146 have shown to affect nucleotide binding by increasing GDP dissociation (Edkins *et al.*, 2006). These activating mutations result in Ras becoming resistant to GAPs and thus remaining GTP-bound. Therefore, cells harbouring the Ras mutation are no longer in a state of equilibrium and instead undergo uncontrolled cellular growth and proliferation, which often leads to transformation of the cell. However, not all of these activating mutations result in equal transformation (Der, Finkel and Cooper, 1986; Miller and Miller, 2012; Winters *et al.*, 2017).

1.6.2. Incidence of Ras mutations

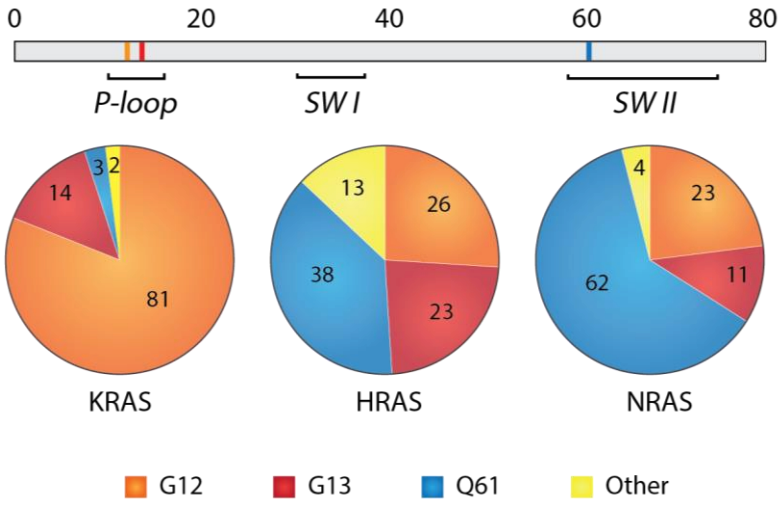

Figure 1.6| Ras mutations – Most common Ras mutations occur in the effector lobe at codons 12, 13 and 61. Percentage of each Ras mutation contributing to the total number of Ras-related cancer cases are shown for each Ras isoform (adapted from Mo, Coulson and Prior, 2018).

Ras mutations are present in around 17% of human cancer cases. Majority of these cases are linked to KRAS mutations (69%), which are predominantly associated with lung, pancreatic

and colorectal carcinomas. The next commonly mutated Ras isoform is NRAS (22%), with over half of these cases being associated to melanomas. The least frequently mutated Ras, HRAS is only present in around 9% of these cases and occur mainly in bladder cancers and head and neck cancers (Mo, Coulson and Prior, 2018).

Another complexity added to the incidences of Ras-associated cancers are the different types of Ras mutations (*Fig. 1.6*). Most of the KRAS mutations (81%) occur at G12, whereas in NRAS cases, a large proportion (62%) are linked to Q61. Differently, HRAS mutations display only a slight bias towards Q61 (38%) compared to G12 (26%), G13 (23%) and other mutations (13%) (Mo, Coulson and Prior, 2018).

1.7. RAS THERAPEUTICS

The high prevalence of Ras mutations in cancers makes it a desirable drug target for cancer therapy. Since its discovery, there have been many attempts at both direct and indirect inhibition, however, an FDA-approved anti-Ras therapy has yet to be discovered (Friedlaender *et al.*, 2020).

1.7.1. Direct inhibitors

At current, therapeutics for direct inhibition have focused on either targeting their activation state, effector binding or dimerization (Lacal and Aaronson, 1986; Spencer-Smith *et al.*, 2017; Friedlaender *et al.*, 2020).

1.7.1.1. KRAS G12C inhibitors

One of the more successful drug targets recognises a pocket in the switch II region of GDP-bound Ras and prevents Sos-GEF activity, as well as effector binding by disrupting both the switch I and II regions. This novel drug specifically binds to the mutant cysteine in KRAS G12C (accounts for 11% of KRAS-mutated cancers) and prevents it from being GTP-bound (Ostrem *et al.*, 2013). Currently, three KRAS G12C small molecule inhibitors are being tested in clinical trials: AMG-510, ARS-3248 and MRTX849, mainly in patients with non-small cell lung carcinoma (NSCLC) where this mutation is most commonly found (Canon *et al.*, 2019; Fell *et al.*, 2020; Friedlaender *et al.*, 2020). The promising findings from the

first clinical trial of AMG-510 revealed that the treatment either partially shrank the tumour or prevented progression of tumour growth in the 13 NSCLC participants (Friedlaender *et al.*, 2020).

Aside from blocking nucleotide exchange, other inhibitors have been used to target effector binding sites. One of the first Ras inhibitors to be discovered was Y13-259, a neutralising monoclonal antibody which blocked effector binding. However, this treatment failed to penetrate cells and therefore was not successful (Lacal and Aaronson, 1986). More promising drugs are being discovered using computational analyses of Ras structures, as these reveal potential ligand binding pockets that could block Ras-effector interactions (Tanaka, Williams and Rabbitts, 2007).

1.7.1.2. Inhibition of Ras dimerization

A more recent approach is to inhibit Ras dimerization, which is considered to be a prerequisite for nanocluster formation and subsequent Ras signalling. A monobody, NS1 has been used to target the α4-α5 region, the proposed dimerization site. Preliminary data reveals that the monobody was able to inhibit Ras dimerization and its consequential signalling. Transformation mediated by oncogenic Ras was abrogated both *in vitro* and *in vivo* (Spencer-Smith *et al.*, 2017).

1.7.2. Indirect inhibitors

The lack of deep binding pockets for small inhibitory molecules observed in structural studies revealed a possible caveat in using direct inhibition as a pharmacological treatment. Therefore, efforts have also been made towards indirect methods, which focus on targeting other factors such as membrane localisation; a fundamental process required for oncogenic Ras activity (Whyte *et al.*, 1997; Zhou *et al.*, 2012; Cho, Park and Hancock, 2013; van der Hoeven *et al.*, 2013).

1.7.2.1. Farnesyltransferase inhibitors

Some of the first attempts at preventing Ras association with the membrane centred on targeting enzymes required for PTMs of the Ras CAAX domain, in particular the inhibition

of FTases (FTIs). However, results soon revealed that KRAS and NRAS were unaffected by FTIs, due to an alternative lipidation process via geranylgeranyltransferases (Whyte *et al.*, 1997). On the other hand, HRAS appears to be dependent on FTases and therefore, FTIs could be beneficial in HRAS-associated cancers. However, its specificity for other substrates may also cause potential toxicity (Cohen-Jonathan *et al.*, 2009).

1.7.2.2. PDEδ inhibitor

Another inhibitor tested was Deltarasin. This drug targets PDEδ, which binds the farnesylated tail of KRAS and is required for efficient membrane localisation (Chandra *et al.*, 2012; Zimmermann *et al.*, 2013). Disruption of this interaction led to KRAS mis-localisation and a reduction in activity (Zimmermann *et al.*, 2013). However, its specificity for KRAS has been questioned as it appears to regulate other Ras isoforms as well as other farnesylated proteins (Chandra *et al.*, 2012).

1.7.2.3. Pharmacological agents against Ras nanoclustering

Other attempts are based on perturbing Ras nanoclustering. An L-type calcium channel blocker called Fendiline has shown to specifically reduce KRAS nanoclustering by redistributing KRAS to other cellular components. However, its actual mechanism is unknown but does not appears to be related to its known role of calcium channel inhibition (van der Hoeven *et al.*, 2013).

Staurosporines and nonsteroidal anti-inflammatory drugs (NSAIDs) have shown to alter the concentration of PS and cholesterol within the plasma membrane, respectively (Zhou *et al.*, 2012; Cho, Park and Hancock, 2013). It appears that staurosporines inhibit KRAS nanoclustering specifically by redistributing PS from the plasma membrane to endomembranes, but the underlying mechanism is not linked to its the role in terms of PKC inhibition (Cho, Park and Hancock, 2013). Whereas NSAIDs like indomethacin perturb lateral segregation between cholesterol-dependent and independent regions in HRAS and NRAS, (Zhou *et al.*, 2012).

1.8. RATIONALE

1.8.1. Isoform-specific differences

It has become increasingly evident that Ras isoforms are not functionally redundant, differing in aspects ranging from localisation to human disease (Prior *et al.*, 2003; Tidyman and Rauen, 2016; Mo, Coulson and Prior, 2018). Ras isoforms are similar in sequence amongst the G-domain region, however main differences occur at the C-terminal which is responsible for membrane localisation. As mentioned previously, these Ras isoforms assemble into spatially distinct nanoscale domains at the plasma membrane, where downstream signalling occur. The occupancy of different locations within the plasma membrane exposes each Ras isoform to a unique combination of lipids and proteins, where the available pool of effectors could differ for each Ras isoform (Zhou and Hancock, 2015).

Previously reported, different Ras isoforms exhibit differences in Ras signalling, whereby KRAS and HRAS are coupled to more potent activation of Raf and PI3K, respectively (Yan *et al.*, 1998). Whereby, this isoform-specific signalling could be due to the orientation of the effector-binding domain (Abankwa *et al.*, 2010). However, more recently, a large-scale short interfering RNA (siRNA) screen highlighted that effector dependence differed according to the cell line investigated (Yuan *et al.*, 2018). It has also been suggested that the use of ectopic overexpression could also distort the signalling outcomes, since the signalling pattern of endogenously expressed Ras differed from those overexpressed (Hood *et al.*, 2019). Although, Ras effector signalling appears to be context-dependent, the variation in signalling between the Ras isoforms cannot be disputed due to the observed functional differences. For example, in mice colonic epithelium, mutant HRAS hindered growth of endodermal progenitors, whereas mutant KRAS stimulated their proliferation (Quinlan *et al.*, 2008).

Another important line of evidence for isoform differences come from clinical studies. Each Ras isoform is biased towards certain cancer types as well as different RASopathies, a group of developmental syndromes caused by germline mutations of Ras or Ras related proteins.

Each RASopathy present unique features in addition to a set of morphological and behavioural traits shared amongst these rare genetic disorders (Tidyman and Rauen, 2016). Both KRAS and NRAS mutations have been found in Noonan syndrome (Schubbert *et al.*, 2006; Cirstea *et al.*, 2010), whereas only HRAS and KRAS mutations are present in Costello (CS) and cardiofaciocutaneous (CFC) syndromes, respectively (Aoki *et al.*, 2005; Niihori *et al.*, 2006). Aside from the common dysmorphic craniofacial features and learning difficulties, CS patients also present with a likelihood of developing malignancies like rhabdomyosarcomas and neuroblastomas (Gripp *et al.*, 2002). Differently, CFC individuals are characterised by the presence of distinct pigmented nevi (Siegel *et al.*, 2011). The manifestation of these different clinical features in association with each Ras isoform presents a clear indication of their fundamental differences.

1.8.2. Project Aims

Ras mutations are responsible for millions of new cancer cases each year (Mo, Coulson and Prior, 2018). The search for a therapeutic drug to target Ras has been longsome and puzzling, which highlights the importance of delving into Ras biology in order to identify new approaches for Ras inhibition. One of the fundamental bases for Ras function stems from its localisation; nanoclustering is required for optimal Ras signalling.

The proteome microenvironment of Ras nanoclusters is not well understood, therefore, identification of novel proteins within Ras nanoclusters that could be vital for its regulation and/or assembly could be of therapeutic interest (*Fig.1.7*). More importantly, distinguishing the differences between the Ras isoform nanoclusters may identify isoform-specific proteins, that could be candidate targets for cancers associated with a certain Ras isoform.

Thus, the project aims are as follows:

1. To investigate the protein microenvironment of all three Ras isoforms in both their inactive and active (GTP-bound and G12V mutant) state.
2. To produce a shortlist of proteins that might play a role in Ras nanoclustering.

3. To explore its relationship with Ras and whether it has an effect on Ras nanoclustering.

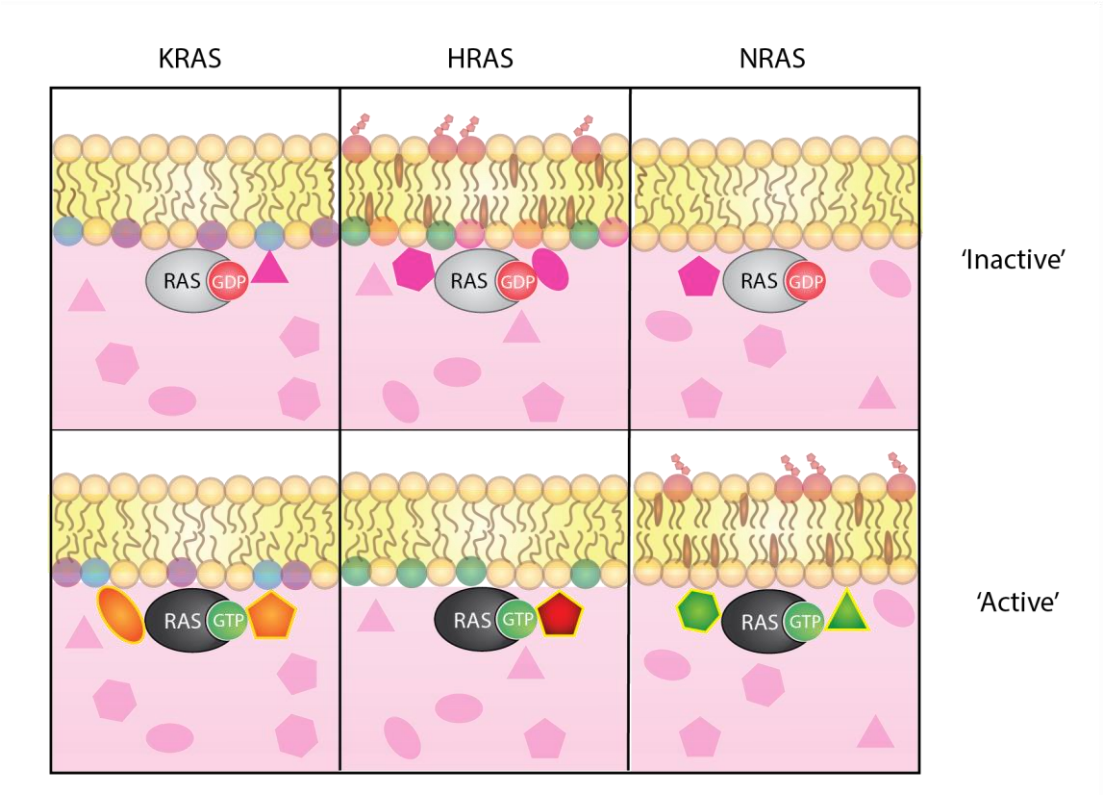

Figure 1.7| Identification of novel Ras nanocluster regulators – Comparison of the protein microenvironments of inactive and active KRAS, HRAS and NRAS isoforms in order to identify potential isoform-specific nanoclustering regulators.

CHAPTER TWO

Material and Methods

2.1. CELL BIOLOGY

All reagents were purchased from Thermo Fisher Scientific unless stated otherwise.

2.1.1. Cell culture

For this project, human cervix carcinoma cell lines, HeLa S3 (ATCC) were used due to their high transfection efficiency. Cells were cultured in Dulbecco's Modified Eagle's Medium (DMEM) with GlutaMAX (31966021) supplemented with 10% fetal bovine serum (FBS (10270) in a humidified incubator maintained at 37°C and 5% CO_2. Every 48-72 hours, cells were washed with phosphate buffered saline (PBS (14200067)) followed by incubation with 0.5% Trypsin-EDTA (15400054) before being passaged at a 1:3 – 1:7 ratio.

2.1.2. DNA transfection

GeneJuice Transfection Reagent (Merck, 70967) was used for transient expression of Ras and annexins in HeLa S3 cells. Seeding density varied for experiment type. For western blots, $3x10^5$ cells/well were seeded into a 6-well plate. Whereas $1.1x10^7$ cells were seeded equally between two $15cm^2$ plate for mass spectrometry. Following overnight incubation, culture medium was replaced with fresh media. Preparation of transfection reagent consisted of adding 6/45µl GeneJuice into 0.1/1ml Opti-MEM (51985026) and incubated for 5 minutes at room temperature. Then 1/15 µg of DNA was mixed into the Opti-MEM solution and left at room temperature for a further 20 minutes. The resulting solution was gently added to the cells and incubated at 37°C for 24 hours before being harvested.

2.1.3. siRNA knockdown

For siRNA knockdown experiments of annexin 2 and 6, ON-TARGETplus Human SMARTpool (5 nmol) of ANXA2 (Dharmacon, L-010741-00- 0005), ANXA6 (Dharmacon, L-011210-00- 0005) and non-targeting control (NT1, Dharmacon, D-001810-10-05) siRNA were used. These were resuspended with 1x siRNA buffer to a stock concentration of 20µM and stored at -20°C before use. The previous day, $1.5x10^5$ cells/well were seeded into a 6-well plate. Then two solutions were prepared for the knockdown, which were initially incubated separately at room temperature for 5 minutes. The first solution consisted of 2µl

siRNA and 83µl Opti-MEM and the second solution was made up of 2µl RNAiMax and 83µl Opti-MEM. After the incubation, the solutions were combined and stored at room temperature for 20 minutes. Media was aspirated from the cells and replaced with 830µl fresh media for each well (6-well plate) before the addition of the siRNA reaction. After 6 hours, media was exchanged for fresh media. Cells were lysed after 48-72 hours.

2.1.4. Cell treatment

Stimulated and serum-starved samples were washed twice with PBS and replaced with serum-free DMEM media post-transfection (24 hours). Cells were starved for 5 hours. For stimulated samples, following serum-starvation, media was exchanged for fresh media supplemented with 20% FBS for 5 minutes before cell lysis.

2.2. MOLECULAR BIOLOGY

All reagents unless otherwise stated were purchased from New England Biolabs.

2.2.1. Primers

Primers (Eurofins Genomics) were designed to amplify the FLAG-tagged APEX2 inserts from the template: APEX2-Actin in pEGFP. In addition to the insert, a restriction endonuclease (RE) site, NheI was introduced to the N-terminus as well as a linker region and another RE site, BglII to the C-terminus.

Name	Sequence (5' – 3')	Length	Tm	GC content
N_APX2_SM	TCCGCTAGCGCTACCGGTCGCCACCATGGACTACAAGGAT	40	>75°C	60.0%
C1_APX2_SM	TCGAGATCTGAGTCCGGAGCCCGAGCCCGAGGTCGAGCCCGAGCCCTTGGCGTCGGCAAATCC	63	>75°C	68.3%
C2_APX2_SM	TCGAGATCTGGAGTCCGGAGCCCGAGCCCGAGGTCGAGCCCGAGCCCTTGGCGTCGGCAAATCC	64	>75°C	68.8%
C3_APX2_SM	TCGAGATCTGAGAGTCCGGAGCCCGAGCCCGAGGTCGAGCCCGAGCCCTTGGCGTCGGCAAATCC	65	>75°C	67.7%

Table 2.1| Summary of primers used for APEX2 cloning.

2.2.2. Plasmids

Plasmids	Company	Catalog no.
EGFP-KRAS WT	As previously described (Prior *et al.*, 2001)	
EGFP-KRAS G12V	As previously described (Prior *et al.*, 2001)	
EGFP-HRAS WT	As previously described (Prior *et al.*, 2001)	
EGFP-HRAS G12V	As previously described (Prior *et al.*, 2001)	
EGFP-NRAS WT	As previously described (Aran and Prior, 2013)	
EGFP-NRAS G12V	As previously described (Aran and Prior, 2013)	
GFP-tK	As previously described (Prior *et al.*, 2001)	
GFP-tH	As previously described (Prior *et al.*, 2001)	
FLAG-APEX2-KRAS WT	Made in house	
FLAG-APEX2-HRAS WT	Made in house	
FLAG-APEX2-NRAS WT	Made in house	
FLAG-APEX2-KG12V	Made in house	
FLAG-APEX2-HG12V	Made in house	
FLAG-APEX2-NG12V	Made in house	
FLAG-APEX2-tK	Made in house	
FLAG-APEX2-tH	Made in house	
FLAG-APEX2	Made in house	
mCherry- KRAS WT	Gift from Dr Luke Chamberlain (Uni. Of Strathclyde)	
mCherry- KG12V	Gift from Dr Luke Chamberlain (Uni. Of Strathclyde)	
mCherry- HRAS WT	Gift from Dr Luke Chamberlain (Uni. Of Strathclyde)	
mCherry- HG12V	Gift from Dr Luke Chamberlain (Uni. Of Strathclyde)	
mCherry- NRAS WT	Gift from Dr Luke Chamberlain (Uni. Of Strathclyde)	
mCherry- NG12V	Gift from Dr Luke Chamberlain (Uni. Of Strathclyde)	
APEX2-Actin in pEGFP	Addgene	66172
pcDNA3.1(+)-N-eGFP-annexin 2	GenScript	Ohu13706C
pcDNA3.1(+)-N-eGFP-annexin 6	GenScript	Ohu00168C
pcDNA3.1(+)-N-eGFP-annexin A7	GenScript	Ohu02797C
pEGFP-C1	Clontech	(Discontinued)
pEGFP-C2	Clontech	6083-1
pEGFP-C3	Clontech	6082-1

Table 2.2| List of plasmids.

2.2.3. Polymerase Chain Reaction

The primers as listed in Table 2.1 were reconstituted with water to a stock concentration of 100pmol/µl. This was further diluted to 20mM using water for use in the polymerase chain reaction (PCR). Each PCR sample consisted of the following 41.5µl water, 5µl dNTPs (25mM), 1µl Pfu Ultra II hot start polymerase, 0.5µl forward primer (20mM), 0.5µl reverse primer and 1µl DNA template (50ng/µl).

For the amplification of FLAG-tagged APEX2 that were capable of insertion into the three pEGFP vectors: C1, C2 and C3, three different inserts were required. Therefore, three different PCRs were set up using the N-APX2_SM as the forward primer and either C1_APX1_SM, C2_APX2_SM or C3_APX2_SM as the reverse primer. Actin-APEX2 in pEGFP was used as the template DNA for the amplification of APEX2 and water was used as a control template. The reactions were placed in a thermal cycler where the samples were heated to 95°C for 2 minutes before undergoing 35 sequential cycles of 30 seconds at 95°C, 30 seconds at 55°C and 30 seconds at 72°C. Followed by 5 minutes at 72°C. The resulting PCR products were visualised using gel electrophoresis and the correct sized gel bands were excised for DNA extraction.

2.2.4. Agarose gel electrophoresis

0.8-1.2% agarose gels were prepared by heating together UltraPure™ Agarose (Invitrogen, 15510-019) and 1X TAE (diluted from 50X TAE (National Diagnostics, EC-872)). Once dissolved, ethidium bromide was added to the solution at a final concentration of 0.5µg/ml, then poured into gel tanks to set at room temperature. Samples were prepared using 6X gel loading dye (B7021S) and ran alongside Quick-Load 1kb plus DNA Ladder (N0550) and/or 100bp DNA ladder (B7025). Typically, the gels were ran in 1X TBE running buffer (diluted from 10X TBE (National Diagnostic, EC-860)) for 50-80 minutes at 120V.

2.2.5. Ligation

DNA was eluted from gel pieces containing either vector or insert DNA using the QIAquick Gel Extraction Kit (Qiagen, 28115). Resulting DNA was mixed in a 3:1 ratio of insert to

vector and adjusted to 9µl with nuclease-free H_2O, then incubated with 10µl Quick Ligase Reaction buffer and 1µl Quick Ligase from the Quick Ligation Kit (M2220) for 5 minutes at room temperature. Then stored on ice before being transformed into competent cells.

2.2.6. TOPO PCR cloning

To generate subcloning vector intermediates containing the APEX2 inserts, the Zero Blunt™ TOPO PCR kit (ThermoFisher Scientific, K283020) was used. Firstly, PCR amplification products were resolved using gel electrophoresis and visualised under UV light for excision. DNA was extracted from the excised gel pieces using the QIAquick Gel Extraction Kit. Resulting blunt-end PCR products were directly inserted into TOPO vector via incubation of both these components with a salt solution for 30 minutes at room temperature. Transformation of these cloning vectors into TOPO10 cells were performed as described in the next subsection.

2.2.7. Bacterial transformation

Ligation products were transformed into either TOPO10 or DH5α cells by a succession of incubations at different temperatures: 20 minutes on ice followed by heat shock at 42°C for 30 seconds and another 2 minutes on ice. The resulting cells were incubated with SOC medium for 1 hour at 37°C in a shaker of 225rpm to encourage bacterial growth. This was spread on LB agar plates containing the relevant antibiotic (100µg/ml ampicillin or 50µg/ml kanamycin) and incubated overnight at 37°C. Colonies were selected and amplified in LB media supplemented with appropriate antibiotic at 37°C with gentle shaking (225rpm) overnight. The bacterial culture was spun down at 15,000g for 10 minutes and plasmid DNA was extracted using the QIAprep Spin Miniprep kit (Qiagen, 27104) following manufacturer's instructions. The resulting plasmid DNA was validated via RE test digests and sent for sequencing (MRC PPU DNA Sequencing and Services, Dundee, Scotland).

Amplification of plasmid DNA was performed using the QIAGEN Plasmid Maxi Kit (Qiagen, 12163) following confirmation of the DNA sequence. In addition, glycerol stocks were made by pelleting 5ml overnight bacterial culture and resuspending in 2ml of 40%

glycerol in LB broth. This was stored at -80°C.

2.2.8. Restriction endonuclease digest

NheI-HF (R3131) and BglII (R1044) enzymes were used to do a test digest of the TOPO10-APEX2 plasmids to check for the FLAG tagged-APEX2 insert. Once confirmed, the same enzymes were used to digest TOPO10-APEX2-C1/C2/C3 and the following vectors: pEGFP-C1, -C2. -C3, -truncated minimal membrane anchors of KRAS (tK) and HRAS (tH). Each RE digest reaction consisted of 2µg DNA, 1µl NheI-HF, 1µl BglII, 4µl NEBuffer™ 2.1 (B7202S) and made up to a total volume of 50µl with dH_2O. The reaction was incubated for 15 hours at 37°C, then in 80°C for 2 minutes. Test digests were scaled to 10µl volume reactions. Resulting products were validated using gel electrophoresis. Gel bands for the APEX2 inserts and EGFP-absent vectors were excised, then DNA was extracted from these gel pieces. The resulting APEX2 inserts was ligated to each vector accordingly to generate APEX2-C1, APEX2-C2, APEX2-C3, APEX2-tK and APEX2-tH.

For the generation of APEX2-KRAS WT, -KG12V, -HRAS WT and -HG12V, SacI-HF and KpnI were used to digest APEX2-C1/C2/C3 and EGFP-KRAS WT/KG12V/HRAS WT/HG12V in NEBuffer™ 2.1 (B7202S) for 4 hours at 37°C, followed by 65°C for 20 minutes. Similarly, APEX2-NRAS WT and -NG12V were cloned using BamHI-HF and SacI-HF. These REs were incubated with either APEX2-C3 or EGFP-NRAS WT/NG12V for 4 hours at 37°C in CutSmart® Buffer (B7204S), then at 65°C for a further 20 minutes. Digested products were ran on an agarose gel and DNA was extracted from the corresponding gel band. The final products were formed via ligation of the APEX2 insert with the respective Ras vector. Lastly, these constructs were verified by DNA sequencing.

2.3. PROTEIN BIOCHEMISTRY

2.3.1. Reagents

Reagent	Company	Catalog No.
Biotin	Sigma-Aldrich	B4501
Biotin phenol	Iris-Biotech	41994-02-9

Bovine Serum Albumin	First Link	41-10-410
Bromophenol blue	Sigma-Aldrich	B0126
DTT	Melford biolaboratories	20291
Glycerol	Sigma-Aldrich	G6279
Glycine	Melford biolaboratories	G0709
Hydrochloric acid	Sigma-Aldrich	320331
Hydrogen Peroxide, 30%	Sigma-Aldrich	H1009
Methanol	Thermo Fisher Scientific	M/4000/PC17
Nonidet P-40 substitute	Fluka	74385
PMSF	G-Biosciences	786-055
Potassium chloride	Sigma-Aldrich	P5405
Protease inhibitor cocktail	Sigma-Aldrich	P8340
Sodium Ascorbate	Sigma-Aldrich	A-7631
Sodium Azide	Sigma-Aldrich	13412
Sodium Carbonate	Sigma-Aldrich	S2127
Sodium Chloride	Thermo Fisher Scientific	S/3160/60
Sodium deoxycholate	Sigma-Aldrich	30970
Sodium dodecyl sulfate	Sigma-Aldrich	L4509
Tris Base	Thermo Fisher Scientific	BP152-1
Trolox	Sigma-Aldrich	238813-25G
Tween	GeneFlow	EC-607
Urea	Sigma-Aldrich	U1363

Table 2.3| List of reagents used for protein biochemistry experiments.

2.3.2. Cell lysis

For non-APEX2 experiments, cells were placed on ice and washed twice in ice cold PBS to remove any traces of media. Then NP40 lysis buffer (0.5% Nonidet P-40 substitute (w/v), 25mM Tris (pH 7.5), 100mM NaCl, 50mM NaF, milliQ water) was added directly to the cells and incubated for 15 minutes with gentle rocking. Lysates were collected and impurities were pelleted by centrifugation (15,000g, 10 minutes, 4°C). Supernatant was collected and protein concentration was measured using the Pierce™ BCA Protein Assay Kit (Thermo Fisher Scientific, 23225).

2.3.3. Proximity labelling

Preliminary experiments using RIPA lysis buffer (50mM Tris, 150mM NaCl, 1% Triton X-100, 0.1% SDS, 0.5% sodium deoxycholate in d H_2O adjusted to pH 7.5) appeared to result in the contamination of genomic DNA on western blots, therefore NP40 lysis buffer was used instead. The NP40 lysis buffer was modified for the APEX2 experiments by supplementation with 1:250 mammalian protease inhibitor (MPI), 1mM PMSF, 10mM sodium ascorbate, 10mM sodium azide and 5mM trolox.

Previous to cell lysis, cell media was replaced with prewarmed DMEM supplemented with biotin phenol (BP, final concentration: 500µM) for 30 minutes (37°C, 5% CO_2) at 24 hours post-transfection. Then hydrogen peroxide (H_2O_2) was added to each well (final concentration – 1mM) for 15-240 seconds. For control samples, no H_2O_2 was added. Media from each well was immediately aspirated after specified incubation period of H_2O_2 and washed three times with quencher solution (10mM sodium ascorbate, 10mM sodium azide, 5mM trolox in PBS). Then NP40 lysis buffer containing MPI and quenchers were added to the cells for 15 minutes with gentle rocking at room temperature (due to the precipitation of trolox if performed on ice). Cell lysates were collected and centrifuged at 15,000g for 10 minutes at 4°C. Supernatant was quantified using the Pierce™ 660nm protein assay then stored at -20°C before use.

For the enrichment of biotinylated proteins, an initial small-scale experiment was performed using 360µg lysate to 20/30/40µl streptavidin beads. This was later scaled up for mass spectrometry experiments, where 2.5mg lysate was incubated with prewashed streptavidin beads (total volume – 2.2ml) for 1 hour on a rotator at room temperature. Here, the sample was divided into two Lo-bind tubes, i.e., 1.25mg lysate with 104.2µl streptavidin beads. Samples were pelleted on a magnetic rack and flowthrough was removed. The remaining beads were washed with a series of buffers in the following order: twice with RIPA buffer (10mM Tris-HCl (pH 7.5), 150mM NaCl, 1% Triton X100, 0.1% SDS (ThermoFisher Scientific), 1% Sodium deoxycholate, milliQ water), once with 1M KCL, 0.1M Na_2CO_3,

5M urea in 10mM Tris-HCl and twice again with RIPA buffer. At each wash step, the beads were vortexed, placed on the rotator for 5 minutes, then pelleted on a magnetic rack.

Proteins were eluted from the beads by boiling the beads with 3X sample buffer (diluted from 6X sample buffer, 276mM Tris-HCl (pH 6.8), 7.9% SDS, 7.3% DTT, 28.4% glycerol, 0.009% bromophenol blue, dH_2O) supplemented with 2mM biotin and 20mM DTT for 10 minutes at 110°C. Samples were vortexed, cooled on ice and then centrifuged at 13,000g at room temperature. The samples were placed back on to the magnetic rack in order to separate the eluate and streptavidin beads. Collected eluate was kept at -20°C before use.

2.3.4. Immunoprecipitation

2.3.4.1. FLAG IP

Immunoprecipitation (IP) of FLAG-tagged protein complexes were achieved using anti-FLAG M2 Affinity Gel (Sigma, A2220), which consists of 4% agarose beads covalently attached to mouse monoclonal anti-FLAG antibody. These beads were prepared via three sequential washes with YP-IP buffer (0.1% NP40 (v/w), 25mM Tris (pH 7.5), 150mM NaCl, dH_2O) at 6000g for 30 seconds per wash.

Cells transfected with FLAG-tagged APEX2-Ras were lysed with NP40 (as mentioned above in section 2.3.2). 0.8mg of lysate was made up to a volume of 800µl using NP40 lysis buffer then incubated with 40µl anti-FLAG beads for 2 hours at 4°C on a rotator (15rpm). Beads were pelleted at 6000g for 2 minutes and supernatant was stored at -20°C. Then beads were washed four times with YP-IP wash buffer. FLAG-tagged proteins were eluted from the beads by boiling the beads with 20µl 2X sample buffer (125mM Tris-HCl (pH 6.8), 4% SDS, 20% glycerol, 0.004% bromophenol blue, dH_2O) at 95°C. Samples were centrifuged at 8200g for 30 seconds, allowing separation of FLAG-tagged proteins from the anti-FLAG beads. Supernatant was stored at -20°C until use.

2.3.4.2. GFP IP

20µl of GFP-NanoTrap beads (made in house) were washed three times with dH_2O at

15,000g for 30 seconds per wash. Once prepared, 1mg/ml lysate of GFP-tagged annexin transfected cells was added to the beads and spun at 15rpm for 30 minutes at 4°C. Following the incubation, beads were pelleted at 15,000g for 30 seconds. Then washed three times with ice cold YP-IP buffer and once with 10mM Tris pH (pH 7.5). GFP-tagged proteins were eluted by boiling samples with 20µl of 2X sample buffer at 95°C for 5 minutes.

2.3.5. SDS-PAGE

Protein samples were prepared for loading on to precast NuPAGE 4-12% Bis-Tris gels (Thermo Fisher Scientific) with 5X sample buffer, then heated to 95°C for 5 minutes. The precast gel was placed into a NuPAGE gel tank and submerged with 1X NuPAGE MOPS SDS running buffer (diluted from 20X (Thermo Fisher Scientific, NP000102).

Typically, 15-20µg of protein was loaded into each well, whereas for pulldowns, the total eluate volume was loaded. Molecular weight was measured using the Full range Amersham™ ECL™ Rainbow™ Marker (Sigma-Aldrich, RPN800E) alongside the samples. The protein gels were ran at an initial voltage of 100V until samples had passed from the wells into the gel, then raised to 180V for the remaining 50-60 minutes.

2.3.6. Western blotting

Proteins from the polyacrylamide gel were transferred on to Amersham™ Protran® Western blotting nitrocellulose membranes (Sigma-Aldrich, GE10600002) using a Royal Genie Blotter (Idea Scientific, 4020) containing transfer buffer (25mM Tris-Glycine, 20% methanol). This was ran at a constant 0.8A (~30V) for 1 hour and 10 minutes. The efficiency of the transfer and quality of the samples were assessed by staining the nitrocellulose membrane with Ponceau-S stain (Sigma-Aldrich, P7170). This stain was removed with multiple washes using H_2O before subsequent blocking and incubation steps.

All the following incubations were done with gentle agitation. The nitrocellulose membrane was placed in block, either 5% bovine serum albumin (BSA) or 5% milk (Marvel) in Tris-buffered saline with Tween (TBST (10mM Tris, 150mM NaCl, 0.1% Tween 20, pH 7.4)) for 1 hour at room temperature. Then replaced with appropriate primary antibody (in block)

overnight at 4°C (see *Table 2.4*). The primary antibody was removed after incubation and any unbound antibody was washed off using three 5-minute TBST washes. Then incubated with the respective IRDye conjugate-secondary antibodies (LI-COR BioSciences) for 1 hour at room temperature. Lastly, the membrane was washed again twice in TBST (5-minutes per wash) and once with TBS (10mM Tris, 150mM NaCl, pH 7.4). The membrane was visualised on the LI-COR Odyssey Imaging System.

2.3.7. Antibodies

Antibody	Company	Catalog No.	Dilution
Anti-Pan Ras *(rabbit)*	Abcam	ab52939	1/5000 in 5% BSA
Anti-FLAG *(rabbit)*	Sigma-Aldrich	F4725	1:1000 in 5% BSA
Anti-NRAS *(mouse)*	Cell Signalling	F155	1/200 in 5% BSA
Anti-ERK *(rabbit)*	Cell Signalling	4695	1/1000 in 5% BSA
Anti-B-Raf *(mouse)*	Cell Signalling	L12G7	1/1000 in 5% BSA
Anti-PI3K-p110α *(rabbit)*	Cell Signalling	C73F8	1/1000 in 5% BSA
Anti-pERK 1/2 *(rabbit)*	Cell Signalling	4370S	1/2000 in 5% milk
Anti-pMEK 1/2 *(rabbit)*	Cell Signalling	9154S	1/1000 in 5% milk
Anti-pAKT *(rabbit)*	Cell Signalling	4060S	1/2000 in 5% milk
Anti-beta actin *(mouse)*	Abcam	ab6276	1/10000 in 5% BSA
Anti-annexin A1 *(rabbit)*	Abcam	ab214486	1/2000 in 5% BSA
Anti-annexin A2 (*rabbit*)	Abcam	ab41803	1/5000 in 5% BSA/milk
Anti-annexin A5 *(mouse)*	Abcam	ab54775	1/500 in 5% BSA
Anti-annexin A6 *(rabbit)*	Abcam	ab201024	1/1000 in 5% BSA/milk
Anti-annexin A7 *(rabbit)*	Abcam	ab197586	1/2000 in 5% BSA/milk
Anti-annexin A11 *(rabbit)*	Abcam	ab137424	1/2000 in 5% BSA
Anti-septin 2 *(rabbit)*	Abcam	ab58657	1:500 in 5% BSA
Anti-GFP *(sheep)*	Made in house by Prof. Prior.		1:5000 in 5% milk
IRDye® 680LT Donkey anti-Mouse IgG (H + L)	LI-COR Biosciences	926-68022	1:10000 in 5% BSA
IRDye® 800CW Donkey anti-Rabbit IgG (H + L)	LI-COR Biosciences	925-32212	1:15000 in 5% BSA
IRDye® 800CW Streptavidin	LI-COR Biosciences	926-32230	1:10000 in 5% BSA

Table 2.4| List of primary and secondary antibodies used for western blots.

2.3.8. Statistical analysis

Statistical analyses were performed when appropriate for experiments with at least three independent repeats using GraphPad Prism 8.0. To determine the type of statistical test required, a normality test was performed to check the distribution of the data so that a statistical test could be chosen accordingly.

2.4. PROTEOMICS

2.4.1. In-gel digest

Eluted samples were loaded into Novex precast gels (4-12% gradient, 10 well, 1.5mm) and ran at 100V for 15 minutes. The gel was fixed with 10% acetic acid and 50% methanol for 10 minutes on a rocker. Once fixed, the gel was washed twice with water then each lane/sample was divided into top and bottom pieces. These pieces were further subdivided into 1mm^2 square gel pieces. Resulting gel pieces were destained with 50mM ammonium bicarbonate (ambic (Sigma-Aldrich, 09830))/acetonitrile (ACN (VWR, 20060320)) at 37°C for 10 minutes at 900rpm. This step was repeated until gel pieces were opaque. Then, gel pieces were dehydrated with ACN for 5 minutes (900rpm, room temperature) before being placed into a speed vacuum for 5 minutes. Subsequent samples were reduced and alkylated using DTT (1hr, 900rpm, 56°C) and IAA (30 mins, 900rpm, room temperature (Sigma-Aldrich, T-6125)), respectively. Then washed with 100mM ambic followed by 50mM ambic/ACN, both at room temperature for 15 minutes at 900rpm. Followed by dehydration using ACN and the speed vacuum. The dehydrated gel pieces were submerged in trypsin gold (Promega, V5280) for over 16 hours.

The following day all supernatants were retained from the samples as well as from a series of incubations with ACN (30 mins, 900rpm, 30°C), 1% formic acid (20 mins at room temperature, repeated twice) and ACN again (10 mins, 900rpm, RT). Collected supernatant was dried in the speed vacuum until no liquid was present. For KRAS and NRAS, samples were processed by Dr Emma Rusilowicz-Jones on the LTP-Orbitrap XL mass spectrometer (Thermo Fisher Scientific) based at the University of Liverpool. The dried peptides of the

remaining samples were resuspended in buffer A (0.5% acetic acid) then loaded on to previously made C18 stage tips that had been prewashed in methanol, buffer B (0.5% acetic acid and 80% ACN) and buffer A. The collected flowthrough was passed through the C18 columns again. Then these columns were washed twice with buffer A, before samples were eluted in 60% ACN. The eluted samples were then further processed and analysed at the Proteomics Research Technology Platform in University of Warwick on the Orbitrap Fusion with UltiMate 3000 RSLCnano System (Thermo Fisher Scientific).

2.4.2. Mass spectrometry data processing

Mass spectrometry data was processed using MaxQuant 1.5.3.8. Group specific parameters were changed to label-free quantification as well as to include variable modifications: oxidation, acetylation, phosphorylation and biotinylation. In addition, carbamidomethyl fixed modification was also added.

Data generated by MaxQuant were exported to Excel. Using the label-free quantification (LFQ) intensities, ratios were calculated using the no H_2O_2 control. These ratios were averaged between the two independent repeats. Then $\log_2$ transformed for shortlisting. To categorise whether proteins were specifically enriched i.e., biotinylated proteins, a two-fold threshold was implemented. Therefore, values greater than two-fold change of biotinylation control (i.e., no H_2O_2) in KRAS, HRAS and/or NRAS samples were termed 'specific', whereas proteins with values less than two-fold were termed 'non-specific'.

2.5. IMAGING

2.5.1. Immunofluorescence

Antibody	Company	Catalog no.	Dilution
Pan-Ras (rabbit)	Abcam	ab52939	1:100 in 3% BSA
Anti-FLAG (mouse)	Sigma-Aldrich	F1804	1:500 in 3% BSA
Anti-mouse Alexa-Fluor™ 488	Thermo Fisher Scientific	A28175	1:500 in 3% BSA
Anti-rabbit Alexa-Fluor™ 594	Thermo Fisher Scientific	A]11012	1:500 in 3% BSA
Streptavidin Alexa Fluor™ 647	Thermo Fisher Scientific	S21374	1:500 in 3% BSA

Table 2.5| List of primary and secondary antibodies used for immunofluorescence.

Cells were seeded at a cell density of 1.8-2x10^5 cells per well containing sterile coverslips (6 well plate), which were transfected the next day. Following 24 hours after transfection, cells were washed twice with ice cold PBS. Then cells were fixed in ice cold methanol for 10 minutes followed by 1 minute with acetone, both steps at -20°C.

The following steps were all performed at room temperature. Cells were washed twice with PBS then blocked with 3% BSA for 30 minutes. Next, the fixed cells were incubated with their primary antibodies in 3% BSA for 2 hours (see *Table 2.5*). The primary antibody was removed via three washes with PBS, each 5 minutes. Then cells were incubated with their secondary antibody (*see Table 2.5)* for 30 minutes before repeating wash steps with PBS. The coverslips were then removed and placed on to slides using MOWIOL 4-88 reagent (Merck, 475904) with added DAPI. Slides were left to dry overnight, then visualised on the Zeiss LSM 800 confocal microscope. Images were processed using FIJI.

2.5.2. Fluorescence Resonance Emission Transfer

2.5.2.1. Sample preparation

HeLa S3 cells were seeded at a cell density of 5x10^4 cells per compartment in a glass bottom, four compartment 35mm dish (Greiner, 627975). The following day, 25µl Opti-MEM, 0.75µl GeneJuice and 0.5µg DNA was added to each compartment for a single transfection. For co-transfections, the GeneJuice volume was doubled to account for the total combined DNA amount of 1µg. Here, cells were either transfected with GFP-annexins and/or mCherry-Ras.

After 24 hours of transfection, cells were placed in a humidified warm (37°C) chamber containing 5% CO_2 to be visualised on the Zeiss LSM 780 confocal microscope using the ZEN software. Images were collected with Dr James Boyd at the Liverpool Centre for Cell Imaging, who also calculated the FRET efficiency using MATLAB.

2.5.2.2. Sensitised emission

Cells were visualised and captured in three different channels: the GFP donor (488nm excitation, 490-535nm emission), the mCherry acceptor (560nm excitation, 595-645nm

emission) and FRET (488nm excitation, 595-645nm emission). The FRET efficiency (*see below*) was calculated in MATLAB, whereby each pixel intensity detected in the FRET channel was corrected using intensity values generated by cross-excitation and bleed-through.

$$FRET\ \varepsilon\ (\%) = [(F_i - (\beta\ x\ D_i) - (\gamma\ x\ A_i))/A_i]\ x\ 100$$

F_ε = FRET efficiency channel
β = Pixel intensity in bleedthrough channel
Fi = Pixel intensity in FRET channel
γ = Pixel intensity in cross-excitation channel
Di = Pixel intensity in donor channel
Ai = Pixel intensity in acceptor channel

2.5.2.3. Photoacceptor bleaching

For photoacceptor bleaching analysis, images of the cells were collected for both channels: GFP and mCherry for three frames prebleach. Then acceptor bleaching was initiated followed by dual channel imaging for a further three frames. Intensities of both channels was measured for whole cells using FIJI, then processed using Microsoft Excel to express values as a percentage of the initial donor/acceptor fluorescence.

2.5.3. Transmission Electron Microscopy

2.5.3.1. Grid preparation

Glass slides were cleaned and dipped into 0.3% pioloform dissolved in chloroform, then left to dry. A razor blade was used to score along the glass slide before moisture was applied and immediately submerged vertically into dH_2O in order to form a pioloform film. 3.05mm Copper Mesh hexagonal grids (G2450C, Agar Scientific) were gently placed on the floating pioloform sheet and collected using a white sticker covered clean glass slide. Slides were stored in a desiccator before use.

2.5.3.2. Single gold labelling

For each sample, 180,000 cells were seeded on a 3cm dish containing 13mm coverslips. Cell were transfected the following day with either mutant (G12V) or WT mCherry-HRAS. For samples with A6, cells were also co-transfected with eGFP-A6.

Previously prepared grids were treated with poly-l-lysine for 10 minutes and subjected to two washes in water before being left to dry for 10 minutes. Coverslips with the adherent cells were removed from the dishes after 24 hours post-transfection and placed cell side down on top of two grids. Filter paper was placed on top and pressure was applied using a rubber bung. KOAC buffer (250mM HEPES, 1.15M Potassium acetate, 25mM $MgCl_2$) was added gently to the coverslips to allow for grids to float and subsequently be attached to membrane 'rip offs'.

Grids were removed and placed in the following solutions: fix (4% PFA, 0.1% glutaraldehyde in KOAC solution) for 10 minutes, 50mM glycine for 3 minutes (x3), block (0.2% BSA, 0.2% fish skin gelatine in PBS) for 20 minutes, gold-conjugated antibody (3.5nm anti-RFP gold) for 30 minutes, block for 3 minutes (x3) and dH_2O for 1 minute (x3). Lastly, the grids were submerged in methylcellulose/uranyl acetate solution (3% uranyl acetate in methylcellulose) and captured using a loop; excess was removed at an angle using filter paper. These were left to dry at room temperature. Once dried, the grids were carefully removed from the loops, then stored for imaging. Grids were imaged at 87,000X magnification on the transmission electron microscope (TEM). Training and assistance for the preparation and visualisation of EM samples were provided by Professor Ian Prior, Miss Alison Beckett and Miss Jo Isherwood.

2.5.3.3. Analysis

Firstly, digital images acquired from the TEM were cropped (765x765nm) and processed to remove background in order to acquire *x* and *y* co-ordinates of gold particles using Adobe Photoshop and ImageJ, respectively. These co-ordinates were used for univariate point pattern analysis, which facilitates Ripley's K function (*see formula below*) to determine the distribution of these gold particles by comparing the calculated number of points within a unit area with the expected normal distribution.

Nanoclustering analysis of processed images (HRAS WT – 21 images, HRAS WT + A6 – 14 images, HG12V – 10 images, HG12V + A6 – 11 images) were carried out by Dr Yong

Zhou (*University of Texas*) using macros on Microsoft Excel. Additional statistical analyses were performed using GraphPad Prism v8.0.

$$K(r) = An^{-2} \sum_{i \neq j} w_{ij} 1 \left(|| x_i - x_j || \leq r \right)$$

$$L(r) - r = \sqrt{(K(r)/\pi)} - r$$

$K(r)$ = Univariate K function

r = Radius (1-240nm, 1nm increment)

A = Area

n = Number of points

w_{ij} = Correction for edge effect

$||x_i - x_j||$ = Euclidean distance

$L(r)-r$ = Linear transformation of $K(r)$

CHAPTER THREE

Establishing APEX2 as a tool to screen the Ras proteome microenvironment

3.1. INTRODUCTION

Protein-protein interactions regulate the structural and signalling processes underlying the functions of a living cell. The 'undruggable' status of Ras makes it increasingly important to map these interactions to further understand Ras biology and to identify potential targets for Ras-associated cancer therapeutics (Cox *et al.*, 2014).

Since the discovery of Ras, many efforts have been focussed into identifying proteins involved in the Ras signalling pathways. Genetic and biochemical techniques such as yeast-2-hybrid (Vojtek, Hollenberg and Cooper, 1993; Hofer *et al.*, 1994) and co-immunoprecipitations (IP) (Koide *et al.*, 1993; Warne, Vician and Downward, 1993) have been key tools in identifying some of the most well-known Ras interactors. Raf was the first Ras effector to be discovered, whereby initial genetic analyses of *Drosophila melanogaster* (Dickson *et al.*, 1992) and *Caenorhabditis elegans (C. elegans)* (Han *et al.*, 1993) highlighted Raf as a downstream component of Ras signalling. It was later shown in mammalian cells that Raf could be co-immunoprecipitated with Ras (Koide *et al.*, 1993), which was then confirmed to be a direct interaction (Warne, Vician and Downward, 1993). Another Ras effector, PI3K was also discovered via co-IP experiments whereby PI3K was present in anti-Ras (Y13-259) immunoprecipitates, which increased in stimulated cells and diminished when blocked with an anti-Ras antibody (Sjölander *et al.*, 1991). In the past few decades, several direct interactors of active Ras other than Raf and PI3K have been identified such as RalGDS, Tiam1, p120GAP, NF1 and PKCζ (Rajalingam *et al.*, 2007)

Aside from Ras effectors, many Ras regulators have also been identified. Similar genetic studies using *Drosophila* and *C.elegans* were fundamental in the discovery of Kinase Suppressor of Ras (KSR) (Sundaram and Han, 1995; Therrien *et al.*, 1995) and SHOC2 (Sieburth, Sun and Han, 1998), which are scaffold proteins that positively regulate signalling by aiding the assembly of signalling complexes to Ras (Nguyen *et al.*, 2002; Matsunaga-Udagawa *et al.*, 2010). Another type of regulator that aids Ras localisation at the inner plasma membrane were found using techniques such as co-IP and affinity purification.

These include galectin-1 (Ashery *et al.*, 2006) and caveolin-1 (Song *et al.*, 1996), respectively, which both regulate isoform-dependent spatial organisation of Ras at the plasma membrane.

Although these techniques have provided key insight into the discovery of direct and indirect Ras interactors, they do however carry fundamental limitations of the identification of predominantly stable and high-affinity protein-protein interactions due to the harsh procedures involved in cell lysis. Additionally, often these experiments are performed *in vitro*, so do not provide physiologically relevant conditions. However, in more recent years, newer techniques that bypass these problems have been developed to map protein-protein interactions such as proximity labelling methods coupled with mass spectrometry (Jiang *et al.*, 2012; Roux *et al.*, 2012; H.-W. Rhee *et al.*, 2013).

Currently, there are three main proximity labelling methods based on the enzymes: horseradish peroxidase (HRP) (Jiang *et al.*, 2012), biotin ligase (BirA) (Roux *et al.*, 2012) and ascorbate peroxidase (APEX) (H. Rhee *et al.*, 2013). The advantage of this type of methodology is that the process occurs in living cells and therefore maintains a physiologically relevant microenvironment. In addition, it has the capacity to detect transient and weak interactions.

The general principle of proximity labelling relies on the fusion of the protein of interest with an enzyme that can convert a substrate into a highly reactive radical that can covalently tag a neighbouring protein with an enzyme substrate. These enzyme substrates are often small, e.g. biotin is 244.31g/mol, to lessen the possibility of modifying the activity or localisation of the protein (Jiang *et al.*, 2012; Roux *et al.*, 2012; H.-W. Rhee *et al.*, 2013). The strong covalent bond between biotin and other proteins are preserved during cell lysis, therefore reducing the number of artefacts (Chapman-Smith and Cronan, 1999). These labelled proteins undergo various stringent washes to remove any non-specific interactions and are enriched for their enzyme substrate tag. Protein elutes can then be used for either western blotting for initial queries or alternatively be used for mass spectrometry to broadly

screen the spatially proximal proteome (Jiang *et al.*, 2012; Roux *et al.*, 2012; H.-W. Rhee *et al.*, 2013).

HRP is a 44kDa heme peroxidase tag. In the presence of H_2O_2, it can convert phenolic compounds like tyramine (selective proteomic proximity labelling assay using tyramide, SPPLAT) (Li *et al.*, 2014) or phenolic aryl azide derivatives (enzyme-mediated activation of radical source, EMARS) (Honke and Kotani, 2012) into tyramide-biotin or fluorescein arylazide/biotin arylazide respectively, which bind electron-rich amino acids of neighbouring proteins. HRP has been used to map the surface of living cells due to its optimal activity in oxidising environments such as extracellular regions or the lumen of the ER or Golgi. Its structurally essential disulphide bonds and Ca^{2+} ion-binding sites are unable to form in reducing environments such as the cytosol, therefore HRP is limited to secretory pathways and extracellular interactomes (Jiang *et al.*, 2012).

Proximity-dependent biotin identification (BioID) uses a promiscuous 35kDa *Escherichia coli*-derived biotin ligase (BirA*). Normally, BirA catalyses the conversion of biotin to a reactive biotinoyl-5'-AMP (bioAMP) in the presence of ATP and strongly retains the intermediate in its active site until its substrate, acetyl-CoA carboxylase or a short acceptor peptide is available. However, engineered biotin ligase, BirA* harbours a R118G mutation in its catalytic site which reduces its affinity for bioAMP and thus dissociates easier to bind to lysine residues of neighbouring proteins (Roux *et al.*, 2012). In water, the half-life of bioAMP has been estimated to be approximately 30 minutes (Xu and Beckett, 1994), however this has shown to be less inside cells, possibly due to the presence of intracellular nucleophiles (Kim *et al.*, 2014).

The application of BioID in the nuclear pore complex has shown that the labelling radius of BioID to be approximately 10nm (Kim *et al.*, 2014), although this can be context-dependent and vary with the length of the flexible linker (Kim *et al.*, 2016). However, BioID has relatively slow kinetics as it requires 15-24 hours of labelling time with biotin supplementation for sufficient biotinylation. BioID was originally used to study a well-

characterised component of the nuclear envelope, an intermediate filament protein called lamin-A (LaA). The method was able to identify known interactors of LaA as well as a novel interacting protein, SLAP75, which was later found to associate with the nuclear envelope (Roux *et al.*, 2012). Following its initial success for screening direct and indirect protein-protein interactions of the nuclear envelope, it has since been applied to studies of previously difficult to investigate insoluble structures such as cell junction complexes (Van Itallie *et al.*, 2014; Fredriksson *et al.*, 2015) and centrosomes (Firat-Karalar *et al.*, 2014; Dong *et al.*, 2016) in mammalian cells.

The smallest enzyme used for proximity labelling, APEX, is 27kDa and is derived from either pea (APEX, first generation) (H.-W. Rhee *et al.*, 2013) or soybean (APEX2, second generation) (Lam *et al.*, 2015). This class I cytosolic plant peroxidase was first engineered to be used in EM, as an alternative to HRP that could be used in reducing microenvironments. APEX catalyses the production of diaminobenzidine (DAB), which in return recruits osmium to produce the high contrast required for high resolution EM images (Martell *et al.*, 2012). In addition to its use for EM, it can also be used as a tool for proteomic mapping. The first-generation APEX has three mutations: K14D, W41F and E112K (H.-W. Rhee *et al.*, 2013), whereas the second generation was developed by yeast display and yields an additional mutation (A134P), which improves its catalytic efficiency and sensitivity (Lam *et al.*, 2015). Similar to the other enzymes, the engineered monomeric APEX catalyses the production of biotin-phenoxyl radicals in the presence of H_2O_2 and its substrate, BP. These free radicals are short-lived (<1ms) (Mortensen and Skibsted, 1997) and attach to tyrosine side chains (H.-W. Rhee *et al.*, 2013) and potentially other electron-rich amino acids such as tryptophan (Bhaskar *et al.*, 2003), cysteine (Rogers *et al.*, 2008) and histidine (Amini, Kodadek and Brown, 2002).

Initial studies in mitochondria demonstrated the use of APEX for proteomic mapping. The first experiment highlighted proteins associated with the human mitochondrial matrix and was able to distinguish proteins between whether they were inner membrane proteins facing

the matrix or the intermembrane space (H.-W. Rhee *et al.*, 2013). Whereas the second experiment focussed on mapping the proteome of a previously impossible to isolate component, the mitochondrial intermembrane space, which aided the identification of 9 novel mitochondrial proteins (Hung *et al.*, 2014). Following the success of these studies based in bound organelles, APEX was later used to map proteomes of open compartments like in primary cilia (Mick *et al.*, 2015) and G-protein coupled receptors (GPCRs) on the plasma membrane (Lobingier *et al.*, 2017; Paek *et al.*, 2017).

The primary aim of this project is to identify regulators of Ras nanoclustering and in the context of different Ras isoforms and activation states. Therefore, it is advantageous to use the novel proximity labelling method to widely screen the different Ras microenvironments, as this technique has the potential to capture transient interactions in live cells and without the need to biochemically isolate the plasma membrane. The choice of labelling enzyme was dependent on which enzyme was most suitable for capturing the dynamic nature of the nanoclustering events that range from 0.1-1 seconds occurring at the inner membrane leaflet (Zhou and Hancock, 2015). At this location, HRP would be inactive and thus, unsuitable for investigating the Ras interactome in this context, whereas APEX2 could tolerate such conditions. Additionally, APEX2 has a faster labelling duration than BirA*, 1 minute (Lam *et al.*, 2015) versus 18-24 hours (Roux *et al.*, 2012). Therefore, APEX2 is more likely to capture more dynamic interactions, whereas BirA* would detect steady state interactions. Furthermore, APEX2 has less potential of interfering with the function and localisation of Ras as it is a smaller enzyme tag than BirA* (27kDa vs 35kDa). Henceforth, the catalytically improved second generation APEX2 will be the labelling enzyme used in this project to spatially map the Ras interactome (*Fig.3.1a*).

3.2. AIMS

3.2.1. To establish the APEX2 method for the study of Ras

The first objective for this project will be to establish APEX2 as a proteomic tool. Therefore, it will require APEX2 to be fused to the protein of interest, Ras. Since different Ras isoforms

will be investigated, several APEX2-Ras fusion constructs need to be generated. Then, multiple steps involved in the APEX2 method (*Fig.3.1b)* will be optimised for the study of Ras.

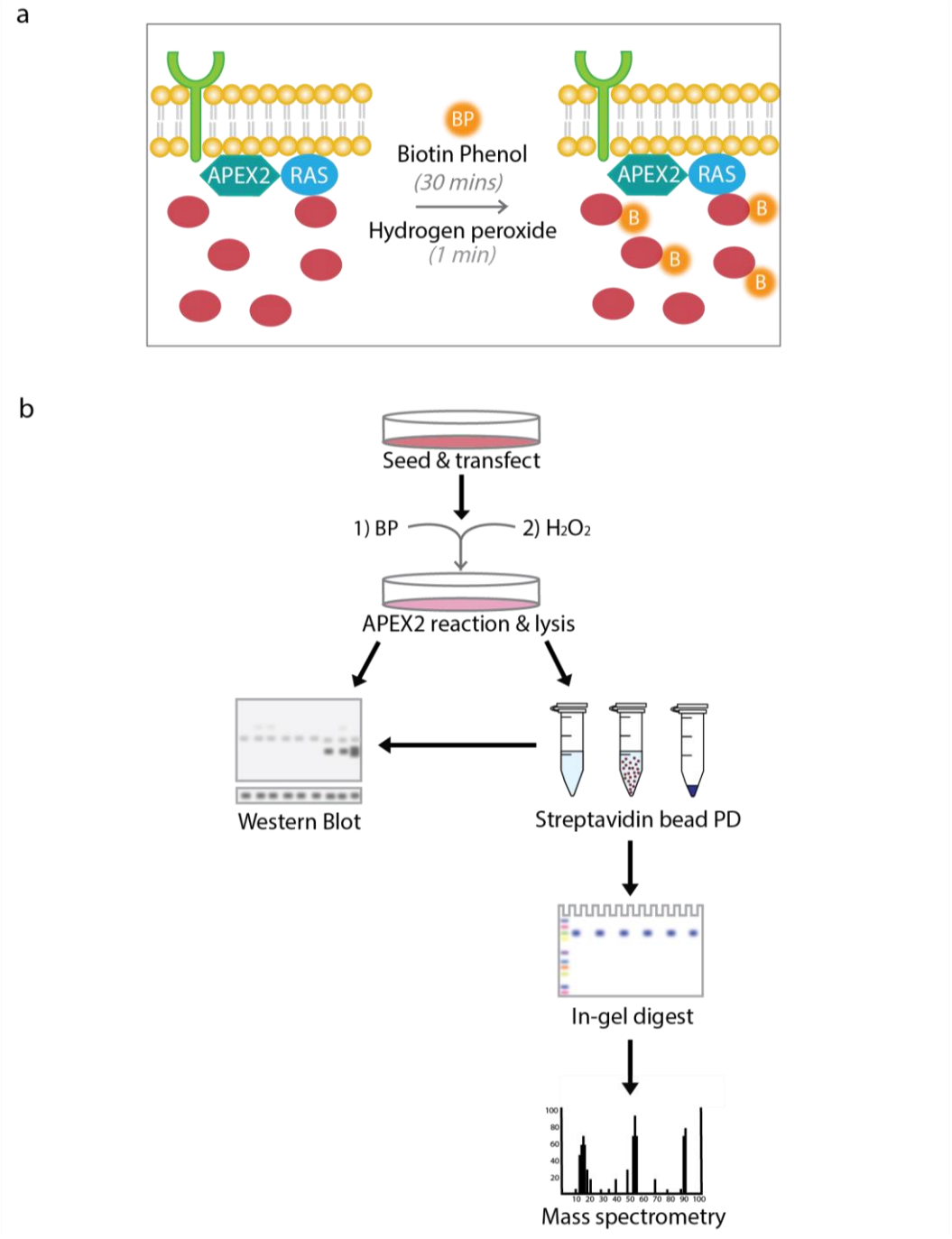

Figure 3.1| Proximity labelling using APEX2 – a) Schematic of the APEX2 reaction. The addition of its substrate: BP (30 minutes) followed by H_2O_2 (1 minute) treatment allows for proteins in close proximity with Ras to be covalently tagged with biotin. (b) The APEX2 methodology involves HeLa S3 cells to be seeded and transfected with FLAG-tagged APEX2-Ras. Cells were lysed and tested initially using western blot. Further experiments using streptavidin bead pulldown were used to enrich for biotinylated proteins, then analysed either by western blot or mass spectrometry.

3.2.2. To identify whether the APEX2 method would be a suitable tool for screening the Ras proteome microenvironment.

The APEX2 method has been used to successfully map the proteome microenvironment of many cellular regions of interest such as the synaptic cleft and mitochondrial intermembrane space. Here, this methodology will be assessed by identifying whether APEX2 can be used to widely screen the Ras proteome without affecting its normal activity and localisation.

3.3. PRODUCTION OF APEX2-TAGGED RAS

In order to perform the APEX2 experiments, a panel of fusion constructs consisting of APEX2 and Ras: KRAS WT (K WT), KG12V, HRAS WT (H WT), HG12V, NRAS WT (N WT) and NG12V were generated (*Appendix 1*). Here, different APEX2-Ras isoforms and their G12V mutants were created so that in later experiments, comparisons can be made between the proteome microenvironments of these various conditions.

An overview of the cloning process can be seen in Figure 3.2. The first step consisted of using APEX2-actin in pEGFP as a template DNA of APEX2. This plasmid consisted of an N-terminal FLAG epitope tag (DYKDDDDK) and APEX2 (soybean), which contains 4 mutations: K14D, W41F, E112K and A134P. Next, N-terminal and C-terminal primers were designed to amplify the FLAG-tagged APEX2 as well as to add restriction sites: NheI and BglII, respectively. The C-terminal primer also contained an additional 13 amino acid linker consisting of glycine and serine residues between the APEX2 and BglII sequence. This short linker was included to minimise the effect of APEX2 on the targeting moiety of Ras. A number of bases were also added before the BglII sequence to alter the frame of the APEX2 insert so that it could be cloned into the appropriate pEGFP-C1/C2/C3 vector.

These amplified inserts were later ligated into an intermediate vector, pCR 4 Blunt TOPO. Once confirmed by DNA sequencing, the APEX2-TOPO plasmids were digested by NheI and BglII for either subcloning into pEGFP-C1/C2/C3 or for direct cloning into pEGFP-tK or -tH. In both cases, pEGFP was replaced with APEX2. For the full-length Ras APEX2 constructs, pEGFP-KRAS WT/KG12V/HRAS WT/HG12V/NRAS WT/NG12V and

APEX2-C1/C2/C3 underwent the appropriate restriction enzyme digest to generate different Ras isoform inserts that could be subcloned into the multiple cloning sites of the respective APEX2 vectors. In all APEX2-Ras constructs, APEX2 was specifically tagged to the N-termini of Ras to prevent alterations to the C-termini, which is fundamental for its localisation (Prior and Hancock, 2012)

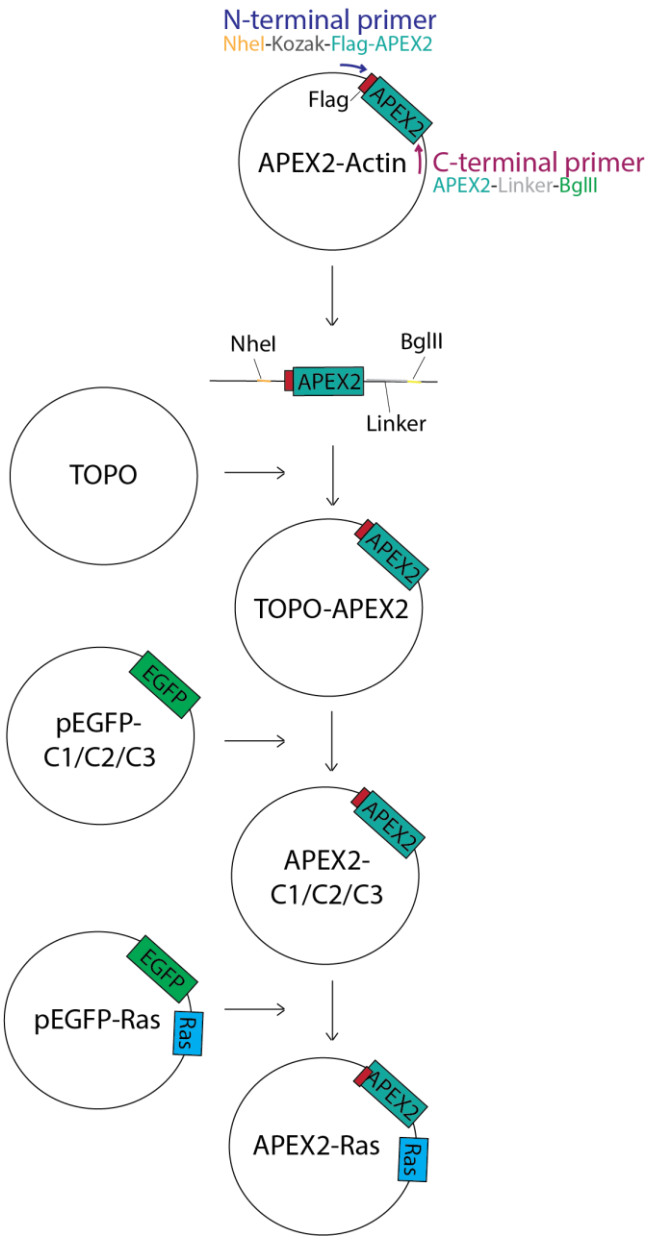

Figure 3.2| Schematic of APEX2-Ras cloning - Using designed primers and PCR, the APEX2 sequence from the template: APEX2-Actin in a pEGFP vector was amplified. The APEX2 insert was subcloned into a TOPO vector for sequencing. Then using REs, the APEX2 insert was removed from the TOPO-APEX2 and was inserted into the position of the EGFP sequence of the pEGFP-C1/C2/C3 vectors. Then the respective full-length Ras sequences were inserted into the multiple cloning sites of these APEX2-C1/C2/C3 vectors in order to generate APEX2-Ras.

3.4. CHARACTERISATION OF APEX2-RAS LOCALISATION AND ACTIVITY

3.4.1. Expression of APEX2-Ras *in vitro*

Having generated a panel of different APEX2-Ras constructs, it was important to check whether cells could efficiently express these constructs and consequently able to biotinylate proteins. Therefore, the presence of FLAG (the N-terminus tag of APEX2-Ras) and biotin were investigated in whole cell lysates.

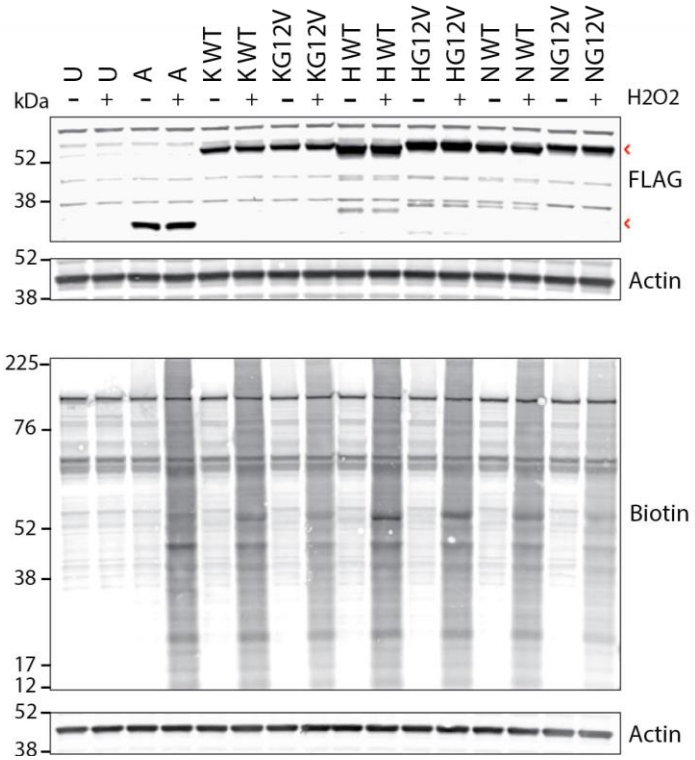

Figure 3.3| Western blot of APEX2-Ras transfected cells – Hela S3 cells were transfected with either APEX2-K WT, -KG12V, -H WT, -HG12V, -N WT or -NG12V. Controls included untransfected (U) and APEX2 only (A). Each condition was subjected to 30 minutes of BP, followed by either with (+) or without (-) H_2O_2 treatment for 1 minute. Cell lysates were blotted for the presence of FLAG (*red arrows*), biotin and actin (loading control). Data representative of 3 biological repeats.

HeLa S3 cells were transiently transfected with either APEX2 only or APEX2-Ras fusion constructs: KRAS WT, KG12V, HRAS WT, HG12V, NRAS WT and NG12V for 24 hours. As a control, untransfected (U) HeLa S3 cells were used. Then for each sample, the media was replaced with media supplemented with BP. After 30 minutes, half of the samples were

treated with H_2O_2 for 1 minute. The reaction was halted by a number of washes with quencher solution, followed by cell lysis. 10µg of total cell lysate from individual samples were ran on an SDS PAGE gel and transferred to a nitrocellulose membrane. Followed by immunoblotting for FLAG, biotin, and actin (loading control).

As expected, FLAG was present only in the transfected samples, i.e., the APEX2 only control and in the APEX2-Ras samples: K WT, KG12V, H WT, HG12V, N WT and NG12V (*indicated by the red arrows in the top blot*), but not in the untransfected control (*Fig.3.3*). The difference between the detection of a lower (~30kDa) and upper FLAG band (~53kDa) is due to the presence of the Ras protein in the APEX2-Ras samples and therefore making it a higher molecular weight. It also appears that there might be slight discrepancies in protein expression levels, since KRAS WT and KG12V have lower expression compared to other isoforms. Overall, it was evident that HeLa S3 cells can be efficiently transfected with the APEX2-Ras constructs, and therefore able to express the APEX2-Ras fusion protein of which biotinylated proteins in the presence of BP and H_2O_2.

Next, it was assessed whether the expressed APEX2-Ras protein could biotinylate proteins. To test this, samples were either untreated (BP only) or treated with H_2O_2 and later whole cell lysates were immunoblotted for biotin. As shown in Figure 3.3 (lower blot), three predominant bands appear at 130kDa, 75kDa and 72kDa in all samples. These are likely to represent naturally biotinylated proteins in humans, in which biotin is a crucial co-factor for metabolic enzymes such as carboxylase and decarboxylases, where post-translation modifications occur via biotin ligase (Hung *et al.*, 2016). In the untransfected controls, less biotinylation can be observed. Whilst in all H_2O_2-treated APEX2 samples, additional bands were present across a large molecular-weight range due to the presence of APEX2-biotinylated proteins. These proteins were likely to represent proteins that were in close proximity to APEX2 or APEX2-Ras. Since APEX2 alone is not specifically targeted to any cellular region, it is likely that these detected proteins represent a population of randomly labelled proteins encountered by APEX2 within the cell. In general, the addition of the

APEX2 enzyme to Ras does not appear to affect its enzymatic activity and the biotinylation of endogenous proteins (with the exception of the three naturally occurring biotinylated proteins) is dependent on the presence of the APEX2 enzyme, BP and H_2O_2.

3.4.2. Localisation of APEX2-Ras *in vitro*

Ras predominantly localises at the plasma membrane and fundamental for this correct localisation is the HVR (Prior and Hancock, 2012). Using immunofluorescence (IF), the localisation of APEX2-Ras within the cell could be investigated to see whether the attachment of APEX2 to the Ras protein affected its localisation to the plasma membrane.

Cells were prepared like previous, supplemented with BP and H_2O_2 then reaction was quenched before preparation for imaging. Here, cells were stained with multiple antibodies: anti-FLAG antibody to detect APEX2-Ras, Pan-Ras antibody to visualise total Ras expression, streptavidin-conjugated Alexa Fluor to check for biotinylation and DAPI for nuclear staining (*Fig.3.4*). As expected, FLAG was present in all APEX2-Ras transfected samples and its pattern of expression was very similar to the expression of Ras, therefore highlighting that most of the Ras detected in the cell is from the exogenous expression of the FLAG-Ras construct. This is further supported by the negative controls, where little Ras/FLAG expression appeared in the untransfected sample. Similarly, in the APEX2 only control, FLAG can be seen due to its presence in the APEX2 construct. However, Ras expression is considerably lower compared to samples containing APEX2-Ras and is likely to reflect the normal levels of endogenous Ras present within the cells.

Majority of the APEX2-Ras fusion proteins: KRAS WT, KG12V, HRAS WT, HG12V and NRAS WT localised predominantly in the plasma membrane, indicating that the attachment of APEX2 to Ras does not appear to affect its localisation. This is reassured by the APEX2 only control, which shows a different pattern of APEX2 localisation, where its expression is mainly cytosolic. APEX2-NG12V is less membrane-bound and more cytosolic than the other isoforms and this could be due to the dynamic cycling between palmitoylated and depalmitoylated states (Laude and Prior, 2008).

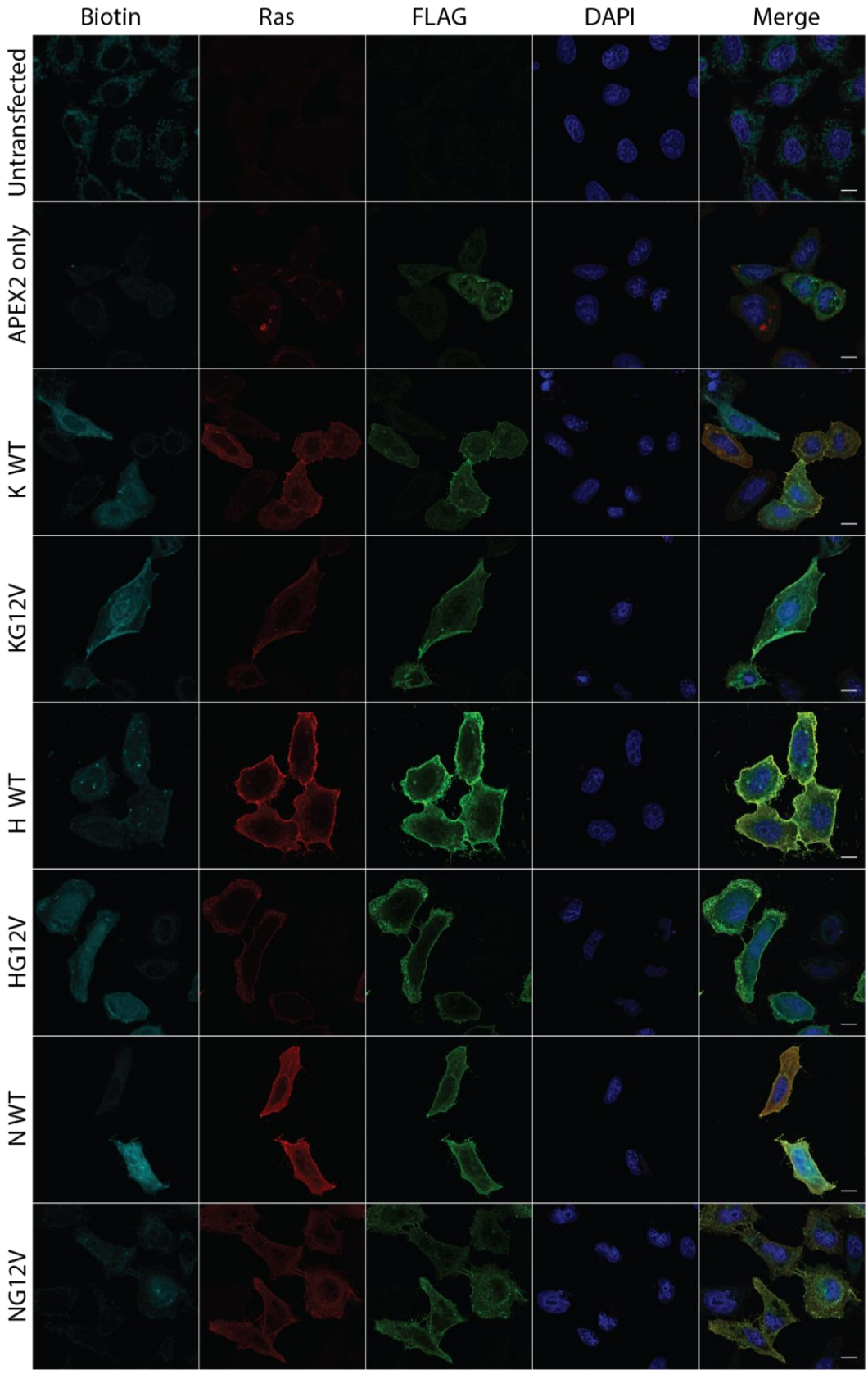

Figure 3.4| Localisation of APEX2-Ras – Representative confocal fluorescent images of cells (n=3) expressing either APEX2-K WT, -KG12V, -H WT, -HG12V, -N WT, -NG12V or APEX2 only. Expression of Ras, APEX2-Ras and biotinylation was visualised using anti-Ras, anti-FLAG, and streptavidin-Alexa Fluor 647 antibodies, respectively. DAPI used as a nuclear stain. Scale bar, 10µm.

Biotinylation was seen in all samples, which is not surprising since this type of assay does not distinguish between endogenously biotinylated proteins and APEX2-biotinylated proteins. However, it can be speculated that there is a higher expression of biotinylated proteins in some of the Ras samples compared to control. Although in some samples the pattern of biotinylation follows the expression of FLAG and Ras, there are some that do not. This could be due to the diffusion of biotinylated proteins from the APEX2-Ras during the H_2O_2 reaction window since Ras is not present in a compartmentalised part of the cell. Overall, the IF experiments have shown that the APEX2-Ras fusion proteins can localise correctly to the plasma membrane.

3.5. OPTIMISATION OF THE APEX2 TECHNIQUE

3.5.1. Stimulation of Ras activity

The aim of this project is to investigate the different Ras isoform interactomes in both their active and non-active states since it has been previously highlighted that GDP- and GTP-bound Ras occupy distinct transient nanoclusters on the plasma membrane for each isoform. Therefore, the assumption would be that the proteome microenvironment would differ between these states. In order to capture the snapshots of these different Ras events, the optimal stimulation for Ras effector activity would be required to establish the conditions that would model Ras in its active form.

HeLa S3 cells expressing APEX2-NRAS WT were firstly serum-starved for 5 hours then stimulated with FBS (20%) for different durations (0.5, 1, 2, 3, 4, 5, 10, 20, 30 minutes) before lysis. In addition, there was a serum-starved (SS) control and normal serum supplemented (20% FBS) with no starvation (CON) control. FBS was chosen to stimulate various growth factor pathways such as EGF, which induces Ras activation. Western blots were performed on the resulting lysates and the phosphorylation of three well-known Ras effectors: MEK, ERK and Akt were immunoblotted along with biotin and actin as loading control (*Fig.3.5*). Bands observed for the three experimental repeats were quantified then ratioed to actin, followed by normalisation to the SS condition for each of the effectors.

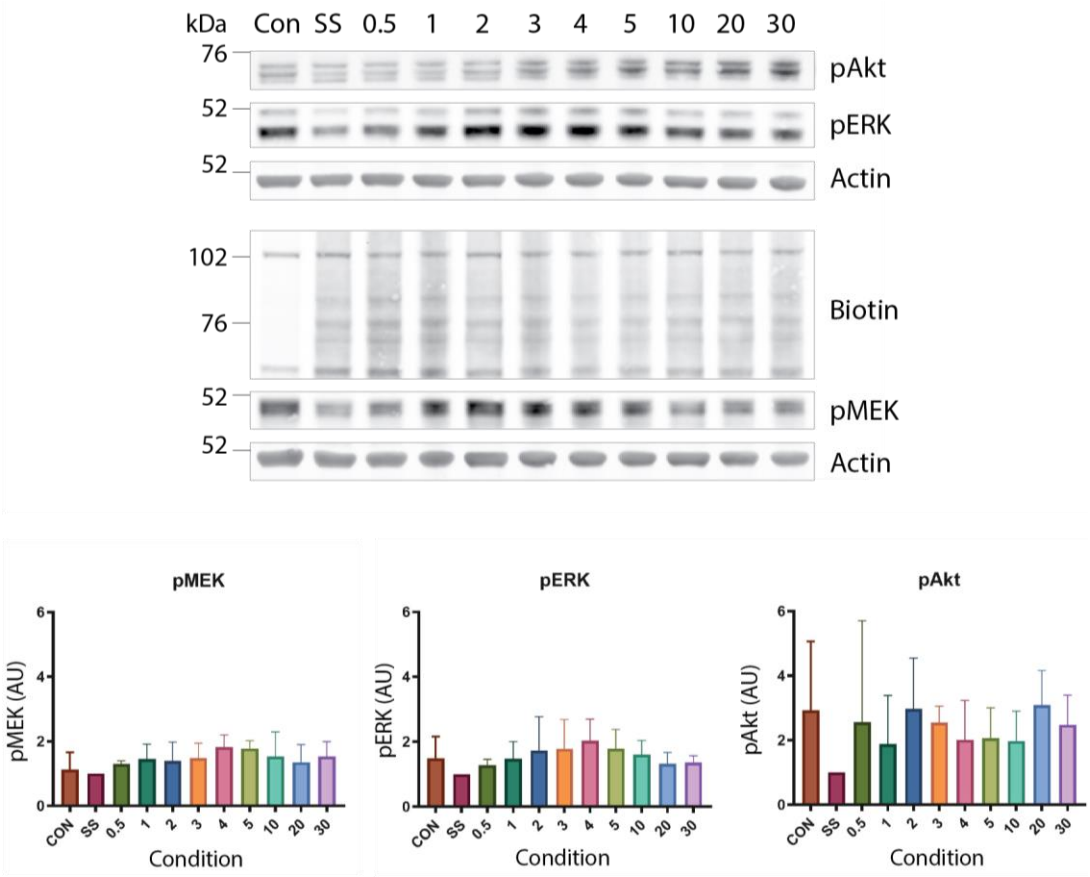

Figure 3.5| Optimisation of Ras stimulation – Different durations of FBS stimulation (0-30 mins) were tested on APEX2-NRAS WT transfected cells. Lysates were blotted for pMEK (S217/S221), pERK (T202/Y204), pAkt (S473), biotin and actin. Bottom graphs show the cumulative pMEK, pERK and pAkt activity of three independent experiments, error bars displayed as mean+SD.

Results indicated that pERK activity increased following stimulation and reached its highest level (mean = 2.03 and 1.79) between 4-5 minutes and similarly, pMEK levels peaked at 4-5 minutes (mean = 1.83 and 1.78) before declining. Whereas pAkt activity displays a prolonged increase following stimulation (*Fig. 3.5*). Since peak pERK and pMEK activity occurred between 4-5 minutes, it seemed that this would be the optimal duration to stimulate cells to model active Ras. Although peak pAkt did not occur during these timepoints, the pAkt levels (mean = 2.01 and 2.07, respectively) observed were still double the levels for SS (mean = 1). Therefore, in combination with current literature, 5 minutes of FBS stimulation should be an appropriate duration to represent active Ras, since levels of activated MEK, ERK and Akt are noticeably higher than the SS control. In addition to testing Ras activity, biotinylation was also checked to see if FBS stimulation resulted in any

changes. As shown from the blot, the biotinylation pattern remained fairly constant amongst the different timepoints and therefore was unaffected by the FBS stimulation.

3.5.2. Duration of biotinylation reaction

The application of APEX has predominantly been used in enclosed membrane-bound compartments. The original protocol suggests that the biotinylation reaction, i.e., H_2O_2 incubation, should occur for 1 minute. However, since Ras localises at the inner leaflet of the plasma membrane, the labelled proteome microenvironment will be relatively larger due to the wider open region and thus a higher chance of non-specific labelling of proteins that are not part of the Ras interactome. The assumption is that the longer the reaction, the larger the biotinylation radius and as a result the more proteins being biotinylated (*Fig. 3.6a*). Therefore, the duration of the reaction is an important factor to consider.

To determine the duration of biotinylation that would produce minimal labelling of non-specific proteins, different durations of H_2O_2 incubation was investigated using western blotting. Durations (0, 15, 30, 45, 60, 120 and 240 seconds) of H_2O_2 were tested in APEX2-NRAS WT transfected cells. In addition, untransfected and APEX2-only were used as controls. Figure. 3.6b shows that the cells expressed APEX2-NRAS WT, as represented by the bands in the lower blot immunoblotted for FLAG (~53kDa). From the three independent repeats, it is evident that there is a time-dependent increase in biotinylation. Whereby the highest level of biotinylation occurred with the longest incubation of 240 seconds, which is comparable to the levels seen for the non-targeted APEX2-only control. However, 240 seconds would not be a suitable timepoint as this might cause cellular toxicity and it could also be speculated that a longer reaction could result in the labelling of more distal proteins. Therefore, an ideal timepoint would be at the shortest duration that results in sufficient biotinylation. Although, biotinylation could be observed from as early as 15 seconds, this would be problematic from a practical perspective and thus 30 seconds was chosen for subsequent experiments instead, which showed to have similar levels of biotinylation as other later timepoints such as at 45, 60 or 120 seconds.

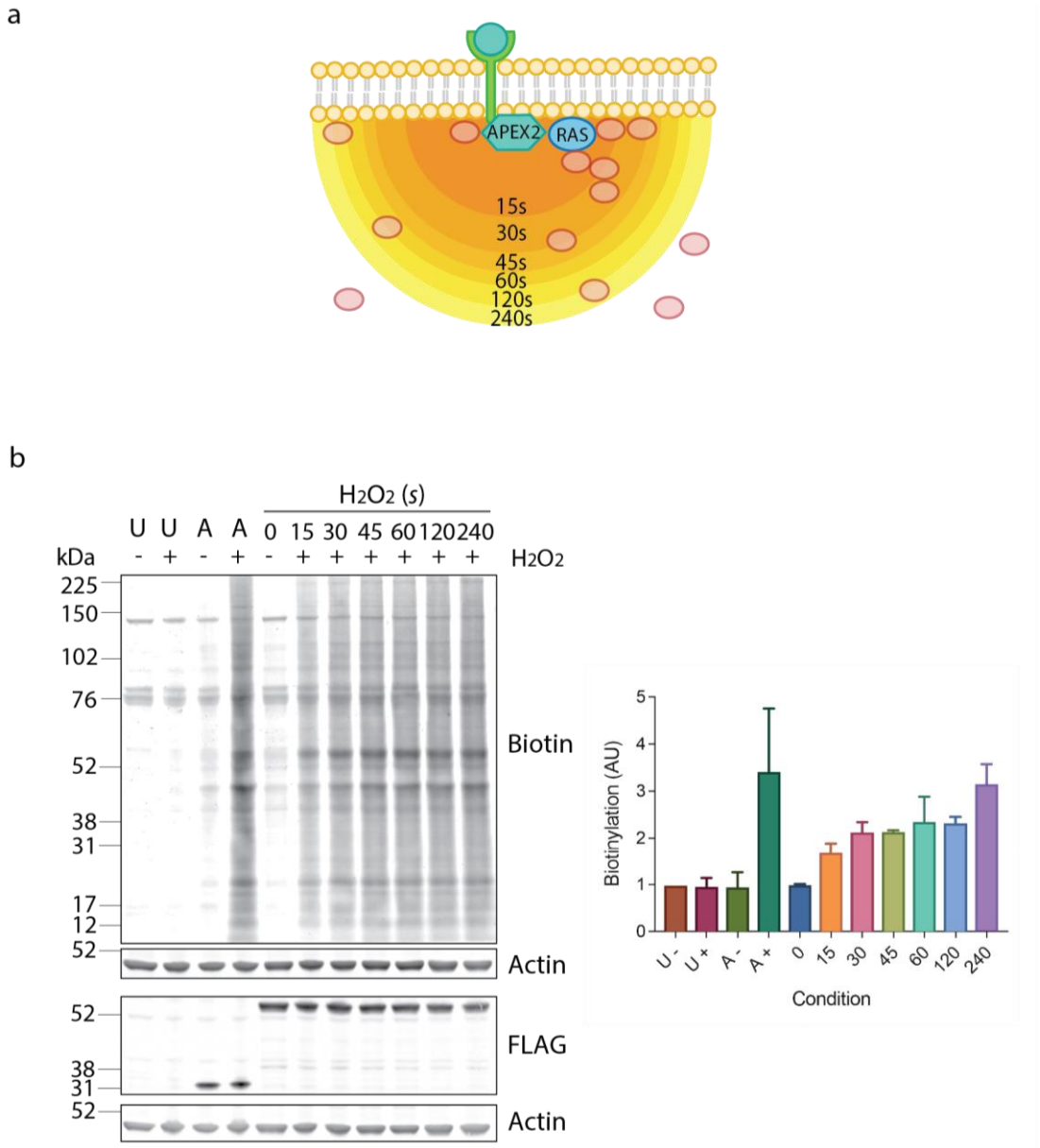

Figure 3.6| Optimisation of the duration of the biotinylation reaction – a) Schematic of the hypothesised relationship between biotinylation radius and duration of H_2O_2 incubation. b) Representative western blot and bar graph summary (n=3) displaying the time-dependent increase in biotinylation (0-240s). Untransfected and APEX2 only controls were either untreated or treated with H_2O_2 for 60s. Actin was used as a loading control. Error bars are mean+SD.

3.5.3. Titration of streptavidin beads used for pulldown

For mass spectrometry experiments, biotinylated proteins need to be enriched using streptavidin beads. The original protocol suggests to incubate 360µg whole cell lysates with 30µl streptavidin beads for 1 hour at room temperature (Hung *et al.*, 2016). Using this as a guideline, the amount of streptavidin beads needed for optimal purification of biotinylated proteins in these experiments was tested.

Using the originally stated protein concentration, 360µg total cell lysate of APEX2-NRAS WT transfected cells was incubated with either 20, 30 or 40µl streptavidin beads for 2 hours at room temperature. Flowthrough was retained to check for any unbound biotinylated proteins. The beads underwent a series of washes in different buffers containing high-salt, -pH and -urea to remove non-biotinylated protein before proteins were eluted. Both flowthrough, eluted proteins and no-bead controls were used for western blotting and the presence of biotinylated proteins was checked.

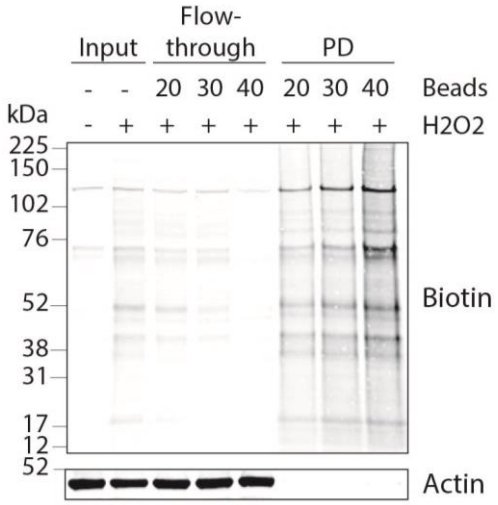

Figure 3.7| Streptavidin bead titration – Optimisation of the amount of streptavidin beads (20, 30, 40µl) required for enrichment of biotinylated proteins. Whole cell lysates (input, 1:36), flowthrough (1:36) and pulldown samples were immunoblotted for biotin. Actin was used as a loading control.

The higher amount of streptavidin beads used resulted in greater enrichment of biotinylated proteins. However, it is evident from Figure 3.7 that 40µl streptavidin beads might be overly saturated as no biotinylated proteins were present in the flowthrough compared to the no beads control, which indicated that even the naturally occurring endogenous biotinylated proteins were being pulled down. It is also possible that a larger volume of beads provides an increased surface area for non-specific binders and thus increases the background signal. The smallest volume of streptavidin beads (20µl) resulted in the least enrichment of biotinylated proteins, which could potentially lead to suboptimal purification of potential proteins. So, for that reason, 30µl streptavidin beads per 360µg protein lysate was chosen to minimise the risk of either low detection or too many non-specific binders and therefore

optimally enriches for specifically labelled proteins generated by APEX2-Ras. Meanwhile, actin was absent from the eluates indicating the specificity of APEX2-Ras as well as the efficiency of the purification steps to achieve the biotinylated fraction.

3.5.4. APEX2 biotinylates Ras effectors

Previous results confirmed efficient transfection of the APEX2-Ras construct into HeLa S3 cells, which was then expressed as fusion proteins that were capable of biotinylation once supplemented with BP and H_2O_2. However, the specificity of this biotinylation reaction is still unknown. To test whether this biotinylation is not random and occurs predominantly within the close vicinity of Ras, detection of proteins associated with Ras were used as positive markers. Using the previously optimised conditions, biotinylation of Ras effectors: PI3K and B-Raf were tested.

Figure 3.8| Specific biotinylation of Raf and PI3K – Lysates from serum-starved and stimulated APEX2-NRAS WT transfected cells underwent enrichment for biotinylated proteins. Input (I), flowthrough (F) and pulldown (P) samples were blotted for PI3K, B-Raf and NRAS (left). Schematic (right) shows the biotinylation reaction within 30 seconds.

As shown by Figure 3.8, pulldown of well-known Ras effectors: PI3K and B-Raf indicated that the APEX2-NRAS WT fusion protein was able to biotinylate relevant proteins that interact with Ras. The pulldown lanes show that within the enrichment of biotinylated proteins that NRAS was detected and therefore reaffirming that the neighbouring APEX2 enzyme was close enough to biotinylate Ras. Additionally, Ras effectors such as PI3K and Raf were also biotinylated and appear to be more abundant in the stimulated samples versus serum-starved, which is to be expected since recruitment of Ras effectors occurs following Ras activation. From this experiment, there is confidence that the APEX2-Ras fusion

proteins are functioning correctly, and the previously optimised conditions would be suitable for a larger-scale application to different Ras isoforms and active states.

3.6. DISCUSSION

In recent years, proximity labelling has been a popular technique for studying protein-protein interactions. They carry advantages over conventional methods as they preserve interactions within a living cell and allow for the detection of transient and weak interactions as well as associated proteins. At the beginning of this project, no studies had used proximity labelling to investigate the Ras interactome, therefore it was of interest to use this novel approach to provide insights into potential interactions that have been previously missed by conventional methods. The benefits of it being a wide screening tool makes it easier to investigate multiple conditions such as different isoforms and activation states. More importantly, it has the capability to capture interactions at the plasma membrane which are fundamental for Ras signalling but are normally disrupted due to cell lysis.

In this chapter, the APEX2 technique was established to study the Ras interactome at the plasma membrane with aims to highlight any potential regulators of Ras nanoclustering. Here, it has been demonstrated via sequencing as well as on a protein-level that all designed constructs were functional and correctly targeted in living cells. This was facilitated in the following experiments that were required to optimise the methodology. The first set of experiments sought to generate a model that represented 'active' Ras to allow for comparisons between both active and non-active Ras protein microenvironments to then identify any specific proteins which regulate the different signalling platforms on the plasma membrane. In this experiment, FBS was used as it consists of multiple growth factors, which activate Ras via the RTK pathway (Gstraunthaler, 2003). High activity levels of Ras effectors: ERK, MEK and Akt were observed at 5 minutes, suggesting this timepoint to be the optimal model for 'active' Ras. This is similar to previously reported, where peak MEK and Akt activity occurred after 5 minutes of EGF stimulation in PC12 cells and HEK293 cells, respectively (Traverse *et al.*, 1992; Borisov *et al.*, 2009). Aside from static snapshots

of effector activity using western blots, single-cell analysis has also demonstrated that the average pERK activity similarly reaches a maximum between 5-10 minutes in PC12 cells. Interestingly, it highlighted heterogeneity in activity occurred amongst the cells in response to EGF stimulation (Ryu *et al.*, 2015). Overall, current literature in support with data generated here provides evidence that the 5-minute stimulation will be sufficient to capture the active state of Ras during the transient activation period. It is also important to note that the concentration and composition of different growth factors affect the stimulation dynamics, therefore the same batch of FBS should be used for subsequent experiments.

Initially, APEX was recommended for the study of compartments within mammalian cells and many original papers were indeed done in membrane-enclosed organelles such as mitochondria and ER (Hung *et al.*, 2017). However, over the years its use has expanded to different model organisms such as yeast (Hwang and Espenshade, 2016) and *Drosophila* (Mannix *et al.*, 2019), as well as in non-membrane enclosed regions like the primary cilia (Mick *et al.*, 2015) and mitochondria nucleoid (Han *et al.*, 2017). The success of APEX in non-enclosed regions showed promise for its use to study Ras at the plasma membrane. However, this required alterations to the original APEX2 method previously described by Hung *et al*, so that it would be suitable for studying open regions (Hung *et al.*, 2016). Modifications to the biotinylation process was needed due to the likelihood of more non-specific labelling as a result of the larger proteome microenvironment. Despite most APEX2 protocols using 1 minute reaction windows (Hung *et al.*, 2016; Han *et al.*, 2017), it was shown here that 30 seconds of H_2O_2 generated sufficient biotinylation. The same duration was used in the study of GPCRs, where they were also investigating dynamic events (Lobingier *et al.*, 2017). It is postulated that shorter reactions would result in a smaller population of biotinylated proteins and consequently reduce the number of non-Ras associated binders. Additionally, it could be speculated that reducing the incubation time would give a better snapshot of the dynamic events during nanoclustering. Given the shortened reaction window and thus reduced number of biotinylated proteins, it was expected that there would also be a change to the ratio of streptavidin beads to lysate.

However, further experimentation indicated that the originally stated amount would be optimal. Lastly, using the optimised conditions, a preliminary small-scale enrichment was carried out to test if known Ras interactors were present in the selectively isolated population of biotinylated proteins. The results demonstrated that PI3K and B-Raf were efficiently detected and differences could be seen between the unstimulated and stimulated Ras.

These initial experiments have demonstrated that the fusion of APEX2 to Ras does not appear to affect Ras localisation or activity and vice versa, Ras does not seem to alter APEX2 function. Having generated a number of APEX2-Ras constructs consisting of the three Ras isoforms in both their WT and G12V mutant forms, as well as a model for active and non-active Ras, the different conditions required for large-scale experiments to investigate the proximity proteome had been established. Furthermore, modifications were made to the APEX2 method so that it was more applicable for the study of open regions. Preliminary results showed that APEX2 was able to biotinylate known interactors of Ras, indicating that APEX2 is a suitable enzyme to screen the Ras interactome and has the potential to capture novel interactions.

CHAPTER FOUR

Using APEX2 to screen the Ras interactome

4.1. INTRODUCTION

Ras nanocluster formation result from the complex interplay between the plasma membrane and Ras. Here, Ras isoforms laterally segregate into non-overlapping nanoclusters, which are also GDP/GTP-dependent (Janosi *et al.*, 2012). This process is required to expose Ras to a suitable proteome and lipidome microenvironment, which favour interactions that lead to downstream Ras signalling (Prior *et al.*, 2003). The plasma membrane is highly heterogenic and consists of different microdomains such as lipid rafts (Prior *et al.*, 2001) or caveolae (Ariotti *et al.*, 2014), which have shown to be important for Ras nanoclustering. Other components such as scaffold proteins, lipid composition and actin also affect nanocluster formation and therefore are crucial determinants of Ras signalling (Plowman *et al.*, 2005; Zhou *et al.*, 2014).

Actin aids Ras nanoclustering via its interaction with the plasma membrane, whereby it facilitates the formation and maintenance of these nanodomains (Plowman *et al.*, 2005). Similarly, cholesterol is another vital component of Ras nanoclustering, its presence has shown to be required for the localisation of HRAS-GTP and NRAS-GDP, whereas HRAS-GDP and NRAS-GTP is cholesterol-independent (Prior *et al.*, 2001). Other lipid species that make up the plasma membrane also vary depending on the isoform and nucleotide state. Examples include: PS, PA, PIP_2, PIP_3, PI_3P and PI_4P (Zhou *et al.*, 2014). One study highlighted that all these lipids were present in KG12V, HG12V and tH nanoclusters. PS and PI_4P were more associated with HRAS, whilst tH appeared to be more enriched for PIP_2 and PI_3P than HG12V. Also, PA was more abundant in HG12V nanoclusters. Whereas, KG12V nanoclusters displayed lower concentrations of PS and PI_4P compared to HRAS but higher amounts of PA (Zhou *et al.*, 2014). Therefore, highlighting the complexity of the lipid microenvironment of Ras.

In terms of scaffold proteins, a few have been identified for the Ras pathway such as KSR (Therrien *et al.*, 1995, 1996), AF6 (Kuriyama *et al.*, 1996) and IQGAP1 (Matsunaga *et al.*, 2014). However, only a few scaffold proteins like Gal-1 (Belanis *et al.*, 2008), Gal-3

(Shalom-Feuerstein *et al.*, 2008), NPM (Inder *et al.*, 2009) and ASPP2 (Posada *et al.*, 2016) have shown to affect Ras nanoclustering. Gal-1 is recruited to the plasma membrane where it interacts with activated HRAS and plays an integral nanocluster component that stabilises the HRAS-GTP nanoclusters (Belanis *et al.*, 2008). Similarly, Gal-3 is recruited from the cytosol to the plasma membrane by KRAS-GTP, where it is involved in the formation and stabilisation of KRAS-GTP nanoclusters (Elad-Sfadia *et al.*, 2004; Shalom-Feuerstein *et al.*, 2008). NPM also specifically interacts with KRAS at the plasma membrane, where it enhances KRAS clustering and activation of MAPK (Inder *et al.*, 2009). Whilst, pan-Ras scaffold protein, ASPP2 increases nanoclustering of all oncogenic Ras G12V isoforms (Posada *et al.*, 2016).

Evidently, Ras nanocluster formation requires input from different types of lipid and protein. These vary depending on the type of Ras isoform present and whether GDP or GTP-bound (Prior *et al.*, 2003). To date, regulation of Ras nanoclustering at the plasma membrane is not very well understood. Since localisation is key to Ras activity, which is fundamental for certain cancer types (Mo, Coulson and Prior, 2018), its crucial to understand its localisation at the plasma membrane and identify regulators that are involved. Elucidating the different protein microenvironments in which these nanoclusters function would provide insight into potential regulators of Ras nanoclustering and subsequently, Ras signalling. The identification of such regulators could be beneficial as alternative pharmacological targets that prevent Ras signalling via abrogation of Ras nanoclustering, since direct inhibition of Ras has shown to be problematic (Brock *et al.*, 2016).

Previous to the use of proximity labelling methods, it would have been likely that purification of the plasma membrane would be required to investigate these types of interactions (Roy *et al.*, 1999; Prior *et al.*, 2001). However, the purification process often introduces contaminants and disrupts interactions. Whereas, traditional methods of proteomic analysis of co-IP carries a bias for strong interactions (Koide *et al.*, 1993; Song *et al.*, 1996a). Therefore, the availability of proximity labelling methods such as APEX2 has

been beneficial as it allows for an unbiased proteomic screen of proteins in close proximity of Ras in intact living cells, therefore allowing detection of both weak and strong, direct and indirect interactors (Lam *et al.*, 2015).

To identify the different Ras proteome microenvironments, the three Ras isoforms: KRAS, HRAS and NRAS were studied using the conditions optimised from the previous chapter. The ease of APEX2 to widely screen the proteome makes it possible to compare multiple conditions. This is advantageous as evidently from previous studies, different Ras isoforms and activation states dictate the type of nanocluster formed. Therefore, different models will be generated to represent these conditions. Ras isoforms: KRAS4B WT, HRAS WT and NRAS WT as well as their G12V mutant forms will be used. In addition, for each WT condition, to mimic the effects of being GDP or GTP-bound, Ras will be either serum-starved or stimulated with FBS. The large number of samples as a result from the different conditions meant it would not be possible to do stable isotope labelling by amino acids in cell culture (SILAC) and therefore label-free mass spectrometry will be used instead.

As a main control, each Ras WT isoform sample will also only be treated with BP and not with H_2O_2, i.e., no biotinylation reaction, to account for any non-specific binders. For additional controls, to aid the identification of predominantly plasma membrane proteins, APEX2 only and tK and tH were used to produce proximity lists of cytosolic and membrane proteins, respectively. Specifically, tK and tH localise in cholesterol-independent and cholesterol-dependent nanoclusters, respectively (Janosi and Gorfe, 2010; Janosi *et al.*, 2012). In this chapter, different Ras proximity proteomes will be investigated with APEX2 to generate a list of hits that could aid the elucidation of possible Ras nanocluster regulators.

4.2. AIMS

4.2.1. To validate APEX2 as a method for screening the Ras interactome.

Preliminary data from the small-scale experiments illustrated that APEX2 could be a suitable tool to screen the Ras interactome, therefore it will be reviewed whether this will be reflected among the mass spectrometry data.

4.2.2. To observe protein networks of different Ras isoforms and active states.

Protein lists generated from the multiple conditions will allow for comparisons between the different protein microenvironments to identify any isoform- or active-specific proteins and/or universal proteins that are relevant for the general Ras interactome.

4.2.3. To produce a shortlist of potential regulators of Ras localisation.

Amongst the generated data, top hits will be selected to shortlist proteins that could potentially regulate Ras localisation and therefore be used for further analysis.

4.2.4. To compare APEX2 to BioID studies.

Validation of the APEX2 dataset generated here via comparisons with other Ras interactomes produced by other proteomic studies could provide insight to the accuracy of the APEX2 data as well as an evaluation of the proximity labelling methods.

4.3. APEX2 AS A METHOD

4.3.1. Experimental setup

For the large-scale experiment, 21 samples were prepped using different Ras isoform constructs and conditions for mass spectrometry (*Fig. 4.1*). Samples included APEX2-tagged KRAS WT, KG12V, HRAS WT, HG12V, NRAS WT and NG12V. In addition, APEX2 alone and APEX2-tagged tK and tH were used as controls.

The main control used for these mass spectrometry experiments was the no H_2O_2 control, which distinguishes between biotinylated and non-biotinylated proteins. In addition, other potential controls: APEX2 only, tK and tH were tested. These controls would essentially act as negative and positive markers respectively and therefore help narrow the shortlisting process to produce a list of membrane-enriched proteins that associate with Ras. The free-flowing APEX2 would act as a negative control and eliminate any non-plasma membrane targeted cytosolic proteins, whereas the tK and tH would act as positive markers of the plasma membrane where the respective Ras molecules localise.

For each Ras isoform, there were 4 conditions: WT control (no H_2O_2 treatment, i.e., no

biotinylation, CON), WT serum-starved (no serum media for 5 hours prior lysis, SS), WT stimulated (serum-starved for 5 hours followed by 5-minute stimulation with 20% FBS before lysis, STIM) and G12V (the mutant G12V form of the Ras isoform in normal 20% FBS supplemented media, G12V). Each sample underwent transfection, treatment with BP and H_2O_2 (or without for control) followed by cell lysis. Resulting lysates were subjected to avidin-based pulldown and ran on a polyacrylamide gel. Peptides were extracted using in-gel digest and analysed by mass spectrometry.

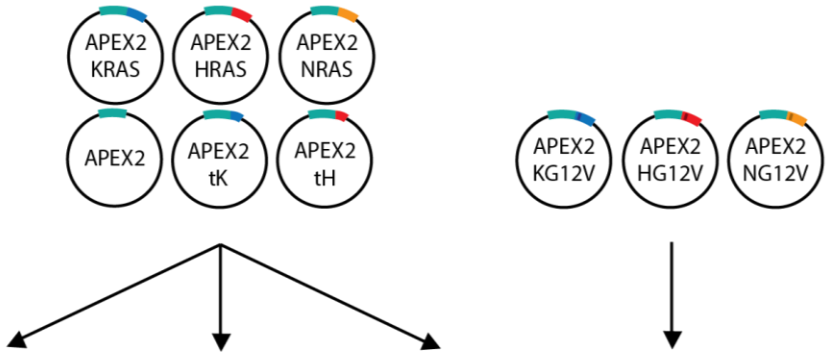

Condition	Control	Serum-starved	Stimulated	Mutant Ras
Phenotype	WT	WT	WT	G12V
Stimulus	Normal	No serum	+FBS (5 mins)	Normal
H_2O_2	-	+	+	+

Figure 4.1| Schematic of the sample preparation workflow for mass spectrometry – Three different Ras isoforms (WT) along with controls: APEX2 only, tK and tH were transfected into HeLa S3 cells and treated accordingly to generate the conditions: control, serum-starved (no serum for 5hrs) and stimulated (no serum for 5hrs followed by 5 min FBS stimulation). The G12V mutant-transfected cells were kept in normal media supplemented with 20% FBS.

4.3.2. Data processing of mass spectrometry data

To analyse the differences between interactomes, the data was processed to a finalised list of proteins detected in each sample. In brief, the LFQ intensities were normalised to the non-

biotinylated samples to identify biotinylated proteins, which were then averaged between the two repeats. These values were log_2-transformed to model any changes in expression proportionately. Then a two-fold limit was set to stringently categorise specifically enriched i.e., biotinylated proteins from non-specifically labelled proteins. Note, with this assay, only increase fold changes were considered and not decreases due to the nature of the no H_2O_2 control. Therefore, any proteins with a value 2-fold greater than control in the KRAS, HRAS and NRAS protein lists were termed 'specific' and listed as a protein present in that specific interactome. Whereas hits with values less than 2-fold were termed 'non-specific'.

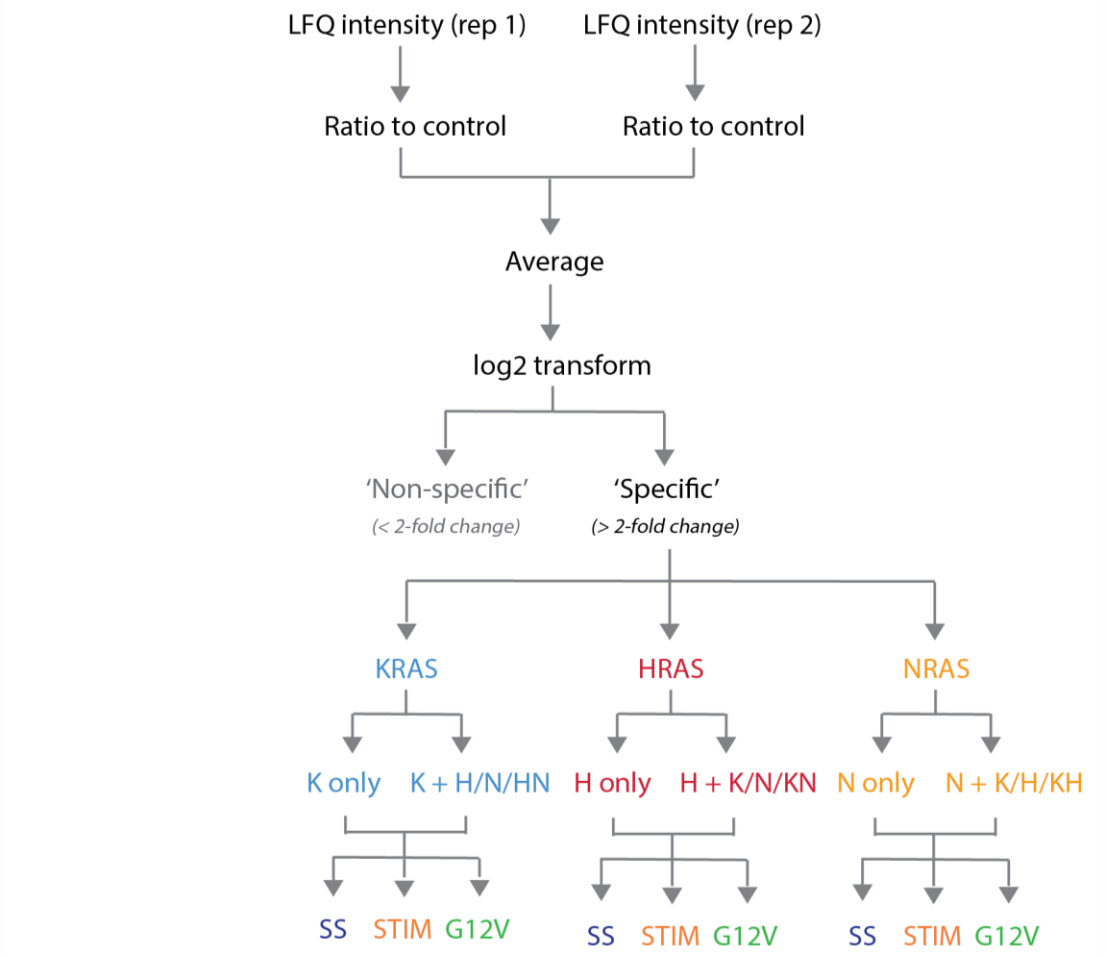

Figure 4.2| Data processing workflow for mass spectrometry results – LFQ intensities generated from MaxQuant used to produce shortlists of specific proteins (>2-fold change compared to no H_2O_2), which were categorised by Ras isoform followed by activation status.

4.3.3. Reproducibility

A total of 5200 proteins (excluding common contaminants) were detected from the two

independent repeats of the 21 samples tested. To check the overall quality of the data, the LFQ intensities between the two experimental repeats were analysed. The graph shown in Figure 4.3a displays a strong correlation (Pearson's correlation = 0.942) between the two sets of LFQ intensities. The little variability between the datasets provides a good indication that the datasets are similar and reproducible. However, only two experimental repeats were performed here due to the time-constraints so further repeats would be needed.

4.3.4. Specificity

Mass spectrometry analysis revealed a total of 5200 hits were detected, in terms of K, H and N, 2212 of these proteins were non-specific i.e., proteins detected in the no H_2O_2 control and 2988 proteins were found to be specific for K, H or N (*Fig. 4.3b*). In order to classify whether a hit was specific for a particular isoform, a 2-fold change in either one of the conditions: serum-starved, stimulated or G12V was required. Due to the classification of non-specific hits as less than 2-fold change, it is difficult to speculate whether there were a high number of non-biotinylated binders during the pulldown process or that many biotinylated binders were not considered to be 'specific' due to being lower than the chosen threshold.

The total number of specific hits for each Ras isoform and controls are displayed in Figure 4.3c. KRAS and NRAS have a similar number of hits (1610 and 1493, respectively), whereas fewer proteins were detected in HRAS (1117). As expected, a smaller number of proteins were detected in the truncated versions of KRAS (1117) and HRAS (903). The least number of proteins was detected in the APEX2 only control (888). The specific hits can be further subcategorised into whether these hits were distinctive to one Ras isoform or shared amongst the other isoforms (*Fig. 4.3b*). Interestingly, KRAS and NRAS samples shared more associated proteins than with HRAS, which seems to be more linked to KRAS than NRAS. Out of the 2988 proteins detected, only 199 proteins were common to all three Ras isoforms, in fact, majority (42-55%) of the proteins were present only in one Ras isoform. Therefore, the results suggest that each of the three Ras isoforms have a very different protein microenvironment.

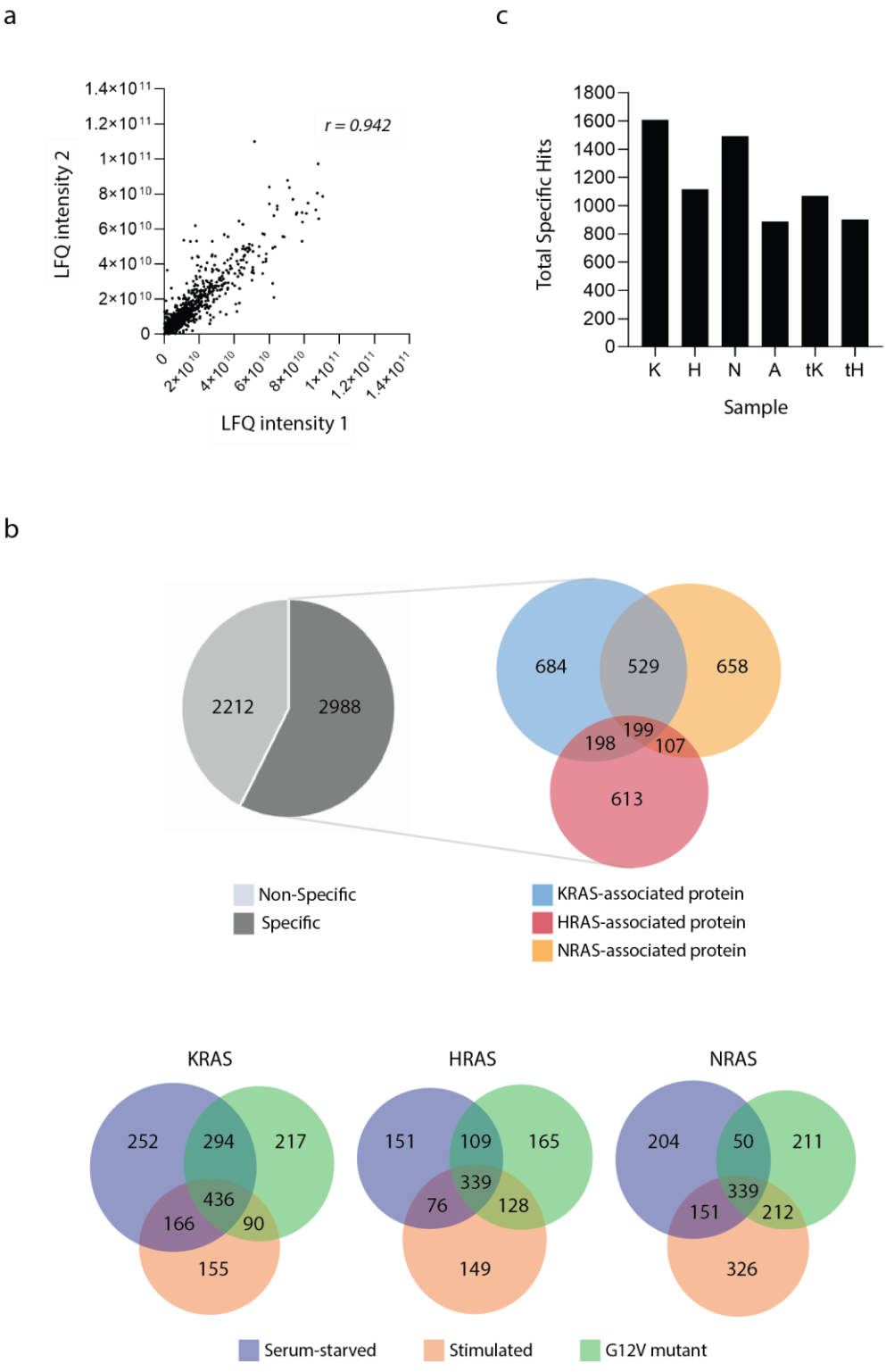

Figure 4.3| **Overview of APEX2 mass spectrometry results** – a) Reproducibility between the two experimental repeats. b) Detected proteins processed into two categories: specific (> 2-fold change compared to control) and non-specific. Specific proteins consist of KRAS-, HRAS- and NRAS-associated proteins, which can be further subdivided into their subsequent conditions: serum-starved, stimulated or G12V mutant. c) Total number of specific hits for each Ras isoform and control.

Each Ras isoform proximity interactome is divided into the three conditions: serum starved, stimulated and G12V mutant (*Fig. 4.3b*). Results showed that 27.0%, 30.3% and 22.7% of the total hits were shared by all the conditions in KRAS, HRAS and NRAS, respectively. This indicates that these hits could potentially form the core interactome for each of the Ras isoforms. It was predicted that G12V and stimulated would share a higher proportion of the interactome, which appears to be the case in HRAS and NRAS but not in KRAS, whereby more similarities were seen between serum-starved and stimulated. NRAS displayed the most commonality between the G12V and stimulated condition (212). This suggests that despite both conditions being a model of 'active' Ras, these two interactomes are more diverse than expected.

In addition, there were fewer proteins present in the stimulated condition than in the serum starved and G12V samples in KRAS, which was surprising as it would be expected that more proteins would be recruited when active. However, the opposite was true for NRAS, whereby the stimulated condition generated more hits than the other two conditions. Whereas, for HRAS, a similar number of unique proteins were detected per condition. Therefore, as a gross overview, it appears that the proximity interactome varies by different degrees dependent on the isoform and condition. For example, mutant KRAS and inactive KRAS proteomes share more similarities, whilst mutant HRAS and NRAS are more alike to stimulated HRAS and NRAS, respectively.

4.3.5. Ras interactors

To check the validity of the dataset, a list of Ras interactors was generated using STRING. The top 50 interactors with high confidence (score >= 0.7) for KRAS, HRAS and NRAS in humans using experiment and database sources were compiled into a list of 76 unique Ras interactors. From this list, 42 interactors were found in our dataset (55.3%), of which 29 were specific for K, H or N and 13 were either non-specific or detected in only controls: tK and/or tH (*Fig. 4.4a*). The breakdown of the number of identified Ras interactors in each sample can be seen in Figure 4.4b.

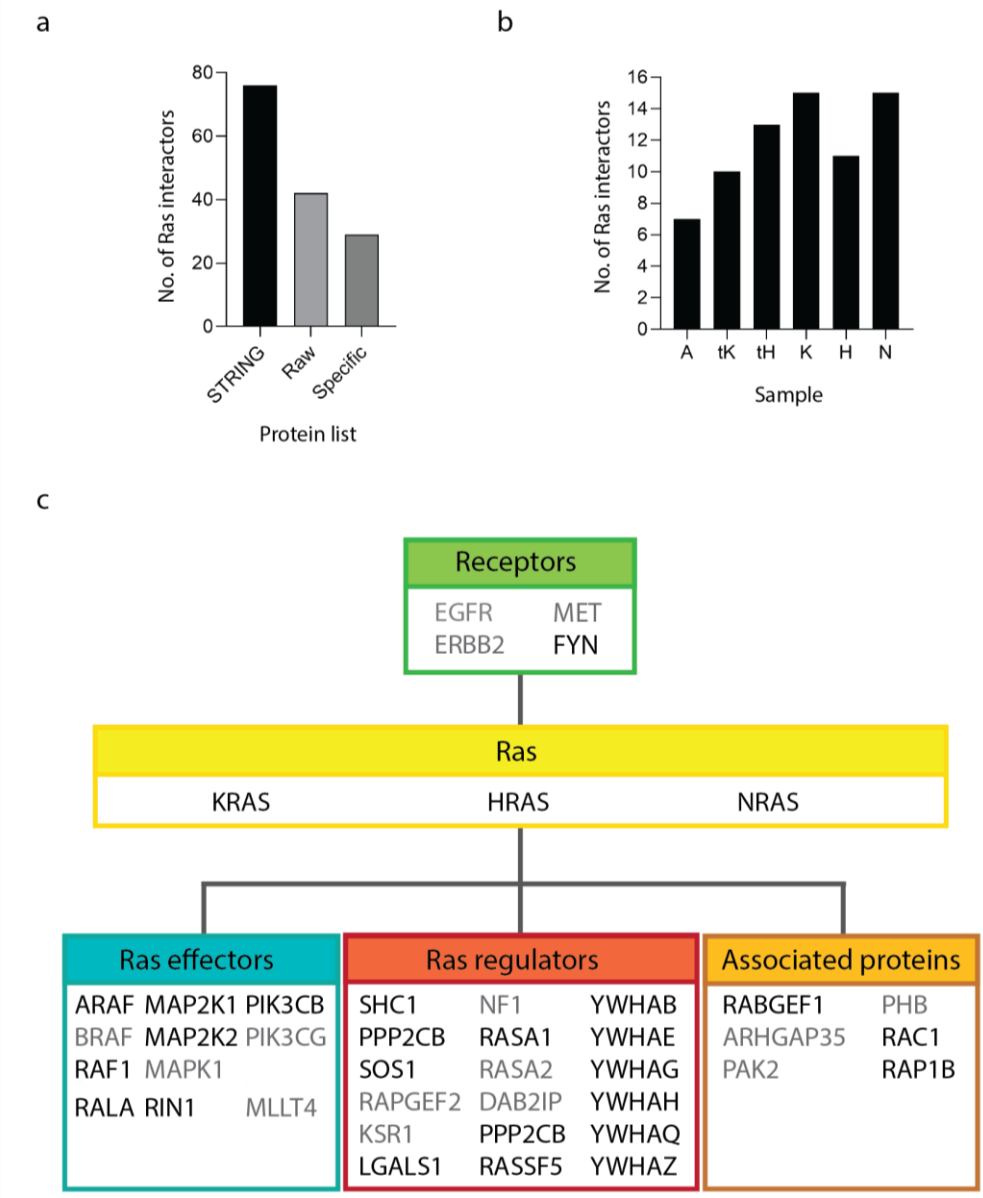

Figure 4.4| Identification of Ras interactors within the Ras-proximal proteome network – Bar charts displaying number of Ras interactors identified in a) STRING versus different protein lists generated here as well as b) a breakdown of these for the different samples. c) Schematic of known Ras interactors detected in the mass spectrometry data. Those listed in black highlight the presence of Ras interactors within the specific K, H, N databases versus hits that were non-specific (grey).

The first key observation is that KRAS, HRAS and NRAS were detected in their respective samples and therefore APEX2 was correctly localised close to Ras in these samples. Secondly, Ras interactors were identified in the dataset and thus relevant proteins were biotinylated in these APEX2 experiments. Thirdly, the Ras isoforms and truncated Ras

markers all consisted of a higher number of Ras interactors compared to the negative non-Ras control, APEX2 only. Although, it is interesting to note that BRAF, PI3KCG, RAC1, PAK2, MAP2K1, MLLT4, RASA2 were all present in the APEX2 only sample, which could suggest its wide presence within the cell might not make it a suitable negative control as it might eliminate potential candidate proteins. Nevertheless, Ras was not detected in the APEX2 control, which indicates that the specific localisation of Ras might have minimised its chances of being non-specifically labelled by free APEX2.

All three Ras isoforms were present in the KRAS sample. But for HRAS and NRAS, only two Ras isoforms were detected in each sample, KRAS and HRAS in the HRAS only sample; HRAS and NRAS in the NRAS only sample. Intriguingly, both HRAS and NRAS were detected in the tK and tH controls, but KRAS was not present in either. Since KRAS was not labelled in the tK control but in the vicinity of the other two Ras isoforms, it is possible that precise localisation of KRAS requires the additional signals that could be provided by its full-length sequence. Identification of the respective Ras isoform and interactors in each sample confirmed that Ras has been efficiently biotinylated, which subsequently should lead to the specific labelling of relevant proteins within the vicinity.

4.3.6. Proteome enriched for Ras signalling and plasma membrane proteins

The detection of known Ras interactors highlighted the potential for the enrichment of other Ras-associated proteins in the detected proteomes for each of the Ras isoforms, Here, biological processes and cellular components associated with the total specific datasets were investigated via Gene Ontology (GO) enrichment analysis using the DAVID 6.7 database with an ease score of 0.1 and count of 2. The total specific dataset lists ($_T$) were used here to give an overview of the overall function and localisation of the Ras isoforms, whereas later, assessment of hits present in only one of the isoforms ($_O$) was used to identify proteins/functions/localisation unique to that isoform.

The total specific datasets of KRAS (K_T), HRAS (H_T) and NRAS (N_T) revealed that all three Ras isoforms were enriched for Ras protein signalling as well as other processes that might

be relevant to nanocluster formation such as actin cytoskeleton and membrane organisation proteins. Similarly, small GTPase mediated signalling was also found to be a significant biological process in KRAS and NRAS, in particular, components involved in Rho protein signalling were detected in KRAS. The absence of these pathways in the APEX2 only control signifies that the enrichment of Ras-related proteins is only present in the relevant Ras samples. Aside from these Ras-related roles, more general processes such as DNA replication, translation, protein transport and stress response were also enriched in all three Ras isoforms. In general, the enriched biological processes appear to be very similar amongst the different isoforms, with the exception of small GTPase mediated signalling, which was absent in HRAS. Additionally, Rho protein signalling, and protein ubiquitination were only present in KRAS and NRAS, respectively. The detected interactomes of tH and tK had similar enrichments as their full-length counterparts, however Ras protein signalling was not present in tK. As shown previously, KRAS was not present in tK, therefore it could be speculated that the lack of KRAS could result in inaccurate localisation and subsequently, an absence of relevant Ras signalling proteins. Nevertheless, APEX2-labelling has shown to effectively capture the functionality of the Ras interactomes.

Fundamentally for this project, the aim is to identify regulators of Ras nanoclustering at the plasma membrane, therefore it is crucial to detect proteins associated with the plasma membrane. Using GO analysis, the cellular localisation of the detected proteins was assessed. As shown by Figure 4.5, the labelled proteins were detected widely around the cell and found to be significantly associated with several components of the cell: plasma membrane, cytoskeleton, cytosol, mitochondria, ER, ribosomes, and nucleoli. Its ubiquitous expression within the cell is not surprising, since it is known that Ras can traffic and signal from various endomembranes (Choy *et al.*, 1999; Rebollo, Pérez-Sala and Martínez-A, 1999; Chiu *et al.*, 2002; Lu *et al.*, 2009). Therefore, it is possible that APEX2 labelling occurs at various timepoints among these locations. The result showed a significant enrichment of endosomal and ER proteins in KRAS and NRAS. It is interesting that these proteins were not as abundant in HRAS, since there is substantial evidence that HRAS can

localise and signal from these different endomembranes (Apolloni *et al.*, 2000; Chiu *et al.*, 2002; Roy, Wyse and Hancock, 2002). More surprisingly, for all three Ras isoforms, proteins associated with the Golgi apparatus appeared to be absent, which is particularly unexpected for HRAS and NRAS, since these isoforms are commonly known to be palmitoylated in the Golgi (Laude and Prior, 2008).

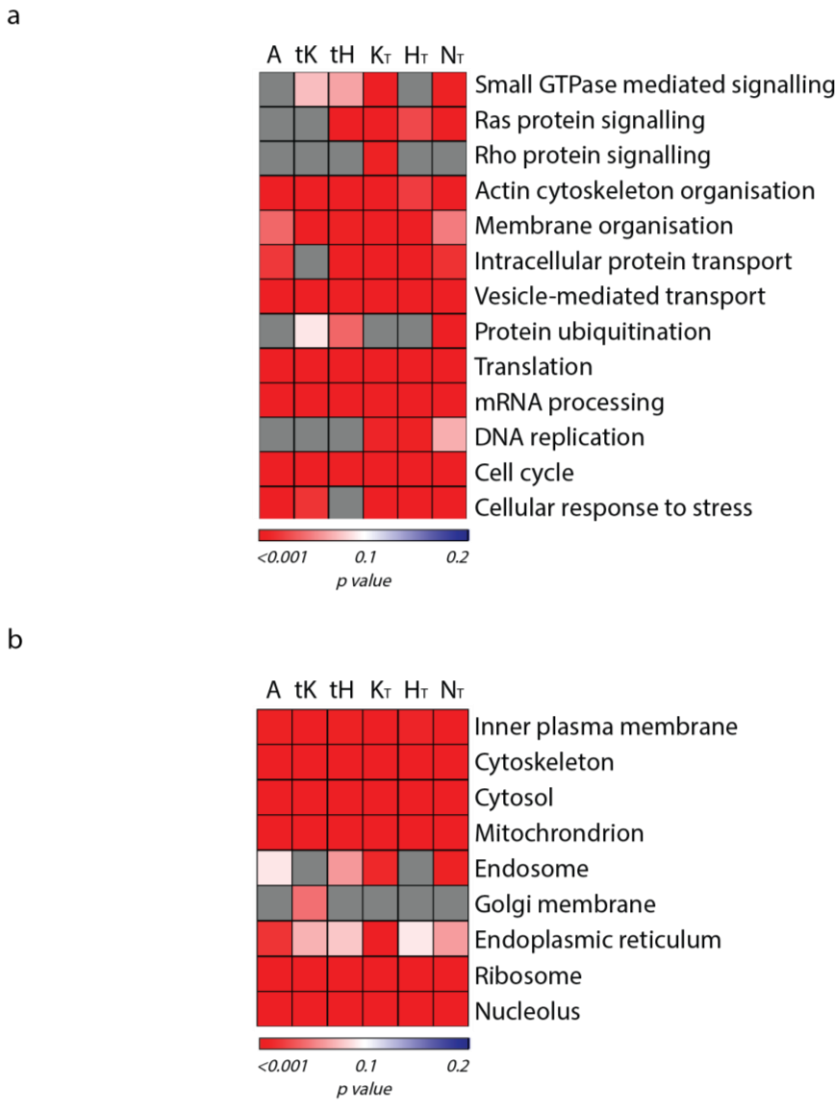

Figure 4.5| GO enrichment analysis of the total specific hits – Datasets of total specific hits ($_T$) of all three Ras isoforms and the controls: A, tK and tH were represented by their a) biological function and b) cellular components. Colour intensity represents the enrichment *p* value.

To conclude, there was a significant enrichment of plasma membrane proteins amongst the total specific datasets, which indicates that a large proportion of APEX2-Ras molecules

localised to the plasma membrane where interactions with potential regulators could have been detected. The GO analysis did however also reveal the noise associated with this type of methodology, which would need to be addressed with additional localisation controls in future experiments.

4.4. PROFILING THE RAS INTERACTOMES

Preliminary analysis has shown promising results that APEX2-Ras labels proteins in the vicinity, which are relevant to Ras biology. Despite the widespread labelling throughout the cell, there was still an enrichment of plasma membrane proteins in the Ras samples, which could be potential regulators. The three Ras isoforms have different signalling platforms on the plasma membrane, which aside from the G-domain and C-terminal membrane anchors, also require additional proteins to facilitate their specific localisation (Belanis *et al.*, 2008; Shalom-Feuerstein *et al.*, 2008; Posada *et al.*, 2016). Dissection of the different Ras interactomes could elucidate proteins unique to each isoform and/or condition. This will aid the shortlisting process to highlight potential hits that could play a role in Ras localisation.

4.4.1. Isoform-dependent interactomes

In the previous section, total hits in each isoform i.e., any hits identified in that isoform irrespective of appearing in other isoforms were used for analysis. However, to investigate the isoform-specific hits (denoted by $_o$), the total hits were categorised into hits that occurred exclusively in one isoform. Hits present in two or all three isoforms were also displayed to show the full dissection of the dataset (*Fig.4.6*). With this breakdown, comparisons could be made between unique proteins present in each isoform (K_o, H_o, N_o) as well as any shared amongst two isoforms or common to all three isoforms.

Analysis of the biological functions amongst these isoform-specific datasets revealed that the hits responsible for the Ras protein signalling enrichment seen previously in all three isoforms was not unique to each isoform and are due to the combinations of proteins found amongst the different Ras isoforms. Interestingly, K_o and H_o were significantly enriched for proteins involved in membrane organisation and more importantly, these proteins were

different between the two isoforms. This raises the question whether these differentially expressed proteins play a role in its localisation.

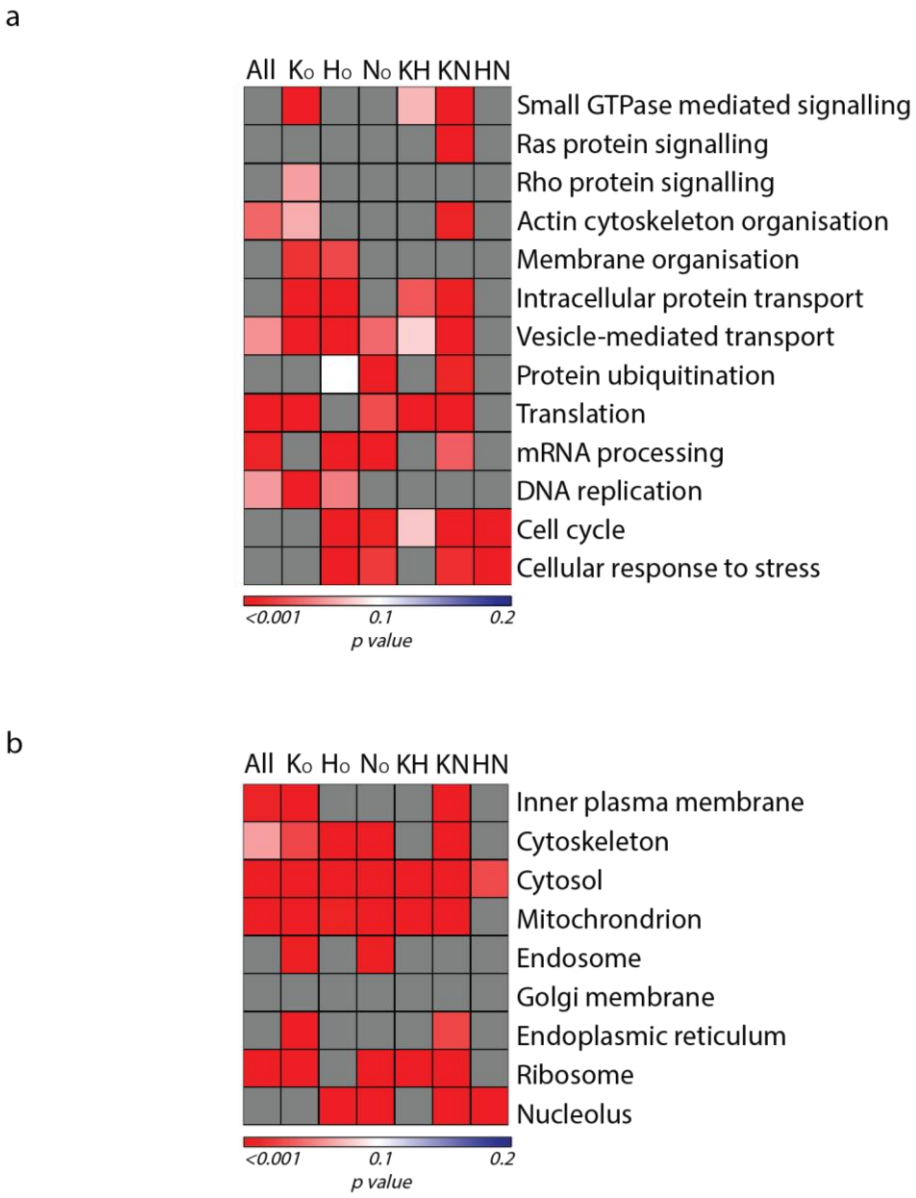

Figure 4.6| **Dissection of isoform-specific proximity proteins** - Heatmap of GO enrichment analysis of hits present in one ($_o$), two or all three Ras isoforms.

The cellular component analysis revealed that proteins common to all three Ras isoforms were enriched for inner plasma membrane proteins. Significant enrichment of these types of proteins were also present exclusively in KRAS as well as in both KRAS and NRAS. From literature, it is known that HRAS and NRAS undergo an exocytic pathway to the plasma membrane via the ER and Golgi, however, proteins associated with these components were

not present in either isoforms nor in the collective group of HRAS and NRAS (HN) (Choy *et al.*, 1999; Apolloni *et al.*, 2000). Overall, it appears that the majority of enriched plasma membrane proteins were shared amongst all isoforms, which could suggest that these different Ras molecules localise closely to each other at the plasma membrane. It is also possible that APEX2 does not have the resolution to distinguish the differences between the different nanoclusters due to their close proximity.

4.4.2. Activation-dependent interactomes

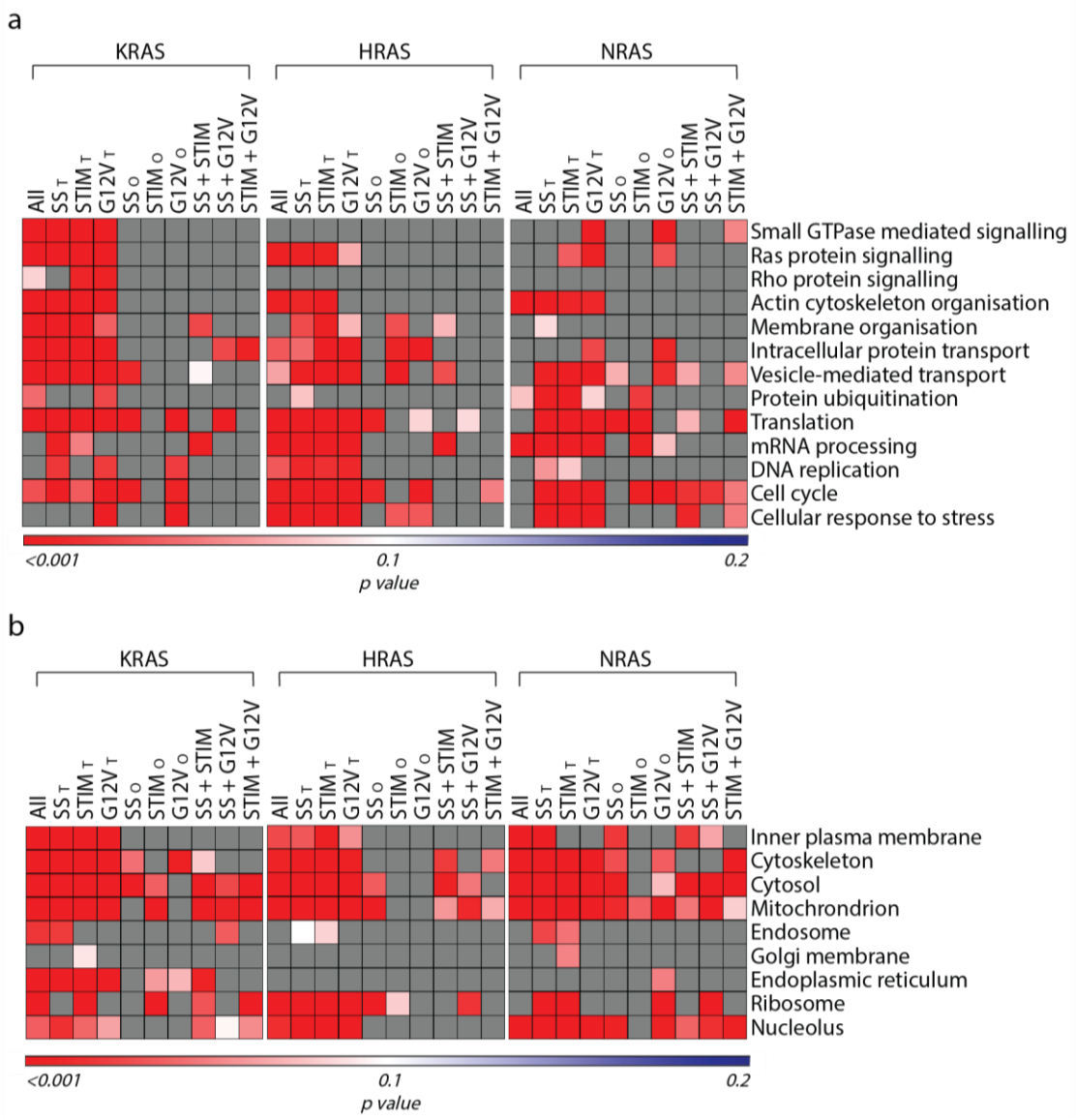

Figure 4.7| **Interrogating proximity proteomes of different activation states** – The effects of serum-starvation, stimulation and the G12V mutation on Ras a) function and b) localisation was investigated using GO enrichment analysis.

Next, the effects of differential activation on Ras signalling and localisation were investigated. Similar to the isoform analysis, each isoform ($_T$) was divided into unique hits for each of the conditions: serum-starved, stimulated and G12V (*Fig. 4.7*). As mentioned previously, the serum-starved condition represented inactive GDP-bound-Ras, whereas stimulated and G12V models active GTP-bound Ras.

Initial findings show that all conditions in KRAS and HRAS were significantly enriched in Ras protein signalling. These hits do not appear to be unique to each of the individual conditions, therefore suggesting that the proteins enriched for Ras protein signalling were predominantly shared amongst both active and inactive Ras. It is possible that the expression levels of these proteins differ between the nucleotide states, however due to the nature of overexpression, exact quantification was limited. Unlike KRAS and HRAS, Ras protein signalling only appears to be significant in active Ras conditions in NRAS. This highlights a possibility that the NRAS proximity proteome varies more considerably with its state of activity compared to other isoforms.

A significant association of inner plasma membrane proteins were present in the collective conditions for each Ras isoform, however none appeared to be unique to a specific condition (with the exception of serum-starved NRAS). Interestingly, there did not appear to be an increased enrichment of plasma membrane proteins in the activated conditions (i.e., STIM and G12V) compared to the serum-starved non-active samples, despite the knowledge that activation of Ras leads to the recruitment of additional proteins to the plasma membrane (Simanshu, Nissley and McCormick, 2017).

4.4.3. Shortlisting of proteins for validation

Analysis revealed that APEX2 in combination with a dynamic protein like Ras generated extensive labelling around the cell. Also, due to the nature of the experiment, accurate comparisons of protein expression levels could not be made. The majority of the enriched plasma membrane proteins did not appear to be isoform nor activation state specific and instead were commonly found to be shared amongst these conditions. The high amount of

labelling of these proteins and their presence in all conditions provided confidence that these proteins were likely to be in close proximity to Ras, where they might play a role in their biology. Therefore, to shortlist proteins that could be of potential interest to Ras nanoclustering, top hits specific for all different conditions were investigated.

A total of 17 proteins were found to be specific for all Ras isoforms: KRAS, HRAS and NRAS, as well as for all three conditions: serum-starved, stimulated, and mutant (*Fig. 4.8a*). Amongst these hits, Ras-associated proteins: ezrin (EZR), galectin-3 (LGALS3/Gal-3) and Ras GTPase-activating protein-binding protein 2 (G3BP2) were present. Gal-3 is a KRAS scaffolding protein (Shalom-Feuerstein *et al.*, 2008), whereas EZR aids the assembly of a protein complex with Ras and SOS (Geißler *et al.*, 2013). Aside from these types of proteins, other hits included enzyme-, actin- and cell division-related proteins. More importantly, two members from the membrane-binding annexin (ANXA or A) family: ANXA11 and ANXA6 (Grewal *et al.*, 2005) were found to be highly present amongst the Ras proximity proteomes, in particular with KRAS and HRAS. Interestingly, other annexins have also appeared in the datasets. Therefore, annexins could be of interest due to its association with the plasma membrane and its observed proximity to Ras.

In the overall dataset, eight types of annexins were detected: ANXA-1, -2, -3. -4, -5, -6, -7 and -11 (*Fig. 4.8b*). All these annexins appeared to be most abundant in KRAS compared to the other two isoforms. Only ANXA6 and ANXA11 were detected in all Ras isoforms and conditions, whereas ANXA1 and ANXA2 were present in all Ras isoforms but not all conditions. The remaining annexins: ANXA-3, -4, -5 and -7 were primarily identified in KRAS, however the latter two annexins were also associated with NRAS. In most cases, the differences between the conditions for each of the Ras isoforms were often subtle. Altogether, it appears that APEX2 might lack the sensitivity and resolution which might be required for an in-depth quantitative comparison of the different isoforms and conditions. Nevertheless, it has been a valuable tool that has highlighted possible candidate proteins such as annexins which will be investigated further using other experimental methodologies.

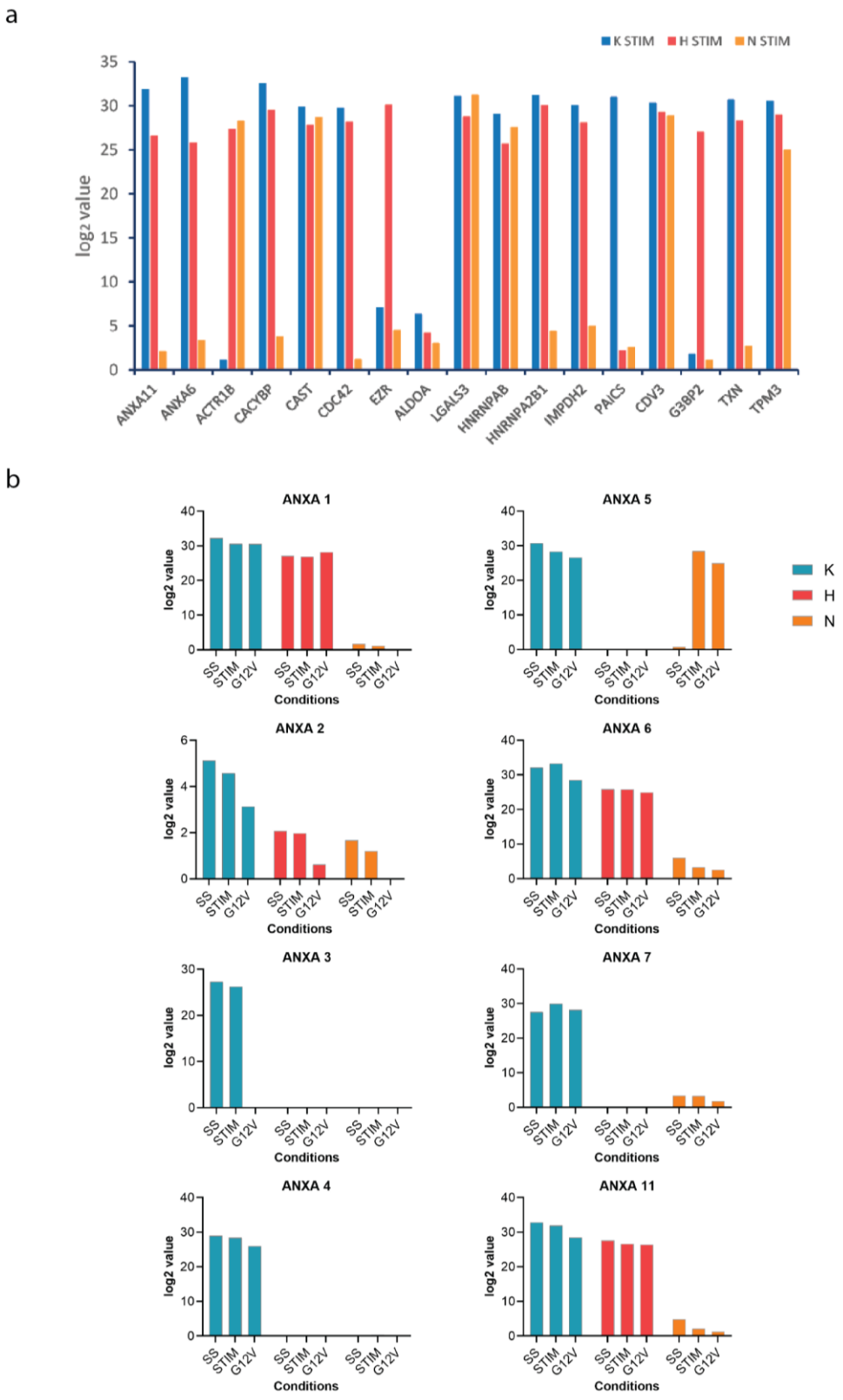

Figure 4.8| **Identification of potential regulators of Ras nanoclusters** – a) Proteins present in all Ras isoforms and activity states represented by their stimulated $\log_2$ value. b) Log_2 values of each Ras isoform and condition are shown for each annexin detected within the APEX2 dataset.

4.4.4. Comparisons to other databases

Proximity labelling has become increasingly popular for screening interactomes, in particular using BioID. In recent years, BioID has been used to study the Ras interactome (Ritchie *et al.*, 2017; Adhikari and Counter, 2018; Kovalski *et al.*, 2019), where these studies focused on identifying therapeutic targets in terms of Ras signalling. However, as of current, no studies have been published using APEX2 to investigate Ras. Therefore, it was of interest to compare the data generated here with the detected interactomes from BioID studies to provide insight into these two methodologies.

Adhikari and Counter investigated the interactomes of oncogenic Ras (G12V) for KRAS, HRAS and NRAS in HEK 293T cells using BioID. In their study, a total of 3148 proteins were detected of which 476 were specifically labelled. Whereas 1984 specific proteins were identified amongst the G12V population in the APEX2 dataset. Between these two datasets, around 115 hits appeared to be common to both (*Fig. 4.9a*). These hits included members of the GTPase family: Rho, Rab and Arf as well as Raf. PIP5K1A was found to be important for KRAS oncogenicity in the BioID study. In concordance, PIP5K1A was also identified in the KG12V and NRAS WT samples in the APEX2 dataset. Therefore, highlighting the capacity of APEX2 to detect hits that were significant in BioID.

The second BioID study by Kovalski *et al* identified the interactomes of KRAS WT/G12D, HRAS WT/G12V and NRAS WT/Q61K in colon (Caco-2)-, bladder (HT-1376)- and skin melanoma (CHL-1)-cancer cell lines, respectively. Here, using their isoform normalised $\log_2$ fold change scores with a cut-off of 4-fold change compared to BirA* control, comparisons were made between their WT data and the combined APEX2 data of serum-starved and stimulated (representing WT Ras) (*Fig. 4.9b*). The overall analysis showed little overlap between the two datasets. Majority of shared proteins for KRAS WT and HRAS WT were related to more general biological processes, whereas hits shared amongst the two databases for NRAS WT were linked to the Ras signalling pathway and plasma membrane. Interestingly, ANXA11 was also detected in their HRAS WT condition.

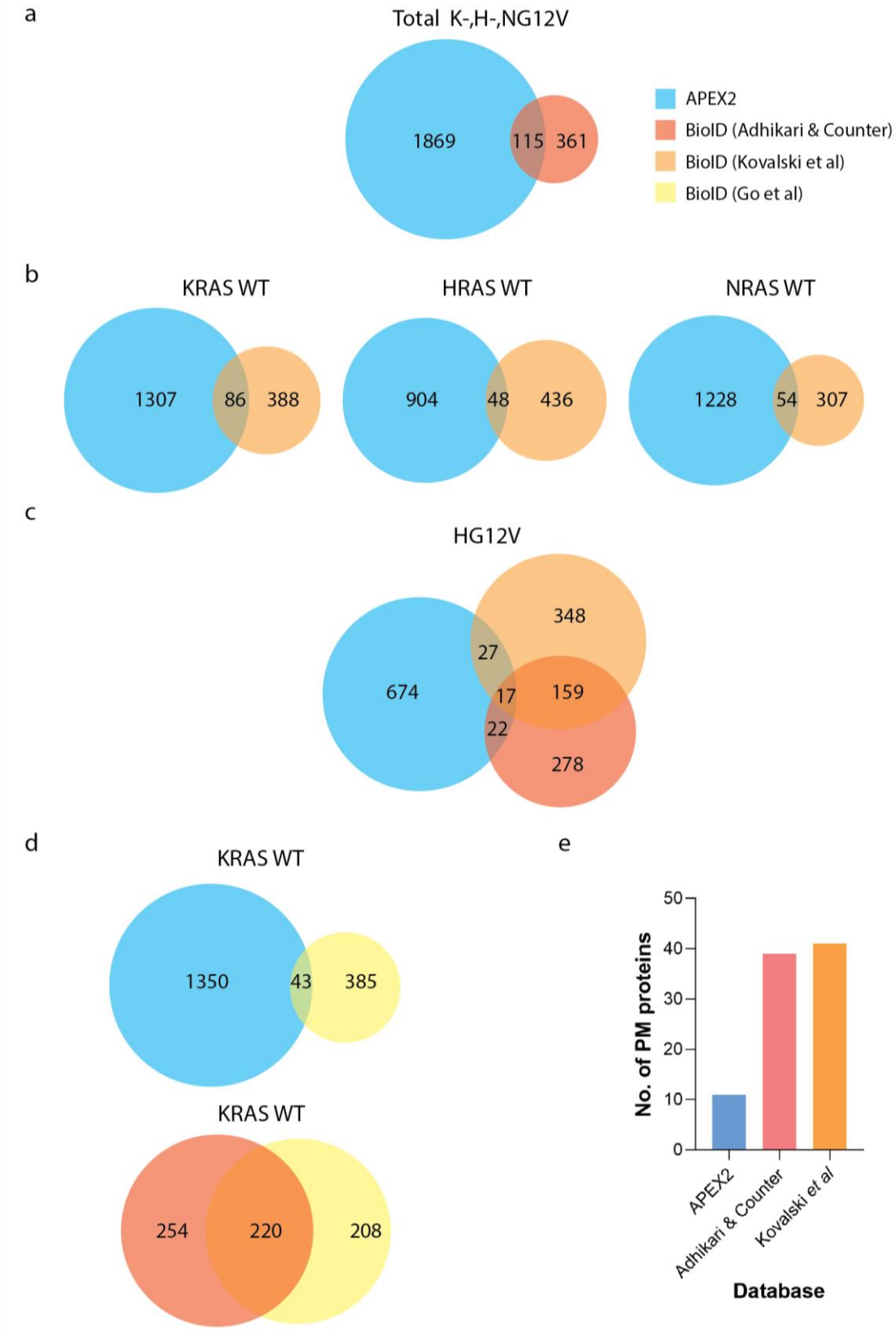

Figure 4.9| **APEX2 vs BioID** – Comparisons made between the APEX2 data and three BioID studies: Adhikari & Counter, Kovalski *et al* and Go *et al*. a) Mutant G12V Ras isoforms. b) WT Ras isoforms. c) HG12V. d) KRAS WT vs tK. e) HG12V vs plasma membrane (PM) proteins.

Presence of the HG12V condition in two of the BioID studies made it possible to compare with the APEX2-generated HG12V dataset (*Fig. 4.9c*). Firstly, the results showed that a higher number of hits were present in APEX2 compared to BioID. Secondly, the two BioID studies displayed more commonality than with APEX2. Lastly, only 17 proteins were present in all three studies. These proteins included the Raf proteins: a-Raf and c-Raf, as well as caveolae component: flotillin-1 (FLOT1). A possible reasoning for the difference in results could be due to the lack of specific (i.e., greater than 2-fold change) labelling of HRAS in the APEX2-generated HG12V condition despite its presence in the dataset, which could ultimately affect the biotinylation of neighbouring proteins.

Another important BioID study is by Go *et al*. Here, they produced a BioID-generated proximity map of HEK 293 Flp-In-T-REx cells using 192 marker proteins as a tool for others to interpret their biotinylation-based proximity labelling data. In their study, 22 bait proteins were used to map the microenvironment of the plasma membrane, which also included tK. Analysis revealed a high level of similarity between the protein lists of Kovalski *et al* and Go *et al*, whereas the APEX2 dataset appeared to be dissimilar (*Fig.4.9d*). Another interesting finding was that the HG12V data from the other two BioID studies were more enriched for the plasma membrane proteins detected in Go *et al* study compared to APEX2 (*Fig.4.9e*). However, nearly a third (120 of the 378) of the plasma membrane proximity proteins generated by BioID were identified in the total specific hits found using APEX2 (*not shown*).

Overall, APEX2 appears to be a noisier method than BioID. The primary indication of this is the presence of considerably more proteins, yet fewer plasma membrane proteins. However, it is possible that the use of additional controls and more stringent cut-offs in other studies aided the deduction of background proteins. In addition, APEX2 captures more transient interactions of which could be more abundant than stable interactions that are thought to be detected by BioID. Nevertheless, differences also occurred between the BioID studies which highlights high variability amongst these types of methodology. The use of

different cell models could contribute to the disparities, such as the type of cell line used and whether expression was transient or stable. Although, it should also be noted that different types of analyses and cut-off points were performed for all studies, which would largely affect the observed final dataset. On the whole, results here have shown differences in protein lists generated by APEX2 and BioID, but a more accurate comparison would be needed whereby the same experimental setup and analyses are used. Nonetheless, it has demonstrated that APEX2 has the capacity to detect potential Ras interactors and/or regulators, however the use of carefully selected markers and controls are required to reduce the noise that is associated with this technique.

4.5 DISCUSSION

In this chapter, the use of APEX2 to profile the Ras interactome was demonstrated, which has not been previously shown before. Here, a large-scale APEX2 experiment was performed using an optimised protocol in combination with mass spectrometry. The overall dataset showed to be reproducible with an r score of 0.942, however further repeats would be needed. Nevertheless, the experiment generated a substantial database consisting of a total of 5200 hits of which 2988 hits were found to be specifically labelled with biotin.

Biotinylation is relatively uncommon within a cell, mainly carboxylases are biotinylated (Chapman-Smith and Cronan, 1999), therefore it was with high confidence that the proteins detected were specifically biotinylated by APEX2-tagged Ras. Also, as shown by the IF images from the previous chapter, background biotinylation was modest and could be due to the combination of naturally biotinylated proteins and cell culture media. However, the high number of non-specific proteins present here which include proteins other than carboxylases indicates that these proteins may have resulted from processes further downstream of the APEX2 protocol. Although, the bead to lysate ratio was optimised previously, it is possible that the scaling-up process could have affected the purity of the enrichment. The large volume of beads may have resulted in suboptimal wash steps during the enrichment process and therefore would require further optimisation for future

experiments.

The specific hits were later categorised into their isoform/s and condition/s, which was then used for GO analysis. Overall, the detected hits showed to be enriched for Ras signalling, membrane organisation and plasma membrane proteins. Additionally, known Ras interactors were also present. Together it was evident that relevant labelling occurred. However, GO analysis of the cellular components revealed that labelling was not occurring exclusively at the plasma membrane, but also in other subcellular regions within the cell in which Ras can traffic to. Since literature has shown that HRAS and NRAS move throughout the cell in a similar manner, it was of interest to see that there was little resemblance between their localisation profiles. Similarly, despite both stimulated and G12V conditions being active models of Ras, these were highly dissimilar in terms of proteins relating to biological function. Nonetheless, both conditions were enriched for plasma membrane proteins.

Interestingly, more proximal proteins were detected in KRAS than in HRAS and NRAS, which could be due to transient transfection, whereby expression levels could vary. GO analysis was used to profile the functions and localisation of these different isoform protein lists. It appeared that KRAS in particular displayed distinctive proximal proteins for membrane organisation and the inner plasma membrane. In terms of the different active and non-active conditions, it did appear that majority of the conditions shared similar proteins for Ras protein signalling (except NRAS) and inner plasma membrane proteins, which might constitute as a core proteome that is supplemented with individually enriched unique proteins that are dependent on the condition.

The level of biotinylation is an indication of its proximity to Ras, i.e., a protein that interacts with Ras should be labelled more than a protein that is in the distance. However, due to the number of conditions used for this experiment, it was not possible to use SILAC and instead the label-free approach was used. The downfall of label-free is that abundance is hard to quantify as the different expression levels cannot be accurately accounted for during analysis, so it was difficult to conclude comparisons made between isoforms without further

experimentation. Therefore, after initial analysis, it became apparent that the results should be interpreted more as an indication of whether a protein was present or not, and not for comparison of expression levels. Using the core set of proteins shared by all Ras isoforms and conditions, a shortlist of 17 proteins was generated. Amongst the list were Ras-related proteins, membrane associated proteins, actin-related proteins, and metabolic enzymes. Since the aim of the project is to identify regulators of Ras nanoclustering organisation at the plasma membrane, it was apparent that membrane proteins present within the list, annexins should be further followed up.

For this project, APEX2 was used as the proximity-labelling method for analysing the Ras interactome, as it was more likely to capture more transient interactions due to the short labelling reaction. During the duration of this project, studies using BioID to investigate Ras were published (Ritchie *et al.*, 2017; Adhikari and Counter, 2018; Go *et al.*, 2019; Kovalski *et al.*, 2019). It was of interest to compare the APEX2 and BioID datasets to understand how these proximity labelling methods differed. Overall, APEX2 generated largely different proximity proteomes compared to those in the BioID studies, which appeared to be more similar to one another. Additionally, more plasma membrane proximity proteins were detected in the BioID studies, although this could be biased as this list of proteins was established using BioID. Nevertheless, APEX2 was able to detect known Ras-related proteins as well as other proteins present in the BioID studies. These proteins are likely to be more stably expressed proteins, whereas the other detected proteins could reflect transient interactions.

Further optimisation of the APEX2 method could reduce the number of non-specific proteins that bind to the streptavidin beads. Also, in light of the analysis, many hits were localised to different cellular components other than the plasma membrane. Markers of these regions could help eliminate proteins that are not localised at the plasma membrane in future experiments, thus reducing the noise to signal ratio.

The observed differences amongst the datasets of the different BioID studies and APEX2

were not surprising, since the biochemistry of the labelling reactions differ. Firstly, the labelling duration determined whether stable or transient interactions were detected. Secondly, BioID labels lysine side chains (Roux *et al.*, 2012), whereas APEX2 tags tyrosine side chains (Lam *et al.*, 2015). Tyrosine is a less abundant amino acid than lysine (Tourasse and Li, 2000; Echols, 2002), which could lead to a bias in the protein population detected. In general, the addition of biotin may also alter the charge and structure of a protein, thus affecting its function. Thirdly, oxidative damage from H_2O_2 could have affected the cellular physiology such as signalling pathways or protein interactions, which could be likely as the GO analysis revealed that the samples were significantly enriched in stress response related proteins. Fourthly, it has been reported that BP is less membrane permeable, which in combination with its short half-life of the unstable free radicals could result in a smaller labelling radius (Hung *et al.*, 2016). However, this might have been more beneficial for this study since regulators of Ras nanoclustering would be expected to be of very close proximity. Variation also occurred amongst the BioID studies, less than half of the total hits were shared between them despite the use of the same labelling duration of 24 hours. Although differences could be due to differences in experimental setup and/or data analysis. In general, it is important to note that the extent in which Ras is affected biochemically by the attachment of these proximity labelling enzymes is still unknown.

Overall, proximity labelling has been an instrumental tool for the wide screening of different proteome microenvironments. Here, APEX2 was successfully used to map proteins proximal to Ras WT (both active and inactive forms) and G12V mutants. A significant number of hits were detected via mass spectrometry of which was used to shortlist annexins as possible regulators of Ras nanoclustering. Therefore, APEX2 has played an important role for this project. However, one of the biggest caveats of this technique is the number of non-plasma membrane proteins detected, which with further optimisation could be resolved. In addition, normalisation of expression via stable transfection in future studies would allow for a more accurate comparison between Ras isoforms.

CHAPTER FIVE

Identification of annexins as Ras interactors

5.1. INTRODUCTION

Annexins are a group of calcium- and acidic phospholipid-binding proteins (Crumpton and Dedman, 1990) that were first discovered in the late 1970s (Creutz, Pazoles and Pollard, 1978). Since then, over 100 different annexin proteins have been identified in a wide range of species such as animals, plant and fungi (Morgan and Pilar Fernandez, 1997). In humans, 12 members have been identified (A1-11, 13), which vary in size ranging from 15kb (A9) to 96kb (A10) (Morgan *et al.*, 1999). A3, -8, -9, -10 and -13 are selectively expressed in neutrophils, skin, tongue, stomach, or small intestine, respectively. Whereas the remaining annexins are ubiquitously expressed (Moss and Morgan, 2004). Within the cell, they are predominantly cytosolic, however some members such as A2 (Eberhard *et al.*, 2001) and A11 (Tomas and Moss, 2003) have been found to localise in the nucleus.

These annexins have high structural homology, where all share a conserved core domain at the C-terminus, which consists of four subunit repeats (except for A6 with eight repeats), each made up of around 70 amino acids (*Fig. 5.1*). The repeats assemble into a tight α-helical disk. Its slightly curved shape gives it a convex surface that contains the calcium- and phospholipid-binding sites, as well as a concave side which associates with the N-terminus and/or potential interactors (Huber, Römisch and Paques, 1990). These calcium-binding sites vary in location and in numbers between the different annexin members. Similarly, the N-terminal domain is unique to each individual annexin, where length and sequence differ between them and mediates interaction with cytoplasmic binding partners like S100A10 (Morel and Gruenberg, 2007), Src (Hayes and Moss, 2009) and PKC (Kheifets *et al.*, 2006). Additionally, the N-terminal domain has shown to modulate membrane association (Wang and Creutz, 1994; Hofmann *et al.*, 2000) and act as a binding site for other annexins, leading to dimerization (Lizarbe *et al.*, 2013).

In general, annexins have shown to be involved in a wide range of processes such as membrane organisation, trafficking as well as extracellular functions. Its hydrophilic nature allows it to bind to negatively charged phospholipids in a reversible calcium-dependent

manner. Whereby, the sensitivity to calcium as well as specificity for particular phospholipid headgroups such as PA, PS or PI differ between each annexin member (Raynal and Pollard, 1994). Typically, external stimuli triggers the release of intracellular calcium and results in the recruitment of annexins to the inner leaflet of the plasma membrane and/or other membranes of various organelles (Reviakine *et al.*, 2000). This allows for annexin regulated membrane reorganisation of the cell in response to different stimuli. For example, A2 and A6 are recruited to sites of actin assembly, where they associate with lipid rafts and cytoskeleton in order to regulate the organisation of non-raft and raft microdomains in smooth muscle cell membranes (Babiychuk and Draeger, 2000). Interactions with the membrane can also be calcium-independent and instead, depend on pH (Gerke and Moss, 2002). For example, the acidic pH in endosomes can induce conformational changes to A6, thus exposing hydrophobic regions to bind the plasma membrane (Golczak *et al.*, 2004).

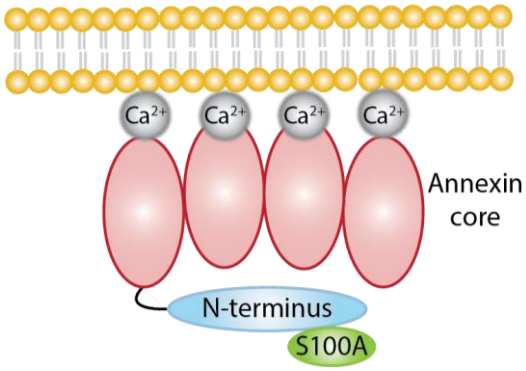

Figure 5.1| Schematic of the annexin structure

Aside from membrane organisation, annexins also play a role in both calcium-dependent and -independent regulated endocytotic and exocytotic events. Studies have shown A2 to be associated with early endosomes in a calcium-independent manner (Babiychuk and Draeger, 2000) as well as the biogenesis of multivesicular endosomes (Mayran, Parton and Gruenberg, 2003). Its subcellular distribution appears to be regulated by cholesterol, as it binds to cholesterol-rich membranes (Mayran, Parton and Gruenberg, 2003). Similarly, A8 has shown to be required for the regulation of late endosomal trafficking (Goebeler *et al.*, 2008). Whereas, A6 regulates the budding of clathrin-coated pits from the plasma membrane of human fibroblast cells (Lin, Südhof and Anderson, 1992).

The pathogenesis or progression of many human diseases have often been linked to annexins. In particular, annexins have been associated with various cancers such as breast (Du *et al.*, 2018), ovarian (Song *et al.*, 2009), gastric (Hua *et al.*, 2018), liver (Sun *et al.*, 2018; Zhao *et al.*, 2018) as well as head and neck cancers (Raulf *et al.*, 2018). In gastric cancer, it has been reported that A11 promotes the proliferation, migration and invasion of cancerous cells via the Akt/GSK-3β pathway (Hua *et al.*, 2018). Whereas, A5 has shown to aid the progression of hepatocarcinoma via the integrin and MEK-ERK pathway (Sun *et al.*, 2018). Another pathway affected by annexins is the NF-kB pathway, which appears to be important for A3-mediated metastasis in breast cancer (Du *et al.*, 2018). Contrastingly, A1 is associated with better prognosis in head and neck cancers despite being previously linked to breast cancer progression, as it regulates EGFR activity (Raulf *et al.*, 2018).

As shown in the previous chapter, A1-7 and A11 were all identified in the APEX2 screen, indicating a possible association with Ras. In particular, A6 and A11 were found to be linked with all Ras isoforms in both their active and inactive states (*Fig. 4.9*). Due to their affinity for phospholipids and role as a membrane scaffold, there is potential that annexins might be involved in Ras nanoclustering. To date, there has been minimal studies looking at the link between Ras and annexins. Two studies from the same research group highlighted a possible relationship between A6 and Ras, where it was hypothesised that A6 aids the recruitment of gap120 to the plasma membrane, resulting in the deactivation of Ras (Grewal *et al.*, 2005; Vilá de Muga *et al.*, 2009). With the exception of these studies, it appears that no further research exists between annexins and Ras. Therefore, in this chapter, the relationship between Ras and annexins will be investigated to establish whether annexins are involved in the organisation of Ras nanoclusters at the plasma membrane.

5.2. AIMS

5.2.1. To determine whether Ras and annexins interact.

Annexins (A1-7, -11) were detected in the APEX2 data, indicating that these annexins are in close vicinity of Ras. However, this does not indicate that Ras and annexins interact.

Therefore, the first objective is to elucidate whether direct or indirect interactions, if any, occur between these two groups of proteins.

5.2.2. To characterise the effect of annexins on Ras biology.

The next objective was to characterise the relationship between annexins and Ras by determining if annexins affect Ras biology. In particular, it is of interest to explore whether annexins are capable of modulating Ras signalling and/or nanoclustering.

5.3. ANNEXINS INTERACT WITH RAS

5.3.1. Validation of annexins in Ras pulldown

Various members of the annexin family were detected in the APEX2 dataset. Before elucidating whether these annexins are important for Ras biology, the detection of annexins was first optimised in order to validate whether annexins were present in the FLAG-Ras pulldown. As mentioned previously, A1-7 and A11 were detected in the dataset. Antibodies against A1, A2, A5, A6, A7 and A11 were tested in HeLa S3 cells transfected with APEX2 tagged-KRAS WT (*Fig. 5.2a*). The results showed that each of these annexins were clearly detectable in the transfected cells.

Next, validation of the mass spectrometry results by western blot was performed. Here, the APEX2 experiment was conducted using the same conditions as stated previously (*Fig. 4.1*). The pulldown of biotinylated proteins was blotted for two proteins that were detected in the APEX2 screen: A6 and septin-2 (SEPT2) (*Fig. 5.2b*). In the previous chapter, SEPT2 was detected in the KRAS and NRAS proximity proteomes. Whereas A6 was more enriched in KRAS and HRAS compared to NRAS. In this experiment, however, A6 was predominantly present in stimulated KRAS and to a lesser extent in serum starved KRAS and HRAS. SEPT2 displayed a similar biotinylation profile to A6, but these results were more reflective of the mass spectrometry data where SEPT2 was found to be mainly enriched in KRAS. Interestingly, the enrichment of both proteins appeared to coincide with the pattern of actin biotinylation. It was of interest to also note that expression of A6 was higher in all Ras-transfected samples compared to control, i.e., untransfected (*Fig. 5.2b, top blot*).

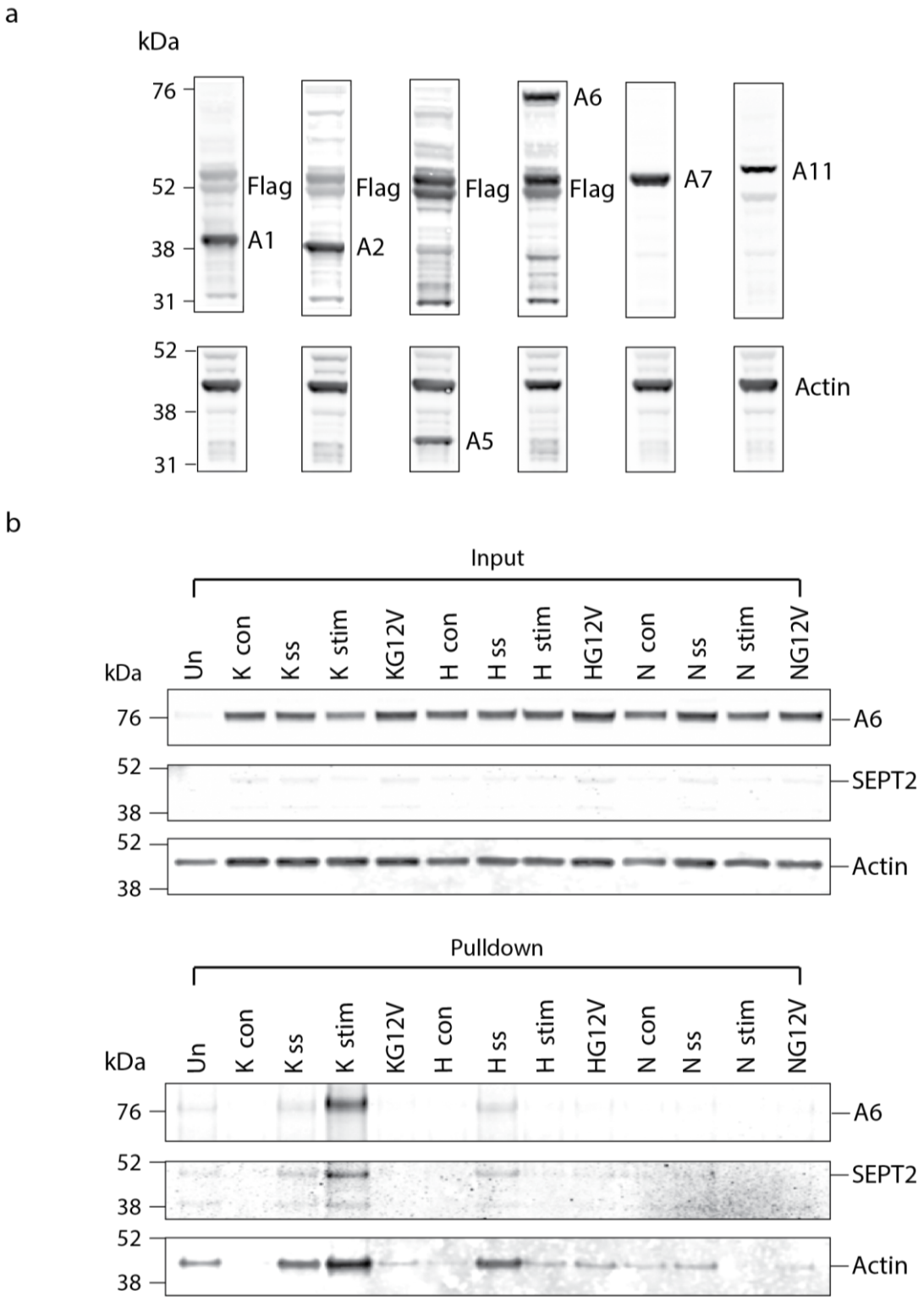

Figure 5.2| Detection of annexins – a) Testing the presence of endogenous annexins in KRAS WT transfected HeLa S3 cells using their respective anti-A1, A2, A5, A6, A7 and A11 antibodies. An anti-FLAG antibody was used to detect the FLAG-tagged APEX2-Ras and actin was used as a loading control. b) Validation of A6 and SEPT2 in the biotinylated population. The input (2.5%) and streptavidin pulldown are shown in the top and bottom blots, respectively.

In addition, the similar expression profiles between A6, SEPT2 and actin could suggest that the streptavidin pulldown process was not as clean as expected, since actin was not previously observed in other pulldown blots. Overall, the results have shown slight discrepancies to the mass spectrometry data seen in the previous chapter, however in general the results suggest that A6 is in close proximity to KRAS and HRAS. Therefore, in the next section, the interaction between A6 and Ras will be investigated.

5.3.2. Identifying interaction between annexin 6 and the different Ras isoforms

The next steps were to explore whether annexins and Ras interact. IP was used to test if a direct interaction occurred between exogenously expressed APEX2-tagged Ras and endogenous annexins. Here, additional annexins were tested alongside A6, since these annexins were also detected before. Specifically, A1, A2, A6 and A7 were measured in the FLAG IPs of APEX2-KRAS WT, -KG12V, -HRAS WT, -HG12V, -NRAS WT and -NG12V transfected HeLa S3 cells (*Fig. 5.3a*).

Previous mass spectrometry data showed that A1, A2 and A6 were present in all three Ras proximal proteomes, however only A6 was present in all conditions, i.e., serum-starved, stimulated and G12V. Whereas A7 predominantly appeared in KRAS. In Figure 5.3b, A1 and A2 are absent in the pulldown lanes, suggesting that these annexins are not direct Ras interactors. Whereas A7 was present in the pulldown of HRAS and NRAS but absent from KRAS (*Fig.5.3c*), however it was later elucidated that these bands were not A7 and instead were caused by off-target labelling by the A2 antibody (*not shown*). Similar to the mass spectrometry data, A6 was detected in the pulldowns of all Ras isoforms (*Fig.5.3b, c*). However, there is a possibility that the observed bands in the pulldown lanes could be non-specific since A6 is also present in the untransfected control. Troubleshooting using a different negative control such as GFP-FLAG as well as a lysate preclearing step with beads did not eliminate the observed problem. Therefore, further optimisation of the FLAG-pulldown protocol is required. Nonetheless, these results do not exclude A6 as a direct interactor of Ras, but alternative experiments will be required to investigate this further.

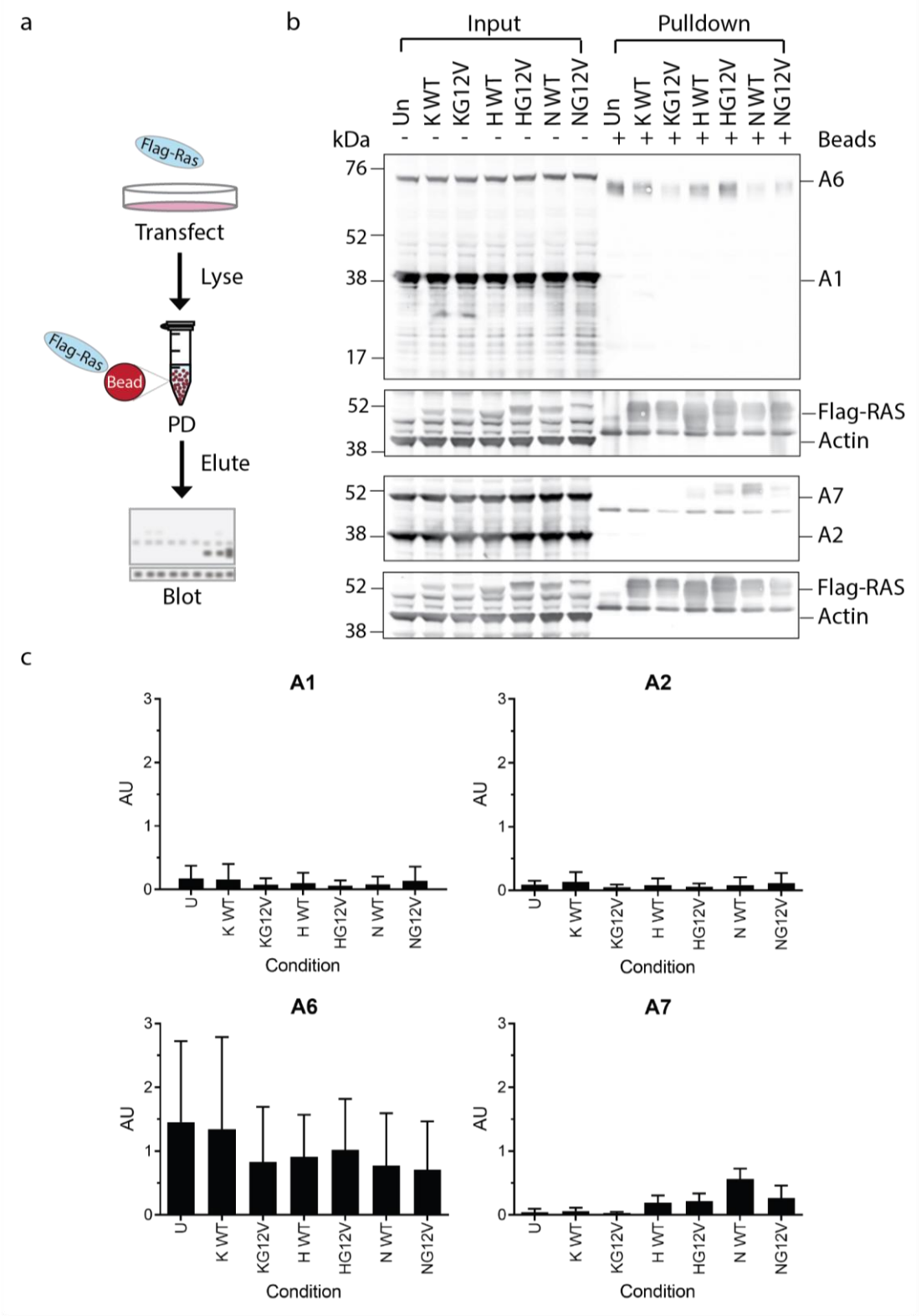

Figure 5.3| Investigation of annexins as direct interactors of Ras – a) Schematic of the FLAG-Ras IP process. b) Representative blot of FLAG-Ras IP. Both input (2.5%) and pulldown samples were blotted for A1, A2, A6, A7, FLAG and actin (loading control). c) Quantification of annexins in the pulldown lanes (*n=3*), results were normalised to untransfected control. Error bars represent mean+SD.

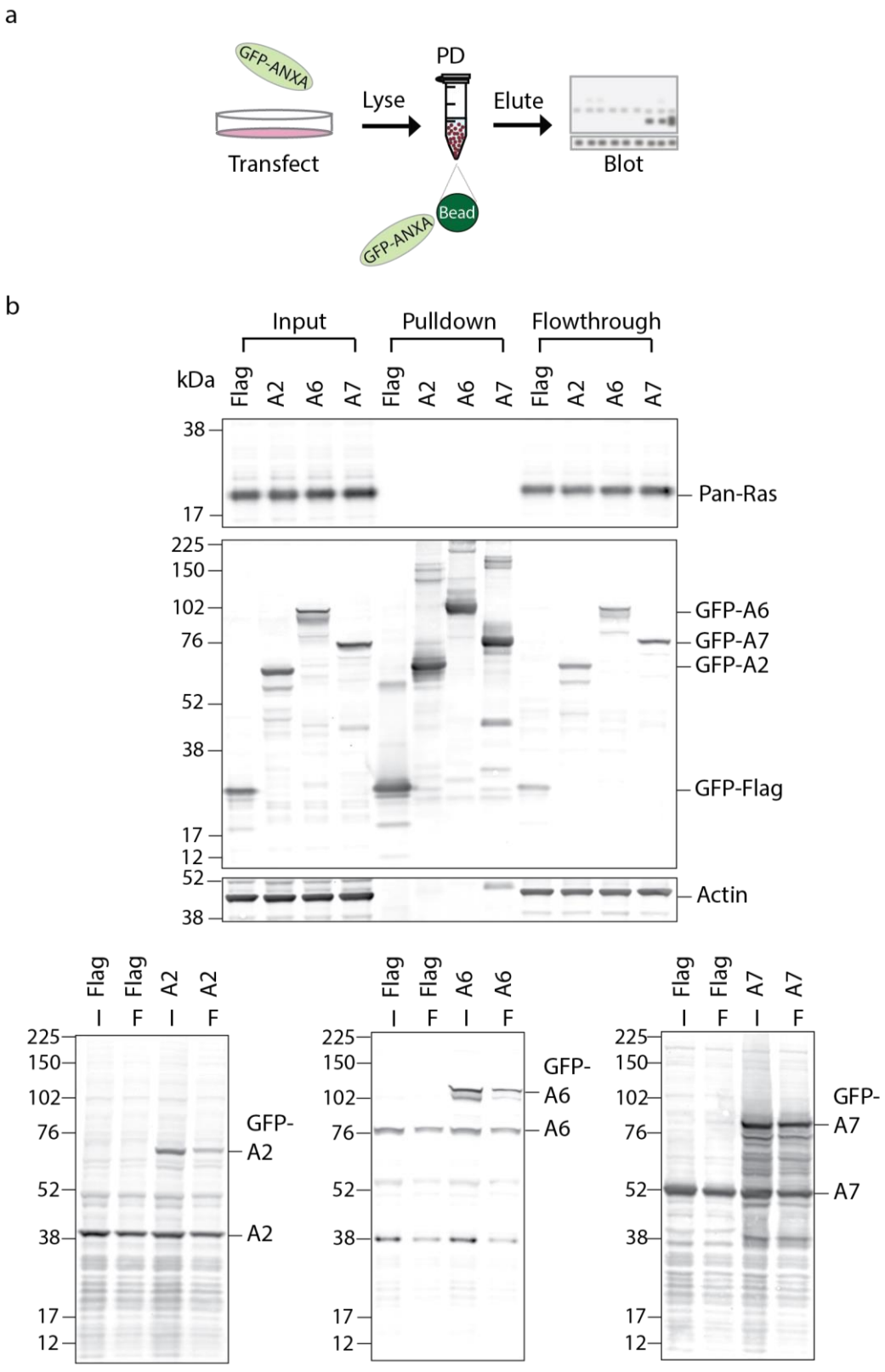

Figure 5.4| Absence of Ras in GFP-annexin pulldowns – a) Schematic of the enrichment of annexins from GFP-ANXA transfected HeLa S3 cell lysates using anti-GFP beads. b) Representative blot (*from n=3*) of measuring endogenous Ras in GFP-ANXA pulldowns (*top*) and validation of enriched GFP-A2, -A6 and -A7 proteins (*bottom*).

To circumvent the possible non-specific enrichment associated with the FLAG IP method, an alternative IP experiment was designed to validate whether the previous results were representative of the Ras and annexin interaction. In these experiments, endogenous Ras was probed in the pulldowns of GFP-tagged annexins. Here, Hela S3 cells were transfected with GFP-FLAG, -A2, -A6 and -A7, then incubated with anti-GFP beads to elute the GFP proteins, which were later used to assess the presence of Ras (*Fig.5.4a*).

As shown by the representative blots (*Fig. 5.4b*), all GFP proteins were successfully enriched. However, Ras was not detected in any of the pulldown lanes of A2, A6 or A7 (*Fig. 5.4b, top blot*). An interesting observation is that all three of these annexins already appear to be abundant within HeLa S3 cells. Therefore, it would be of interest to know whether the endogenous Ras preferentially interacts with the endogenous annexins over the transiently transfected GFP-tagged annexins. The lack of Ras in the IP was consistently seen across all three experimental repeats (*not shown*), which could either indicate that Ras does not interact with A2, A6 or A7, or that IPs might not be a suitable technique for capturing the transient interaction that may occur between these two proteins.

5.3.3. Visualisation of the Ras-annexin interaction

Results from the previous experiments regarding the interaction between Ras and annexins remained fairly inconclusive. IPs have the disadvantage of only being able to capture strong or stable interactions, due to the harsh conditions of cell lysis and enrichment steps. Therefore, FRET was used to circumvent this problem and assess whether weak or transient interactions occur between annexins and Ras.

The principal of FRET is based on the excitation of one fluorophore (donor) with light of one wavelength, followed by a non-radiative transfer of energy to another fluorophore (acceptor), which emits light of another wavelength. This phenomenon can only occur when the two molecules are within approximately 10nm (100Å); energy transfer is highly sensitive to the distance between the fluorophores (Sekar and Periasamy, 2003). These fluorophores are chosen so that an overlap occurs between the spectrums of the donor

emission and the acceptor excitation in order for energy transfer to occur. In addition, there must be sufficient separation between the donor and acceptor emission spectrums so that fluorescence of each fluorophore can be measured (Sekar and Periasamy, 2003).

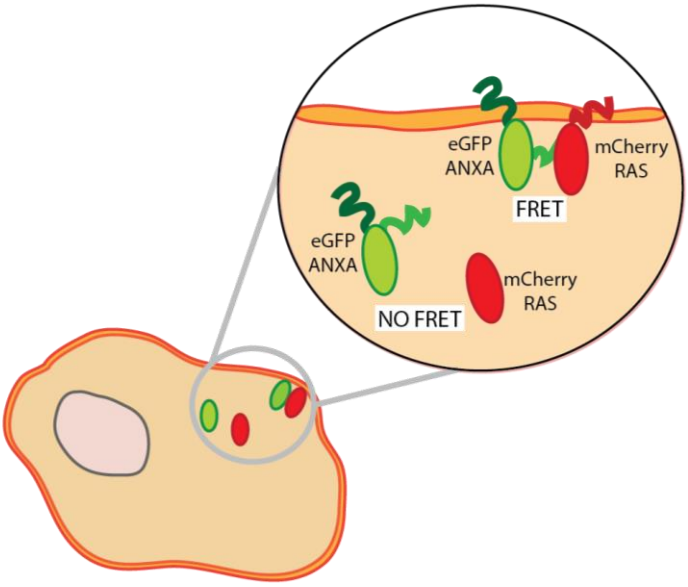

Figure 5.5| Schematic of FRET

For these experiments, eGFP-annexins: A2, A6 and A7 and a panel of mCherry-tagged Ras isoforms and G12V mutants were used (*Fig.5.5*). These were co-transfected into HeLa S3 cells and visualised live 24 hours post-transfection. In addition to these samples, single transfections of A2, A6 or A7 were used as negative controls and to account for donor bleedthrough into the FRET channel. A positive control of co-expressed eGFP-HRAS WT and mCherry-HRAS WT was also used.

To measure FRET, two types of analyses were performed: sensitised emission (SE) and acceptor photobleaching. For SE analysis, the co-transfected cells were visualised under three channels: eGFP, mCherry and FRET. If protein-protein interaction occurred, FRET was observed, whereby donor (eGFP) excitation led to acceptor excitation (mCherry) and subsequently, emission of the mCherry wavelength would be observed in the FRET channel. The increased emission of the acceptor (mCherry) results in a decrease of the donor (eGFP) emission, which forms the basis of the second type of FRET analysis: acceptor photobleaching. Where in this scenario, bleaching of the acceptor (mCherry) fluorophore

will increase the fluorescence of the donor fluorophore if the two molecules are in close proximity.

Images taken of these co-transfected cells revealed that both types of fluorophores: eGFP-annexin and mCherry-Ras were efficiently expressed (*Fig.5.6)*. In general, annexins were predominantly expressed in the cytosol, whereas Ras expression varied depending on the partnering annexin. Interestingly the morphology differed between the different annexins. A6-transfected cells exhibited normal morphology, whereas both A2- and A7-transfected cells had a more rounded cell appearance. In addition, A2 cells appeared to have enlarged nuclei and Ras appeared to be mainly present in puncta, presumably endosomes. Whereas in A7-expressing cells, large vacuoles can be seen, which could be a result of A7 activity since A7 has been previously been implicated in the fusion of vesicles (Creutz, Pazoles and Pollard, 1978). Here, the distribution of Ras was similar to A2-expressing cells, where it was mainly found in endosomes. Unlike A2 and A7, Ras distribution was generally more cytosolic, or plasma membrane bound in A6-expressing cells.

FRET efficiency ($FRET_{\varepsilon}$) for each pixel within an image was calculated by the subtraction of the cross-excitation (i.e., excitation of donor via excitation of acceptor) and bleedthrough (i.e., detection of donor in the acceptor channel) intensities from the FRET intensity and expressed as a percentage of the acceptor intensity. Observation of the $FRET_{\varepsilon}$ images revealed varying levels of FRET amongst the different samples. The positive control displayed high levels of FRET along the plasma membrane as expected, whereas the negative control: A6, showed little FRET (*Fig.5.6a*), which was similar to the A2 and A7 controls (*not shown*). Images showed that FRET was present in the majority of A6- (*Fig.5.6a & b*) and A7-expressing (*Fig.5.6c*) cells, however little to no FRET was observed in the A2-transfected cells. For most A6 and A7 samples, FRET was present in the cytosol and plasma membrane, but absent from the nucleus. In A7, FRET also occurred in the observed puncta.

To quantify FRET in a number of cells, acceptor photobleaching was used. Here, confocal images were taken before and after bleaching. Whole cell fluorescence was measured for

each cell and used to calculate the percentage difference in fluorescence after acceptor photobleaching. As shown by Figure 5.7, cells were efficiently photobleached, indicated by the significant decrease in acceptor fluorescence after frame 3, when acceptor photobleaching was initiated. For the HRAS WT-HRAS WT positive control, only a minute increase in donor fluorescence was seen (*Fig.5.7a*). However, it is likely that this small change in fluorescence reflects the observed FRET at the plasma membrane, which represents only a small proportion of the cell and therefore would only be portrayed as a small percentage for whole cell analysis.

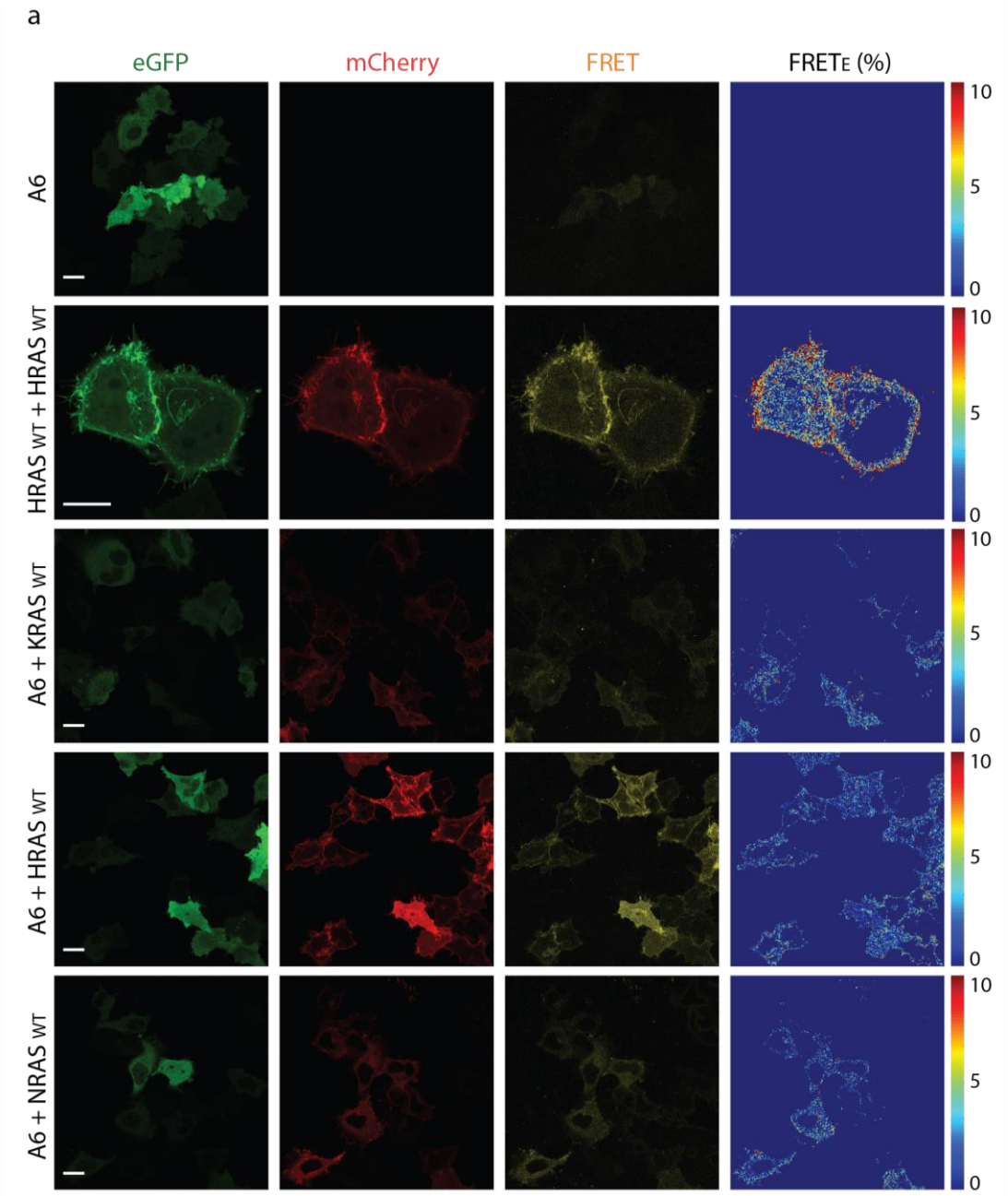

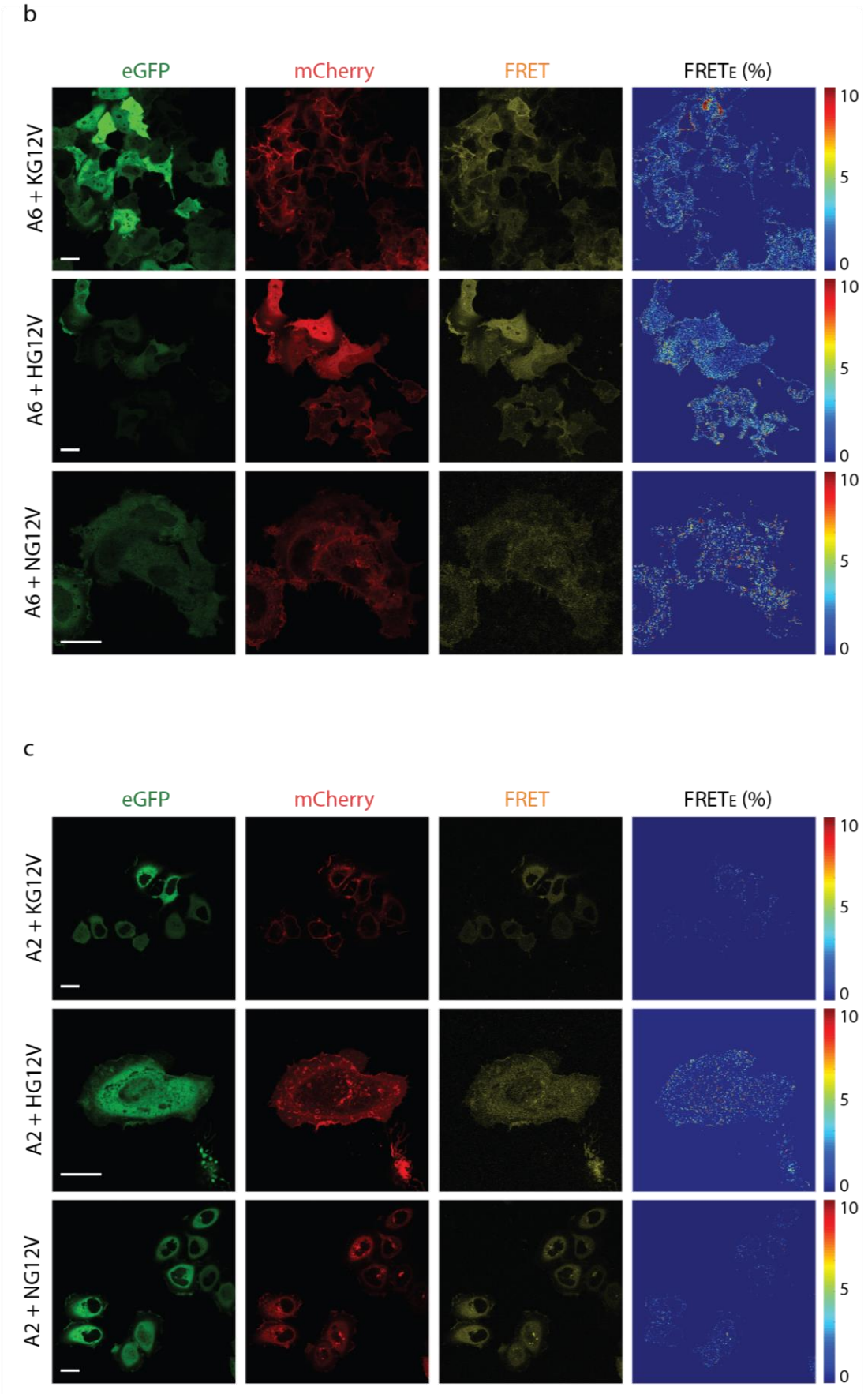
b
eGFP
mCherry
FRET
FRETE (%)
A6 + KG12V
A6 + HG12V
A6 + NG12V
10
5
0
c
eGFP
mCherry
FRET
FRETE (%)
A2 + KG12V
A2 + HG12V
A2 + NG12V
10
5
0

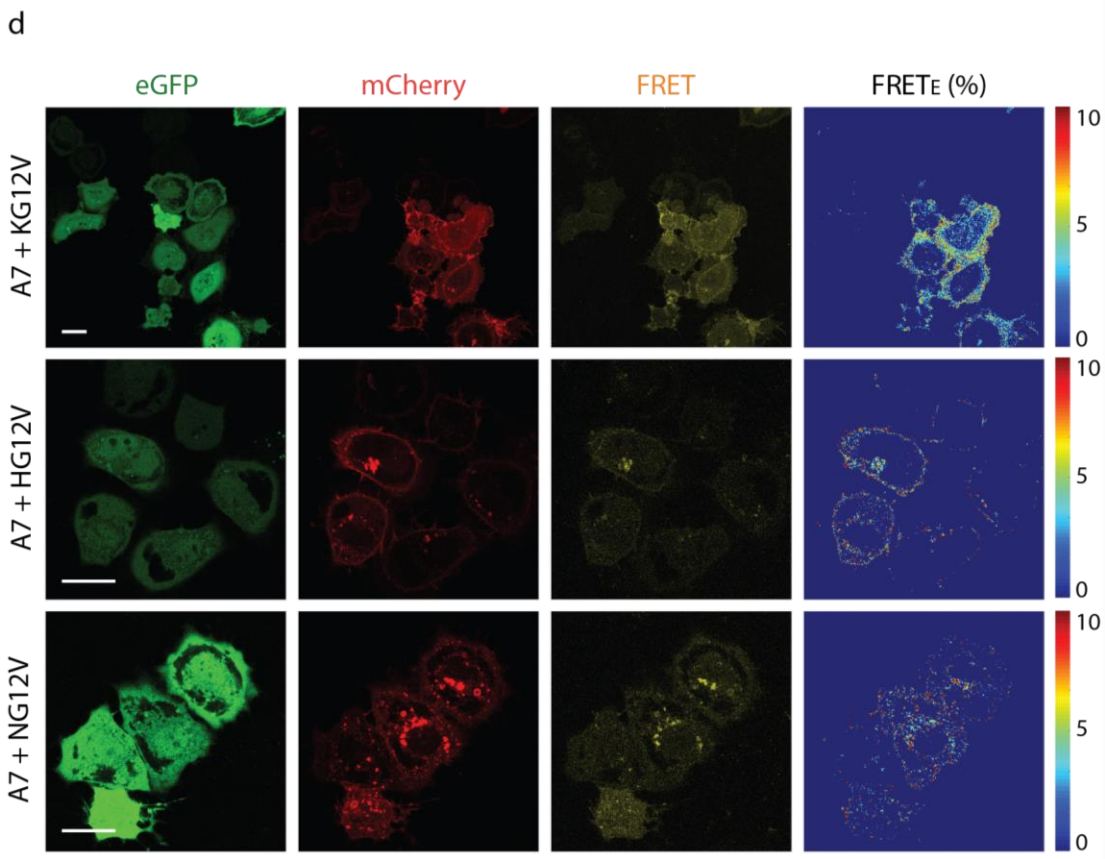

Figure 5.6| Representative images of cells co-transfected with Ras and annexins - Confocal images of HeLa S3 cells co-transfected with a) eGFP-A6 and mCherry-Ras WT and b) G12V. A6 serves as a donor-only control and eGFP- and mCherry-HRAS WT was used as a positive control. Other annexins: c) A2 and d) A7 with mutant G12V Ras are also shown. Each column represents the fluorescence channel, FRET and $FRET_E$. $FRET_E$ (%) was calculated per pixel, correcting for bleedthrough and cross-excitation. Scale bar, 20µm.

As for the A6-transfected samples, KRAS WT and KG12V displayed a similar level increase in donor fluorescence as the HRAS WT-HRAS WT positive control. Whereas the donor fluorescence increased more notably in the A6 and HRAS WT/G12V samples, indicating that eGFP-A6 and mCherry-HRAS WT/G12V were likely to be in close proximity to each other or potentially interacting. Differently, A2 and A7 did not show an increase in donor fluorescence and instead showed degradation in fluorescence, therefore alterations to the bleaching process will be required to accommodate this problem. Overall, acceptor photobleaching along with SE analysis has revealed a possible interaction amongst A6 and HRAS WT/G12V.

a

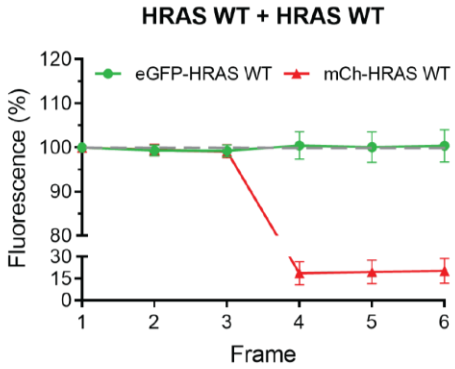
HRAS WT + HRAS WT
eGFP-HRAS WT
mCh-HRAS WT
Fluorescence (%)
120
110
100
90
80
30
15
0
1
2
3
4
5
6
Frame

b

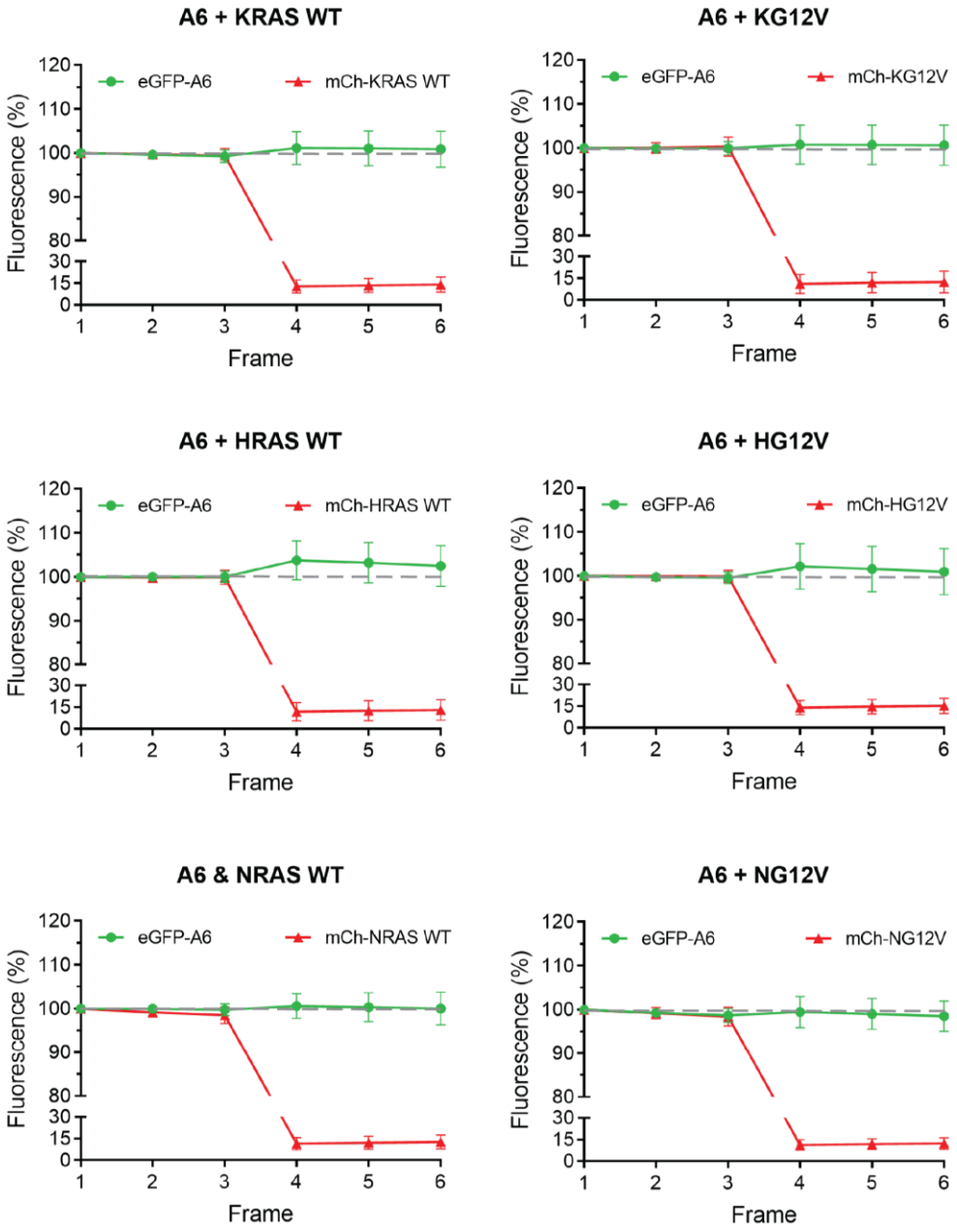
A6 + KRAS WT
eGFP-A6
mCh-KRAS WT
A6 + KG12V
mCh-KG12V
A6 + HRAS WT
mCh-HRAS WT
A6 + HG12V
mCh-HG12V
A6 & NRAS WT
mCh-NRAS WT
A6 + NG12V
mCh-NG12V
Fluorescence (%)
Frame

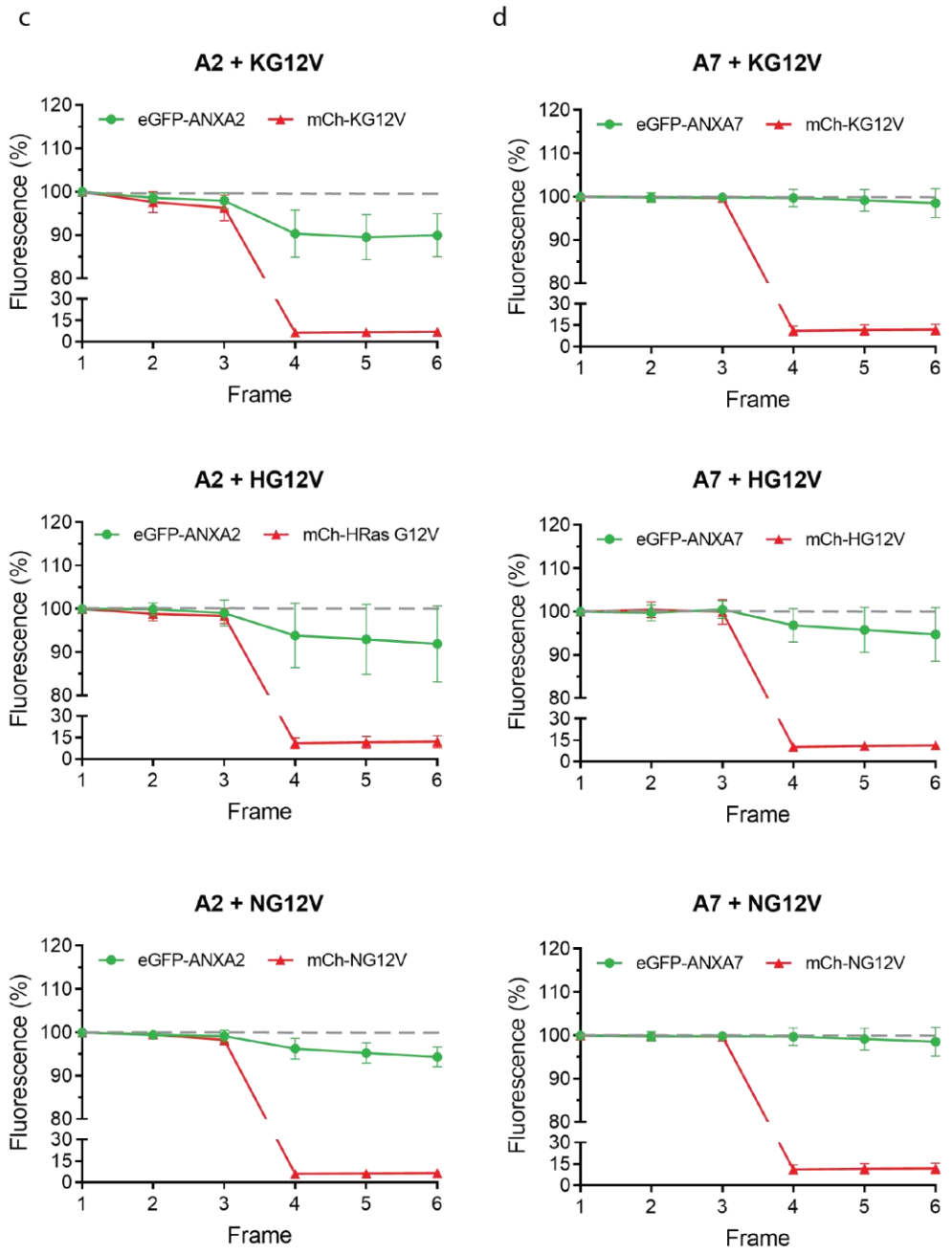

Figure 5.7| Whole cell analysis of annexin and Ras FRET through acceptor photobleaching - HeLa S3 cells were co-transfected with either a) eGFP-HRAS WT and mCherry-HRAS WT, b) eGFP-A6 and mCherry-Ras, c) eGFP-A2 and mCherry-mutant Ras or d) eGFP-A7 and mCherry-mutant Ras. Images were taken before and after bleaching (frame 3). Error bars indicate SD for 30 cells per A6 condition and double-labelled HRAS WT or 13 cells per A2 and A7 condition from 3 independent experiments.

5.4. RAS ACTIVITY REDUCED BY ANNEXINS

5.4.1. Knockdown of A2 or A6 increases Ras activity

As demonstrated previously, HeLa S3 cells endogenously express Ras, A2 and A6. Therefore, siRNAs could be used to reduce A2 or A6 expression to investigate their effect on Ras activity. The duration of siRNA treatment was optimised to achieve a sufficient reduction in its expression levels (*Fig 5.8*). Here, cells were treated with non-targeting (NT1), A2 or A6 siRNA for 48 or 72 hours. Measurements of A2 and A6 expression levels at 48 hours revealed a reduction of 46.5% and 84.9% respectively, compared to control. Whereas at 72 hours, levels decreased to 30.9% in A2 and 10.4% in A6. Subsequently, 72 hours was chosen as it resulted in the lowest expression of A2 and A6. It is to be noted that two isoforms of A6 exist due to alternative splicing of the *A6* gene. siRNA treatment targets both isoforms but for all other experiments, isoform 1 (A6-1) was used for exogenous expression of A6 (Smith *et al.*, 1994)

In these knockdown experiments (*Fig.5.8b*), cells were either non-stimulated or stimulated with FBS for 5 minutes following 5 hours of serum-starvation. Expression levels of activated Ras effectors: MEK, ERK and pAkt were measured along with Ras and A2 or A6. The first observation is that both A2 and A6 expression was successfully reduced with 72 hours siRNA treatment. Secondly, very low levels of pMEK, pERK and pAkt were seen across the non-stimulated samples, of which were elevated in the stimulated samples. Interestingly, knockdown of either A2 or A6 in the stimulated samples resulted in a further increase of Ras effectors: pERK and pAkt. Modest increases of pERK levels were detected in both annexin knockdowns, although it was more noticeable in the A6 siRNA treated sample. The most dramatic change was seen in pAkt activity, where reduced expression of either A2 or A6 resulted in an increase of pAkt. Whereas pMEK levels remained relatively constant irrespective of A2 or A6 siRNA treatment. Overall, reduction of A2 or A6 expression led to increased activation of downstream Ras effector pathways (*no statistical significance*), suggesting that A2 and A6 might play a role in reducing Ras activity.

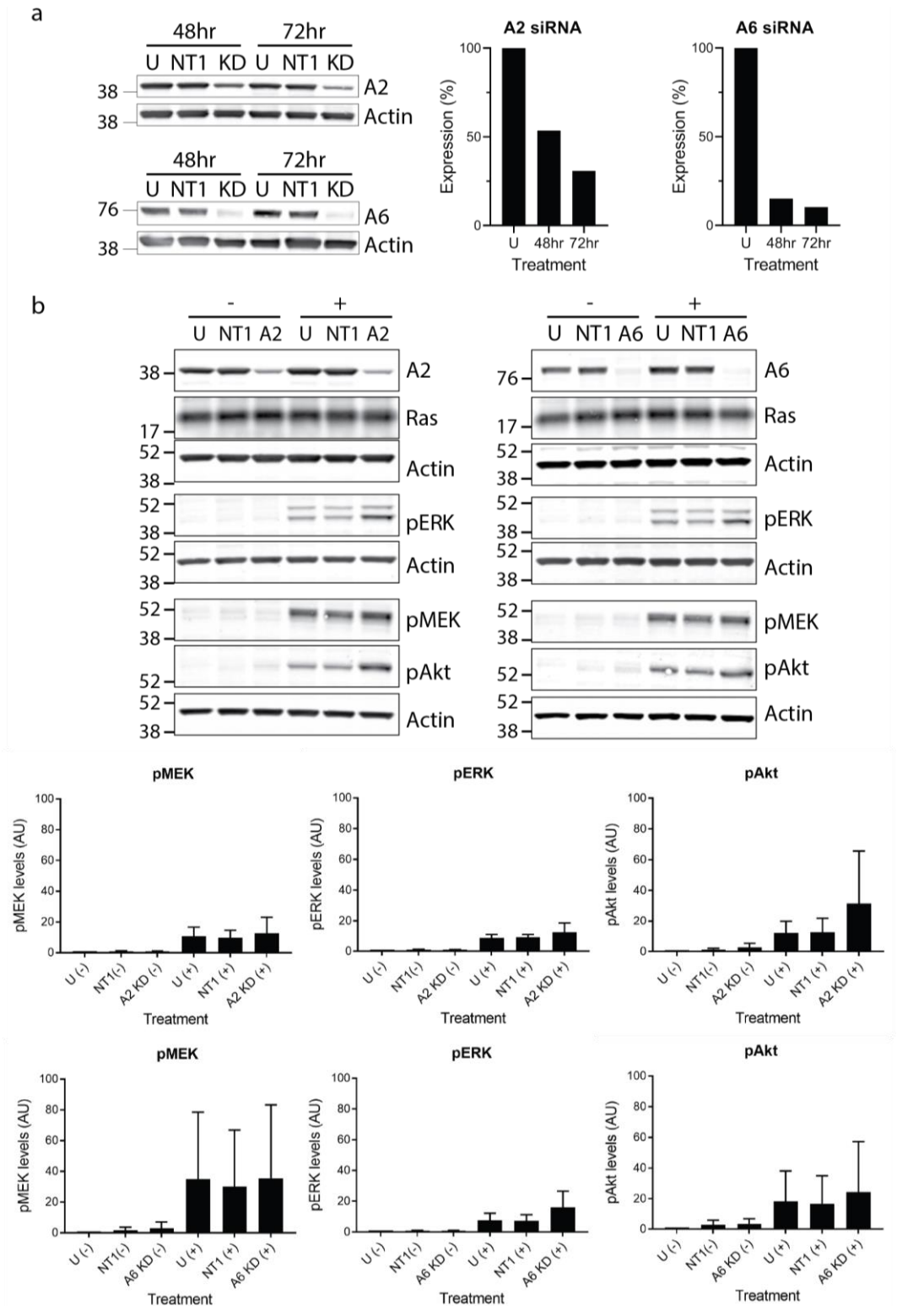

Figure 5.8| **Reduced A2 and A6 expression increased Ras effector activation** – a) Optimisation of siRNA treatment. b) Representative blots of Ras effector activity following A2 or A6 knockdown. Cells were subjected to NT1, A2 or A6 siRNA for 72hrs, then either untreated (-) or activated with FBS (+). Summary graphs (top panel – A2, bottom panel - A6, n=3) show the level of pMEK, pERK and pAkt expression (1AU) normalised to non-stimulated untransfected samples, error bars indicate SD.

5.5. EVALUATING THE EFFECT OF ANNEXIN 6 ON RAS NANOCLUSTERING

5.5.1. A6 increases the random distribution of Ras.

So far, it has been demonstrated that A6 and HRAS potentially interact and that A6 perturbs downstream Ras effector signalling. For these reasons, it was of interest to investigate whether A6 could play a role in Ras nanoclustering. One of the methods to investigate nanoclustering is via high resolution EM. Ras is a small protein that has a low electron-density, therefore direct visualisation of Ras is not viable. However, conjugation of a larger more electron dense molecule such as a gold particle to Ras detecting antibodies can aid the visualisation of their spatial patterns on the plasma membrane (Prior *et al.*, 2003).

For these experiments, gold-tagged red fluorescent protein (RFP) antibodies were used to label mCherry-Ras proteins. HeLa S3 cells were co-transfected with mCherry-HRAS WT/G12V and GFP-A6. Single transfections of mCherry-HRAS WT or mCherry-HG12V were used as controls. These transfected cells were used to provide membrane samples for visualisation. Ras proteins on these plasma membrane samples were labelled with 3.5nm anti-RFP gold. Digital images of gold labelling were obtained, then spatial patterning of the gold particles (i.e., Ras) was evaluated using univariate Ripley's K function. The non-linear transformation of the Ripley's K function, *L(r)-r* reveals the spatial patterning of Ras between 0-240nm (*r*). Where, random distribution is depicted by an *L(r)-r* value of 0, whilst positive and negative values imply clustering and dispersion, respectively.

The gold particle spatial patterning of Ras was analysed for each image per condition, the average of these *L(r)-r* values for each 1nm increment between 0-240nm is displayed in Figure 5.9a. Comparisons between Ras distribution with and without additional A6 expression were made. Overall, the *L(r)-r* curves revealed that the Ras proteins were predominantly randomly distributed in all the tested conditions. It is well-established that Ras proteins form nanoclusters at the plasma membrane (Prior *et al.*, 2003; Plowman *et al.*, 2005; Zhou and Hancock, 2015), therefore the observed random distribution is most likely

a reflection of poor labelling using the 3.5nm anti-RFP antibodies. From the curves and maximum *L(r)-r* (L_{max}) values, it appears that in co-transfected conditions, i.e., samples with additional A6 expression, Ras proteins were more randomly distributed than their single-transfection counterparts: HRAS WT and HG12V (*Fig. 5.9a & b*). This was more evident in HRAS WT than in HG12V, where a reduction in L_{max} value from 0.543 to 0.346 can be seen when exogenous A6 was present. However, bootstrap analysis of the *L(r)-r* clustering did not show statistical significance.

5.5.2. Higher ordered HG12V oligomers are reduced by A6

Due to the low labelling intensities, significant changes of the overall Ras nanoclustering when co-expressed with A6 were not observed. However, for both HRAS WT and HG12V, the addition of A6 resulted in a consistent trend towards a more random/less clustered distribution (*Fig. 5.9a & b*). For further analysis, the population distribution of these Ras molecules was investigated using Ripley's K function to count the number of gold particles for a defined distance of 15nm.

As shown by Figure 5.9c & d, the majority of detected gold particles existed as monomers (>80%) for all conditions. This was expected since the previous results indicated a lack of clustering. The remaining gold particles decreased in frequency with increasing oligomer size for both HRAS WT and HG1V. For HRAS WT samples, differences in population distribution were minor with only a 2.3% decrease in monomers and slight incremental changes in dimers (+0.9%), trimers (+1.1%) and multimers (+0.26) in the presence of A6. Contrastingly, an increase in monomers (+5.6%) can be seen in HG12V and A6 co-expressed samples compared to HG12V only. In accordance, a smaller percentage of higher ordered HG12V oligomers contributed to the total population when A6 was present. In particular, a significant decrease in trimers ($p=0.009$) was observed. Overall, the results suggest that A6 reduces HG12V clustering, possibly as a result of alterations to the population distribution but has no significant effect on the population distribution of HRAS WT proteins.

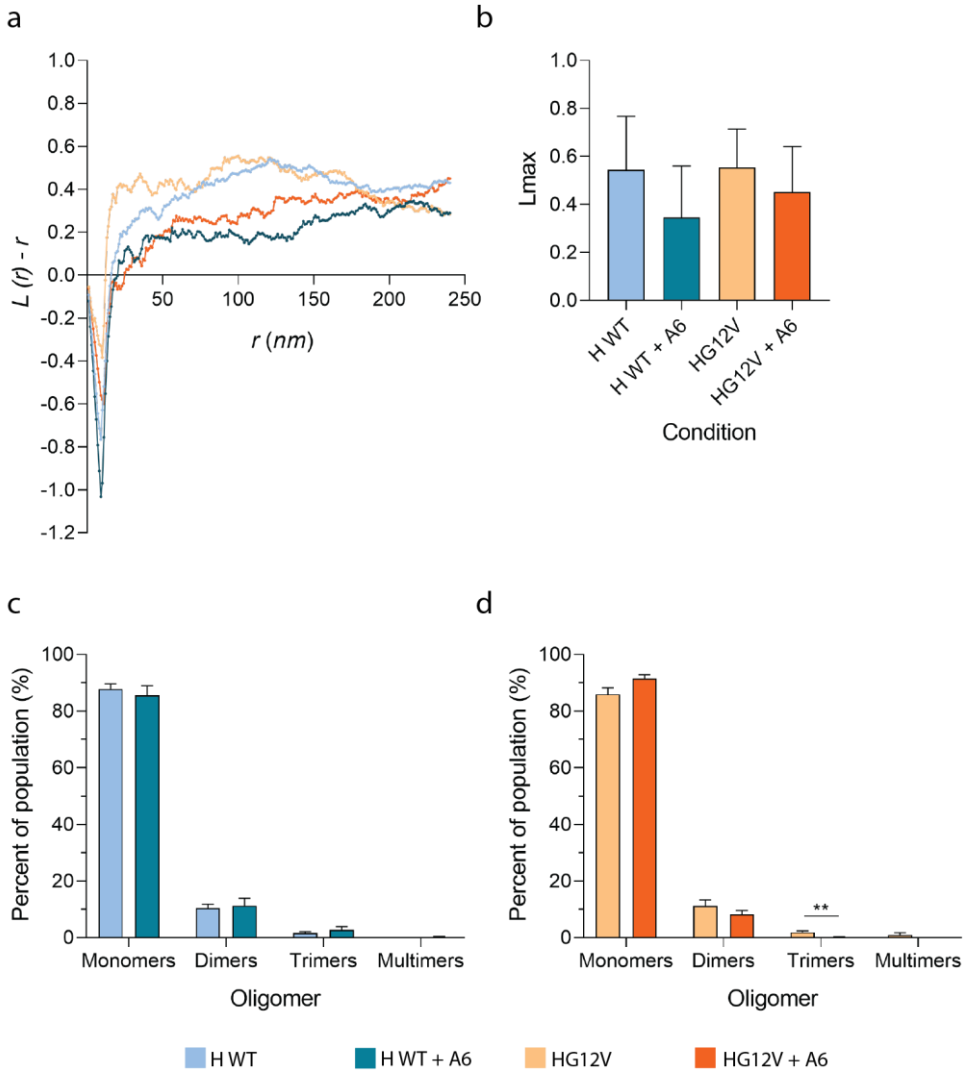

Figure 5.9| A6 redistributes Ras populations – Digital images of gold-labelling in transfected-samples: HRAS WT (n=21), HG12V (n=10), HRAS WT and A6 (n=14) and HG12V and A6 (n=11) were acquired. For each condition, (a) the average *L(r)-r* values between 0-240nm were plotted as well as their (b) maximum *L(r)-r* values (L_{max}) +SEM. Population analysis of (c) HRAS WT and (d) HG12V +SEM is shown above. ** $p < 0.01$.

5.6. DISCUSSION

The detection of multiple annexins during the APEX2 screen and in the shortlisted proteins, as well as their link to the plasma membrane deemed them to be prospective regulators of Ras nanoclustering. The mass spectrometry data showed promising results of correctly biotinylated proteins, i.e., proteins proximal to Ras, such as Ras effectors: Raf and MEK, however reaffirmation of whether annexins was biotinylated by other means was required before conducting further investigations. Western blotting revealed the presence of A6 in

enriched biotinylated lysates generated from a repeat of the conditions used in the APEX2 experiments. Although, there were slight discrepancies to the mass spectrometry data. Irrespectively, A6 was detected in KRAS (serum-starved and stimulated) and HRAS (serum-starved). Interestingly, A6 expression was similar to SEPT2 and actin. It has been previously reported using latrunculin that KG12V and tH nanoclusters but not HG12V have a dependence on actin (Plowman *et al.*, 2005). From this, it could be speculated that there might be a possible link between A6, SEPT2, actin and Ras. Although further experimentation would be required to investigate whether this was an artefact of inefficient enrichment, since actin was not detected in the streptavidin pulldown experiments demonstrated previously using NRAS.

With the validation that annexin is proximal to Ras, the interaction between annexins and Ras was explored. The co-IP experiments did not evidently show an interaction between annexins: A1, A2, A6 or A7 with Ras. This is supported by another study, in which A6 was not present in the Ras pulldown and vice versa, Ras was not detected in the A6 pulldown (de Vilá Muga *et al.*, 2009). An interaction was only seen in this study when cells were stimulated with EGF (de Vilá Muga *et al.*, 2009).

Interestingly, FRET revealed interactions between A6 and the different Ras isoforms (HRAS>KRAS>NRAS), in particular A6 and HRAS WT/G12V (*Fig. 5.7*). It also highlighted a possible interaction between A7 and Ras, but the cell morphology was vastly different from normal cells, possibly due to the overexpression of A7. Lastly, A2 did not appear to interact with Ras. These novel findings are of interest since the relationship between A2/A7 and Ras have not been previously explored. Whereas, the relationship between A6 and Ras has been previously investigated (Grewal *et al.*, 2005; de Vilá Muga *et al.*, 2009). One study revealed FRET was more abundant in HG12V compared to HRAS WT, which differs from the results presented here as there were no evident discrepancies between the two forms of HRAS (de Vilá Muga *et al.*, 2009). However, it is to be noted that FRET efficiency was calculated differently in their study, since the percentage represents

the normalisation of donor post- and pre-bleach intensities by the donor post-bleach value (de Vilá Muga *et al.*, 2009). Nevertheless, both set of results showed that FRET occurred between A6 and HRAS. Although, the interaction was not detected in the co-IP experiments, this did not negate that no direct interaction occurred but instead raised the possibility that these interactions might be either weak and/or transient. In general, results presented in this chapter confirm that A6 is an interactor of Ras, which is consistent with other studies.

To understand the consequence of the interaction between A6 and Ras, the effect of A6 on Ras activity was investigated. Reducing endogenous expression of either A2 or A6 resulted in the elevated activation of ERK and Akt (*Fig. 5.8*). Although, MEK activity did not increase and remained fairly similar to control. It is possible that MEK activity had already peaked around 4 minutes as shown in Chapter 3. Therefore, since cells were lysed at the 5-minute timepoint, this could have been missed, so repeat experiments using additional timepoints should be investigated to see whether this is the case. In another study, transient expression of A6 in A6-absent BT20 cell lines appeared to reduce both Pan Ras and MEK activity compared to normal BT20 cells (de Vilá Muga *et al.*, 2009). Interestingly, the observed effect occurred following 3 minutes of EGF stimulation, which further supports that it likely that peak MEK activity was missed in the knockdown experiments performed here (de Vilá Muga *et al.*, 2009). The observed increase in ERK has also been formerly shown in EGF-stimulated HeLa cells that were treated prior with siRNA treatment against A6 (Grewal *et al.*, 2005). Although the results presented here do not formally demonstrate that Ras activity is affected by A6, it has shown that A6 reduced the activity of downstream Ras effectors: Raf and PI3K, therefore highlighting their possible relevance to Ras biology.

Altogether, the previous results indicated that A6 affected Ras downstream signalling and consequently could have an effect on Ras nanoclustering. This was investigated using EM immunogold labelling, however, results revealed a lack of Ras clustering even in control samples, i.e., single transfection of HRAS WT or HG12V. Typically, L_{max} values in previous EM nanoclustering studies have ranged from 1.75 to 6 for GFP-tH, -HRAS and -HG12V

(Prior *et al.*, 2003; Plowman *et al.*, 2005; Belanis *et al.*, 2008). Since HRAS WT and HG12V samples have consistently shown to exhibit nanoclustering, it raises the probability that issues arose here. The choice of cells does not appear to be the problem, as it has been previously shown that nanoclustering can be measured efficiently in HeLa cells and it would be expected that HeLa S3 cells would be similar (Eisenberg *et al.*, 2011; Barceló *et al.*, 2013). From observation, the presence of membrane rip offs was often scarce and difficult to detect in samples. Additionally, there was also a lack of gold-labelling. These could all be contributing factors towards the lack of nanoclustering seen across the samples. Addressing these issues for future experiments could provide confidence as to whether the observed reduced clustering of HRAS WT and HG12V in the presence of A6 can be consistently seen.

Analysing the population distribution of the gold-labelled Ras particles revealed that over 80% of the observed population existed as monomers (*Fig. 5.9c & d*), which is considerably more than the previously reported percentage of 60% (Tian *et al.*, 2010). A6 increased the percentage of monomeric Ras proteins in HG12V with a concomitant reduction in the number of multimers (*Fig. 5.9d*). It has previously been shown that Ras nanoclusters but not monomers can recruit Raf (Tian *et al.*, 2007; Plowman *et al.*, 2008). Therefore, the lack of nanoclusters and subsequent increase in monomers in the presence of A6 indicates A6 promotes the disassembly of Ras nanoclusters. This could represent a form of novel negative Ras nanocluster regulators since only positive regulators to date have been discovered. As a result of decreased Ras clustering, it could be speculated that the number of signalling platforms would be reduced, thus affecting Ras activity. This is coherent with the results observed in the siRNA knockdown experiments where reduced A6 expression resulted in an increase in Ras effector activity. However, it would be important to repeat the nanocluster experiments with the conditions of the siRNA knockdown to directly confirm that the observed increase in Ras effector activity in the presence of low A6 expression was due to elevated clustering of HRAS proteins on the plasma membrane.

Although, these experiments would require further repeats with more reliable controls, the results nevertheless indicate that A6 promotes Ras inactivity in HG12V. This has been reported by other studies with the suggestion that A6 bridges the connection between Ras and gap120 via a calcium-dependent manner (Grewal *et al.*, 2005). However, HG12V mutants are resistant to gap120 inactivation and therefore it is unlikely that this is the mechanism in which A6 inactivates Ras (Smith, Neel and Ikura, 2013).

Collectively, the results suggest A6 reduces Ras nanoclustering in HRAS WT and HG12V, which has not been previously explored. In addition, results here suggest that A6-induced Ras effector inactivity in HG12V might occur due to the disassembly of signalling platforms, although the exact mechanism is unclear and will be elucidated in future studies.

CHAPTER SIX

Discussion

The primary aim of this project was to identify proteins involved in the regulation of Ras nanocluster organisation. Here, APEX2 was used to investigate the proximal proteomes of the three Ras isoforms: KRAS, HRAS and NRAS. This novel screen of the Ras microenvironment generated the first APEX2-Ras database, of which consists of over 2900 Ras proximal proteins. Analysis of this database later revealed that a group of membrane-associated proteins, annexins, could be of interest. Investigations into the relationship between annexins and Ras demonstrated that A6 interacts with HRAS and can negatively regulate HRAS nanoclustering.

6.1. APEX2 AS A SCREENING TOOL

In order to produce a shortlist of candidate proteins that might be involved in Ras nanoclustering, a wide unbiased screening methodology was adopted. Proximity labelling combined with mass spectrometry has become popular in use, with many studies showing success via the identification of novel interactors and regulators (Roux *et al.*, 2012; H.-W. Rhee *et al.*, 2013; Firat-Karalar *et al.*, 2014; Hung *et al.*, 2014; Van Itallie *et al.*, 2014; Fredriksson *et al.*, 2015; Mick *et al.*, 2015; Dong *et al.*, 2016; Lobingier *et al.*, 2017; Paek *et al.*, 2017). BioID and APEX are the forerunners of this type of methodology, with both offering different advantages. APEX generate substrates with a shorter half-life than BioID, thus more likely to capture dynamic transient proteome microenvironments (Roux *et al.*, 2012; Lam *et al.*, 2015). Therefore, due to the short-lived nature of Ras nanoclusters, APEX seemed be the more suitable choice of enzyme for this project and so APEX2, the improved second-generation APEX was used.

6.1.1. First APEX2 screen of the Ras proteome

The preliminary experiments consisted of generating the tools for Ras proximity labelling in HeLa S3 cells, as well as adapting the original protocol based on the labelling of the mitochondrial intermembrane space for the study of the Ras proteome instead. Here, 6 different APEX2-tagged Ras constructs: APEX2-KRAS WT, -KG12V, -HRAS WT, -HG12V, -NRAS WT, -NG12V and 2 controls: APEX2-tH and -tK were designed and

generated. The full-length Ras constructs were able to localise correctly to the plasma membrane and additionally showed to activate downstream effectors such as Raf and PI3K. Various conditions such as the stimulation of Ras activity, biotinylation duration and bead quantity for the streptavidin pulldown were also optimised. This modified protocol with the newly made Ras constructs were used for the later large-scale mass spectrometry experiments.

Here, the first APEX2-based proximity labelling of the Ras proteome was performed. Different Ras isoforms were tested in their unstimulated WT form, as well as in their active state (stimulated or in its mutant G12V form). As a result, a collective database of 2988 proximal proteins was generated for the different conditions. The number of proteins detected with APEX2 was considerably higher than their respective conditions identified in other studies using BioID (Adhikari and Counter, 2018; Go *et al.*, 2019; Kovalski *et al.*, 2019). The main reasons that could have attributed to these differences include the kinetics and biochemistry of the two labelling methods. Another possibility could be due to the analysis. LFQ was used here due to the number of conditions, whereas the BioID studies utilized SILAC-based mass spectrometry approaches. Although SILAC is better for accurate comparisons between conditions, the number of comparisons that could be made are limited to only three or less conditions.

GO analysis revealed that the detected proteins belonged to various subcellular regions. Therefore, it appeared that the combination of the fast-labelling kinetics associated with APEX2 and the dynamic nature of Ras trafficking resulted in widespread labelling throughout the cell. As a result, shortlisting for potential candidates was problematic due to the large protein population. This highlighted the importance of reliable localisation markers for non-enclosed regions, as they aid the elimination of proteins that are not in the area of interest. Despite tK and tH being used, these were not as useful as expected, as they followed similar dynamics to the full-length Ras. Therefore, more stable well-known membrane proteins should be used instead as membrane markers. Nevertheless, in-depth analysis of

the dataset helped narrow down a group of membrane-related proteins proximal to Ras.

Due to the time constraints of this project, transient expression of APEX2-Ras was used, which carries the disadvantage of varying protein expression. Therefore, only crude comparisons could be made between the Ras isoforms and in this case, merely an indication of whether a protein is present in the proximity of Ras within a particular sample, as opposed to absolute comparison of protein levels between the different conditions. However, for future experiments, stable expression of APEX2-Ras should be considered for a better assessment of the differences and similarities amongst the different isoforms and conditions.

6.1.2. Newer proximity labelling techniques

Since the invention of BioID and APEX, newer biotin-based enzymatic tags have been created such as TurboID, MiniTurbo and split-BioID/APEX (De Munter *et al.*, 2017; Xue *et al.*, 2017; Branon *et al.*, 2018). The use of BioID has generally been favoured over APEX, possibly due to toxicity concerns of H_2O_2 treatment. Therefore, most recent advancements in proximity labelling methods were based on BioID (De Munter *et al.*, 2017; Branon *et al.*, 2018). TurboID and MiniTurbo were both developed using the BirA* tag with the addition of further mutagenesis of the reactive biotin-5'-AMP binding motif. The MiniTurbo is essentially a smaller version of the TurboID with two less mutations. These tags have a better labelling efficiency and shorter labelling duration (~10min) compared to BioID (Branon *et al.*, 2018).

Whereas split-BioID/APEX consists of dividing the enzyme into N- and C-terminal fragments that can be fused to two different proteins (De Munter *et al.*, 2017; Xue *et al.*, 2017). This type of tag forms the basis of conditional protein-fragment complementation, whereby activity of the enzyme is regained when the two proteins associate (De Munter *et al.*, 2017; Xue *et al.*, 2017). These newer labelling techniques should be considered for future experiments as they could provide potential advantages over APEX2. For example, split-APEX2 could be used to investigate proteins in the vicinity of active Ras with more accuracy, since the APEX2 fragments could be split between Ras and Raf, thus ensuring

that labelling only occurs when Ras is engaged to Raf.

Overall, APEX2 has shown to be a valuable tool for investigating the Ras proteome. It has efficiently labelled well-known Ras-associated proteins, as well as highlighted possible novel Ras interactors and regulators. Through the process, it became apparent that it carries the main disadvantage of widespread labelling, which could be circumvented using a thorough selection of negative and positive localisation controls. Nonetheless, this large-scale experiment has created a database that can be later used to support other studies of Ras.

6.2. ANNEXIN 6 REDUCES HRAS NANOCLUSTERING

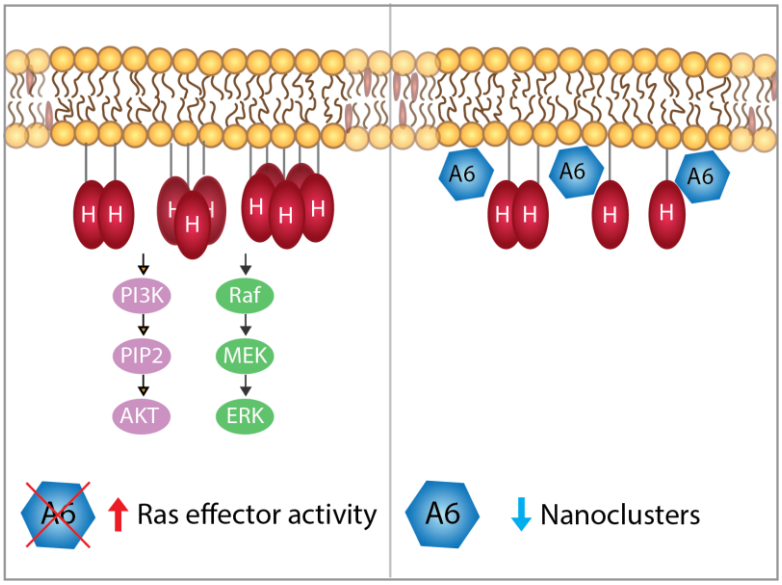

Figure 6.1| Overview of Ras biology in relation to A6 – Schematic of the observed results in this study, A6 siRNA knockdown resulted in the reduction of Ras effector activity. Whereas overexpression of A6 led to decreased HRAS clustering on the plasma membrane.

6.2.1. Key findings of the relationship between A6 and Ras

The APEX2 methodology highlighted various annexins within the Ras proximal proteome, of which a select few were chosen for further analysis of their relationship with Ras. The main finding was that A6 interacted predominantly with the HRAS isoform in both its WT and G12V form. This interaction was most likely transient as it was not clearly detected in the IP experiments but evident using FRET. A6 also affected downstream Ras effector

pathways, whereby reduced A6 expression resulted in elevated Raf and PI3K activity (*Fig. 6.1*).

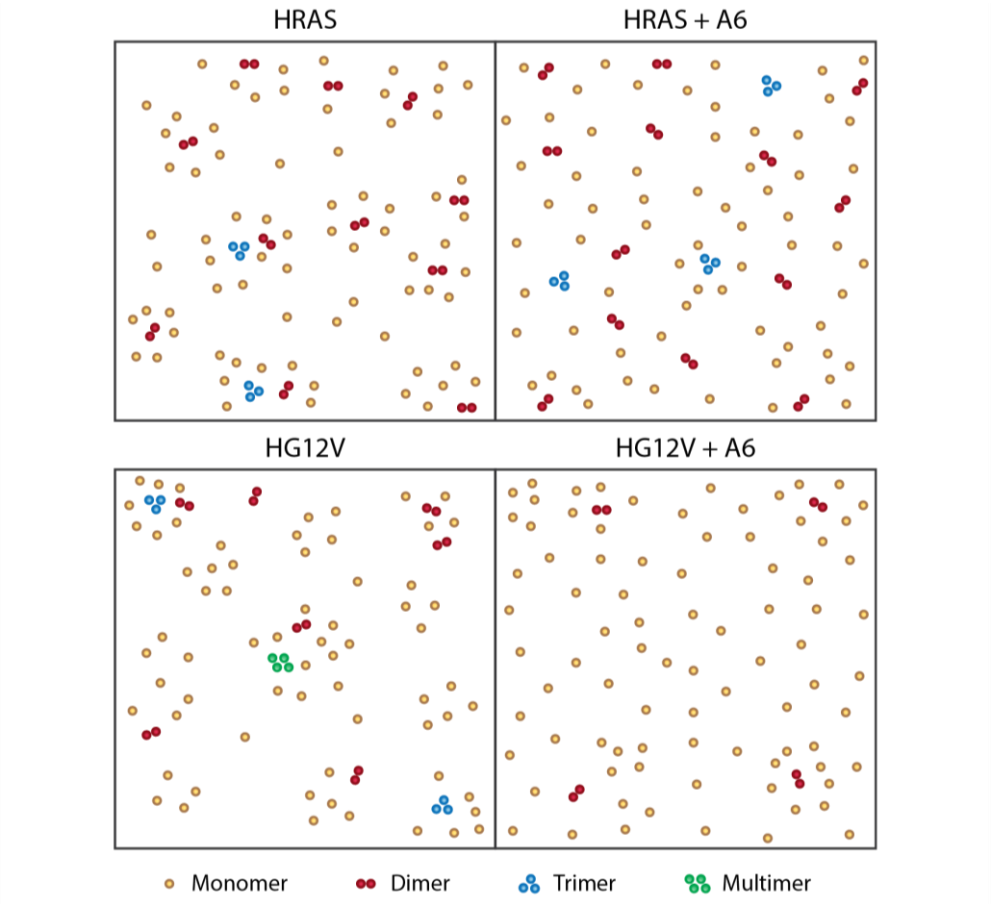

Figure 6.2| Schematic modelling of the effect of A6 on HRAS WT and HG12V distribution on the plasma membrane – Example spatial patterns of gold-labelled HRAS WT and HG12V proteins with/without A6 based on data generated.

These findings have only ever been previously reported by another lab group, which suggested that the mechanism behind the observed A6 and active HRAS interaction was that A6 recruits gap120 in a calcium-dependent manner to the plasma membrane to inactivate Ras (Grewal *et al.*, 2005; de Vilá Muga *et al.*, 2009). More intriguingly, their results showed that A6 only interacted with HG12V, which seems to be contradictory of their proposed mechanism since its widely known that G12V mutants are insensitive to GAPs (Smith, Neel and Ikura, 2013). The lack of both follow-up studies as well as supporting evidence from other groups deemed it necessary to independently investigate this interaction in order to elucidate the underlying mechanism.

Ras nanoclustering was investigated due to the observed effects of A6 on downstream Ras effector signalling. Using EM immunogold labelling, the spatial patterning of HRAS on the plasma membrane was analysed. On the whole, gold-labelling was not as abundant as expected, but the results demonstrated a novel finding that A6 reduced the clustering of both HRAS WT and HG12V (*Fig. 6.1 & 6.2*). For HRAS WT, the population distribution was unaltered by A6, therefore it is likely that the observed overall reduced clustering effect was a result of Ras proteins being generally more dispersed in the presence of A6 (*Fig 6.2*). However, for HG12V, nanoclustering was likely decreased by the significant reduction of higher ordered oligomers (*Fig 6.2*). This phenomenon has not been observed previously and demonstrates a novel process in which Ras nanoclustering is negatively regulated.

6.2.2. Clinical relevance of the A6-HRAS relationship

Similar to Ras, A6 is also associated with cancer. Ras is often mutated, whereas A6 expression vary dependent on the cancer type. It has been reported that A6 plays a potential tumour suppressor role in melanoma, breast and gastric cancers, but promotes tumorigenesis in other cancers such as cervical cancer and lymphoblastic leukaemia (Francia *et al.*, 1996; Smith *et al.*, 2002; Lomnytska *et al.*, 2011; Sakwe *et al.*, 2011; Koumangoye *et al.*, 2013; X. Wang *et al.*, 2013).

In this project, A6 dampened Ras effector activity in the cervical epithelial cancer cell line: HeLa S3, which should consequently result in decreased cellular growth, although further experimentation using growth assays would be required to formally confirm this outcome. This differs from the currently reported role for A6 in cervical cancers, whereby A6 expression improves prognosis, however, it is to be noted that cervical cancers are not primarily Ras driven (Mo, Coulson and Prior, 2018). However, it does highlight that the role of A6 is highly context-dependent and emphasises the importance of testing different cell lines.

In colorectal cancer, a positive correlation between KRAS mutations and A1 overexpression has been observed (Su *et al.*, 2010). Therefore, it is possible that this A6-HRAS relationship

could be of relevance to certain types of cancer, for example, melanoma, which has been linked to both low A6 expression and Ras mutations (Francia *et al.*, 1996; Mo, Coulson and Prior, 2018).

6.2.3. Interaction between A6 and Ras

This study has revealed that A6 interacts with HRAS and that its expression can reduce the clustering of HRAS WT/G12V proteins. It could be speculated that the observed nanoclustering effect is concomitant of the A6 and HRAS interaction, however double immunogold labelling of both proteins would be required for validation. These main findings were established using A6-1, which are predominantly expressed in normal cells, whereas the A6 siRNA used for knockdown experiments targeted both isoforms. It has been reported that A6-2 is the more abundant isoform present in transformed cell lines, therefore A6-2 may also be important for Ras biology.

Annexins can operate in either a calcium-dependent or independent manner. For A6, calcium binding sites are located in domains: 1, 2, 4, 5, 6 and 8 of the annexin core (Huber *et al.*, 1990). However, it is unclear here whether A6 requires calcium to interact with Ras and is a factor to consider in future experiments. Past literature has shown that the A6-Ras interaction was increased when cells were treated with ionomycin, however under physiological conditions, it is unknown whether A6 is dependent on calcium in order to interact with Ras (de Vilá Muga *et al.*, 2009).

Future studies using structural analysis will be vital for understanding their interaction, as it would provide insight as to whether A6 directly blocks Ras from clustering with other Ras proteins, or indirectly via other means such as allosteric hindrance of possible dimerization sites or induction of conformational changes to Ras.

6.2.4. Possible mechanisms behind A6-modulated Ras nanoclustering

The fundamental process in which A6 reduces HRAS clustering is unknown, however some suggestions could be inferred from the current known or suggested roles of A6. Annexins are recognised for their ability to bind phospholipids as well as being instrumental for the

organisation of the plasma membrane and actin cytoskeleton. All of which are vital factors that are essential for the formation of Ras nanoclusters. Therefore, it is highly possible that these connections form the basis of this novel A6 regulatory role.

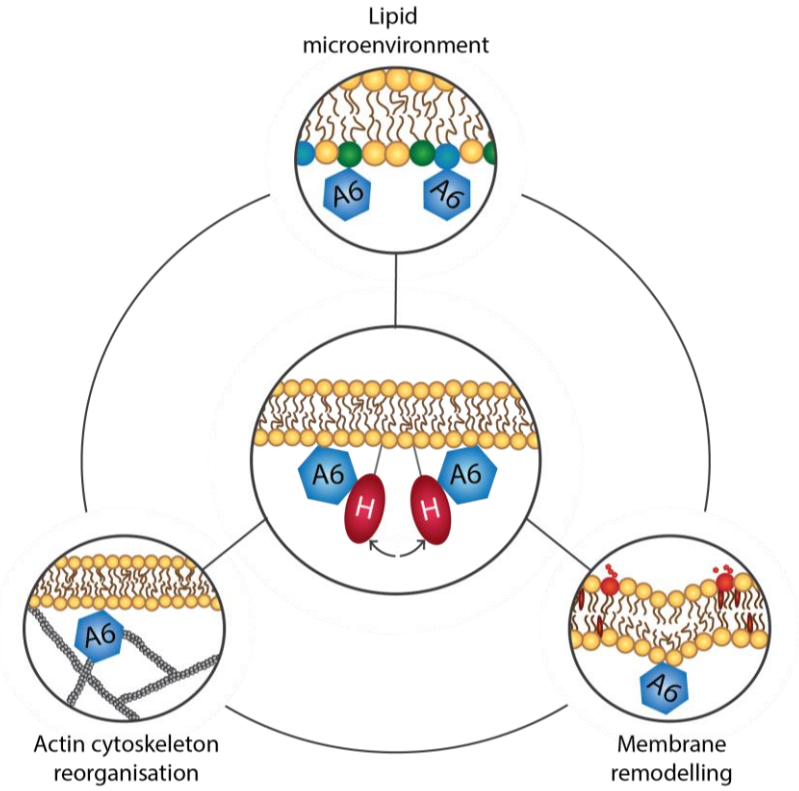

Figure 6.3| Possible factors governing A6-modulated HRAS nanoclustering – A6 has different affinities for various lipid species and is commonly known for its role in mediating changes amongst the actin cytoskeleton and/or plasma membrane. These interlinked factors could contribute to its novel role as a negative regulator of HRAS nanoclustering.

6.2.4.1. Lipid microenvironment

A6 is the largest annexin with a unique double annexin core that allows it to connect up to two distinct membranes. Each domain within the core can bind up to three phospholipid polar head groups (Rescher and Gerke, 2004; Lizarbe *et al.*, 2013). Since its been reported that only the first four annexin core domains are required for the modulation of Ras activity, the remaining domains should be available to bind other components, such as phospholipids, when bound to Ras (de Vilá Muga *et al.*, 2009). It could be speculated that the ability of A6 to bind to phospholipids in the plasma membrane in either a calcium-dependent or independent manner might be a prerequisite to bring A6 into close proximity to HRAS for

an interaction to occur (Golczak *et al.*, 2004; Lizarbe *et al.*, 2013).

As discovered here, A6 interacts predominantly with HRAS WT and HG12V nanoclusters, which are exclusively localised in raft and non-raft domains containing specific phospholipids, respectively. This is consistent with studies showing that A6 can localise to both types of microdomains as well as caveolae and clathrin-coated pits (Kamal, Ying and Anderson, 1998; Alvarez-Guaita *et al.*, 2015). It is thought that each annexin exhibits a preference for certain lipid species, but it is unknown which lipids are preferentially bound by A6 (Lizarbe *et al.*, 2013). It is known that A6 can bind to PS, which is more prevalent in KRAS nanoclusters. Therefore, it would have been expected that interactions would be more noticeable between A6 and KRAS rather than HRAS (Pikuta *et al.*, 1996; Cho, Park and Hancock, 2013). Although, the FRET data shows that KRAS could possibly interact with A6, it was not investigated whether A6 affects KRAS nanoclustering. Nevertheless, PS is also present in HRAS nanoclusters. It is possible that if phospholipids were an important component for governing exclusively the A6-HRAS interaction, then A6 could be more associated with lipid species that are specifically enriched in HRAS microdomains such as PI_4P (Zhou and Hancock, 2015).

6.2.4.2. Membrane remodelling and actin cytoskeleton reorganisation

The process in which A6 modulates Ras nanoclustering could occur directly or indirectly. Direct hinderance of Ras could prevent its association with other Ras proteins or the plasma membrane. Alternatively, A6 could perturb nanoclustering indirectly via membrane remodelling and/or reorganisation of the actin cytoskeleton.

A6 has often been proposed to be involved in membrane organisation due to its ability to bind to phospholipids in the plasma membrane and cytoskeletal proteins (Lizarbe *et al.*, 2013). However, direct evidence supporting this hypothesis has often been lacking, until more recently, a study confirmed A6 can alter the membrane structure (Alvarez-Guaita *et al.*, 2015). Results demonstrated in live A431 cells that upregulation of A6 led to a decrease in membrane order. Depletion of cortical actin using latrunculin B increased the membrane

order of A6-expressing A431 cells compared to control, indicating the importance of the actin cytoskeleton for A6 remodelling of the plasma membrane (Alvarez-Guaita *et al.*, 2015).

Latrunculin B has also been used to show that HRAS WT but not HG12V nanoclusters require intact actin for their formation (Plowman *et al.*, 2005). This raises the possibility that the actin cytoskeleton might be an important factor for the observed A6-modulated reduction in HRAS WT clustering. The authors also suggest that A6 indirectly modulates membrane order via alterations to cholesterol homeostasis, which was not directly evident in their study but shown in their previous study where A6 depleted cholesterol levels in membrane fractions (Cubells *et al.*, 2007; Alvarez-Guaita *et al.*, 2015). However, the reliability of these conclusions is questionable since membrane fractionation experiments generate artefacts and the use of latrunculin B could cause global changes to the cell.

In the same study, cluster analysis revealed that A6 expression increased the clustering of non-raft (Src15) markers greater than raft (Lck10) markers in A431 cells, whereas clustering of both markers were equally increased in mouse embryonic fibroblasts (MEF)-WT cells (Alvarez-Guaita *et al.*, 2015). Although a direct comparison cannot be made, it is of interest that A6 exhibited almost an opposite effect in HeLa S3 cells, where clustering of both HRAS WT and HG12V were reduced, which respectively represented raft and non-raft domains. Therefore, highlighting that the role of A6 in terms of microdomain clustering is likely to be cell-type dependent.

In general, the study performed here has contributed to the understanding of A6 in the context of Ras. The ability of A6 to interact with both HRAS WT and HG12V indicates that not only does A6 modulate both their respective raft and non-raft microdomains but also that A6 localises to these structures. Since A6 could reduce Ras nanoclustering in both HRAS WT and HG12V, it could be speculated that these unique microenvironments composed of different proteins and lipids provides a combinational signal that determines the mechanism in which A6 restructures these domains, possibly via the actin cytoskeleton,

in order to reduce HRAS clustering. The population distribution analysis showed that HG12V nanoclusters could be potentially reduced by the disassembly of higher ordered oligomers in the presence of A6, suggesting HG12V nanoclusters undergoes a different kind of remodelling compared to HRAS WT. In summary, it could be hypothesized that A6 remodels microdomains in order to disrupt HRAS nanoclustering, which could form the basis of future investigations.

6.3. FUTURE WORK

Majority of this project was based on establishing the APEX2 method for the study of Ras and subsequently generating the proximity proteome database. The initial work was instrumental for the discovery of the A6-HRAS interaction and preliminary results have demonstrated a novel role for A6 in the context of Ras nanoclustering. However, further experiments are required such as:

1. To repeat the comprehensive survey of the Ras proximity proteome with more accuracy, i.e., use of stably expressed APEX2-tagged Ras and reliable localisation markers. This will allow for more precise comparisons between isoforms and conditions, as well as aid the shortlisting process of membrane proteins.

2. To fully characterise the role of A6 in Ras nanoclustering in all three Ras isoforms. Double immunogold labelling could be used to assess A6 in addition to Ras, since annexins have also shown to dimerize. This will provide insight of the spatial relationship between A6 and Ras on a nanoscale resolution. Due to the possibility of context-dependent effects, other cell lines should also be considered.

3. To elucidate the A6-Ras interaction and the mechanism behind the regulation of HRAS nanoclustering by A6. Structural analysis could reveal how A6 and HRAS interact and provide insight on if other domains on A6 are available to bind lipids or other proteins. In terms of nanoclustering, it should be examined whether A6 alters Ras clustering directly, or indirectly via the actin cytoskeleton and/or lipid microdomains on the plasma membrane.

6.4. CONCLUDING REMARKS

To summarise, APEX2 was used to do a comprehensive survey of the proximity proteome microenvironment of all three Ras isoforms: KRAS, HRAS and NRAS in different conditions. This produced an extensive database that could be processed to understand the types of proteins present, as well as shortlist potential proteins that could regulate Ras nanoclustering. Following a series of different interaction studies and nanoclustering experiments, A6 was found to interact with HRAS (both WT and mutant) and reduce the clustering of these Ras proteins at the plasma membrane. Possibly as a consequence, downstream Ras effector pathways were also negatively affected by A6. Although A6 cannot be used as a therapeutic target in Ras-driven cancers due to its universal role within the cell, it has been imperative to understand their interaction with Ras. Thus, APEX2 has been fundamental for advancing our knowledge of the Ras proteome and more importantly, the discovery of the first negative regulator of Ras nanoclustering.

References

Abankwa, D. *et al.* (2008) 'A novel switch region regulates H-ras membrane orientation and signal output', *EMBO Journal*. European Molecular Biology Organization, 27(5), pp. 727–735. doi: 10.1038/emboj.2008.10.

Abankwa, D. *et al.* (2010) 'Ras membrane orientation and nanodomain localization generate isoform diversity', *Proceedings of the National Academy of Sciences of the United States of America*, 107(3), pp. 1130–1135. doi: 10.1073/pnas.0903907107.

Abdelmohsen, K. and Gorospe, M. (2012) 'RNA-binding protein nucleolin in disease', *RNA Biology*. Taylor and Francis Inc., pp. 799–808. doi: 10.4161/rna.19718.

Adhikari, H. and Counter, C. M. (2018) 'Interrogating the protein interactomes of RAS isoforms identifies PIP5K1A as a KRAS-specific vulnerability', *Nature Communications*. Nature Publishing Group, 9(1), p. 3646. doi: 10.1038/s41467-018-05692-6.

Agamasu, C. *et al.* (2019) 'KRAS Prenylation Is Required for Bivalent Binding with Calmodulin in a Nucleotide-Independent Manner', *Biophysical Journal*. Biophysical Society, 116(6), pp. 1049–1063. doi: 10.1016/j.bpj.2019.02.004.

Alvarez-Guaita, A. *et al.* (2015) 'Evidence for annexin A6-dependent plasma membrane remodelling of lipid domains', *British Journal of Pharmacology*. John Wiley and Sons Inc., 172(7), pp. 1677–1690. doi: 10.1111/bph.13022.

Ambrogio, C. *et al.* (2018) 'KRAS Dimerization Impacts MEK Inhibitor Sensitivity and Oncogenic Activity of Mutant KRAS', *Cell*. Cell Press, 172(4), pp. 857-868.e15. doi: 10.1016/j.cell.2017.12.020.

Amini, F., Kodadek, T. and Brown, K. C. (2002) 'Protein affinity labeling mediated by genetically encoded peptide tags.', *Angewandte Chemie (International ed. in English)*, 41(2), pp. 356–9. doi: 10.1002/1521-3773(20020118)41:2<356::aid-anie356>3.0.co;2-m.

Aoki, Y. *et al.* (2005) 'Germline mutations in HRAS proto-oncogene cause Costello syndrome', *Nature Genetics*, 37(10), pp. 1038–1040. doi: 10.1038/ng1641.

Apolloni, A. *et al.* (2000) 'H-ras but Not K-ras Traffics to the Plasma Membrane through the Exocytic Pathway', *Molecular and Cellular Biology*. American Society for Microbiology, 20(7), pp. 2475–2487. doi: 10.1128/mcb.20.7.2475-2487.2000.

Aran, V. and Prior, I. A. (2013) 'Compartmentalized Ras signaling differentially contributes to phenotypic outputs', *Cellular Signalling*. Elsevier, 25(9), pp. 1748–1753. doi: 10.1016/j.cellsig.2013.05.004.

Ariotti, N. *et al.* (2014) 'Caveolae regulate the nanoscale organization of the plasma membrane to remotely control Ras signaling.', *The Journal of cell biology*. The Rockefeller University Press, 204(5), pp. 777–92. doi: 10.1083/jcb.201307055.

Ashery, U. *et al.* (2006) 'Spatiotemporal organization of Ras signaling: Rasosomes and the galectin switch', *Cellular and Molecular Neurobiology*. Springer, 26(4–6), pp. 471–495. doi: 10.1007/s10571-006-9059-3.

Babiychuk, E. B. and Draeger, A. (2000) *Annexins in Cell Membrane Dynamics: Ca 2-regulated Association of Lipid Microdomains*, *The Journal of Cell Biology*. Available at: http://www.jcb.org (Accessed: 25 February 2020).

Barceló, C. *et al.* (2013) 'Oncogenic K-ras segregates at spatially distinct plasma membrane signaling platforms according to its phosphorylation status', *Journal of Cell Science*. The Company of Biologists Ltd, 126(20), pp. 4553–4559. doi: 10.1242/jcs.123737.

Belanis, L. *et al.* (2008) 'Galectin-1 is a novel structural component and a major regulator of H-Ras nanoclusters', *Molecular Biology of the Cell*. American Society for Cell Biology, 19(4), pp. 1404–1414. doi: 10.1091/mbc.E07-10-1053.

Bhaskar, B. *et al.* (2003) 'A novel heme and peroxide-dependent tryptophan-tyrosine cross-link in a mutant of cytochrome c peroxidase', *Journal of Molecular Biology*. Academic Press, 328(1), pp. 157–166. doi: 10.1016/S0022-2836(03)00179-7.

Birchenall-Roberts, M. C. *et al.* (2006) 'K-Ras4B proteins are expressed in the nucleolus: Interaction with nucleolin', *Biochemical and Biophysical Research Communications*. Biochem Biophys Res Commun, 348(2), pp. 540–549. doi: 10.1016/j.bbrc.2006.07.094.

Bishop, A. L. and Hall, A. (2000) 'Rho GTPases and their effector proteins', *Biochemical Journal*, pp. 241–255. doi: 10.1042/0264-6021:3480241.

Bivona, T. G. *et al.* (2003) 'Phospholipase Cγ activates Ras on the Golgi apparatus by means of RasGRP1', *Nature*. Nature Publishing Group, 424(6949), pp. 694–698. doi: 10.1038/nature01806.

Bivona, T. G. *et al.* (2006) 'PKC regulates a farnesyl-electrostatic switch on K-Ras that promotes its association with Bcl-XL on mitochondria and induces apoptosis', *Molecular Cell*, 21(4), pp. 481–493. doi: 10.1016/j.molcel.2006.01.012.

Blaževitš, O. *et al.* (2016) 'Galectin-1 dimers can scaffold Raf-effectors to increase H-ras nanoclustering', *Scientific Reports*. Nature Publishing Group, 6. doi: 10.1038/srep24165.

Boriack-Sjodin, P. A. *et al.* (1998) 'The structural basis of the activation of Ras by Sos', *Nature*. Nature Publishing Group, 394(6691), pp. 337–343. doi: 10.1038/28548.

Borisov, N. *et al.* (2009) 'Systems-level interactions between insulin-EGF networks amplify mitogenic signaling', *Molecular Systems Biology*, 5. doi: 10.1038/msb.2009.19.

Bos, J. L., Rehmann, H. and Wittinghofer, A. (2007) 'GEFs and GAPs: Critical Elements in the Control of Small G Proteins', *Cell*. Cell Press, pp. 865–877. doi: 10.1016/j.cell.2007.05.018.

Bourne, H. R., Sanders, D. A. and McCormick, F. (1990) 'The GTPase superfamily: A conserved switch for diverse cell functions', *Nature*, pp. 125–132. doi: 10.1038/348125a0.

Bourne, H. R., Sanders, D. A. and McCormick, F. (1991) 'The GTPase superfamily: conserved structure and molecular mechanism', *Nature*, pp. 117–127. doi: 10.1038/349117a0.

Box, J. K. *et al.* (2016) 'Nucleophosmin: From structure and function to disease development', *BMC Molecular Biology*. BioMed Central Ltd., 17(1), p. 19. doi: 10.1186/s12867-016-0073-9.

Boyartchuk, V. L., Ashby, M. N. and Rine, J. (1997) 'Modulation of ras and a-factor function by carboxyl-terminal proteolysis', *Science*, 275(5307), pp. 1796–1800. doi: 10.1126/science.275.5307.1796.

Branon, T. C. *et al.* (2018) 'Efficient proximity labeling in living cells and organisms with TurboID', *Nature Biotechnology*. Nature Publishing Group, 36(9), pp. 880–898. doi: 10.1038/nbt.4201.

Brock, E. J. *et al.* (2016) 'How to Target Activated Ras Proteins: Direct Inhibition vs. Induced Mislocalization.', *Mini reviews in medicinal chemistry*. NIH Public Access, 16(5), pp. 358–69. doi: 10.2174/1389557515666151001154002.

Brunet, A., Datta, S. R. and Greenberg, M. E. (2001) 'Transcription-dependent and -independent control of neuronal survival by the PI3K-Akt signaling pathway', *Current Opinion in Neurobiology*. Elsevier Ltd, pp. 297–305. doi: 10.1016/S0959-4388(00)00211-7.

Buday, L. and Downward, J. (1993) 'Epidermal growth factor regulates p21ras through the formation of a complex of receptor, Grb2 adapter protein, and Sos nucleotide exchange factor', *Cell*, 73(3), pp. 611–620. doi: 10.1016/0092-8674(93)90146-H.

Canon, J. *et al.* (2019) 'The clinical KRAS(G12C) inhibitor AMG 510 drives anti-tumour immunity', *Nature*. Nature Publishing Group, 575(7781), pp. 217–223. doi: 10.1038/s41586-019-1694-1.

Casey, P. J. and Seabra, M. C. (1996) 'Protein prenyltransferases', *Journal of Biological Chemistry*, pp. 5289–5292. doi: 10.1074/jbc.271.10.5289.

Chandra, A. *et al.* (2012) 'The GDI-like solubilizing factor PDEδ sustains the spatial organization and signalling of Ras family proteins', *Nature Cell Biology*. Nature Publishing Group, 14(2), pp. 148–158. doi: 10.1038/ncb2394.

Chang, F. *et al.* (2003) 'Signal transduction mediated by the Ras/Raf/MEK/ERK pathway from cytokine receptors to transcription factors: Potential targeting for therapeutic intervention', *Leukemia*. Nature Publishing Group, pp. 1263–1293. doi: 10.1038/sj.leu.2402945.

Chapman-Smith, A. and Cronan, J. E. (1999) 'In vivo enzymatic protein biotinylation', *Biomolecular Engineering*. Elsevier, 16(1–4), pp. 119–125. doi: 10.1016/S1050-3862(99)00046-7.

Cherfils, J. and Zeghouf, M. (2013) 'Regulation of small GTPases by GEFs, GAPs, and GDIs', *Physiological Reviews*. Physiol Rev, pp. 269–309. doi: 10.1152/physrev.00003.2012.

Chiu, V. K. *et al.* (2002) 'Ras signalling on the endoplasmic reticulum and the Golgi', *Nature Cell Biology*. Nature Publishing Group, 4(5), pp. 343–350. doi: 10.1038/ncb783.

Cho, K. J., Park, J. H. and Hancock, J. F. (2013) 'Staurosporine: A new tool for studying phosphatidylserine trafficking', *Communicative and Integrative Biology*, 6(4). doi: 10.4161/cib.24746.

Choy, E. *et al.* (1999) 'Endomembrane trafficking of ras: The CAAX motif targets proteins to the ER and Golgi', *Cell*. Cell Press, 98(1), pp. 69–80. doi: 10.1016/S0092-8674(00)80607-8.

Cirstea, I. C. *et al.* (2010) 'A restricted spectrum of NRAS mutations causes Noonan syndrome', *Nature Genetics*, 42(1), pp. 27–29. doi: 10.1038/ng.497.

Cohen-Jonathan, E. *et al.* (2009) 'Farnesyltransferase Inhibitors Potentiate the Antitumor Effect of Radiation on a Human Tumor Xenograft Expressing Activated HRAS1', *http://dx.doi.org/10.1667/0033-7587(2000)154[0125:FIPTAE]2.0.CO;2*. doi: 10.1667/0033-7587(2000)154[0125:FIPTAE]2.0.CO;2.

Connor, J. *et al.* (1992) 'Bidirectional transbilayer movement of phospholipid analogs in human red blood cells. Evidence for an ATP-dependent and protein-mediated process', *Journal of Biological Chemistry*, 267(27), pp. 19412–19417.

Contente, S., Yeh, T. J. A. and Friedman, R. M. (2011) 'H-ras localizes to cell nuclei and varies with the cell cycle', *Genes and Cancer*. Genes Cancer, 2(2), pp. 166–172. doi: 10.1177/1947601911405042.

Cox, A. D. *et al.* (2014) 'Drugging the undruggable RAS: Mission Possible?', *Nature Reviews Drug Discovery*. Nature Publishing Group, pp. 828–851. doi: 10.1038/nrd4389.

Creutz, C. E., Pazoles, C. J. and Pollard, H. B. (1978) 'Identification and purification of an adrenal medullary protein (synexin) that causes calcium-dependent aggregation of isolated chromaffin granules', *Journal of Biological Chemistry*, 253(8), pp. 2858–2866.

Crumpton, M. J. and Dedman, J. R. (1990) 'Protein terminology tangle [7]', *Nature*. Nature Publishing Group, p. 212. doi: 10.1038/345212a0.

Cubells, L. *et al.* (2007) 'Annexin a6-Induced alterations in cholesterol transport and caveolin export from the Golgi complex', *Traffic*. Wiley-Blackwell, 8(11), pp. 1568–1589. doi: 10.1111/j.1600-0854.2007.00640.x.

Cutler, R. E. *et al.* (1998) 'Autoregulation of the Raf-1 serine/threonine kinase', *Proceedings of the National Academy of Sciences of the United States of America*. National Academy of Sciences, 95(16), pp. 9214–9219. doi: 10.1073/pnas.95.16.9214.

D'Souza-Schorey, C. and Chavrier, P. (2006) 'ARF proteins: Roles in membrane traffic and beyond', *Nature Reviews Molecular Cell Biology*, pp. 347–358. doi: 10.1038/nrm1910.

Dai, Q. *et al.* (1998) 'Mammalian prenylcysteine carboxyl methyltransferase is in the endoplasmic reticulum', *Journal of Biological Chemistry*. American Society for Biochemistry and Molecular Biology, 273(24), pp. 15030–15034. doi: 10.1074/jbc.273.24.15030.

Daniels, M. A. *et al.* (2006) 'Thymic selection threshold defined by compartmentalization of Ras/MAPK signalling', *Nature*. Nature Publishing Group, 444(7120), pp. 724–729. doi: 10.1038/nature05269.

Der, C. J., Finkel, T. and Cooper, G. M. (1986) 'Biological and biochemical properties of human rasH genes mutated at codon 61', *Cell*. Cell, 44(1), pp. 167–176. doi: 10.1016/0092-8674(86)90495-2.

Der, C. J., Krontiris, T. G. and Cooper, G. M. (1982) 'Transforming genes of human bladder and lung carcinoma cell lines are homologous to the ras genes of Harvey and Kristen sarcoma viruses', *Proceedings of the National Academy of Sciences of the United States of America*. National Academy of Sciences, 79(11 I), pp. 3637–3640. doi: 10.1073/pnas.79.11.3637.

Dickson, B. *et al.* (1992) 'Raf functions downstream of Rasl in the Sevenless signal transduction pathway', *Nature*, 360(6404), pp. 600–603. doi: 10.1038/360600a0.

Dong, J.-M. *et al.* (2016) 'Proximity biotinylation provides insight into the molecular composition of focal adhesions at the nanometer scale', *Science Signaling*, 9(432), pp. rs4–rs4. doi: 10.1126/scisignal.aaf3572.

Du, R. *et al.* (2018) 'Downregulation of annexin A3 inhibits tumor metastasis and decreases drug resistance in breast cancer', *Cell Death and Disease*. Nature Publishing Group, 9(2), p. 126. doi: 10.1038/s41419-017-0143-z.

Duncan, J. A. and Gilman, A. G. (1998) 'A cytoplasmic acyl-protein thioesterase that removes palmitate from G protein α subunits and p21(RAS)', *Journal of Biological Chemistry*. American Society for Biochemistry and Molecular Biology, 273(25), pp. 15830–15837. doi: 10.1074/jbc.273.25.15830.

Eberhard, D. A. *et al.* (2001) 'Control of the nuclear-cytoplasmic partitioning of annexin II by a nuclear export signal and by p11 binding', *Journal of Cell Science*, 114(17), pp. 3155–3166.

Ebner, M. *et al.* (2017) 'PI(3,4,5)P3 Engagement Restricts Akt Activity to Cellular

Membranes', *Molecular Cell*. Cell Press, 65(3), pp. 416-431.e6. doi: 10.1016/j.molcel.2016.12.028.

Echols, N. (2002) 'Comprehensive analysis of amino acid and nucleotide composition in eukaryotic genomes, comparing genes and pseudogenes', *Nucleic Acids Research*. Oxford University Press (OUP), 30(11), pp. 2515–2523. doi: 10.1093/nar/30.11.2515.

Edkins, S. *et al.* (2006) 'Recurrent KRAS codon 146 mutations in human colorectal cancer', *Cancer Biology and Therapy*. Landes Bioscience, 5(8), pp. 928–932. doi: 10.4161/cbt.5.8.3251.

Eisenberg, S. *et al.* (2011) 'Raft Protein Clustering Alters N-Ras Membrane Interactions and Activation Pattern', *Molecular and Cellular Biology*. American Society for Microbiology, 31(19), pp. 3938–3952. doi: 10.1128/mcb.05570-11.

Elad-Sfadia, G. *et al.* (2004) 'Galectin-3 augments K-ras activation and triggers a ras signal that attenuates ERK but not phosphoinositide 3-kinase activity', *Journal of Biological Chemistry*. American Society for Biochemistry and Molecular Biology, 279(33), pp. 34922–34930. doi: 10.1074/jbc.M312697200.

Ellis, R. W. *et al.* (1981) 'The p21 src genes of Harvey and Kirsten sarcoma viruses originate from divergent members of a family of normal vertebrate genes', *Nature*. Nature Publishing Group, 292(5823), pp. 506–511. doi: 10.1038/292506a0.

Fantl, W. J., Johnson, D. E. and Williams, L. T. (1993) 'Signalling by Receptor Tyrosine Kinases', *Annual Review of Biochemistry*. Annual Reviews, 62(1), pp. 453–481. doi: 10.1146/annurev.bi.62.070193.002321.

Fell, J. B. *et al.* (2020) 'Identification of the Clinical Development Candidate MRTX849, a Covalent KRASG12C Inhibitor for the Treatment of Cancer', *Journal of Medicinal Chemistry*. American Chemical Society. doi: 10.1021/acs.jmedchem.9b02052.

Filippov, A., Orädd, G. and Lindblom, G. (2004) 'Lipid Lateral Diffusion in Ordered and Disordered Phases in Raft Mixtures', *Biophysical Journal*. Biophysical Society, 86(2), pp. 891–896. doi: 10.1016/S0006-3495(04)74164-8.

Firat-Karalar, E. N. *et al.* (2014) 'Proximity Interactions among Centrosome Components Identify Regulators of Centriole Duplication', *Current Biology*, 24(6), pp. 664–670. doi: 10.1016/j.cub.2014.01.067.

Francia, G. *et al.* (1996) 'Identification by differential display of Annexin-VI, a gene differentially expressed during melanoma progression', *Cancer Research*, 56(17), pp. 3855–3858.

Frech, M. *et al.* (1994) 'Role of Glutamine-61 in the Hydrolysis of GTP by p21H-ras: An Experimental and Theoretical Study', *Biochemistry*. Biochemistry, 33(11), pp. 3237–3244. doi: 10.1021/bi00177a014.

Fredriksson, K. *et al.* (2015) 'Proteomic Analysis of Proteins Surrounding Occludin and Claudin-4 Reveals Their Proximity to Signaling and Trafficking Networks', *PLOS ONE*. Edited by T. Wang, 10(3), p. e0117074. doi: 10.1371/journal.pone.0117074.

Friedlaender, A. *et al.* (2020) 'KRAS as a druggable target in NSCLC: Rising like a phoenix after decades of development failures', *Cancer Treatment Reviews*. W.B. Saunders Ltd, p. 101978. doi: 10.1016/j.ctrv.2020.101978.

Garnett, M. J. *et al.* (2005) 'Wild-type and mutant B-RAF activate C-RAF through distinct mechanisms involving heterodimerization', *Molecular Cell*. Cell Press, 20(6), pp. 963–969. doi: 10.1016/j.molcel.2005.10.022.

Geißlera, K. J. *et al.* (2013) 'Regulation of Son of sevenless by the membrane-actin linker protein ezrin', *Proceedings of the National Academy of Sciences of the United States of America*. National Academy of Sciences, 110(51), pp. 20587–20592. doi: 10.1073/pnas.1222078110.

Gerke, V. and Moss, S. E. (2002) 'Annexins: From structure to function', *Physiological Reviews*. American Physiological Society, pp. 331–371. doi: 10.1152/physrev.00030.2001.

Ghosh, S. *et al.* (1996) 'Raf-1 kinase possesses distinct binding domains for phosphatidylserine and phosphatidic acid: Phosphatidic acid regulates the translocation of Raf-1 in 12-O-tetradecanoylphorbol-13-acetate-stimulated Madin-Darby canine kidney cells', *Journal of Biological Chemistry*. American Society for Biochemistry and Molecular Biology Inc., 271(14), pp. 8472–8480. doi: 10.1074/jbc.271.14.8472.

Go, C. D. *et al.* (2019) 'A proximity biotinylation map of a human cell', *bioRxiv*. Cold Spring Harbor Laboratory, p. 796391. doi: 10.1101/796391.

Goebeler, V. *et al.* (2008) 'Annexin A8 regulates late endosome organization and function', *Molecular Biology of the Cell*. American Society for Cell Biology, 19(12), pp. 5267–5278. doi: 10.1091/mbc.E08-04-0383.

Golczak, M. *et al.* (2004) 'Structure of human annexin A6 at the air-water interface and in a membrane-bound state', *Biophysical Journal*. Biophysical Society, 87(2), pp. 1215–1226. doi: 10.1529/biophysj.103.038240.

Goodwin, J. S. *et al.* (2005) 'Depalmitoylated Ras traffics to and from the Golgi complex via a nonvesicular pathway', *Journal of Cell Biology*. The Rockefeller University Press, 170(2), pp. 261–272. doi: 10.1083/jcb.200502063.

Gorfe, A. A., Grant, B. J. and McCammon, J. A. (2008) 'Mapping the Nucleotide and Isoform-Dependent Structural and Dynamical Features of Ras Proteins', *Structure*. Howard Hughes Medical Institute, 16(6), pp. 885–896. doi: 10.1016/j.str.2008.03.009.

Grant, B. M. M. *et al.* (2020) 'Calmodulin disrupts plasma membrane localization of farnesylated KRAS4b by sequestering its lipid moiety', *Science Signaling*. American Association for the Advancement of Science, 13(625). doi: 10.1126/scisignal.aaz0344.

Grewal, T. *et al.* (2005) 'Annexin A6 stimulates the membrane recruitment of p120GAP to modulate Ras and Raf-1 activity', *Oncogene*, 24(38), pp. 5809–5820. doi: 10.1038/sj.onc.1208743.

Gripp, K. W. *et al.* (2002) 'Five additional Costello syndrome patients with rhabdomyosarcoma: Proposal for a tumor screening protocol', *American Journal of Medical Genetics*, 108(1), pp. 80–87. doi: 10.1002/ajmg.10241.

Gstraunthaler, G. (2003) 'Alternatives to the use of fetal bovine serum: serum-free cell culture.', *ALTEX : Alternativen zu Tierexperimenten*, 20(4), pp. 275–281.

Gupta, S. *et al.* (2007) 'Binding of Ras to Phosphoinositide 3-Kinase p110α Is Required for Ras- Driven Tumorigenesis in Mice', *Cell*, 129(5), pp. 957–968. doi: 10.1016/j.cell.2007.03.051.

Haga, R. B. and Ridley, A. J. (2016) 'Rho GTPases: Regulation and roles in cancer cell biology', *Small GTPases*. Taylor and Francis Inc., pp. 207–221. doi: 10.1080/21541248.2016.1232583.

Hall, A. *et al.* (1983) 'Identification of transforming gene in two human sarcoma cell lines as a new member of the ras gene family located on chromosome 1', *Nature*. Nature Publishing Group, 303(5916), pp. 396–400. doi: 10.1038/303396a0.

Han, M. *et al.* (1993) 'C. elegans lin-45 raf gene participates in let-60 ras-stimulated vulval differentiation.', *Nature*, 363(6425), pp. 133–40. doi: 10.1038/363133a0.

Han, S. *et al.* (2017) 'Proximity Biotinylation as a Method for Mapping Proteins Associated with mtDNA in Living Cells', *Cell Chemical Biology*. Elsevier Ltd, 24(3), pp. 404–414. doi: 10.1016/j.chembiol.2017.02.002.

Hanahan, D. and Weinberg, R. A. (2011) 'Hallmarks of cancer: The next generation', *Cell*, pp. 646–674. doi: 10.1016/j.cell.2011.02.013.

Hancock, J. F. *et al.* (1989) 'All ras proteins are polyisoprenylated but only some are palmitoylated', *Cell*, 57(7), pp. 1167–1177. doi: 10.1016/0092-8674(89)90054-8.

Hancock, J. F., Paterson, H. and Marshall, C. J. (1990) 'A polybasic domain or palmitoylation is required in addition to the CAAX motif to localize p21ras to the plasma membrane', *Cell*, 63(1), pp. 133–139. doi: 10.1016/0092-8674(90)90294-O.

Harvey, J. J. (1964) 'An unidentified virus which causes the rapid production of tumours in mice [33]', *Nature*. Nature Publishing Group, pp. 1104–1105. doi: 10.1038/2041104b0.

Hayes, M. J. and Moss, S. E. (2009) 'Annexin 2 has a dual role as regulator and effector of v-Src in cell transformation', *Journal of Biological Chemistry*, 284(15), pp. 10202–10210. doi: 10.1074/jbc.M807043200.

Heerklotz, H. (2002) 'Triton promotes domain formation in lipid raft mixtures', *Biophysical*

Journal. Biophysical Society, 83(5), pp. 2693–2701. doi: 10.1016/S0006-3495(02)75278-8.

Hekman, M. *et al.* (2002) 'Associations of B- and C-raf with cholesterol, phosphatidylserine, and lipid second messengers: Preferential binding of raf to artificial lipid rafts', *Journal of Biological Chemistry*. American Society for Biochemistry and Molecular Biology, 277(27), pp. 24090–24102. doi: 10.1074/jbc.M200576200.

Hemmings, B. A. and Restuccia, D. F. (2012) 'PI3K-PKB/Akt pathway', *Cold Spring Harbor Perspectives in Biology*. Cold Spring Harbor Laboratory Press, 4(9). doi: 10.1101/cshperspect.a011189.

Henis, Y. I., Hancock, J. F. and Prior, I. A. (2009) 'Ras acylation, compartmentalization and signaling nanoclusters (Review)', *Molecular Membrane Biology*. Taylor & Francis, 26(1–2), pp. 80–92. doi: 10.1080/09687680802649582.

Hernandez-Valladares, M. and Prior, I. A. (2015) 'Comparative proteomic analysis of compartmentalised Ras signalling', *Scientific Reports*. Nature Publishing Group, 5. doi: 10.1038/srep17307.

van der Hoeven, D. *et al.* (2013) 'Fendiline Inhibits K-Ras Plasma Membrane Localization and Blocks K-Ras Signal Transmission', *Molecular and Cellular Biology*. American Society for Microbiology, 33(2), pp. 237–251. doi: 10.1128/mcb.00884-12.

Hofer, F. *et al.* (1994) 'Activated Ras interacts with the Ral guanine nucleotide dissociation stimulator', *Proceedings of the National Academy of Sciences of the United States of America*, 91(23), pp. 11089–11093. doi: 10.1073/pnas.91.23.11089.

Hofmann, A. *et al.* (2000) 'The annexin A3-membrane interaction is modulated by an N-terminal tryptophan', *Biochemistry*. American Chemical Society, 39(26), pp. 7712–7721. doi: 10.1021/bi992359+.

Honke, K. and Kotani, N. (2012) 'Identification of Cell-Surface Molecular Interactions under Living Conditions by Using the Enzyme-Mediated Activation of Radical Sources (EMARS) Method', *Sensors*, 12(12), pp. 16037–16045. doi: 10.3390/s121216037.

Hood, F. E. *et al.* (2019) 'Isoform-specific Ras signaling is growth factor dependent', *Molecular Biology of the Cell*. Edited by J. Chernoff. American Society for Cell Biology, 30(9), pp. 1108–1117. doi: 10.1091/mbc.E18-10-0676.

Hooper, N. M. (1999) 'Detergent-insoluble glycosphingolipid/cholesterol-rich membrane domains, lipid rafts and caveolae', *Molecular Membrane Biology*, pp. 145–156. doi: 10.1080/096876899294607.

Howe, L. R. *et al.* (1992) 'Activation of the MAP kinase pathway by the protein kinase raf', *Cell*, 71(2), pp. 335–342. doi: 10.1016/0092-8674(92)90361-F.

Hua, K. *et al.* (2018) 'Downregulation of annexin A11 (ANXA11) inhibits cell proliferation,

invasion, and migration via the AKT/GSK-3β pathway in gastric cancer', *Medical Science Monitor*. International Scientific Information, Inc., 24, pp. 149–160. doi: 10.12659/MSM.905372.

Huber, R. *et al.* (1990) 'The calcium binding sites in human annexin V by crystal structure analysis at 2.0 A resolution Implications for membrane binding and calcium channel activity', *FEBS Letters*. FEBS Lett, 275(1–2), pp. 15–21. doi: 10.1016/0014-5793(90)81428-Q.

Huber, R., Römisch, J. and Paques, E. P. (1990) 'The crystal and molecular structure of human annexin V, an anticoagulant protein that binds to calcium and membranes.', *The EMBO Journal*. Wiley, 9(12), pp. 3867–3874. doi: 10.1002/j.1460-2075.1990.tb07605.x.

Hung, V. *et al.* (2014) 'Proteomic mapping of the human mitochondrial intermembrane space in live cells via ratiometric APEX tagging.', *Molecular cell*. NIH Public Access, 55(2), pp. 332–41. doi: 10.1016/j.molcel.2014.06.003.

Hung, V. *et al.* (2016) 'Spatially resolved proteomic mapping in living cells with the engineered peroxidase APEX2.', *Nature protocols*. NIH Public Access, 11(3), pp. 456–75. doi: 10.1038/nprot.2016.018.

Hung, V. *et al.* (2017) 'Proteomic mapping of cytosol-facing outer mitochondrial and ER membranes in living human cells by proximity biotinylation.', *eLife*. eLife Sciences Publications, Ltd, 6. doi: 10.7554/eLife.24463.

Hunter, J. C. *et al.* (2015) 'Biochemical and structural analysis of common cancer-associated KRAS mutations', *Molecular Cancer Research*. American Association for Cancer Research Inc., 13(9), pp. 1325–1335. doi: 10.1158/1541-7786.MCR-15-0203.

Hwang, J. and Espenshade, P. J. (2016) 'Proximity-dependent biotin labelling in yeast using the engineered ascorbate peroxidase APEX2', *Biochemical Journal*. Portland Press Ltd, 473(16), pp. 2463–2469. doi: 10.1042/BCJ20160106.

Inder, K. L. *et al.* (2009a) 'Nucleophosmin and nucleolin regulate K-ras plasma membrane interactions and MAPK signal transduction', *Journal of Biological Chemistry*, 284(41), pp. 28410–28419. doi: 10.1074/jbc.M109.001537.

Inder, K. L. *et al.* (2009b) 'Nucleophosmin and nucleolin regulate K-ras plasma membrane interactions and MAPK signal transduction', *Journal of Biological Chemistry*. American Society for Biochemistry and Molecular Biology, 284(41), pp. 28410–28419. doi: 10.1074/jbc.M109.001537.

Inder, K. L., Hill, M. M. and Hancock, J. F. (2010) 'Nucleophosmin and nucleolin regulate K-Ras signaling', *Communicative and Integrative Biology*. Landes Bioscience, 3(2), pp. 188–190. doi: 10.4161/cib.3.2.10923.

Inouye, K. *et al.* (2000) 'Formation of the Ras dimer is essential for Raf-1 activation',

Journal of Biological Chemistry. American Society for Biochemistry and Molecular Biology, 275(6), pp. 3737–3740. doi: 10.1074/jbc.275.6.3737.

Ismail, S. A. *et al.* (2011) 'Arl2-GTP and Arl3-GTP regulate a GDI-like transport system for farnesylated cargo', *Nature Chemical Biology*. Nature Publishing Group, 7(12), pp. 942–949. doi: 10.1038/nchembio.686.

Van Itallie, C. M. *et al.* (2014) 'Biotin ligase tagging identifies proteins proximal to E-cadherin, including lipoma preferred partner, a regulator of epithelial cell–cell and cell–substrate adhesion', *Journal of Cell Science*, 127(4), pp. 885–895. doi: 10.1242/jcs.140475.

Janosi, L. *et al.* (2012) 'Organization, dynamics, and segregation of Ras nanoclusters in membrane domains', *Proceedings of the National Academy of Sciences of the United States of America*. National Academy of Sciences, 109(21), pp. 8097–8102. doi: 10.1073/pnas.1200773109.

Janosi, L. and Gorfe, A. A. (2010) 'Segregation of negatively charged phospholipids by the polycationic and farnesylated membrane anchor of Kras', *Biophysical Journal*. Biophysical Society, 99(11), pp. 3666–3674. doi: 10.1016/j.bpj.2010.10.031.

Jiang, S. *et al.* (2012) 'A proteomics approach to the cell-surface interactome using the enzyme-mediated activation of radical sources reaction', *PROTEOMICS*, 12(1), pp. 54–62. doi: 10.1002/pmic.201100551.

Johannes, L., Jacob, R. and Leffler, H. (2018) 'Galectins at a glance', *Journal of Cell Science*. Company of Biologists Ltd, 131(9). doi: 10.1242/jcs.208884.

John, J. *et al.* (1993) 'Kinetic and structural analysis of the Mg2+-binding site of the guanine nucleotide-binding protein p21(H-ras)', *Journal of Biological Chemistry*. J Biol Chem, 268(2), pp. 923–929.

Jura, N. *et al.* (2006) 'Differential modification of Ras proteins by ubiquitination', *Molecular Cell*, 21(5), pp. 679–687. doi: 10.1016/j.molcel.2006.02.011.

Kamal, A., Ying, Y. S. and Anderson, R. G. W. (1998) 'Annexin VI-mediated loss of spectrin during coated pit budding is coupled to delivery of LDL to lysosomes', *Journal of Cell Biology*. J Cell Biol, 142(4), pp. 937–947. doi: 10.1083/jcb.142.4.937.

Kheifets, V. *et al.* (2006) 'Protein kinase C δ (δPKC)-annexin V interaction: A required step in δPKC translocation and function', *Journal of Biological Chemistry*, 281(32), pp. 23218–23226. doi: 10.1074/jbc.M602075200.

Kidger, A. M. *et al.* (2017) 'Dual-specificity phosphatase 5 controls the localized inhibition, propagation, and transforming potential of ERK signaling', *Proceedings of the National Academy of Sciences of the United States of America*. National Academy of Sciences, 114(3), pp. E317–E326. doi: 10.1073/pnas.1614684114.

Kim, D. I. *et al.* (2014) 'Probing nuclear pore complex architecture with proximity-

dependent biotinylation.', *Proceedings of the National Academy of Sciences of the United States of America*. National Academy of Sciences, 111(24), pp. E2453-61. doi: 10.1073/pnas.1406459111.

Kim, D. I. *et al.* (2016) 'An improved smaller biotin ligase for BioID proximity labeling', *Molecular Biology of the Cell*. Edited by Y. Zheng, 27(8), pp. 1188–1196. doi: 10.1091/mbc.E15-12-0844.

Kirsten, W. H. and Mayer, L. A. (1967) 'Morphologic responses to a murine erythroblastosis virus', *Journal of the National Cancer Institute*, 39(2), pp. 311–335. doi: 10.1093/jnci/39.2.311.

Koide, H. *et al.* (1993) 'GTP-dependent association of Raf-1 with Ha-Ras: identification of Raf as a target downstream of Ras in mammalian cells.', *Proceedings of the National Academy of Sciences of the United States of America*. National Academy of Sciences, 90(18), pp. 8683–6. doi: 10.1073/pnas.90.18.8683.

Kong, E. *et al.* (2013) 'Dynamic palmitoylation links cytosol-membrane shuttling of acyl-protein thioesterase-1 and acyl-protein thioesterase-2 with that of proto-oncogene H-Ras product and growth-associated protein-43', *Journal of Biological Chemistry*. American Society for Biochemistry and Molecular Biology, 288(13), pp. 9112–9125. doi: 10.1074/jbc.M112.421073.

Kötting, C. *et al.* (2008) 'The GAP arginine finger movement into the catalytic site of Ras increases the activation entropy', *Proceedings of the National Academy of Sciences of the United States of America*. National Academy of Sciences, 105(17), pp. 6260–6265. doi: 10.1073/pnas.0712095105.

Koumangoye, R. B. *et al.* (2013) 'Reduced annexin A6 expression promotes the degradation of activated epidermal growth factor receptor and sensitizes invasive breast cancer cells to EGFR-targeted tyrosine kinase inhibitors', *Molecular Cancer*. Mol Cancer, 12(1). doi: 10.1186/1476-4598-12-167.

Kovalski, J. R. *et al.* (2019) 'The Functional Proximal Proteome of Oncogenic Ras Includes mTORC2', *Molecular Cell*. Cell Press, 73(4), pp. 830-844.e12. doi: 10.1016/j.molcel.2018.12.001.

Kuriyama, M. *et al.* (1996) 'Identification of AF-6 and Canoe as putative targets for Ras', *Journal of Biological Chemistry*, 271(2), pp. 607–610. doi: 10.1074/jbc.271.2.607.

Kusumi, A. and Sako, Y. (1996) 'Cell surface organization by the membrane skeleton', *Current Opinion in Cell Biology*. Elsevier Ltd, 8(4), pp. 566–574. doi: 10.1016/S0955-0674(96)80036-6.

Lacal, J. C. and Aaronson, S. A. (1986) 'Monoclonal antibody Y13-259 recognizes an epitope of the p21 ras molecule not directly involved in the GTP-binding activity of the protein.', *Molecular and Cellular Biology*. American Society for Microbiology, 6(4), pp.

1002–1009. doi: 10.1128/mcb.6.4.1002.

Lam, S. S. *et al.* (2015) 'Directed evolution of APEX2 for electron microscopy and proximity labeling', *Nature Methods*. Nature Publishing Group, 12(1), pp. 51–54. doi: 10.1038/nmeth.3179.

Laude, A. J. and Prior, I. A. (2008) 'Palmitoylation and localisation of RAS isoforms are modulated by the hypervariable linker domain', *Journal of Cell Science*. Company of Biologists Ltd, 121(4), pp. 421–427. doi: 10.1242/jcs.020107.

Leevers, S. J. and Marshall, C. J. (1992) 'Activation of extracellular signal-regulated kinase, ERK2, by p21ras oncoprotein.', *The EMBO Journal*. Wiley, 11(2), pp. 569–574. doi: 10.1002/j.1460-2075.1992.tb05088.x.

Leevers, S. J., Paterson, H. F. and Marshall, C. J. (1994) 'Requirement for Ras in Raf activation is overcome by targeting Raf to the plasma membrane', *Nature*, 369(6479), pp. 411–414. doi: 10.1038/369411a0.

Lemmon, M. A. and Schlessinger, J. (2010) 'Cell signaling by receptor tyrosine kinases', *Cell*. NIH Public Access, pp. 1117–1134. doi: 10.1016/j.cell.2010.06.011.

Li, X.-W. *et al.* (2014) 'New Insights into the DT40 B Cell Receptor Cluster Using a Proteomic Proximity Labeling Assay', *Journal of Biological Chemistry*, 289(21), pp. 14434–14447. doi: 10.1074/jbc.M113.529578.

Lin, H. C., Südhof, T. C. and Anderson, R. G. (1992) 'Annexin VI is required for budding of clathrin-coated pits.', *Cell*, 70(2), pp. 283–91. doi: 10.1016/0092-8674(92)90102-i.

Lizarbe, M. A. *et al.* (2013) 'Annexin-phospholipid interactions. Functional implications', *International Journal of Molecular Sciences*. Multidisciplinary Digital Publishing Institute (MDPI), pp. 2652–2683. doi: 10.3390/ijms14022652.

Lobingier, B. T. *et al.* (2017) 'An Approach to Spatiotemporally Resolve Protein Interaction Networks in Living Cells.', *Cell*. NIH Public Access, 169(2), pp. 350-360.e12. doi: 10.1016/j.cell.2017.03.022.

Lomnytska, M. I. *et al.* (2011) 'Differential expression of ANXA6, HSP27, PRDX2, NCF2, and TPM4 during uterine cervix carcinogenesis: Diagnostic and prognostic value', *British Journal of Cancer*. Br J Cancer, 104(1), pp. 110–119. doi: 10.1038/sj.bjc.6605992.

Lowy, D. R. and Willumsen, B. M. (1993) 'Function and Regulation of Ras', *Annual Review of Biochemistry*. Annual Reviews, 62(1), pp. 851–891. doi: 10.1146/annurev.bi.62.070193.004223.

Lu, A. *et al.* (2009) 'A clathrin-dependent pathway leads to KRas signaling on late endosomes en route to lysosomes', *Journal of Cell Biology*. The Rockefeller University Press, 184(6), pp. 863–879. doi: 10.1083/jcb.200807186.

Luo, Z. *et al.* (1997) 'An intact Raf zinc finger is required for optimal binding to processed

Ras and for ras-dependent Raf activation in situ.', *Molecular and Cellular Biology*. American Society for Microbiology, 17(1), pp. 46–53. doi: 10.1128/mcb.17.1.46.

Macara, I. G. (2001) 'Transport into and out of the Nucleus', *Microbiology and Molecular Biology Reviews*. American Society for Microbiology, 65(4), pp. 570–594. doi: 10.1128/mmbr.65.4.570-594.2001.

Mannix, K. M. *et al.* (2019) ' Proximity labeling reveals novel interactomes in live Drosophila tissue ', *Development*. The Company of Biologists, 146(14), p. dev176644. doi: 10.1242/dev.176644.

Marshall, C. J., Hall, A. and Weiss, R. A. (1982) 'A transforming gene present in human sarcoma cell lines', *Nature*. Nature Publishing Group, 299(5879), pp. 171–173. doi: 10.1038/299171a0.

Martell, J. D. *et al.* (2012) 'Engineered ascorbate peroxidase as a genetically encoded reporter for electron microscopy', *Nature Biotechnology*, 30(11), pp. 1143–1148. doi: 10.1038/nbt.2375.

Matsunaga-Udagawa, R. *et al.* (2010) 'The scaffold protein Shoc2/SUR-8 accelerates the interaction of Ras and Raf', *Journal of Biological Chemistry*, 285(10), pp. 7818–7826. doi: 10.1074/jbc.M109.053975.

Matsunaga, H. *et al.* (2014) 'IQGAP1 selectively interacts with K-Ras but not with H-Ras and modulates K-Ras function', *Biochemical and Biophysical Research Communications*, 444(3), pp. 360–364. doi: 10.1016/j.bbrc.2014.01.041.

Mayran, N., Parton, R. G. and Gruenberg, J. (2003) 'Annexin II regulates multivesicular endosome biogenesis in the degradation pathway of animal cells.', *The EMBO journal*, 22(13), pp. 3242–53. doi: 10.1093/emboj/cdg321.

Mick, D. U. *et al.* (2015) 'Proteomics of Primary Cilia by Proximity Labeling', *Developmental Cell*, 35(4), pp. 497–512. doi: 10.1016/j.devcel.2015.10.015.

Milburn, M. V. *et al.* (1990) 'Molecular switch for signal transduction: Structural differences between active and inactive forms of protooncogenic ras proteins', *Science*. American Association for the Advancement of Science, 247(4945), pp. 939–945. doi: 10.1126/science.2406906.

Miller, M. S. and Miller, L. D. (2012) 'RAS mutations and oncogenesis: Not all RAS mutations are created equally', *Frontiers in Genetics*. Frontiers Media SA. doi: 10.3389/fgene.2011.00100.

Misaki, R. *et al.* (2010) 'Palmitoylated ras proteins traffic through recycling endosomes to the plasma membrane during exocytosis', *Journal of Cell Biology*. The Rockefeller University Press, 191(1), pp. 23–29. doi: 10.1083/jcb.200911143.

Mo, S. P. S. P., Coulson, J. M. J. M. and Prior, I. A. I. A. (2018) 'RAS variant signalling',

Biochemical Society Transactions, 46(5), pp. 1325–1332. doi: 10.1042/BST20180173.

Mor, A. *et al.* (2007) 'The lymphocyte function-associated antigen-1 receptor costimulates plasma membrane Ras via phospholipase D2', *Nature Cell Biology*, 9(6), pp. 713–719. doi: 10.1038/ncb1592.

Morel, E. and Gruenberg, J. (2007) 'The p11/S100A10 light chain of annexin A2 is dispensable for annexin A2 association to endosomes and functions in endosomal transport', *PLoS ONE*, 2(10), p. e1118. doi: 10.1371/journal.pone.0001118.

Morgan, R. O. *et al.* (1999) 'Novel human and mouse annexin A10 are linked to the genome duplications during early chordate evolution', *Genomics*. Academic Press Inc., 60(1), pp. 40–49. doi: 10.1006/geno.1999.5895.

Morgan, R. O. and Pilar Fernandez, M. (1997) 'Distinct annexin subfamilies in plants and protists diverged prior to animal annexins and from a common ancestor.', *Journal of molecular evolution*, 44(2), pp. 178–88. doi: 10.1007/pl00006134.

Mortensen, A. and Skibsted, L. H. (1997) 'Importance of Carotenoid Structure in Radical-Scavenging Reactions', *Journal of Agricultural and Food Chemistry*, 45(8), pp. 2970–2977. doi: 10.1021/jf970010s.

Moss, S. E. and Morgan, R. O. (2004) 'The annexins', *Genome Biology*, p. 219. doi: 10.1186/gb-2004-5-4-219.

Muñoz-Maldonado, C., Zimmer, Y. and Medová, M. (2019) 'A comparative analysis of individual ras mutations in cancer biology', *Frontiers in Oncology*. Frontiers Media S.A., 9(OCT), p. 1088. doi: 10.3389/fonc.2019.01088.

Munro, S. (2003) 'Lipid Rafts: Elusive or Illusive?', *Cell*. Cell Press, pp. 377–388. doi: 10.1016/S0092-8674(03)00882-1.

De Munter, S. *et al.* (2017) 'Split-BioID: a proximity biotinylation assay for dimerization-dependent protein interactions', *FEBS Letters*. Wiley Blackwell, pp. 415–424. doi: 10.1002/1873-3468.12548.

Murakoshi, H. *et al.* (2004) 'Single-molecule imaging analysis of Ras activation in living cells', *Proceedings of the National Academy of Sciences of the United States of America*. National Academy of Sciences, 101(19), pp. 7317–7322. doi: 10.1073/pnas.0401354101.

Nan, X. *et al.* (2015) 'Ras-GTP dimers activate the Mitogen-Activated Protein Kinase (MAPK) pathway', *Proceedings of the National Academy of Sciences of the United States of America*. National Academy of Sciences, 112(26), pp. 7996–8001. doi: 10.1073/pnas.1509123112.

Nassar, N. *et al.* (1995) 'The 2.2 Å crystal structure of the Ras-binding domain of the serine/threonine kinase c-Raf1 in complex with RaplA and a GTP analogue', *Nature*, 375(6532), pp. 554–560. doi: 10.1038/375554a0.

Newlaczyl, A. U., Coulson, J. M. and Prior, I. A. (2017) 'Quantification of spatiotemporal patterns of Ras isoform expression during development', *Scientific Reports*. Nature Publishing Group, 7(1), pp. 1–7. doi: 10.1038/srep41297.

Nguyen, A. *et al.* (2002) 'Kinase Suppressor of Ras (KSR) Is a Scaffold Which Facilitates Mitogen-Activated Protein Kinase Activation In Vivo', *Molecular and Cellular Biology*. American Society for Microbiology, 22(9), pp. 3035–3045. doi: 10.1128/mcb.22.9.3035-3045.2002.

Niihori, T. *et al.* (2006) 'Germline KRAS and BRAF mutations in cardio-facio-cutaneous syndrome', *Nature Genetics*, 38(3), pp. 294–296. doi: 10.1038/ng1749.

Ogawara, Y. *et al.* (2002) 'Akt enhances Mdm2-mediated ubiquitination and degradation of p53', *Journal of Biological Chemistry*. American Society for Biochemistry and Molecular Biology, 277(24), pp. 21843–21850. doi: 10.1074/jbc.M109745200.

Örtegren, U. *et al.* (2004) 'Lipids and glycosphingolipids in caveolae and surrounding plasma membrane of primary rat adipocytes', *European Journal of Biochemistry*. Eur J Biochem, 271(10), pp. 2028–2036. doi: 10.1111/j.1432-1033.2004.04117.x.

Ostrem, J. M. *et al.* (2013) 'K-Ras(G12C) inhibitors allosterically control GTP affinity and effector interactions', *Nature*, 503(7477), pp. 548–551. doi: 10.1038/nature12796.

Ozaki, K. *et al.* (2001) 'Erk pathway positively regulates the expression of sprouty genes', *Biochemical and Biophysical Research Communications*. Academic Press Inc., 285(5), pp. 1084–1088. doi: 10.1006/bbrc.2001.5295.

Paek, J. *et al.* (2017) 'Multidimensional Tracking of GPCR Signaling via Peroxidase-Catalyzed Proximity Labeling.', *Cell*, 169(2), pp. 338-349.e11. doi: 10.1016/j.cell.2017.03.028.

Pai, E. F. *et al.* (1989) 'Structure of the guanine-nucleotide-binding domain of the Ha-ras oncogene product p21 in the triphosphate conformation', *Nature*, 341(6239), pp. 209–214. doi: 10.1038/341209a0.

Parker, J. A. *et al.* (2018) 'K-Ras Populates Conformational States Differently from Its Isoform H-Ras and Oncogenic Mutant K-RasG12D', *Structure*. Cell Press, 26(6), pp. 810-820.e4. doi: 10.1016/j.str.2018.03.018.

Parker, J. A. and Mattos, C. (2015) 'The Ras-membrane interface: Isoform-specific differences in the catalytic domain', *Molecular Cancer Research*. American Association for Cancer Research Inc., pp. 595–603. doi: 10.1158/1541-7786.MCR-14-0535.

Parton, R. G. and Hancock, J. F. (2004) 'Lipid rafts and plasma membrane microorganization: Insights from Ras', *Trends in Cell Biology*. Elsevier Current Trends, pp. 141–147. doi: 10.1016/j.tcb.2004.02.001.

Paz, A. *et al.* (2001) 'Galectin-1 binds oncogenic H-Ras to mediate Ras membrane

anchorage and cell transformation', *Oncogene*. Oncogene, 20(51), pp. 7486–7493. doi: 10.1038/sj.onc.1204950.

Pikuta, J. B. *et al.* (1996) 'Interaction of annexins IV and VI with phosphatidylserine in the presence of Ca2+', *Molecular Membrane Biology*. Informa UK Limited, 13(4), pp. 241–250. doi: 10.3109/09687689609160602.

Plowman, S. J. *et al.* (2005) 'H-ras, K-ras, and inner plasma membrane raft proteins operate in nanoclusters with differential dependence on the actin cytoskleton', *Proceedings of the National Academy of Sciences of the United States of America*. National Academy of Sciences, 102(43), pp. 15500–15505. doi: 10.1073/pnas.0504114102.

Plowman, S. J. *et al.* (2008) 'Electrostatic Interactions Positively Regulate K-Ras Nanocluster Formation and Function', *Molecular and Cellular Biology*. American Society for Microbiology, 28(13), pp. 4377–4385. doi: 10.1128/mcb.00050-08.

Plowman, S. J. and Hancock, J. F. (2005) 'Ras signaling from plasma membrane and endomembrane microdomains', *Biochimica et Biophysica Acta - Molecular Cell Research*. Elsevier, pp. 274–283. doi: 10.1016/j.bbamcr.2005.06.004.

Plowman, S.J. and Hancock, J. F. (2005) 'Ras signaling from plasma membrane and endomembrane microdomains', *Biochimica et Biophysica Acta (BBA) - Molecular Cell Research*, 1746(3), pp. 274–283. doi: 10.1016/j.bbamcr.2005.06.004.

Popescu, N. C. *et al.* (1985) 'Chromosomal localization of three human ras genes by in situ molecular hybridization', *Somatic Cell and Molecular Genetics*. Kluwer Academic Publishers-Plenum Publishers, 11(2), pp. 149–155. doi: 10.1007/BF01534703.

Posada, I. M. D. *et al.* (2016) 'ASPP2 is a novel pan-ras nanocluster scaffold', *PLoS ONE*. Edited by J.-I. Park. Public Library of Science, 11(7), p. e0159677. doi: 10.1371/journal.pone.0159677.

Prior, I. A. *et al.* (2001) 'GTP-dependent segregation of H-ras from lipid rafts is required for biological activity', *Nature Cell Biology*. Nature Publishing Group, 3(4), pp. 368–375. doi: 10.1038/35070050.

Prior, I. A. *et al.* (2003) 'Direct visualization of ras proteins in spatially distinct cell surface microdomains', *Journal of Cell Biology*. The Rockefeller University Press, 160(2), pp. 165–170. doi: 10.1083/jcb.200209091.

Prior, I. A. and Hancock, J. F. (2001) 'Compartmentalization of Ras proteins', *Journal of Cell Science*, 114(9), pp. 1603–1608. Available at: https://jcs.biologists.org/content/114/9/1603.short (Accessed: 11 June 2020).

Prior, I. A. and Hancock, J. F. (2012) 'Ras trafficking, localization and compartmentalized signalling', *Seminars in Cell and Developmental Biology*. Elsevier Ltd, pp. 145–153. doi: 10.1016/j.semcdb.2011.09.002.

Qu, L. *et al.* (2019) 'The ras superfamily of small gtpases in non-neoplastic cerebral diseases', *Frontiers in Molecular Neuroscience*. Frontiers Media S.A., p. 121. doi: 10.3389/fnmol.2019.00121.

Quinlan, M. P. *et al.* (2008) 'Activated Kras, but Not Hras or Nras, May Initiate Tumors of Endodermal Origin via Stem Cell Expansion', *Molecular and Cellular Biology*. American Society for Microbiology, 28(8), pp. 2659–2674. doi: 10.1128/mcb.01661-07.

Rajakulendran, T. *et al.* (2009) 'A dimerization-dependent mechanism drives RAF catalytic activation', *Nature*. Nature Publishing Group, 461(7263), pp. 542–545. doi: 10.1038/nature08314.

Rajalingam, K. *et al.* (2007) 'Ras oncogenes and their downstream targets', *Biochimica et Biophysica Acta - Molecular Cell Research*, pp. 1177–1195. doi: 10.1016/j.bbamcr.2007.01.012.

Rameh, L. E. and Cantley, L. C. (1999) 'The role of phosphoinositide 3-kinase lipid products in cell function', *Journal of Biological Chemistry*. American Society for Biochemistry and Molecular Biology, pp. 8347–8350. doi: 10.1074/jbc.274.13.8347.

Raulf, N. *et al.* (2018) 'Annexin A1 regulates EGFR activity and alters EGFR-containing tumour-derived exosomes in head and neck cancers', *European Journal of Cancer*. Elsevier Ltd, 102, pp. 52–68. doi: 10.1016/j.ejca.2018.07.123.

Raynal, P. and Pollard, H. B. (1994) 'Annexins: the problem of assessing the biological role for a gene family of multifunctional calcium- and phospholipid-binding proteins', *BBA - Reviews on Biomembranes*. Elsevier, pp. 63–93. doi: 10.1016/0304-4157(94)90019-1.

Rebollo, A., Pérez-Sala, D. and Martínez-A, C. (1999) 'Bcl-2 differentially targets K-, N-, and H-Ras to mitochondria in IL-2 supplemented or deprived cells: Implications in prevention of apoptosis', *Oncogene*, 18(35), pp. 4930–4939. doi: 10.1038/sj.onc.1202875.

Reddy, E. P. *et al.* (1982) 'A point mutation is responsible for the acquisition of transforming properties by the T24 human bladder carcinoma oncogene', *Nature*. Nature Publishing Group, 300(5888), pp. 149–152. doi: 10.1038/300149a0.

Reiss, Y. *et al.* (1990) 'Inhibition of purified p21ras farnesyl:protein transferase by Cys-AAX tetrapeptides', *Cell*, 62(1), pp. 81–88. doi: 10.1016/0092-8674(90)90242-7.

Rescher, U. and Gerke, V. (2004) 'Annexins - Unique membrane binding proteins with diverse functions', *Journal of Cell Science*. J Cell Sci, pp. 2631–2639. doi: 10.1242/jcs.01245.

Reviakine, I. *et al.* (2000) 'Surface topography of the p3 and p6 annexin V crystal forms determined by atomic force microscopy', *Journal of Structural Biology*, 131(3), pp. 234–239. doi: 10.1006/jsbi.2000.4286.

Rhee, H.-W. *et al.* (2013) 'Proteomic Mapping of Mitochondria in Living Cells via Spatially

Restricted Enzymatic Tagging', *Science*, 339(6125), pp. 1328–1331. doi: 10.1126/science.1230593.

Rhee, H. *et al.* (2013) 'Proteomic Mapping of Mitochondria', *Science*, 339(March), p. 1328. doi: 10.1126/science.1230593.

Ritchie, C. *et al.* (2017) 'Analysis of K-Ras Interactions by Biotin Ligase Tagging.', *Cancer genomics & proteomics*. International Institute of Anticancer Research, 14(4), pp. 225–239. doi: 10.21873/cgp.20034.

Ritt, D. A. *et al.* (2010) 'Impact of Feedback Phosphorylation and Raf Heterodimerization on Normal and Mutant B-Raf Signaling', *Molecular and Cellular Biology*. American Society for Microbiology, 30(3), pp. 806–819. doi: 10.1128/mcb.00569-09.

Rocks, O. *et al.* (2005) 'An acylation cycle regulates localization and activity of palmitoylated ras isoforms', *Science*. Science, 307(5716), pp. 1746–1752. doi: 10.1126/science.1105654.

Rocks, O. *et al.* (2010) 'The palmitoylation machinery is a spatially organizing system for peripheral membrane proteins', *Cell*. Elsevier, 141(3), pp. 458–471. doi: 10.1016/j.cell.2010.04.007.

Rodriguez-Viciana, P. *et al.* (1994) 'Phosphatidylinositol-3-OH kinase direct target of Ras', *Nature*. Nature Publishing Group, 370(6490), pp. 527–532. doi: 10.1038/370527a0.

Rogers, M. S. *et al.* (2008) 'Cross-link formation of the cysteine 228-tyrosine 272 catalytic cofactor of galactose oxidase does not require dioxygen.', *Biochemistry*, 47(39), pp. 10428–39. doi: 10.1021/bi8010835.

Rotblat, B. *et al.* (2004) 'Galectin-1(L11A) Predicted from a Computed Galectin-1 Farnesyl-Binding Pocket Selectively Inhibits Ras-GTP', *Cancer Research*. Cancer Res, 64(9), pp. 3112–3118. doi: 10.1158/0008-5472.CAN-04-0026.

Rothberg, K. G. *et al.* (1992) 'Caveolin, a protein component of caveolae membrane coats', *Cell*. Cell, 68(4), pp. 673–682. doi: 10.1016/0092-8674(92)90143-Z.

Roux, K. J. *et al.* (2012) 'A promiscuous biotin ligase fusion protein identifies proximal and interacting proteins in mammalian cells.', *The Journal of cell biology*, 196(6), pp. 801–10. doi: 10.1083/jcb.201112098.

Roy, S. *et al.* (1999) 'Dominant-negative caveolin inhibits H-Ras function by disrupting cholesterol-rich plasma membrane domains', *Nature Cell Biology*, 1(2), pp. 98–105. doi: 10.1038/10067.

Roy, S. *et al.* (2005) 'Individual Palmitoyl Residues Serve Distinct Roles in H-Ras Trafficking, Microlocalization, and Signaling', *Molecular and Cellular Biology*. American Society for Microbiology, 25(15), pp. 6722–6733. doi: 10.1128/mcb.25.15.6722-6733.2005.

Roy, S., Wyse, B. and Hancock, J. F. (2002) 'H-Ras Signaling and K-Ras Signaling Are Differentially Dependent on Endocytosis', *Molecular and Cellular Biology*. American Society for Microbiology, 22(14), pp. 5128–5140. doi: 10.1128/mcb.22.14.5128-5140.2002.

Rozakis-Adcock, M. *et al.* (1993) 'The SH2 and SH3 domains of mammalian Grb2 couple the EGF receptor to the Ras activator mSos1', *Nature*. Nature, 363(6424), pp. 83–85. doi: 10.1038/363083a0.

Rushworth, L. K. *et al.* (2006) 'Regulation and Role of Raf-1/B-Raf Heterodimerization', *Molecular and Cellular Biology*. American Society for Microbiology, 26(6), pp. 2262–2272. doi: 10.1128/mcb.26.6.2262-2272.2006.

Ryu, H. *et al.* (2015) 'Frequency modulation of <scp>ERK</scp> activation dynamics rewires cell fate', *Molecular Systems Biology*, 11(11), p. 838. doi: 10.15252/msb.20156458.

Sakwe, A. M. *et al.* (2011) 'Annexin A6 contributes to the invasiveness of breast carcinoma cells by influencing the organization and localization of functional focal adhesions', *Experimental Cell Research*. Academic Press Inc., 317(6), pp. 823–837. doi: 10.1016/j.yexcr.2010.12.008.

Santos, E. *et al.* (1984) 'Malignant activation of a K-ras oncogene in lung carcinoma but not in normal tissue of the same patient', *Science*, 223(4637), pp. 661–664. doi: 10.1126/science.6695174.

Santra, T. *et al.* (2019) 'An Integrated Global Analysis of Compartmentalized HRAS Signaling', *Cell Reports*. Elsevier B.V., 26(11), pp. 3100-3115.e7. doi: 10.1016/j.celrep.2019.02.038.

Sarkar-Banerjee, S. *et al.* (2017) 'Spatiotemporal Analysis of K-Ras Plasma Membrane Interactions Reveals Multiple High Order Homo-oligomeric Complexes', *Journal of the American Chemical Society*. American Chemical Society, 139(38), pp. 13466–13475. doi: 10.1021/jacs.7b06292.

Scheffzek, K. *et al.* (1997) 'The Ras-RasGAP complex: Structural basis for GTPase activation and its loss in oncogenic ras mutants', *Science*, 277(5324), pp. 333–338. doi: 10.1126/science.277.5324.333.

Schlichting, I. *et al.* (1990) 'Time-resolved X-ray crystallographic study of the conformational change in Ha-Ras p21 protein on GTP hydrolysis', *Nature*. Nature, 345(6273), pp. 309–315. doi: 10.1038/345309a0.

Schmick, M. *et al.* (2014) 'KRas localizes to the plasma membrane by spatial cycles of solubilization, trapping and vesicular transport', *Cell*. Cell Press, 157(2), pp. 459–471. doi: 10.1016/j.cell.2014.02.051.

Schmick, M., Kraemer, A. and Bastiaens, P. I. H. (2015) 'Ras moves to stay in place', *Trends in Cell Biology*. Elsevier Ltd, pp. 190–197. doi: 10.1016/j.tcb.2015.02.004.

Schubbert, S. *et al.* (2006) 'Germline KRAS mutations cause Noonan syndrome', *Nature Genetics*, 38(3), pp. 331–336. doi: 10.1038/ng1748.

Scolnick, E. M., Papageorge, A. G. and Shih, T. Y. (1979) *Guanine nucleotide-binding activity as an assay for src protein of rat-derived murine sarcoma viruses (Kirsten murine sarcoma virus/transformation)*.

Segev, N. (2001) 'Ypt and Rab GTPases: Insight into functions through novel interactions', *Current Opinion in Cell Biology*. Elsevier Current Trends, pp. 500–511. doi: 10.1016/S0955-0674(00)00242-8.

Sekar, R. B. and Periasamy, A. (2003) 'Fluorescence resonance energy transfer (FRET) microscopy imaging of live cell protein localizations', *Journal of Cell Biology*. The Rockefeller University Press, pp. 629–633. doi: 10.1083/jcb.200210140.

Shalom-Feuerstein, R. *et al.* (2008) 'K-Ras nanoclustering is subverted by overexpression of the scaffold protein galectin-3', *Cancer Research*. NIH Public Access, 68(16), pp. 6608–6616. doi: 10.1158/0008-5472.CAN-08-1117.

Shima, F. *et al.* (2010) 'Structural basis for conformational dynamics of GTP-bound ras protein', *Journal of Biological Chemistry*. American Society for Biochemistry and Molecular Biology, 285(29), pp. 22696–22705. doi: 10.1074/jbc.M110.125161.

Shimizu, K., Goldfarb, M., Perucho, M., *et al.* (1983) 'Isolation and preliminary characterization of the transforming gene of a human neuroblastoma cell line', *Proceedings of the National Academy of Sciences of the United States of America*. National Academy of Sciences, 80(2 I), pp. 383–387. doi: 10.1073/pnas.80.2.383.

Shimizu, K., Goldfarb, M., Suard, Y., *et al.* (1983) 'Three human transforming genes are related to the viral ras oncogenes', *Proceedings of the National Academy of Sciences of the United States of America*. National Academy of Sciences, 80(8 I), pp. 2112–2116. doi: 10.1073/pnas.80.8.2112.

Sieburth, D. S., Sun, Q. and Han, M. (1998) 'SUR-8, a conserved Ras-binding protein with leucine-rich repeats, positively regulates Ras-mediated signaling in C. elegans.', *Cell*, 94(1), pp. 119–30. doi: 10.1016/s0092-8674(00)81227-1.

Siegel, D. H. *et al.* (2011) 'Dermatological findings in 61 mutation-positive individuals with cardiofaciocutaneous syndrome', *British Journal of Dermatology*. NIH Public Access, 164(3), pp. 521–529. doi: 10.1111/j.1365-2133.2010.10122.x.

Silvius, J. R., Del Giudice, D. and Lafleur, M. (1996) 'Cholesterol at different bilayer concentrations can promote or antagonize lateral segregation of phospholipids of differing acyl chain length', *Biochemistry*, 35(48), pp. 15198–15208. doi: 10.1021/bi9615506.

Simanshu, D. K., Nissley, D. V. and McCormick, F. (2017) 'RAS Proteins and Their Regulators in Human Disease', *Cell*. Cell Press, pp. 17–33. doi: 10.1016/j.cell.2017.06.009.

Simons, K. and Sampaio, J. L. (2011) 'Membrane organization and lipid rafts', *Cold Spring Harbor Perspectives in Biology*. Cold Spring Harbor Laboratory Press, pp. 1–17. doi: 10.1101/cshperspect.a004697.

Singer, S. J. and Nicolson, G. L. (1972) 'The fluid mosaic model of the structure of cell membranes', *Science*, 175(4023), pp. 720–731. doi: 10.1126/science.175.4023.720.

Sjölander, A. *et al.* (1991) 'Association of p21ras with phosphatidylinositol 3-kinase.', *Proceedings of the National Academy of Sciences of the United States of America*. National Academy of Sciences, 88(18), pp. 7908–12. doi: 10.1073/pnas.88.18.7908.

Smith, D. L. *et al.* (2002) 'Changes in the proteome associated with the action of Bcr-Abl tyrosine kinase are not related to transcriptional regulation.', *Molecular & cellular proteomics : MCP*. Mol Cell Proteomics, 1(11), pp. 876–884. doi: 10.1074/mcp.M200035-MCP200.

Smith, M. J., Neel, B. G. and Ikura, M. (2013) 'NMR-based functional profiling of RASopathies and oncogenic RAS mutations', *Proceedings of the National Academy of Sciences of the United States of America*. National Academy of Sciences, 110(12), pp. 4574–4579. doi: 10.1073/pnas.1218173110.

Smith, P. D. *et al.* (1994) 'Structure of the human annexin VI gene', *Proceedings of the National Academy of Sciences of the United States of America*. National Academy of Sciences, 91(7), pp. 2713–2717. doi: 10.1073/pnas.91.7.2713.

Song, J. *et al.* (2009) 'Suppression of annexin A11 in ovarian cancer: Implications in chemoresistance', *Neoplasia*. Neoplasia, 11(6), pp. 605–614. doi: 10.1593/neo.09286.

Song, K. S. *et al.* (1996a) 'Co-purification and direct interaction of Ras with caveolin, an integral membrane protein of caveolae microdomains: Detergent-free purification of caveolae membranes', *Journal of Biological Chemistry*. American Society for Biochemistry and Molecular Biology Inc., 271(16), pp. 9690–9697. doi: 10.1074/jbc.271.16.9690.

Song, K. S. *et al.* (1996b) 'Co-purification and Direct Interaction of Ras with Caveolin, an Integral Membrane Protein of Caveolae Microdomains', *Journal of Biological Chemistry*, 271(16), pp. 9690–9697. doi: 10.1074/jbc.271.16.9690.

Spector, A. A. and Yorek, M. A. (1985) 'Membrane lipid composition and cellular function', *Journal of Lipid Research*, pp. 1015–1035.

Spencer-Smith, R. *et al.* (2017) 'Inhibition of RAS function through targeting an allosteric regulatory site', *Nature Chemical Biology*. Nature Publishing Group, 13(1), pp. 62–68. doi: 10.1038/nchembio.2231.

Sperlich, B. *et al.* (2016) 'Regulation of K-Ras4B Membrane Binding by Calmodulin', *Biophysical Journal*. Biophysical Society, 111(1), pp. 113–122. doi: 10.1016/j.bpj.2016.05.042.

Spoerner, M. *et al.* (2001) 'Dynamic properties of the Ras switch I region and its importance for binding to effectors', *Proceedings of the National Academy of Sciences of the United States of America*. National Academy of Sciences, 98(9), pp. 4944–4949. doi: 10.1073/pnas.081441398.

Stouten, P. F. W. *et al.* (1993) 'How does the switch II region of G-domains work?', *FEBS Letters*. FEBS Lett, pp. 1–6. doi: 10.1016/0014-5793(93)81644-F.

Su, N. *et al.* (2010) 'Increased expression of annexin A1 is correlated with K-ras mutation in colorectal cancer', *Tohoku Journal of Experimental Medicine*. Tohoku J Exp Med, 222(4), pp. 243–250. doi: 10.1620/tjem.222.243.

Sun, X. *et al.* (2018) 'Annexin A5 regulates hepatocarcinoma malignancy via CRKI/II-DOCK180-RAC1 integrin and MEK-ERK pathways', *Cell Death and Disease*. Nature Publishing Group, 9(6), p. 637. doi: 10.1038/s41419-018-0685-8.

Sundaram, M. and Han, M. (1995) 'The C. elegans ksr-1 gene encodes a novel raf-related kinase involved in Ras-mediated signal transduction', *Cell*, 83(6), pp. 889–901. doi: 10.1016/0092-8674(95)90205-8.

Swarthout, J. T. *et al.* (2005) 'DHHC9 and GCP16 constitute a human protein fatty acyltransferase with specificity for H- and N-Ras', *Journal of Biological Chemistry*, 280(35), pp. 31141–31148. doi: 10.1074/jbc.M504113200.

Tall, G. G. *et al.* (2001) 'Ras-Activated Endocytosis Is Mediated by the Rab5 Guanine Nucleotide Exchange Activity of RIN1', *Developmental Cell*, 1(1), pp. 73–82. doi: 10.1016/S1534-5807(01)00008-9.

Tanaka, T., Williams, R. L. and Rabbitts, T. H. (2007) 'Tumour prevention by a single antibody domain targeting the interaction of signal transduction proteins with RAS', *EMBO Journal*, 26(13), pp. 3250–3259. doi: 10.1038/sj.emboj.7601744.

Terrell, E. M. and Morrison, D. K. (2019) 'Ras-mediated activation of the Raf family kinases', *Cold Spring Harbor Perspectives in Medicine*. Cold Spring Harbor Laboratory Press, 9(1). doi: 10.1101/cshperspect.a033746.

Therrien, M. *et al.* (1995) *KSR, a Novel Protein Kinase Required for RAS Signal Transduction*, *Cell*.

Therrien, M. *et al.* (1996) 'KSR modulates signal propagation within the MAPK cascade', *Genes and Development*. Cold Spring Harbor Laboratory Press, 10(21), pp. 2684–2695. doi: 10.1101/gad.10.21.2684.

Tian, T. *et al.* (2007) 'Plasma membrane nanoswitches generate high-fidelity Ras signal transduction', *Nature Cell Biology*. Nature Publishing Group, 9(8), pp. 905–914. doi: 10.1038/ncb1615.

Tian, T. *et al.* (2010) 'Mathematical modeling of K-Ras nanocluster formation on the plasma

membrane', *Biophysical Journal*. Biophysical Society, 99(2), pp. 534–543. doi: 10.1016/j.bpj.2010.04.055.

Tidyman, W. E. and Rauen, K. A. (2016) 'Expansion of the RASopathies', *Current Genetic Medicine Reports*. Springer Science and Business Media LLC, 4(3), pp. 57–64. doi: 10.1007/s40142-016-0100-7.

Tomas, A. and Moss, S. E. (2003) 'Calcium- and cell cycle-dependent association of annexin 11 with the nuclear envelope', *Journal of Biological Chemistry*, 278(22), pp. 20210–20216. doi: 10.1074/jbc.M212669200.

Tong, L. *et al.* (1989) 'Structure of ras protein ', *Science*. American Association for the Advancement of Science, p. 244. doi: 10.1126/science.2665078.

Tourasse, N. J. and Li, W. H. (2000) 'Selective constraints, amino acid composition, and the rate of protein evolution', *Molecular Biology and Evolution*. Society for Molecular Biology and Evolution, 17(4), pp. 656–664. doi: 10.1093/oxfordjournals.molbev.a026344.

Travers, T. *et al.* (2018) 'Molecular recognition of RAS/RAF complex at the membrane: Role of RAF cysteine-rich domain', *Scientific Reports*. Nature Publishing Group, 8(1), pp. 1–15. doi: 10.1038/s41598-018-26832-4.

Traverse, S. *et al.* (1992) 'Sustained activation of the mitogen-activated protein (MAP) kinase cascade may be required for differentiation of PC12 cells. Comparison of the effects of nerve growth factor and epidermal growth factor', *Biochemical Journal*, 288(2), pp. 351–355. doi: 10.1042/bj2880351.

de Vilá Muga, S. *et al.* (2009) 'Annexin A6 inhibits Ras signalling in breast cancer cells', *Oncogene*. Nature Publishing Group, 28(3), pp. 363–377. doi: 10.1038/onc.2008.386.

Vojtek, A. B., Hollenberg, S. M. and Cooper, J. A. (1993) 'Mammalian Ras interacts directly with the serine/threonine kinase raf', *Cell*, 74(1), pp. 205–214. doi: 10.1016/0092-8674(93)90307-C.

Wagner, M. J. *et al.* (2013) 'Molecular mechanisms of SH2- and PTB-Domain-containing proteins in receptor tyrosine kinase signaling', *Cold Spring Harbor Perspectives in Biology*. Cold Spring Harbor Laboratory Press, 5(12). doi: 10.1101/cshperspect.a008987.

Wang, W. and Creutz, C. E. (1994) 'Role of the Amino-Terminal Domain in Regulating Interactions of Annexin I with Membranes: Effects of Amino-Terminal Truncation and Mutagenesis of the Phosphorylation Sites', *Biochemistry*, 33(1), pp. 275–282. doi: 10.1021/bi00167a036.

Wang, X. *et al.* (2013) *Annexin A6 is down-regulated through promoter methylation in gastric cancer*, *Am J Transl Res*. e-Century Publishing Corporation. Available at: www.ajtr.org (Accessed: 3 July 2020).

Wang, Z. *et al.* (2013) 'N terminus of ASPP2 binds to Ras and enhances Ras/Raf/MEK/ERK

activation to promote oncogene-induced senescence', *Proceedings of the National Academy of Sciences of the United States of America*. Proc Natl Acad Sci U S A, 110(1), pp. 312–317. doi: 10.1073/pnas.1201514110.

Warne, P. H., Vician, P. R. and Downward, J. (1993) *Direct interaction of Ras and the amino-terminal region of Raf-1 in vitro*, *Nature*. Nature Publishing Group. doi: 10.1038/364352a0.

Warnock, D. E. *et al.* (1993) 'Determination of plasma membrane lipid mass and composition in cultured Chinese hamster ovary cells using high gradient magnetic affinity chromatography', *Journal of Biological Chemistry*, 268(14), pp. 10145–10153.

Weber, C. K. *et al.* (2001) 'Active ras induces heterodimerization of cRaf and BRaf', *Cancer Research*. American Association for Cancer Research, 61(9), pp. 3595–3598.

Whyte, D. B. *et al.* (1997) 'K- and N-Ras are geranylgeranylated in cells treated with farnesyl protein transferase inhibitors', *Journal of Biological Chemistry*, 272(22), pp. 14459–14464. doi: 10.1074/jbc.272.22.14459.

Winters, I. P. *et al.* (2017) 'Multiplexed in vivo homology-directed repair and tumor barcoding enables parallel quantification of Kras variant oncogenicity', *Nature Communications*. Nature Publishing Group, 8(1). doi: 10.1038/s41467-017-01519-y.

Wittinghofer, F. *et al.* (1991) 'Three-dimensional structure of p21 in the active conformation and analysis of an oncogenic mutant', in *Environmental Health Perspectives*, pp. 11–15. doi: 10.1289/ehp.919311.

Wolfman, J. C. *et al.* (2006) 'Structural and functional consequences of c-N-Ras constitutively associated with intact mitochondria', *Biochimica et Biophysica Acta - Molecular Cell Research*. Elsevier, 1763(10), pp. 1108–1124. doi: 10.1016/j.bbamcr.2006.07.015.

Wright, L. P. and Philips, M. R. (2006) 'CAAX modification and membrane targeting of Ras', *Journal of Lipid Research*. J Lipid Res, pp. 883–891. doi: 10.1194/jlr.R600004-JLR200.

Xu, Y. and Beckett, D. (1994) 'Kinetics of Biotinyl-5'-adenylate Synthesis Catalyzed by the Escherichia coli Repressor of Biotin Biosynthesis and the Stability of the Enzyme-Product Complex', *Biochemistry*. American Chemical Society, 33(23), pp. 7354–7360. doi: 10.1021/bi00189a041.

Xue, M. *et al.* (2017) 'Optimizing the fragment complementation of APEX2 for detection of specific protein-protein interactions in live cells', *Scientific Reports*. Nature Publishing Group, 7(1). doi: 10.1038/s41598-017-12365-9.

Yan, J. *et al.* (1998) 'Ras isoforms vary in their ability to activate Raf-1 and phosphoinositide 3-kinase', *Journal of Biological Chemistry*, 273(37), pp. 24052–24056. doi: 10.1074/jbc.273.37.24052.

Yuan, T. L. *et al.* (2018) 'Differential Effector Engagement by Oncogenic KRAS', *Cell Reports*. Elsevier B.V., 22(7), pp. 1889–1902. doi: 10.1016/j.celrep.2018.01.051.

Zabel, B. U. *et al.* (1985) 'Chromosome mapping of genes on the short arm of human chromosome 11: Parathyroid hormone gene is at 11p15 together with the genes for insulin, c-harvey-ras 1, and β-hemoglobin', *Cytogenetic and Genome Research*, 39(3), pp. 200–205. doi: 10.1159/000132135.

Zhao, Y. *et al.* (2018) 'AnnexinA7 down-regulation might suppress the proliferation and metastasis of human hepatocellular carcinoma cells via MAPK/ERK pathway', *Cancer Biomarkers*. IOS Press, 23(4), pp. 527–537. doi: 10.3233/CBM-181651.

Zhou, Y. *et al.* (2012) 'Nonsteroidal anti-inflammatory drugs alter the spatiotemporal organization of Ras proteins on the plasma membrane', *Journal of Biological Chemistry*. American Society for Biochemistry and Molecular Biology, 287(20), pp. 16586–16595. doi: 10.1074/jbc.M112.348490.

Zhou, Y. *et al.* (2014) 'Signal Integration by Lipid-Mediated Spatial Cross Talk between Ras Nanoclusters', *Molecular and Cellular Biology*. American Society for Microbiology, 34(5), pp. 862–876. doi: 10.1128/mcb.01227-13.

Zhou, Y. *et al.* (2017) 'Lipid-Sorting Specificity Encoded in K-Ras Membrane Anchor Regulates Signal Output', *Cell*. Cell Press, 168(1–2), pp. 239-251.e16. doi: 10.1016/j.cell.2016.11.059.

Zhou, Y. and Hancock, J. F. (2015) 'Ras nanoclusters: Versatile lipid-based signaling platforms', *Biochimica et Biophysica Acta - Molecular Cell Research*. Elsevier B.V., pp. 841–849. doi: 10.1016/j.bbamcr.2014.09.008.

Zimmermann, G. *et al.* (2013) 'Small molecule inhibition of the KRAS-PDEδ interaction impairs oncogenic KRAS signalling', *Nature*, 497(7451), pp. 638–642. doi: 10.1038/nature12205.

Appendixes

Appendix 1| Plasmid maps of APEX2-Ras constructs.

FLAG-APEX2-KRAS WT

Origin of vector: pEGFP-C3-KRASWT

Origin of insert: TOPO-pFLAG-APEX2-C3

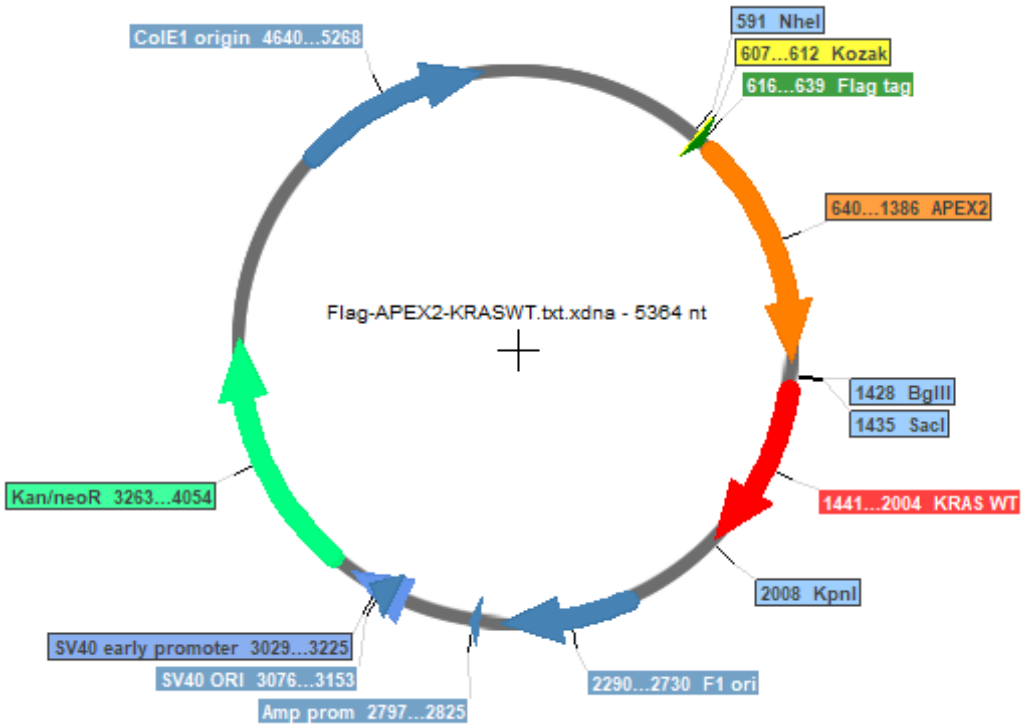

FLAG-APEX2-HRAS WT

Origin of vector: pEGFP-C3-HRASWT

Origin of insert: TOPO-pFLAG-APEX2-C3

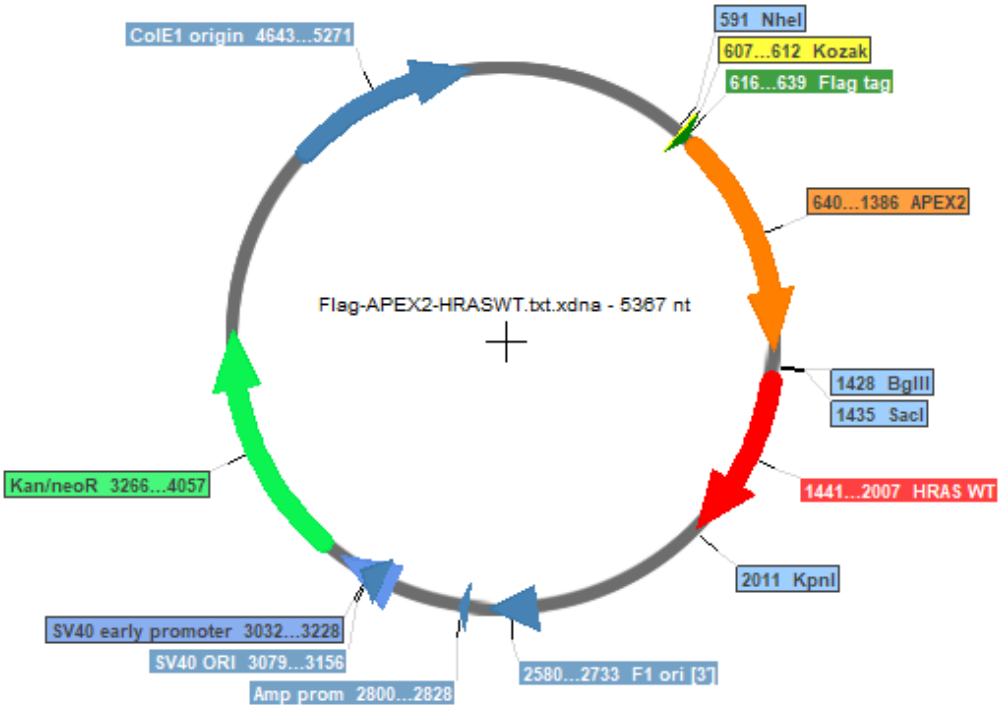

FLAG-APEX2-NRAS WT

Origin of vector: pEGFP-C3-NRASWT

Origin of insert: TOPO-pFLAG-APEX2-C3

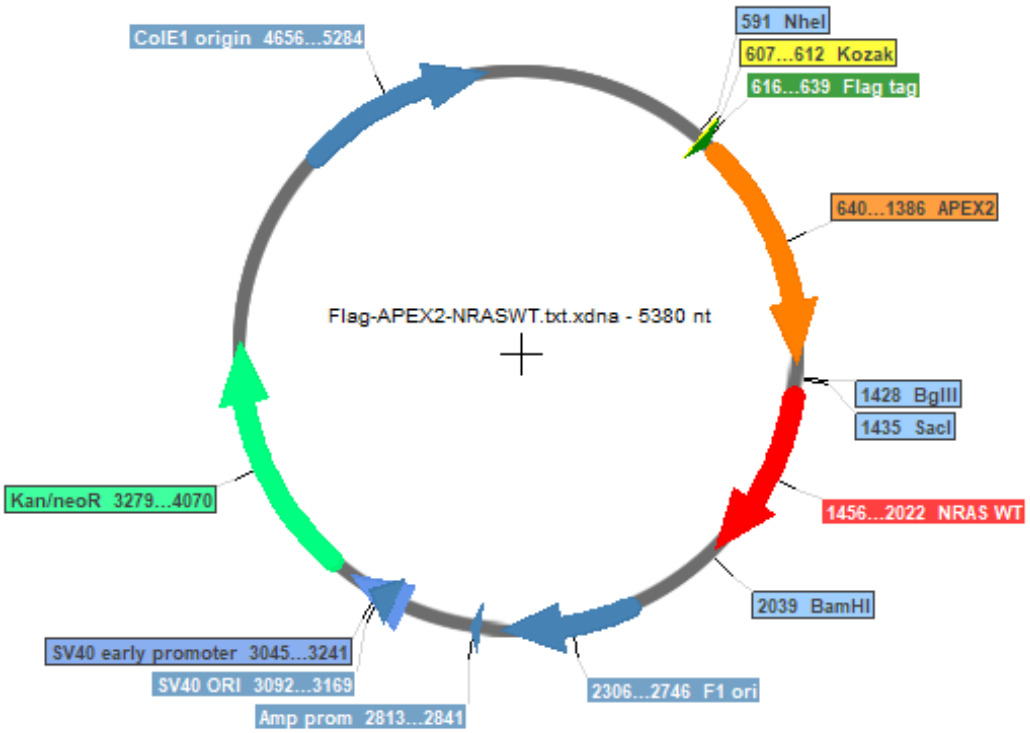

FLAG-APEX2-KG12V

Origin of vector: pEGFP-C2-KG12V

Origin of insert: TOPO- pFLAG-APEX2-C2

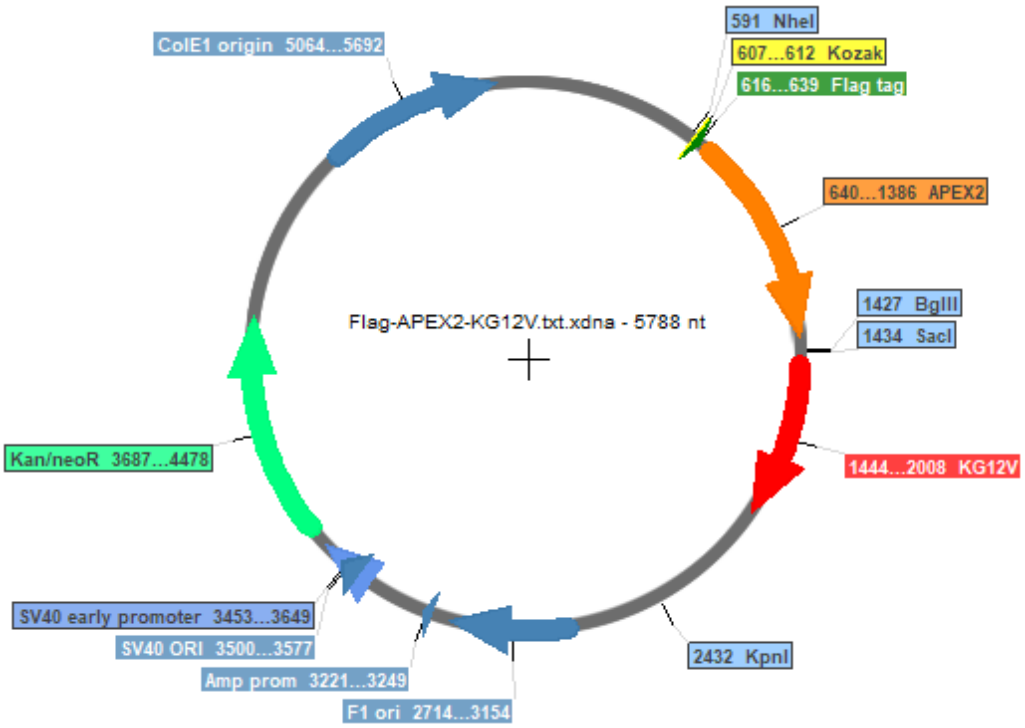

FLAG-APEX2-HG12V

Origin of vector: pEGFP-C1-HG12V

Origin of insert: TOPO-pFLAG-APEX2-C1

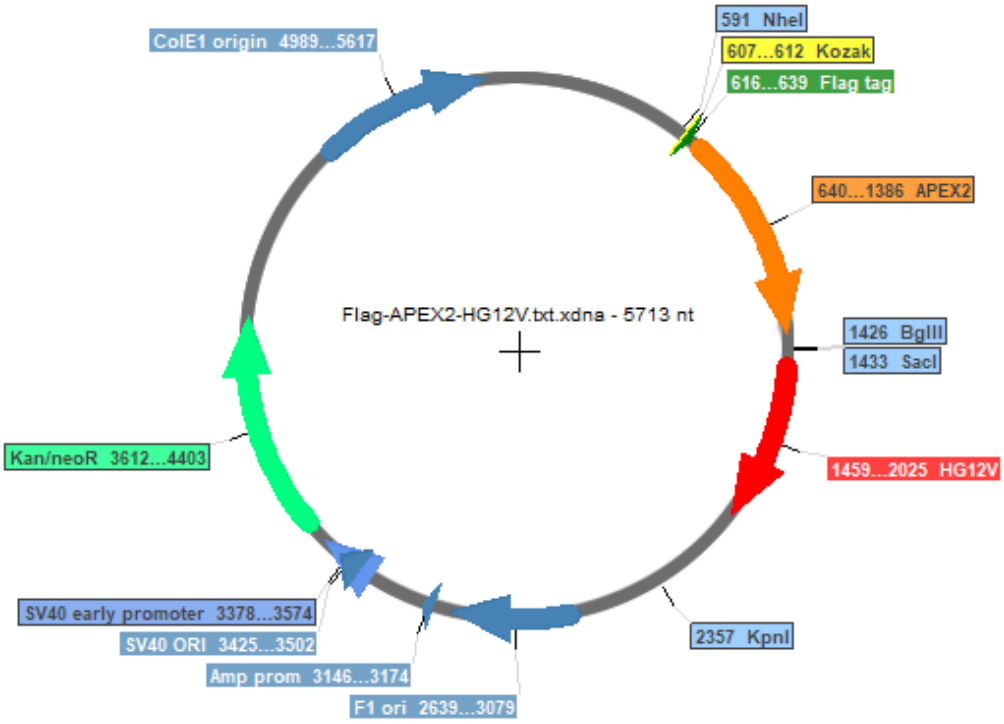

FLAG-APEX2-NG12V

Origin of vector: pEGFP-C3-NG12V

Origin of insert: TOPO-pFLAG-APEX2-C3

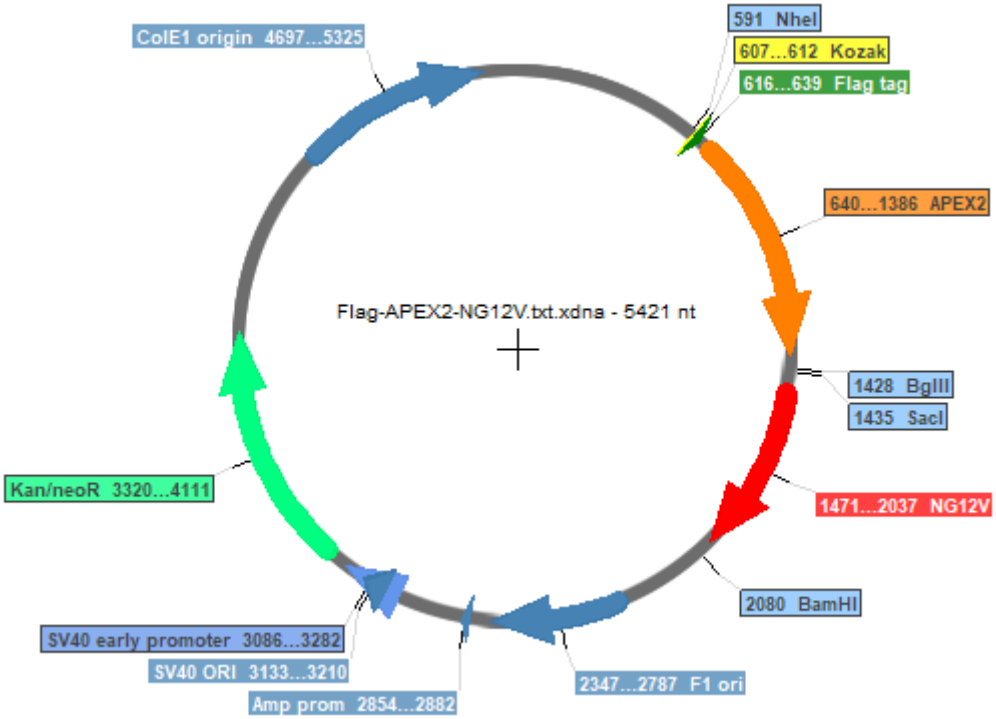

FLAG-APEX2-tK

Origin of vector: pEGFP-C1-tK

Origin of insert: TOPO-pFLAG-APEX2-C1

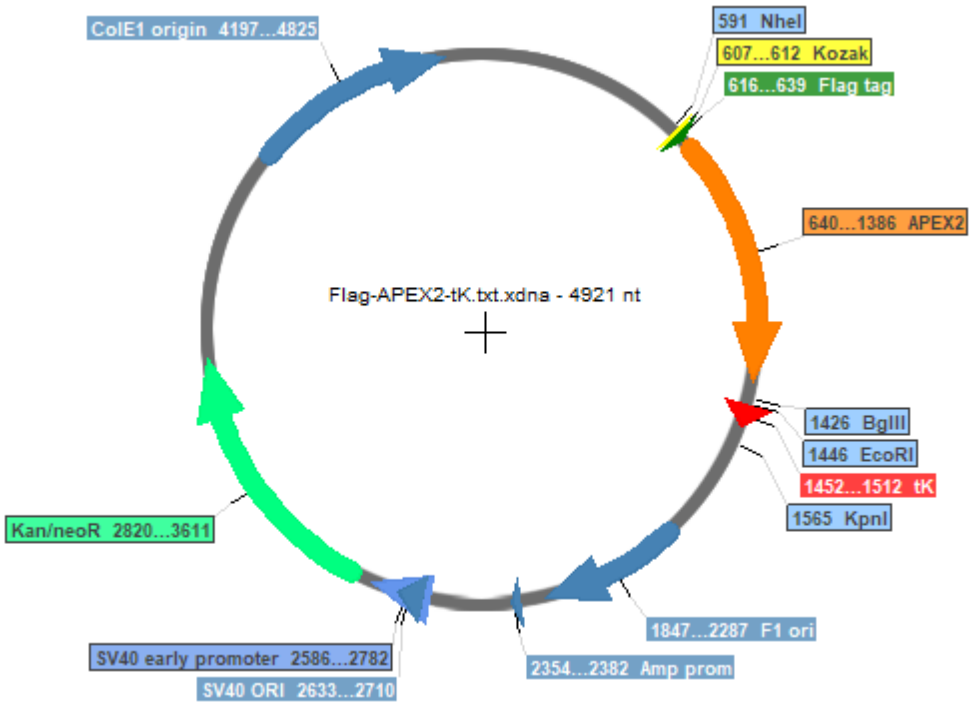

FLAG-APEX2-tH

Origin of vector: pEGFP-C1-tH

Origin of insert: TOPO-pFLAG-APEX2-C1

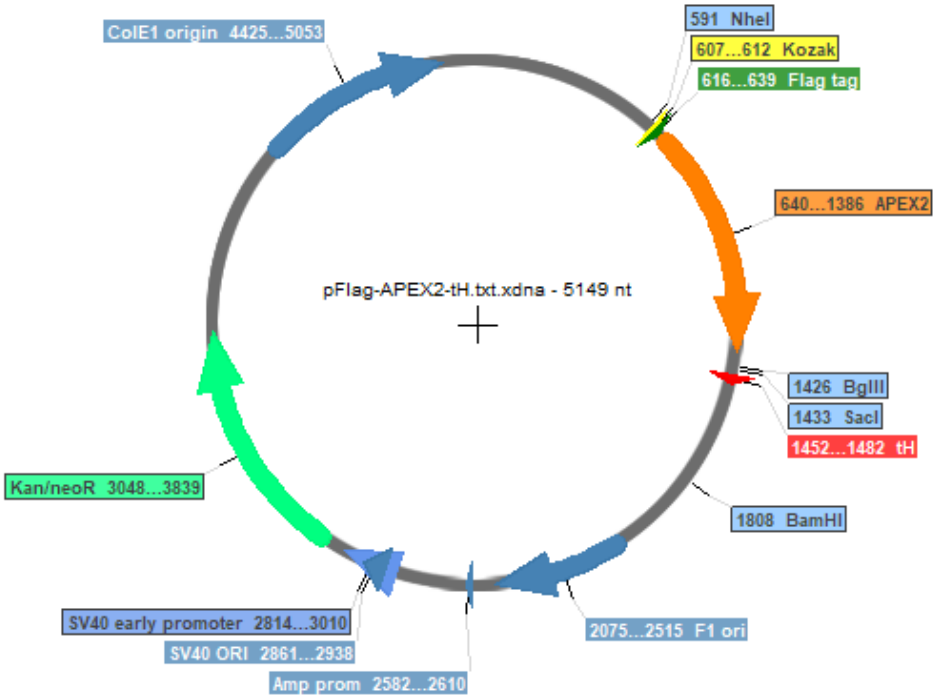

Appendix 2| Shortlisted proteins – LFQ, fold change and average log values for the two experimental repeats of each Ras isoform (KRAS, HRAS and NRAS) in the different treatment conditions (SS, STIM and G12V). For the full list of proteins: https://doi.org/10.17638/datacat.liverpool.ac.uk/1131

KRAS

	LFQ values - 1st replicate				LFQ values - 2nd replicate				Fold change - 1st replicate			Fold change - 2nd replicate		
	CON	SS	STIM	G12V	CON	SS	STIM	G12V	SS	STIM	G12V	SS	STIM	G12V
ANXA11	0.1	28586000	2.35E+08	14459000	0.1	1.49E+09	5.61E+08	60090000	2.86E+08	2.35E+09	1.45E+08	1.49E+10	5.61E+09	6.01E+08
ANXA6	0.1	46529000	5.8E+08	20405000	0.1	9.03E+08	1.46E+09	55968000	4.65E+08	5.8E+09	2.04E+08	9.03E+09	1.46E+10	5.6E+08
ACTR1B	40704000	85198000	1.4E+08	1.33E+08	0.1	56529000	0.1	0.1	2.093111	3.444379	3.265527	5.65E+08	1	1
CACYBP	31280000	2.88E+08	1.62E+09	1.01E+08	0.1	2.9E+09	1.26E+09	3.84E+08	9.194054	51.81266	3.227621	2.9E+10	1.26E+10	3.84E+09
CAST	0.1	0.1	74052000	0.1	0.1	1.63E+08	1.25E+08	36893000	1	7.41E+08	1	1.63E+09	1.25E+09	3.69E+08
CDC42	0.1	33296000	1.02E+08	15332000	0.1	2.51E+08	77964000	47817000	3.33E+08	1.02E+09	1.53E+08	2.51E+09	7.8E+08	4.78E+08
EZR	14961000	5.02E+08	2.39E+09	3.2E+08	40401000	6.61E+09	4.66E+09	1.04E+09	33.53452	159.8088	21.39563	163.6197	115.2447	25.86075
ALDOA	56096000	1.36E+09	5.41E+09	4.68E+08	76165000	1.29E+10	5.4E+09	2.54E+09	24.31189	96.39012	8.335888	168.8833	70.93416	33.28694
LGALS3	0.1	28227000	2.7E+08	17650000	0.1	9.18E+08	2.01E+08	86709000	2.82E+08	2.7E+09	1.77E+08	9.18E+09	2.01E+09	8.67E+08
HNRNPAB	15833000	24396000	39803000	0.1	0.1	1.32E+08	1.11E+08	24135000	1.540832	2.513927	6.32E-09	1.32E+09	1.11E+09	2.41E+08
HNRNPA2B1	15684000	1.63E+08	6.04E+08	1.23E+08	0.1	2.65E+09	4.93E+08	3.29E+08	10.40487	38.51186	7.818159	2.65E+10	4.93E+09	3.29E+09
IMPDH2	0.1	63125000	2.29E+08	62899000	64772000	6.59E+08	2.13E+08	57989000	6.31E+08	2.29E+09	6.29E+08	10.17291	3.293398	0.895279
PAICS	20941000	2.16E+08	4E+08	50137000	0.1	1.16E+09	4.41E+08	2.22E+08	10.30323	19.1094	2.394203	1.16E+10	4.41E+09	2.22E+09
CDV3	0.1	27509000	1.09E+08	25629000	0.1	2.29E+08	1.62E+08	53881000	2.75E+08	1.09E+09	2.56E+08	2.29E+09	1.62E+09	5.39E+08
G3BP2	12874000	31151000	62259000	59267000	30756000	1.58E+08	64492000	66667000	2.419683	4.836026	4.60362	5.124854	2.096892	2.16761
TXN	0.1	24015000	1.04E+08	19442000	0.1	6.09E+08	2.46E+08	24134000	2.4E+08	1.04E+09	1.94E+08	6.09E+09	2.46E+09	2.41E+08
TPM3	0.1	71063000	83110000	0.1	0.1	3.39E+08	2.29E+08	1.33E+08	7.11E+08	8.31E+08	1	3.39E+09	2.29E+09	1.33E+09

CON = Control SS = Serum-starved STIM = Stimulated G12V = Mutant

HRAS

	LFQ values - 1st replicate				LFQ values - 2nd replicate				Fold change - 1st replicate			Fold change - 2nd replicate		
	CON	SS	STIM	G12V	CON	SS	STIM	G12V	SS	STIM	G12V	SS	STIM	G12V
ANXA11	0.1	13438000	0.1	13089000	0.1	28241000	20478000	4168200	1.34E+08	1	1.31E+08	2.82E+08	2.05E+08	41682000
ANXA6	0.1	7514000	0.1	6534500	0.1	4834500	11801000	0.1	75140000	1	65345000	48345000	1.18E+08	1
ACTR1B	77495000	80195000	0.1	61589000	0.1	74194000	34015000	81682000	1.034841	1.29E-09	0.794748	7.42E+08	3.4E+08	8.17E+08
CACYBP	5642700	55766000	47315000	22913000	0.1	98818000	1.55E+08	26062000	9.882857	8.38517	4.060645	9.88E+08	1.55E+09	2.61E+08
CAST	37183000	64637000	38938000	0.1	0.1	50778000	48111000	79221000	1.738348	1.047199	2.69E-09	5.08E+08	4.81E+08	7.92E+08
CDC42	1.05E+08	53569000	55454000	43232000	0.1	42396000	60751000	37585000	0.511838	0.529849	0.413071	4.24E+08	6.08E+08	3.76E+08
EZR	0.1	47316000	53404000	1.11E+08	0.1	1.8E+08	1.84E+08	32043000	4.73E+08	5.34E+08	1.11E+09	1.8E+09	1.84E+09	3.2E+08
ALDOA	47908000	4.16E+08	3.94E+08	2.34E+08	21796000	6.93E+08	6.26E+08	1.65E+08	8.686441	8.220339	4.881648	31.78932	28.73738	7.580749
LGALS3	0.1	0.1	34074000	19122000	0.1	55664000	58731000	26054000	1	3.41E+08	1.91E+08	5.57E+08	5.87E+08	2.61E+08
HNRNPAB	27025000	27168000	32155000	26218000	0.1	21023000	10743000	18703000	1.005291	1.189824	0.970139	2.1E+08	1.07E+08	1.87E+08
HNRNPA2B1	0.1	2.01E+08	2.29E+08	62120000	56319000	4.93E+08	5.18E+08	1.33E+08	2.01E+09	2.29E+09	6.21E+08	8.760276	9.201868	2.37007
IMPDH2	0.1	26290000	15467000	10732000	0.1	37595000	41536000	22516000	2.63E+08	1.55E+08	1.07E+08	3.76E+08	4.15E+08	2.25E+08
PAICS	27787000	1.25E+08	1.37E+08	74588000	35779000	1.16E+08	1.51E+08	48713000	4.512182	4.930363	2.684277	3.24492	4.21057	1.361497
CDV3	0.1	25990000	77369000	22298000	0.1	77081000	56521000	13349000	2.6E+08	7.74E+08	2.23E+08	7.71E+08	5.65E+08	1.33E+08
G3BP2	30132000	34225000	37617000	29949000	0.1	41094000	27981000	23262000	1.135836	1.248407	0.993927	4.11E+08	2.8E+08	2.33E+08
TXN	0.1	42567000	0.1	0.1	0.1	62939000	68004000	45775000	4.26E+08	1	1	6.29E+08	6.8E+08	4.58E+08
TPM3	0.1	1.37E+08	55836000	64353000	0.1	1.27E+08	48893000	16793000	1.37E+09	5.58E+08	6.44E+08	1.27E+09	4.89E+08	1.68E+08

CON = Control SS = Serum-starved STIM = Stimulated G12V = Mutant

NRAS

	LFQ values - 1st replicate				LFQ values - 2nd replicate				Fold change - 1st replicate			Fold change - 2nd replicate		
	CON	SS	STIM	G12V	CON	SS	STIM	G12V	SS	STIM	G12V	SS	STIM	G12V
ANXA11	19563000	28635000	1.14E+08	38118000	14156000	7.94E+08	42028000	41882000	1.463733	5.826305	1.948474	56.07092	2.968918	2.958604
ANXA6	22905000	71584000	1.68E+08	46775000	3058700	3.98E+08	39761000	31025000	3.125256	7.338136	2.042131	130.1991	12.99931	10.1432
ACTR1B	37817000	62234000	1.05E+08	37637000	0.1	53014000	66146000	69840000	1.645662	2.765687	0.99524	5.3E+08	6.61E+08	6.98E+08
CACYBP	41541000	1.78E+08	9.81E+08	1.25E+08	63679000	9.26E+08	2.49E+08	2.09E+08	4.286368	23.60632	3.013408	14.54121	3.911651	3.288839
CAST	0.1	31485000	67549000	38496000	0.1	84708000	19535000	66368000	3.15E+08	6.75E+08	3.85E+08	8.47E+08	1.95E+08	6.64E+08
CDC42	41652000	45940000	79683000	54864000	9069000	1.51E+08	25970000	39530000	1.102948	1.913065	1.3172	16.62366	2.863601	4.358805
EZR	55137000	1.06E+09	2.33E+09	7.17E+08	1.53E+08	4.03E+09	6.86E+08	5.22E+08	19.24842	42.29828	13.00724	26.27388	4.473231	3.403195
ALDOA	3.21E+08	8.57E+08	2.84E+09	1.09E+09	2.59E+08	4.87E+09	2.07E+09	1.53E+09	2.666604	8.853097	3.404295	18.77612	7.972014	5.902012
LGALS3	0.1	40503000	4E+08	1.11E+08	0.1	2.95E+08	1.17E+08	81939000	4.05E+08	4E+09	1.11E+09	2.95E+09	1.17E+09	8.19E+08
HNRNPAB	0.1	22631000	40835000	24877000	6510600	74012000	28542000	28584000	2.26E+08	4.08E+08	2.49E+08	11.36792	4.383928	4.390379
HNRNPA2B1	22119000	2.23E+08	5.86E+08	1.55E+08	17299000	4.5E+08	2.87E+08	1.49E+08	10.09358	26.47272	7.010715	26.02809	16.58131	8.63865
IMPDH2	6693800	91329000	4.06E+08	76901000	54986000	8.79E+08	1.3E+08	56556000	13.64382	60.69796	11.48839	15.98771	2.356964	1.028553
PAICS	57964000	1.69E+08	6.3E+08	2.87E+08	1.32E+08	4.94E+08	1.22E+08	96604000	2.908357	10.86692	4.955662	3.743786	0.927326	0.73207
CDV3	0.1	34846000	76230000	34501000	0.1	0.1	23027000	36253000	3.48E+08	7.62E+08	3.45E+08	1	2.3E+08	3.63E+08
G3BP2	41871000	66365000	55894000	27173000	12540000	42033000	38518000	88619000	1.584987	1.33491	0.648969	3.351914	3.071611	7.066906
TXN	10861000	41887000	1.16E+08	8223000	11998000	1.3E+08	26909000	52813000	3.856643	10.66016	0.757113	10.86514	2.24279	4.401817
TPM3	16885000	64186000	2.8E+08	36765000	0.1	68109000	6850300	1.05E+08	3.801362	16.61001	2.177376	6.81E+08	68503000	1.05E+09

CON = Control SS = Serum-starved STIM = Stimulated G12V = Mutant

Average log values

	KRAS			HRAS			NRAS		
Gene name	SS	STIM	G12V	SS	STIM	G12V	SS	STIM	G12V
ANXA11	32.8	31.9	28.5	27.6	26.6	26.4	4.8	2.1	1.3
ANXA6	32.1	33.2	28.5	25.9	25.8	25.0	6.1	3.3	2.6
ACTR1B	28.1	1.2	1.1	28.5	27.3	28.6	28.0	28.3	28.4
CACYBP	33.8	32.6	30.8	28.9	29.5	27.0	3.2	3.8	1.7
CAST	29.6	29.9	27.5	27.9	27.8	28.6	29.1	28.7	29.0
CDC42	30.4	29.7	28.2	27.7	28.2	27.5	3.1	1.3	1.5
EZR	6.6	7.1	4.6	30.1	30.1	29.4	4.5	4.5	3.0
ALDOA	6.6	6.4	4.4	4.3	4.2	2.6	3.4	3.1	2.2
LGALS3	32.1	31.1	29.0	28.1	28.8	27.8	30.6	31.3	29.8
HNRNPAB	29.3	29.1	26.8	26.6	25.7	26.5	26.8	27.6	26.9
HNRNPA2B1	33.6	31.2	30.6	29.9	30.1	28.2	4.2	4.4	3.0
IMPDH2	28.2	30.1	28.2	28.3	28.1	27.3	3.9	5.0	2.6
PAICS	32.4	31.0	30.0	2.0	2.2	1.0	1.7	2.6	1.5
CDV3	30.3	30.3	28.6	28.9	29.3	27.4	27.4	28.9	28.4
G3BP2	1.9	1.8	1.8	27.6	27.1	26.8	1.3	1.1	1.9
TXN	31.6	30.7	27.7	29.0	28.3	27.8	2.9	2.7	1.4
TPM3	30.9	30.5	29.3	30.3	29.0	28.6	28.3	25.0	29.0

SS = Serum-starved STIM = Stimulated G12V = Mutant